TECHNICAL REPORT

ISO/TR 19905-2

First edition
2012-##-##

Petroleum and natural gas industries — Site-specific assessment of mobile offshore units —

Part 2: Jack-ups commentary and detailed sample calculation

Industries du pétrole et du gaz naturel — Évaluation liée au site des unités marines mobiles —

Partie 2: Compléments sur les plates-formes auto-élévatrices

PROOF/ÉPREUVE

Reference number
ISO/TR 19905-2:2012(E)

ISO copyright office
Case postale 56 • CH-1211 Geneva 20
Tel. + 41 22 749 01 11
Fax + 41 22 749 09 47
E-mail copyright@iso.org
Web www.iso.org

Published in Switzerland

Contents

Page

Foreword

ISO (the International Organization for Standardization) is a worldwide federation of national standards bodies (ISO member bodies). The work of preparing International Standards is normally carried out through ISO technical committees. Each member body interested in a subject for which a technical committee has been established has the right to be represented on that committee. International organizations, governmental and non-governmental, in liaison with ISO, also take part in the work. ISO collaborates closely with the International Electrotechnical Commission (IEC) on all matters of electrotechnical standardization.

International Standards are drafted in accordance with the rules given in the ISO/IEC Directives, Part 2.

The main task of technical committees is to prepare International Standards. Draft International Standards adopted by the technical committees are circulated to the member bodies for voting. Publication as an International Standard requires approval by at least 75 % of the member bodies casting a vote.

In exceptional circumstances, when a technical committee has collected data of a different kind from that which is normally published as an International Standard ("state of the art", for example), it may decide by a simple majority vote of its participating members to publish a Technical Report. A Technical Report is entirely informative in nature and does not have to be reviewed until the data it provides are considered to be no longer valid or useful.

Attention is drawn to the possibility that some of the elements of this document may be the subject of patent rights. ISO shall not be held responsible for identifying any or all such patent rights.

ISO/TR 19905-2 was prepared by Technical Committee ISO/TC 67, *Materials, equipment and offshore structures for petroleum, petrochemical and natural gas industries*, Subcommittee SC 7, *Offshore structures*.

ISO 19905 consists of the following parts, under the general title *Petroleum and natural gas industries — Site-specific assessment of mobile offshore units*:

— *Part 1: Jack-ups*

— *Part 2: Jack-ups commentary and detailed sample calculation* [Technical Report]

The following part is under preparation:

— *Part 3: Floating units*

ISO 19905 is one of a series of International Standards for offshore structures. The full series consists of the following International Standards:

— ISO 19900, *Petroleum and natural gas industries — General requirements for offshore structures*

— ISO 19901-1, *Petroleum and natural gas industries — Specific requirements for offshore structures — Part 1: Metocean design and operating considerations*

— ISO 19901-2, *Petroleum and natural gas industries — Specific requirements for offshore structures — Part 2: Seismic design procedures and criteria*

— ISO 19901-3, *Petroleum and natural gas industries — Specific requirements for offshore structures — Part 3: Topsides structure*

— ISO 19901-4, *Petroleum and natural gas industries — Specific requirements for offshore structures — Part 4: Geotechnical and foundation design considerations*

— ISO 19901-5, *Petroleum and natural gas industries — Specific requirements for offshore structures — Part 5: Weight control during engineering and construction*

— ISO 19901-6, *Petroleum and natural gas industries — Specific requirements for offshore structures — Part 6: Marine operations*

— ISO 19901-7, *Petroleum and natural gas industries — Specific requirements for offshore structures — Part 7: Stationkeeping systems for floating offshore structures and mobile offshore units*

— ISO 19901-8[1)], *Petroleum and natural gas industries — Specific requirements for offshore structures — Part 8: Marine soil investigations*

— ISO 19902, *Petroleum and natural gas industries — Fixed steel offshore structures*

— ISO 19903, *Petroleum and natural gas industries — Fixed concrete offshore structures*

— ISO 19904-1, *Petroleum and natural gas industries — Floating offshore structures — Part 1: Monohulls, semi-submersibles and spars*

— ISO 19905-1, *Petroleum and natural gas industries — Site-specific assessment of mobile offshore units — Part 1: Jack-ups*

— ISO/TR 19905-2, *Petroleum and natural gas industries — Site-specific assessment of mobile offshore units — Part 2: Jack-ups commentary and detailed sample calculation*

— ISO/TR 19905-3[1)], *Petroleum and natural gas industries — Site-specific assessment of mobile offshore units — Part 3: Floating units*

— ISO 19906, *Petroleum and natural gas industries — Arctic offshore structures*

1) Under preparation.

Introduction

The series of International Standards applicable to types of offshore structures, ISO 19900 to ISO 19906, addresses design requirements and assessments for all offshore structures used by the petroleum and natural gas industries worldwide. Through their application, the intention is to achieve reliability levels appropriate for manned and unmanned offshore structures, whatever the type of structure and the nature or combination of the materials used.

It is important to recognize that structural integrity is an overall concept comprising models for describing actions, structural analyses, design or assessment rules, safety elements, workmanship, quality control procedures and national requirements, all of which are mutually dependent. The modification of one aspect of the design or assessment in isolation can disturb the balance of reliability inherent in the overall concept or structural system. The implications involved in modifications, therefore, need to be considered in relation to the overall reliability of offshore structural systems.

The series of International Standards applicable to the various types of offshore structure is intended to provide a wide latitude in the choice of structural configurations, materials and techniques without hindering innovation. Sound engineering judgement is therefore necessary in the use of these International Standards.

ISO 19905-1 was developed from SNAME T&R Bulletin 5-5A[5], but has been considerably altered from that original document. Some of the alterations have involved a restructuring and modification of terminology, but there have been additional changes of greater technical consequence. New material has been added based on studies undertaken since the original development of SNAME T&R 5-5A; new calculation techniques have been addressed because of improved computational capabilities allowing more complex assessments; gaps that existed in the original SNAME T&R 5-5A have been filled, thereby ensuring a more thorough assessment; and changes have been made to align ISO 19905-1 with other standards within the 19900 series. A description of the more important changes, along with the reasoning for the changes, can be found in a series of papers published in 2012 by Offshore Technology Conference. These papers can be of considerable value in helping the analyst, particularly those who are familiar with SNAME T&R 5-5A, in understanding ISO 19905-1. The papers, part of the Technical Session *ISO 19905-1: A Site-Specific Assessment of Mobile Jack-Up Units* are listed in the Bibliography:

— Reference [6], *Background to the ISO 19905-Series and an Overview of the New ISO 19905-1 for the Site-Specific Assessment of Mobile Jack-Up Units*

— Reference [7], *Environmental Actions in the New ISO for the Site-Specific Assessment of Mobile Jack-Up Units*

— Reference [8], *Structural Modeling and Response Analysis in the New ISO Standard for the Site-Specific Assessment of Mobile Jack-Up Units*

— Reference [9], *Foundation Modeling and Assessment in the New ISO Standard 19905-1*

— Reference [10], *Long-Term Applications in the ISO Standard for Site Specific Assessment of Mobile Jack-Up Units and the Use of Skirted Spudcans*

— Reference [11], *Structural Acceptance Criteria in the New ISO for the Site-Specific Assessment of Mobile Jack-Up Units*

— Reference [12], *The Benchmarking of the New ISO for the Site-Specific Assessment of Mobile Jack-Up Units*

This part of ISO 19905, which has been developed from SNAME T&R Bulletin 5-5A, provides a commentary to some clauses of ISO 19905-1 including background information, supporting documentation, and additional or alternative calculation methods as applicable and also provides a detailed sample “go-by” calculation in Annex A. The reader is advised that the information presented herein is intended for use in conjunction with ISO 19905-1 and that the cautions and limitations discussed in ISO 19905-1 apply.

Petroleum and natural gas industries — Site-specific assessment of mobile offshore units —

Part 2:
Jack-ups commentary and detailed sample calculation

1 Scope

This part of ISO 19905 provides a commentary to some clauses of ISO 19905-1 including background information, supporting documentation, and additional or alternative calculation methods as applicable and also provides a detailed sample 'go-by' calculation. ISO 19905-1 specifies requirements and guidance for the site-specific assessment of independent leg jack-up units for use in the petroleum and natural gas industries.

2 References

The following referenced documents are indispensable for the application of this document. For dated references, only the edition cited applies. For undated references, the latest edition of the referenced document (including any amendments) applies.

ISO 19905-1:2012, *Petroleum and natural gas industries — Site-specific assessment of mobile offshore units — Part 1: Jack-ups*

3 Terms and definitions

For the purposes of this document the terms and definitions given in ISO 19905-1 apply.

4 Symbols

4.1 Symbols for Clause 6

C_D	drag coefficient
$C_{De}D_e$	equivalent drag coefficient times effective diameter
d	water depth
D_2	depth attenuation
$D(\theta)$	directional spreading function from ISO 19901-1
$F(\alpha)$	directional spreading function from SNAME
f	frequency (Hz)
g	acceleration due to gravity

H	wave height
H_{det}	reduced wave height which may be used in deterministic/regular wave force calculations
H_{max}	maximum wave height for a given return period; used for airgap calculations
H_{mpm}	wave height associated with H_{srp}, equivalent to the height between the extreme crest and the following trough
H_{mo}	estimate of H_s significant wave height (meters)
H_s	scaled significant wave height to be used in irregular seas simulation (meters)
H_{srp}	significant wave height for assessment return period
k	wave number
m	power constant in the $\left[\cos(\alpha)\right]^{2m}$ spreading function
$S_{nn}(f)$	power density of wave surface elevation as a function of wave frequency
T	wave period (seconds)
T	wind averaging tome (seconds)
T_0	standard reference time averaging interval for wind speed of 1 hr = 3600 s
T_p	peak period in wave spectrum (seconds)
T_z	zero-upcrossing period of wave spectrum (seconds)
U	wind speed
$U_{w,T}(10)$	is the sustained wind speed at 10 m height above mean sea level
U_{w0}	is the 1 h sustained wind speed at the reference elevation 10 m above mean sea level
u	the computed velocity for long crested waves
u_{red}	the reduced horizontal velocity
V	current velocity
α	equilibrium range parameter
α_3	skewness
α_4	kurtosis
γ	peak enhancement factor
γ_d	scaling of drag forces
κ	kinematics reduction factor
η	crest elevation by Airy theory

η_s crest elevation by Stokes

ϕ directional spreading factor defined in ISO 19901-1

σ spectral peakwidth parameter

4.2 Symbols for Clause 7

A cross-sectional area of member

A_e equivalent area of leg per unit height

A_i equivalent area of element

A_s sum of projected areas for all members in the considered plane

A_t total projected envelope area of the considered plane

C_A added mass coefficient

C_D drag coefficient

C_{Do} drag coefficient for chord at direction $\theta = 0°$

C_{D1} drag coefficient for flow normal to the rack, $\theta = 90°$

C_{De} equivalent drag coefficient

C_{Dei} equivalent drag coefficient of member i

C_{Di} drag coefficient of an individual member, related to D_i

$C_{Dpr}(\theta)$ drag coefficient to the projected diameter

C_{Drough} drag coefficient for a rough member

$C_{Dsmooth}$ drag coefficient for a smooth member

C_M inertia coefficient

C_{Me} equivalent inertia coefficient

C_{Mei} equivalent inertia coefficient of member i

C_{Mi} inertia coefficient of a member, related to D_i

d mean, undisturbed water depth (positive)

D member diameter

D_e equivalent diameter of leg bay

D_F face width of leg, outside dimensions

D_i reference dimension of individual leg members

$D_{pr}(\theta)$ projected diameter of the chord

f_i fundamental vibration frequencies of the member

H_s significant wave height

k	roughness height
k/D	relative roughness
KC	Keulegan-Carpenter number
l_i	length of member "i" node to node
m_a	added mass contribution (per unit length) for the member
N	constant in wind velocity power law
$\dot{r}_n$	velocity of the considered member, normal to the member axis and in the direction of the combined particle velocity
$\ddot{r}_n$	acceleration of the considered member, normal to the member axis and in the direction of the combined particle velocity
Re	Reynolds number
s	length of one bay, or part of bay considered
S	Strouhal number
S	average wave steepness
S	outer diameter of an array of tubulars
T	wave period
T_n	first natural period of sway motion
T_z	zero-upcrossing period
u	particle velocity
u_n	particle velocity normal to the member
$\dot{u}_n$	particle acceleration normal to the member
$u_x, \dot{u}_x$	horizontal water particle velocity and acceleration
U	flow velocity at the depth of the considered element
U_C	current particle velocity
U_m	maximum orbital particle velocity
U_{red}	reduced particle velocity for regular waves
U_W	representative wave particle velocity
v_n	total flow velocity normal to the member
V_C	reduced current velocity for use in the hydrodynamic model; V_C should not be taken as less than $0{,}7V_f$
V_{Cn}	current velocity normal to member used in the hydrodynamic model
V_f	far field (undisturbed) current

W dimension from backplate to pitch point of triangular chord or dimension from root of one rack to tip of other rack of split tubular chord

W width of the structure

z coordinate measured vertically upward from the mean water surface

z' modified coordinate to be used in particle velocity formulation

α indicator for relative velocity, 0 or 1

α_i angle defining flow direction relative to member

β ratio of Re/KC, a parameter to describe the test environment

β_i angle defining the member inclination

ΔF_{drag} drag force per unit length

$\Delta F_{inertia}$ inertia force per unit length

$\Delta F_{inertiaH}$ horizontal inertia force per unit length

λ wave length

ν kinematic viscosity

θ angle in degrees for waves relative to the chord orientation

θ_o angle where half the backplate is hidden behind the rackplate

ρ mass density of water or air

ζ instantaneous water surface elevation (same axis system as z)

ζ_o wave crest elevation (same axis system as z)

4.3 Symbols for Clause 8

K_o lateral stiffness without axial load

K_1 lateral stiffness with axial load

K_E sum of individual leg stiffnesses

L distance from the spudcan point of rotation to the hull centre of gravity

P axial load in one leg

P_G total gravity load only

P_g effective hull gravity load; includes hull weight and weight of the legs above the hull

y_0 deflection without axial load P

y_1 additional lateral deflection due to axial load P

y_{max} total lateral deflection

4.4 Symbols for Clause 9

a depth interpolation parameter

B_S soil buoyancy of spudcan below bearing area, i.e. the submerged weight of soil displaced by the spudcan below D, the greatest depth of maximum cross-sectional spudcan bearing area below the sea floor

F_H horizontal force applied to the spudcan due to the assessment load case

F_V gross vertical force acting on the soil beneath the spudcan due to the assessment load case

Q_V gross ultimate vertical foundation capacity

V_{Lo} maximum vertical reaction under the spudcan considered required to support the in-water weight of the jack-up during the entire preloading operation (this is not the soil capacity)

W_{BF} submerged weight of the backfill

$\gamma_{R,PRE}$ preload resistance factor

4.5 Symbols for Clause 10

A axial area of one leg (equals sum of effective chord areas, including a contribution from rack teeth; see ISO 19905-1:2012, A.8.3.3, Note)

A_s effective shear area of one leg

d distance between upper and lower guides

D_{hyst} hysteretic damping

E Young's modulus

F shear transmitted from the hull

F_g geometric factor; = 1,125 (three-leg jack-up), 1,0 (four-leg jack-up)

F_h factor to account for horizontal soil stiffness, K_{hs}, and horizontal leg-hull connection stiffness, K_{hh}

F_h modification factor to be applied to the leg lateral deformation stiffness

F_n factor to account for the number of chords; = 0,5 (three-chord leg), 1,0 (four-chord leg)

F_r modification factor to be applied to the leg-hull connection stiffness

F_v factor to account for vertical soil stiffness, K_{vs}, and vertical leg-hull connection stiffness, K_{vh}

g acceleration due to gravity

h distance between chord centres (opposed pinion chords) or pinion pitch points (single rack chords)

I second moment of area of leg

I_H representative second moment of area of the hull girder joining two legs about a horizontal axis normal to the line of environmental action

K_A effective horizontal stiffness due to axial deformation

K_B	effective bending stiffness
K_e	effective stiffness associated with one leg
k_f	combined vertical stiffness of all fixation system components on one chord
K_{hh}	horizontal leg-hull connection stiffness
K_{hull}	hull rotational stiffness
k_j	combined vertical stiffness of all jacking system components on one chord
K_{rh}	leg-hull connection rotational stiffness
K_{rs}	leg-soil connection rotational stiffness
k_u	total lateral stiffness of upper guides with respect to lower guides
K_{vh}	effective stiffness due to the series combination of all vertical pinion or fixation system stiffnesses, allowing for combined action with shock-pads, where fitted
L	length of leg considered
M_e	effective mass associated with one leg
M_h	moment on leg-hull spring
M_{hull}	full mass of hull including maximum variable load
M_{la}	mass of leg above lower guide (in the absence of a clamping mechanism) or above the centre of the clamping mechanism
M_{lb}	mass of leg below the point described for M_{la}, including added mass for the submerged part of the leg ignoring spudcan
M_s	moment on leg-soil spring
N	number of legs
P	axial load in leg
P	mean force due to vertical fixed load and variable load acting on one leg
P_E	Euler buckling force of one leg
T_n	highest (or first mode) natural period
x_h	hull deflection
Y	distance between centre of one leg and line joining centres of the other two legs (three-leg jack-up), or distance between windward and leeward leg rows for direction under consideration (four-leg jack-up)
ν	Poisson's ratio
δ_{axial}	axial deflection
Δ_{horz}	horizontal hull deflection
θ_{hull}	hull rotation

4.6 Symbols for Clause 12

F_y yield strength, in stress units, taken as the minimum of the yield strength and 90 % of the ultimate tensile strength (UTS; see ISO 19905-1:2012, A.12.2.2)

M_p nominal bending strength

Z plastic section modulus

5 Commentary on ISO 19905-1:2012, Clauses 5 and A.5

No commentary is offered.

6 Commentary on ISO 19905-1:2012, Clauses 6 and A.6

TR.6.4.1 Metocean data — General

ISO 19905-1 permits the use of either 50-year return period individual extremes or 100-year joint probability environmental data with associated and different load factors; see ISO 19905-1:2012, 6.4. For these alternative environmental formulations, adjustments for season and directionality are permitted as given below:

— Seasonally adjusted data may be used if appropriate (ISO 19905-1:2012, 6.4).

NOTE When seasonal data are specified, the data should not be divided into periods of less than one month and the values so calculated should generally be factored such that the extreme for the most severe period equals the all-year value for the required assessment return period.

— Where directional data are available, these may be considered (ISO 19905-1:2012, 6.4).

NOTE When directional data are specified, the data should normally not be divided into sectors of less than 30° and the directional values so calculated should generally be factored such that the extreme for the most severe sector equals the omni-directional value for the required assessment return period and season where applicable. In certain areas 30° sectors may be inappropriate; caution should be exercised if an assessment heading falls marginally outside a sector with higher data or if data is highly directional.

— The downwind (vector) component of the maximum surface flow of the mean spring tidal current is specified rather than the maximum spring tidal current (ISO 19905-1:2012, A.6.4.3).

— Site-specific information may be used to determine an appropriate combination of wind-driven and surge currents (ISO 19905-1:2012, A.6.4.3).

TR.6.4.2 Waves

TR.6.4.2.2 Extreme wave height

The wave heights utilized by ISO 19905-1 for wave load calculations are related to the return period significant wave height for a three-hour storm, H_{srp}. ISO 19905-1 however recognizes that this data may not always be available to the assessor and therefore provides relationships between H_{srp} and H_{max}, the individual extreme wave height for the assessment return period with an annual probability of exceedance of 1/(return period). If the assessment return period is taken as 50 years, $H_{max(50)}$ is the wave height with a 2 % annual probability of exceedance.

H_{srp} and the associated period are normally determined through a direct extrapolation of measured or hindcast site-specific significant wave heights. H_{max} may be determined either from an extrapolation of the distribution of individual wave heights over the assessment return period or by the application of a multiplication factor to H_{srp}.

It is noted that the "extreme wave height" of a regular wave, H_{mpm}, determined from a three-hour storm segment is the most probable maximum (MPM) wave height, defined as the distance from the extreme crest to the following trough. Using this definition, the MPM wave height from the three-hour storm segment is given by:

$$H_{mpm} = 1{,}68\ H_{srp} \qquad \text{(TR.6.4-1)}$$

This relationship is confirmed by the data of Reference [6-1] for individual storms. However, H_{mpm} must not be confused with H_{max} and must not be used to determine the value of H_{srp} on which an assessment is based. This is because H_{max} includes site-specific considerations of potentially longer durations of storms (including build up and decay) and the additional probability contributions of other return period storms (i.e. 20-, 30-, 40-, 100-year, etc. return period storms). Consequently, the ratio H_{max}/H_{srp} is larger than the ratio H_{mpm}/H_{srp}.

A consequence of the site-specific nature of the derivation of H_{max} is that there is no unique relationship between H_{max} and H_{srp} applicable to all areas of the world. Thus, if a specified return period maximum wave height is given at a particular location there is no consistent way to derive H_{srp} without knowledge of how the maximum H_{max} wave height was derived originally.

Average factors between H_{srp} and H_{max} have been derived for a North Sea and a Gulf of Mexico location for a 50-year return period. Without further information, the North Sea factors can be generalized to any non-tropical revolving storm area and the Gulf of Mexico factors can be generalized to tropical revolving storm areas. These factors are:

Environmental conditions	H_{max}/H_{srp}
Tropical revolving storms	1,75
Non-tropical storms	1,86

TR.6.4.2.3 Deterministic waves

The selection of wave height to be applied in a particular analysis approach (regular or irregular waves) is recommended based on matching the loads resulting from the combination of the wave height and kinematics models, as recommended in ISO 19905-1:2012, A.7.3.3.3.1. The scaling of wave heights is introduced as an alternative to the scaling of drag coefficients.

For regular wave analyses using an appropriate wave theory, the wave asymmetry is properly accounted for, but the irregularity of the sea surface and the wave spreading may not be modelled properly.

Considering that the computations with regular waves are made with a kinematics model that has been documented in Reference [6-4] to be somewhat conservative, a reduction factor is appropriate to arrive at realistic force estimates.

As indicated in Tables TR.6.4.2.2-1 and TR.6.4.2.2-2, a reduction factor is required to give similar forces as predicted by an irregular seas simulation if $H_{max} = 1{,}86H_s$. There are a few ways that the reduction factor could be realized in the assessment. In Reference [6-2] a reduction of the drag coefficient by a factor of 0,7 is chosen and in Reference [6-3] a reduction of wave kinematics is chosen. Some classification societies may specify lower C_D values than specified in ISO 19905-1:2012, A.7.3.4, and these apply to regular wave analyses.

Accepting that a scaling factor on kinematics is applicable, the kinematics reduction factor κ is introduced in ISO 19905-1:2012, A.6.4.2.3 for application to the kinematics obtained from H_{max} (preferred) or, alternatively, to scale the wave height, but not both.

In the development of the SNAME T&R Bulletin 5-5A[5] it was chosen to follow a practical way of implementing the reduction in the Practice by reducing the wave height to be used for force computations in regular wave analyses. This was found to be more practical than using a factor on kinematics, as most software on the market did not allow such a scaling factor to be used. Equivalent wave heights are suggested as:

$$H_{det} = 1{,}60H_{srp} \qquad \text{(TR.6.4-2)}$$

The scaling factors on kinematics could be implemented assuming that the load effect is proportional to wave height to the power 2,2, remembering that drag coefficients (C_D) should not be scaled. As a comparison with previous practices, the relationship $H_{det} \approx 1{,}60 H_{srp}$ can also be compared with the reduction of C_D by a factor of 0,7 as recommended in Reference [6-2] in combination with the wave height $H_{max} = 1{,}86 H_s$. By assuming that load effects are proportional to the ratio of wave heights to the power 2,2, the scaling becomes $(1{,}60/1{,}86)^{2,2} = (0{,}86)^{2,2} = 0{,}72$, indicating that this is not lower than current practice. The computational results of Table TR.6.4.2.2-2 indicate also that scaling of 0,66 would give similar static forces as the irregular seas simulation at large water depths. See also Appendix TR.7.B for a comparison of the computational results, related to other practices. In effect, in the SNAME T&R Bulletin 5-5A, the above resulted in a kinematic reduction factor of 0,86 (= 1,60/1,86).

In the course of developing ISO 19905-1, new technology was introduced (see ISO 19905-1:2012, Reference [A.6.4-1]), replacing the above definition of equivalent wave height H_{det}. The directional spreading factor defined in ISO 19901-1 was taken as the basis. This factor ϕ may be applied directly as a kinematics reduction factor κ. Depending on the type of storm region (see TR.6.4.2.2 above) and the latitude, ϕ may vary between 0,87 and 0,94.

In short-crested waves, the wave energy propagates in different directions around the main wave direction. The peak particle velocities under waves become smaller as the waves become more spread. As a result, the directional spreading of waves tends to result in peak loading that is somewhat smaller than that predicted for uni-directional seas. Design codes and practices have accounted for spreading by introducing a factor on horizontal kinematics (either directly or via the wave height) in conjunction with the regular wave approach. The reduction factor reflects the reduced kinematics under the highest point of the wave crest and is thus appropriate for the calculation of quasi-static loads on a single pile. However, it does not account for all the effects of spreading. The loads on offshore structures are reduced further due to the spatial distribution of the wave-loaded structural components.

Thorough inclusion of both 3D and nonlinear effects of waves can reduce the extreme loads computed for a jack-up. In the study reported in ISO 19905-1:2012, Reference [A.6.4-1], a systematic study of a variety of jack-ups (LeTourneau 82SDC, LeTourneau 116C, F&G Mod V, LeTourneau Super 300 and MSC CJ70) in different water depths and environments was performed to generalize the applicability of results. A formula was developed which can robustly represent the above effects in an assessment context, without having to perform the more complex and time consuming direct evaluation. The formulation is given in ISO 19905-1:2012, A.6.4.2.3 in Equations (A.6.4-4) through (A.6.4-7).

The development of the formula was based on fitting the total wave actions on the legs of a typical jack-up by regular wave analysis to the most probable maximum extreme (MPME) results from a stochastic wave analysis. The fitting was done by a kinematic reduction factor. The stochastic wave analyses were performed using the ISO directional spreading factor as the basis and a second order directional wave theory for the irregular extreme wave kinematics coupled with an analysis model which simulates jack-up quasi-static loading. The response quantities assessed were the base shear and the overturning moment. Using the formulae given in ISO 19905-1:2012, A.6.4.2.3, the accuracy of the fit compared to the stochastic loads is within ± 5 %. For the majority of the cases analysed, the resulting κ was between 0,70 and 0,85, but there were cases that produced higher wave loads than the original SNAME ($\kappa = 0{,}86$), so with $\kappa > 0{,}86$.

Caution should be exercised if the above formulation is applied to cases other than three-legged drag-dominated (truss legs) jack-ups in extreme storm conditions. The main reason for this is that only these typical jack-up designs in ultimate limit state (ULS) conditions have been considered in the calculations that form the basis of the formulation. For these jack-up types and conditions, the results are valid; for others, caution is necessary.

TR.6.4.2.3.1 Comparison of wave loads obtained using different wave theories for regular and irregular wave analyses

The Dean's stream function/Stokes' fifth order theories predict higher peak than trough amplitudes, increasing the maximum velocities and the wetted surface compared with the Airy theory. In Figure TR.7.3.3.3-2 the difference in the profiles is illustrated. Using the same specified wave height, this difference can be seen in terms of the overturning moment, base shear and/or deck displacement.

A number of computations were performed to determine the differences due to wave kinematics on selected jack-up designs. Some results are summarized in Tables TR.6.4.2.2-1 and TR.6.4.2.2-2. See also Appendix TR.7.B.

Table TR.6.4.2.2-1 — Regular wave analysis normalized results, $C_{De}D_e$ = 5,13 over the full water depth

Theory	Water depth m	Wave H_{max} & T m/s	Crest amp. m	Base shear MN	Overturning. moment MNm	Dean's overturning/ other
Airy Const.	30	15/14	7,5	3,577	91,607	1,74
Airy Wheeler		15/14	7,5	3,266	82,782	1,93
Stokes' fifth		15/14	10,22	5,211	156,16	1,02
Dean's stream		15/14	10,42	5,243	159,45	1,0
Airy Const.	70	15/14 28/16	7,5 14,0	2,916 14,121	160,83 677,69	1,12 1,44
Airy Wheeler		15/15 28/16	7,5 14,0	2,563 13,446	138,80 636,53	1,30 1,53
Stokes' fifth		15/14 28.16	8,41 19,17	3,171 18,264	180,80 976,62	1,00 1,00
Dean's stream		15/14 28/16	8,41 19,33	3,161 18,136	180,30 972,54	1,0 1,0

In Table TR.6.4.2.2-2 the deterministic analysis is based on application of various H_{max} to H_s relationships. The stochastic analysis refers to extreme values determined from time domain analyses by fitting a three-parameter Weibull distribution to the response peaks and reading the extreme as the 0,999 fractile, approximating a three-hour storm extreme.

The results show dependence on the choice of wave kinematics differing with wave height.

Table TR.6.4.2.2-2 — Scaling factor γ_d on loads to comply with Airy Wheeler in irregular seas[6-10]

		Airy Wheeler	Airy No stretch	Airy Constant	Stokes' Fifth
BASE SHEAR					
Stochastic irregular seas		1,00	1,03	0,83	-
Deterministic regular waves	a	0,79	0,84	0,69	0,66
	b	0,66	0,69	0,56	0,66
	c	0,71	0,75	0,61	0,66
	d	—	—	—	0,92
OVERTURNING MOMENT					
Stochastic irregular seas		1,00	1,10	0,79	—
Deterministic regular waves	a	0,81	0,93	0,69	0,66
	b	0,67	0,76	0,56	0,66
	c	0,72	0,83	0,61	0,66
	d	—	—	—	0,93
Water depth 110 m, H_s = 13,0m, T_p = T_{ass} = 17,0 s, uniform current V = 0,4 m/s. Wheeler stretching basis for normalized results, i.e. Airy Wheeler stochastic load = γ_d (other load).					
a H_{max} = 1,86H_s. b Crest as Stokes. c H_{max} = 1,86H_s × 1,07 except Stokes. d H_{max} = 1,60H_s (see Reference [5]).					

TR.6.4.2.4 Wave crest elevation

Wave crest elevations are specified in ISO 19905-1 with the intention of determining minimum hull elevation and airgap to avoid storm waves impinging on the jack-up hull; see ISO 19905-1:2012, A.6.4.2.4 and 13.6.

TR.6.4.2.5 Wave spectrum

In Reference [5] the wave spectrum is represented by the power density of wave surface elevation $S_{\eta\eta}(f)$ as a function of wave frequency by:

$$S_{\eta\eta}(f) = [16I_0(\gamma)]^{-1}H_s^2T_p(T_pf)^{-5}\exp[-1{,}25/(T_pf)^4]\gamma^q \quad \text{(TR.6.4-3)}$$

where

q = $\exp[-(T_pf - 1)^2/2\sigma^2]$ with:

σ = 0,07 for $T_pf <= 1{,}0$;

σ = 0,09 for $T_pf > 1{,}0$; (Carter 1982, ISO 19905-1:2012, Reference [A.6.4-4])

and

H_s is the significant wave height (meters), including depth correction, according to TR.6.4.2.6;

T_p is the peak period (seconds);

f is the frequency (hertz);

γ is the peak enhancement factor;

$I_0(\gamma)$ is discussed below.

The above definition yields a single-parameter Pierson-Moskowitz spectrum when γ = 1 and $T_p = 5\sqrt{(H_s)}$, with H_s in meters. In this case an appropriate T_p/T_z ratio is 1,406 (see below).

When considering a JONSWAP spectrum, the peak enhancement factor γ varies between 1 and 7 with a most probable average value of 3,3. There is no firm relationship between γ, H_s and T_p. Relationships between variables for different values of γ according to Carter (1982), ISO 19905-1:2012, Reference [A.6.4-4], are as follows (see also ISO 19905-1:2012, A.6.4.2.7):

γ	$I_0(\gamma)$	T_p/T_z
1	0,200	1,406
2	0,249	1,339
3	0,293	1,295
3,3	0,305	1,286
4	0,334	1,260
5	0,372	1,241
6	0,410	1,221
7	0,446	1,205

Alternatively:

$$\left[I_0(\gamma) = \frac{0{,}2}{1 - 0{,}287 \mathrm{Ln}\ (\gamma)} \right]$$

A comparison wave of spectra calculated according to ISO 19901-1:2005, A.8.6, and those calculated according to the SNAME T&R Bulletin 5-5A formulation is shown in Figure TR.6.4.2.5-1. The comparison shows equivalence between the calculated spectra.

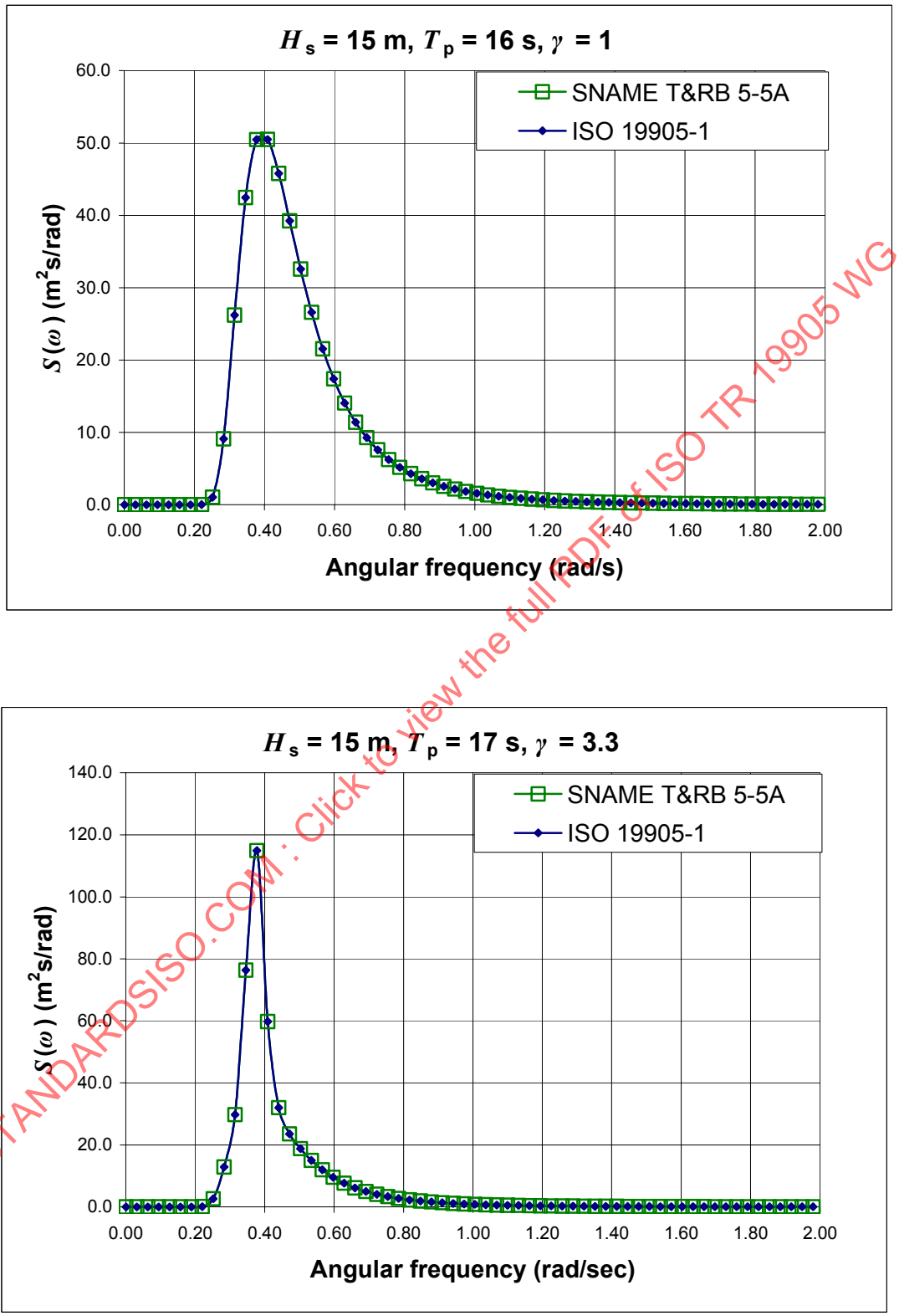

Figure TR.6.4.2.5-1 — Comparison of ISO 19901-1 and SNAME T&R 5-5A wave spectrum formulations

The following alternative, and rather restrictive, representation of the wave spectrum by the power density of wave surface elevation $S_{\eta\eta}(f)$ as a function of wave frequency may be used:

$$S_{\eta\eta}(f) = \alpha g^2(2\pi)^{-4}(f)^{-5}\exp[-1{,}25/(T_p f)^4]\gamma^q \quad \text{(TR.6.4-4)}$$

where

α is the equilibrium range parameter = $0{,}036 - 0{,}005\,6 T_p/\sqrt{H_{m0}^2}$

g is the acceleration due to gravity

q = $\exp[-(T_p f - 1)^2/2\sigma^2]$

σ is the spectral peakwidth parameter = 0,07 for $T_p f \leq 1$

= 0,09 for $T_p f > 1$

H_{m0} is the estimate of H_s significant wave height (m)

T_p is the spectral peak period (s)

f is the frequency (Hz)

γ is the peak enhancement factor

= $\exp[1/0{,}287(1-0{,}197\,5\alpha T_p^4/H_{m0}^2)]$

The above definition yields a Pierson-Moskowitz spectrum when γ = 1,0 and $T_p = 5\sqrt{(H_s)}$, with T_p in seconds and H_s in meters.

TR.6.4.2.6 Airy wave height correction for stochastic analysis

Airy theory may be applicable together with a stochastic irregular seas analysis, and in ISO 19905-1:2012, A.7.3.3.3.2, the Wheeler stretching is recommended for describing the kinematics to the instantaneous surface.

It is accepted that the increasing asymmetry described by higher order theories such as Stokes is appropriate. The asymmetry can also be seen in recorded data as skewness of the waves, as shown in Figure TR.6.4.2.6-1. Since Airy theory has certain limitations, a practical way to compensate for the asymmetry is to increase the significant wave height used as input to the force computations. In order to show that a scaling of significant wave height is appropriate, and to determine the absolute values of the scaling factors, one needs to decide which theory is correct at a given wave condition. Based on the good fit to test results in wave tank measurements[6-5], the Wheeler stretching is found to be a best fit. However, due to the asymmetry of wind-generated ocean waves in shallow water, this agreement is judged to be valid only for large water depths. In Reference [6-6] it is also indicated that a higher peak than trough is appropriate.

Here it is assumed that the significant wave height should have a scaling factor close to 1,0 for Wheeler stretching at water depths equal to or greater than 110 m using irregular wave analysis. At shallower water depths a scaling factor in excess of 1,0 should be due to the wave asymmetry.

In Reference [6-7], a scaling of wave crests is suggested based on the Stokes wave profiles. Comparisons are made both with data for North Sea conditions (d = 70 m) (see also Figure TR.6.4.2.6-1) and shallow waters ($d \approx$ 5,0 m) in the Baltic Sea, implying that this may be a general model. A correction proportional to wave steepness is deduced which shows fair agreement with the data.

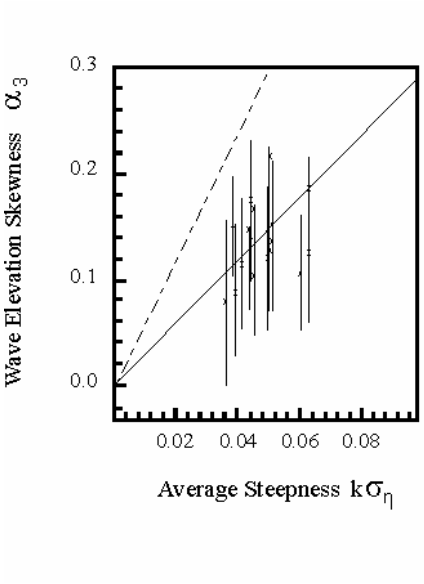

Tp(s)	<1	7-8	8-9	9-10	10-11	11-12	12-13	13-14	14-15
Hs (m) <2	0.076 2.996 1021								
2-3	0.105 2.974 194	0.102 2.966 61	0.107 2.671 1						
3-4		0.121 3.001 43	0.118 3.007 59	0.088 2.912 11					
4-5			0.184 2.991 3	0.147 3.001 33	0.111 2.912 11				
5-6				0.194 2.674 1	0.135 3.021 20	0.148 2.934 9			
6-7						0.126 2.936 3	0.174 2.978 7	0.148 3.018 2	
7-8							0.209 2.875 2	0.141 3.086 3	
8-9								0.168 3.096 1	
9-10									0.256 2.548 1

Figure TR.6.4.2.6-1 — Comparison of wave crest elevation predicted skewness and observed data at 70 m in the North Sea[6-7]

The crest height correction formula may be simplified, neglecting the higher order terms[6-7], to be:

$$\eta_s/\eta \approx 1{,}0 + 0{,}6\alpha_3 + 0{,}5(\alpha_4 - 3) \qquad \text{(TR.6.4-5)}$$

where

η_s is the crest elevation by Stokes

η is the crest elevation by Airy

α_3 = $2{,}5D_2\, H_s / T_p^2$, $\alpha_4 - 3 \approx (1{,}6\alpha_3)^2$: Skewness & kurtosis relations

D_2 = coth (kd) [1 + 3/(2sinh$^2(kd)$)] : Depth attenuation

k = $(2\pi/T)^2/g$: Wave number

The data and the model indicate that the skewness, α_3, is about 0,08 to 0,2 for large seastates at 70 m water depths giving a correction of 1,05 to 1,12 on the crest height compared with a linear model. The forces on a jack-up structure increase proportionally as the square (or more) of the elevation. Applying a correction for the square of the bias in wave crest, the correction for 70m should be in the range 1,10 to 1,25, depending on wave steepness.

By combining the above suggested formulae, a correction for the Wheeler stretching in a stochastic analysis may be deduced as:

$$H_s = 1{,}0 + 1{,}5D_2\, H_{srp} / T_p^2 \qquad \text{(TR.6.4-6)}$$

The D_2 factor includes a dependence on the wave number for individual waves. This is not suitable for the purpose of inclusion in ISO 19905-1, since there is no unique wave number for a seastate.

The elevation is not the only parameter to be considered; others are as follows:

— the depth attenuation over water depth;

— the profiles are not similar in horizontal directions;

— forces at some distance lose correlation.

This gives a different scaling to that deduced from the wave crest height only.

Based on the above a significant wave height for stochastic/irregular wave analysis using Airy waves and Wheeler stretching is recommended as:

$$H_s = [1 + (10H_s/T_p^2)e^{(-d/25)}]H_{srp} \quad \text{(TR.6.4-7)}$$

This removes the direct link to the Stokes profile as suggested in Reference [6-7], but contains the linear dependence on steepness and a depth dependence with an exponential decay.

A similar scaling on wave height for Airy/Wheeler stretching is currently being applied indirectly in design specifications[6-8] where it is stated that the wave heights according to Airy should be two times the peak amplitude predicted by the Stokes wave profile.

The above scaling is an approximation. It would be more correct to account for the wave asymmetry directly in the generation of the sea surface elevation by, for example, the methods indicated in Reference [6-7]. The significant wave height H_{srp} could then be applied directly.

Scaling for other stretching techniques combined with Airy waves may be deduced for stochastic, irregular waves and based on computational comparisons for different wave heights and water depths. However, this will not give exactly the same force profile over the leg and discrepancies in force prediction will occur. Such scaling is therefore not included in ISO 19905-1.

For computational comparisons using this wave height scaling, see also Appendix TR.7.B.

TR.6.4.2.8 Short-crested stochastic waves

TR.6.4.2.8.1 Directional spreading functions according to SNAME

According to SNAME T&R Bulletin 5-5A, subclause 3.5.4, the directional spreading may, in the absence of more reliable data, be taken as

$$F(\alpha) = C \cdot \left[\cos(\alpha)\right]^{2m} \quad \text{for } -\frac{\pi}{2} \le \alpha \le \frac{\alpha}{2} \quad \text{(TR.6.4-9)}$$

where

m is the power constant

C is a constant chosen such that $\int_{-\pi/2}^{\pi/2} F(\alpha) \cdot d\alpha = 1{,}0$

The power constant should normally not be taken as less than

m = 2,0 for fatigue analysis

m = 4,0 for extreme analysis

The above provides a formulation which may be used to incorporate the effects of wave spreading in the analysis. The power constants recommended[6-9] imply that the extreme seastate is close to long-crested, and that there is therefore little angular distribution of wave energy about the mean direction.

It should be noted that where significant spreading exists, it may be non-conservative to assume a long-crested sea.

In Reference [6-3] a reduction formula is suggested which reduces the velocity by a factor "primarily accounting for wave spreading":

$u_{red}/u = \sqrt{[(2m + 1)/(2m + 2)]}$ (TR.6.4-10)

where

u_{red} is the reduced horizontal velocity;

u is the computed velocity for long-crested waves;

m is the exponent in the $\cos^{2m}\theta$ spreading function at T_p.

For a range of the spreading exponent, $2 < m < 3$, the range of the scaling is:

$0{,}91 < u_{red} / u < 0{,}94$

This corresponds to a reduction of the forces by a factor ranging from 0,833 to 0,875. To use such a spreading factor in reducing overall forces on a structure is debatable, and especially so for jack-up structures. There may be cases where the inclusion of the spreading in irregular seas results in higher forces for some headings. If the leg spacing corresponds to a wave period, inducing opposing wave forces for different legs coinciding with the first resonance period, the forces will in fact be amplified when spreading is included. For jack-ups where the resonance period may often be as high as 4 s to 7 s, the effect of wave spreading is believed to reduce forces. However, the size of the reduction is dependent on the structure. See ISO 19905-1:2012, Reference [A.6.4-1], for a thorough discussion on inclusion of wave spreading and resulting effects on wave loads and dynamics of jack-ups.

TR.6.4.2.8.2 Directional spreading functions according to ISO 19901-1

In ISO 19901-1:2005, A.8.7.1, the directional spreading function $D(\theta)$ is described with alternative symmetric functions around the mean direction $\bar{\theta}$. In the absence of information to the contrary, the mean wave direction can be assumed to coincide with the mean wind direction. The three expressions for $D(\theta)$ are:

$$D_1(\theta) = C_1(n)\cdot\left[\cos\left(\theta-\bar{\theta}\right)\right]^n \quad \text{for} \quad -\frac{1}{2}\pi \le \left(\theta-\bar{\theta}\right) \le +\frac{1}{2}\pi \qquad \text{(TR.6.4-11)}$$

$$D_2(\theta) = C_2(s)\cdot\left[\cos\left(\frac{\theta-\bar{\theta}}{2}\right)\right]^{2s} \quad \text{for} \quad -\pi \le \left(\theta-\bar{\theta}\right) \le +\pi \qquad \text{(TR.6.4-12)}$$

$$D_3(\theta) = C_3(\sigma)\cdot\frac{1}{\sigma\sqrt{2\pi}}\cdot\exp\left[-\frac{\left(\theta-\bar{\theta}\right)^2}{2\sigma^2}\right] \quad \text{for} \quad -\frac{1}{2}\pi \le \left(\theta-\bar{\theta}\right) \le +\frac{1}{2}\pi \qquad \text{(TR.6.4-13)}$$

$$D_1(\theta) = D_2(\theta) = D_3(\theta) = 0 \quad \text{for all other } \left(\theta-\bar{\theta}\right) \qquad \text{(TR.6.4-14)}$$

where

$$C_1(n) = \frac{\Gamma(n/2+1)}{\sqrt{\pi}\,\Gamma(n/2+1/2)}$$

$$C_2(s) = \frac{\Gamma(s+1)}{2\sqrt{\pi}\,\Gamma(s+1/2)}$$

$$C_3(\sigma) = 1$$

The functions all have a peak at $\theta = \bar{\theta}$, the sharpness of which depends on the exponent n in $D_1(\theta)$ or s in $D_2(\theta)$, or the standard deviation of the normal distribution $D_3(\theta)$. The coefficients C are normalizing factors dependent on n, s or σ, which are determined such that the integral of $D(\theta)$ over all θ is equal to 1,0.

In engineering applications,

$D_1(\theta)$ is often used with n = 2 to n = 4 for wind seas, and n = 6 or higher for swells,

$D_2(\theta)$ may be used with typical values s = 6 to 15 for wind seas, and s = 15 to 75 for swells.

TR.6.4.2.8.3 Comparison of directional spreading functions in SNAME T&R Bulletin 5-5A and ISO 19901-1

The curves in Figure TR.6.4.2.8.3-1 show parameter values in the directional spreading functions in ISO 19901-1 giving a directional spreading function that is equivalent to the SNAME formulation, with values of the parameter m along the horizontal axis.

Directional spreading functions for $F(\alpha)$ with m = 4, $D_1(\theta)$ with n = 8, $D_2(\theta)$ with s = 15, and $D_3(\theta)$ with σ = 0,34 are shown in Figure TR.6.4.2.8.3-2.

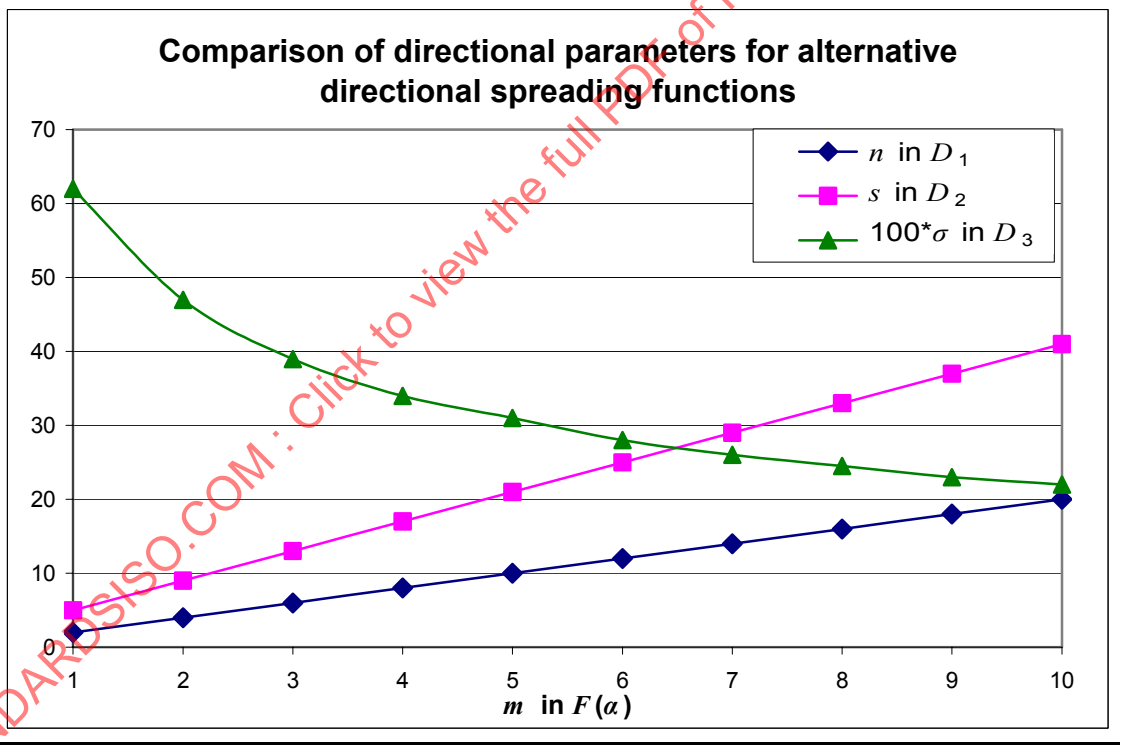

Figure TR.6.4.2.8.3-1 — Comparison of parameters for ISO 19901-1 and SNAME T&R Bulletin 5-5A directional spreading functions

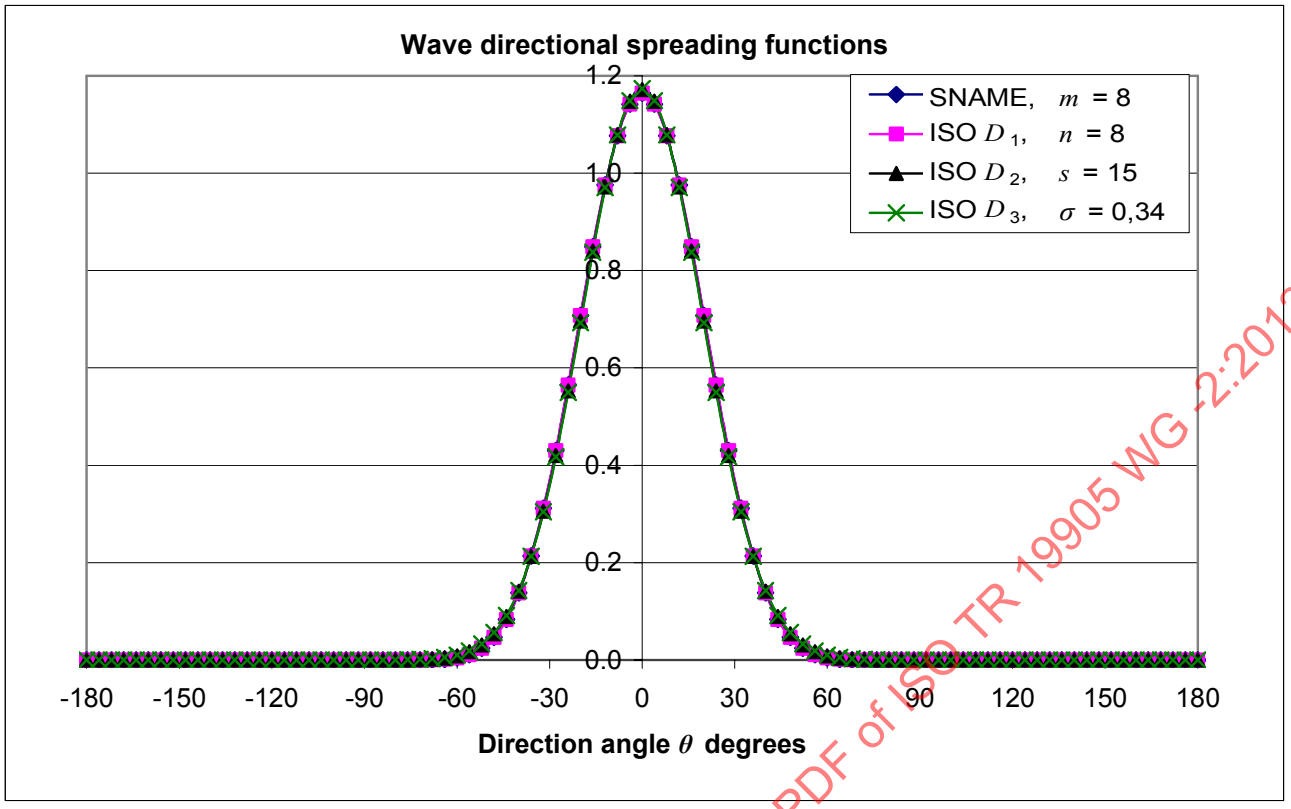

Figure TR.6.4.2.8.3-2 — Comparison of directional spreading functions

TR.6.4.3 Current

According to ISO 19901-1:2005, A.9.3, a power law current profile can be used where appropriate, e.g. in areas dominated by tidal current in shallow waters such as the southern North Sea. The power law exponent is typically 1/7, and stretching of the current profile to the wave crests and troughs when combining with waves is advised.

The profile in ISO 19905-1:2012, A.6.4.3, with constant tidal and surge current speed profile, with addition of linear varying wind-driven current can be applied as a simple and slightly conservative estimate of the current profile. This profile is used as part of the SNAME recipe for jack-up site assessment.

The base shear and overturning moment calculated using the ISO 19901-1 power law profile for tidal current, combined with linear varying wind-driven current have been compared with formulations in ISO 19905-1:2012, A.6.4.3 for a tidal current speed of 1 m/s at sea level and a wind-driven current of 0,3 m/s. The water depth is taken as 100 m. The comparison shows that the base shear is 27 % higher and the overturning moment 13 % higher for the ISO 19905-1:2012, A.6.4.3 formulation than for the ISO 19901-1 power law profile.

Calculations with the above current combined with a wave with a height of 24,3 m and period of 14,7 s, and with stretching of the current and wave profiles to the instantaneous water level, gives a maximum base shear which is 5 % higher and a maximum overturning moment which is 2,3 % higher for the ISO 19905-1:2012, A.6.4.3 formulation than for the ISO 19901-1 power law profile.

Typically, the combined effect current and waves for the ISO 19905-1:2012, A.6.4.3 recipe may be up to 8 % to 10 % on the conservative side compared to the ISO 19901-1 power law profile.

TR.6.4.4 Water depths

ISO 19905-1 references water depths to the lowest astronomical tide (LAT). In some instances the water depth may be referenced to Chart Datum. It is modern practice for these reference levels in hydrographic

surveys to be the same, however caution should be exercised when using older data or navigation charts and the relation of Chart Datum to LAT should be checked and any necessary corrections applied.

See also ISO 19905-1:2012, A.6.4.2.4 regarding wave heights for airgap determination.

TR.6.4.5 Wind

TR.6.4.5.1 General

ISO 19901-1:2005, A.7.3, specifies a logarithmic function for the vertical variation of the mean wind speed. It is also noted in ISO 19901-1:2005, A.7.3 that the logarithmic equations may be approximated by a power law.

In the ISO 19901-1 equations, the wind speed as function of averaging time and height above mean sea level is defined based on a reference wind speed for an averaging period of 1 h and at 10 m height above mean sea level. From these equations, the following expression for conversion of reference wind speed between different averaging periods at 10 m height above mean sea level can be developed:

$$U_{w,T}(10) = [1 - 0{,}024\ 6 \ln(T / 3\ 600)]\ U_{w0} - 0{,}001\ 058 \ln(T / 3\ 600)\ U_{w0}^2 \quad \text{(TR.6.4-15)}$$

where

$U_{w,T}(10)$ is the sustained wind speed at 10 m height above mean sea level, averaged over a time interval $T < 3\ 600$ s;

U_{w0} is the 1 h sustained wind speed at the reference elevation 10 m above mean sea level and is the standard reference speed for sustained winds;

T is the time averaging interval with $T < T_0 = 3\ 600$ s;

T_0 is the standard reference time averaging interval for wind speed of 1 h = 3 600 s

In case the reference wind speed needed for a 1 min average and the average time for the given wind speed is different from 1 h, e.g. 10 min, the above equation should first be solved to get the 1 h average wind speed. Thereafter the 1 min reference wind speed can be calculated from the equation based on the 1 h average speed.

A comparison of different reference wind speeds as function of the 1 h average speed is shown in Figure TR.6.4.5-1.

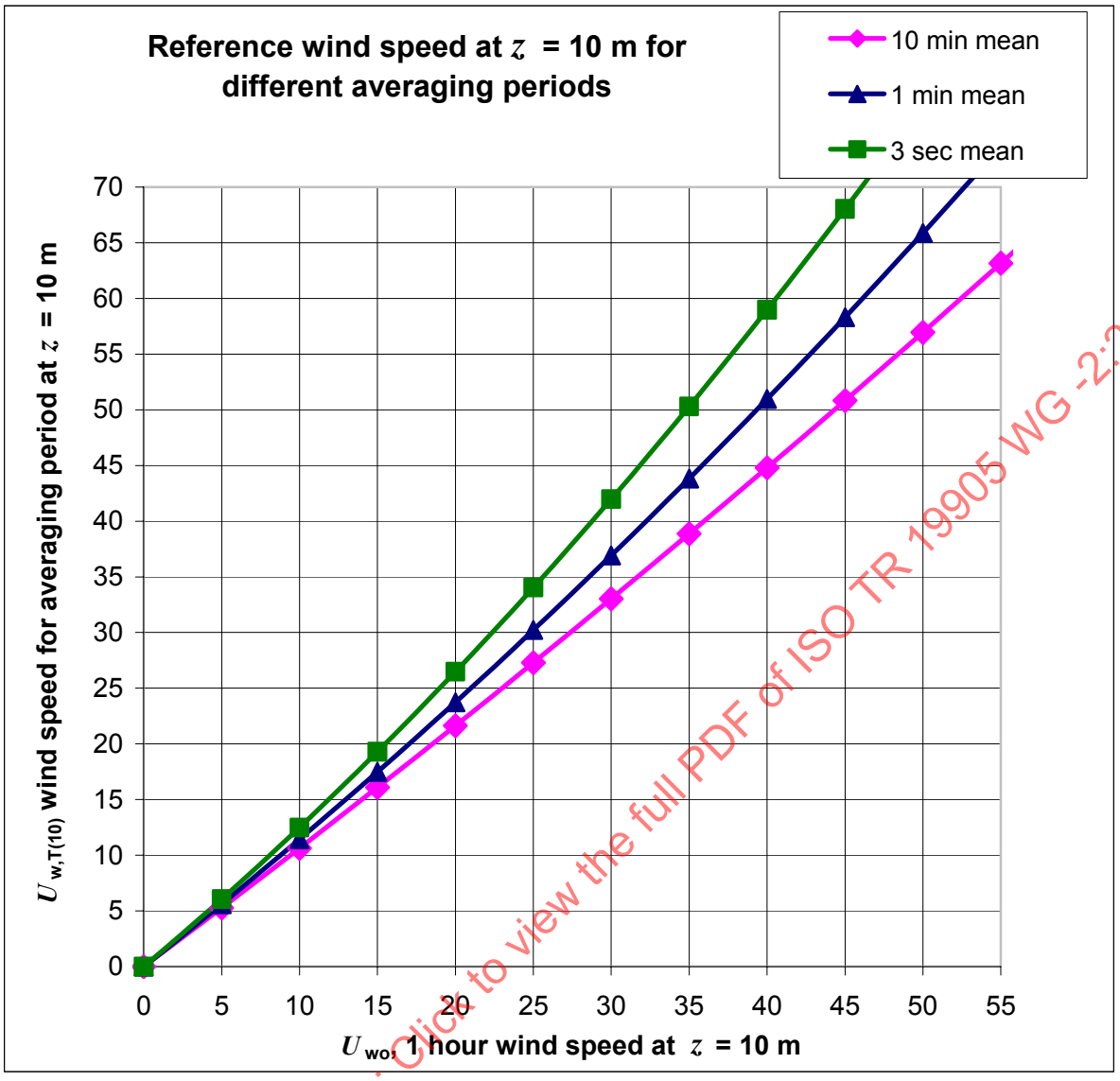

Figure TR.6.4.5-1 — Reference wind speed at z = 10 m for different averaging periods

In ISO 19905-1 the vertical variation of the wind speed may be approximated by a power law based on the 1 min sustained wind for determining the wind loadings on the jack-up.

The effect of the power law approximation compared to the logarithmic formulations of ISO 19901-1 is illustrated in Figure TR.6.4.5-2 and Figure TR.6.4.5-3. Comparisons are made for different values of the 1 min average wind speed at 10 m above mean sea level. It is seen that the power law approximation is slightly on the conservative side. For the most relevant heights, i.e. 20 m to 50 m above sea level, it is seen that the average effect is in the range of 7 % for the 1 min average wind speed at 10 m above sea level, equal to 20 m/s, and 2 % for the 1 min average wind speed at 10 m above sea level, equal to 40 m/s.

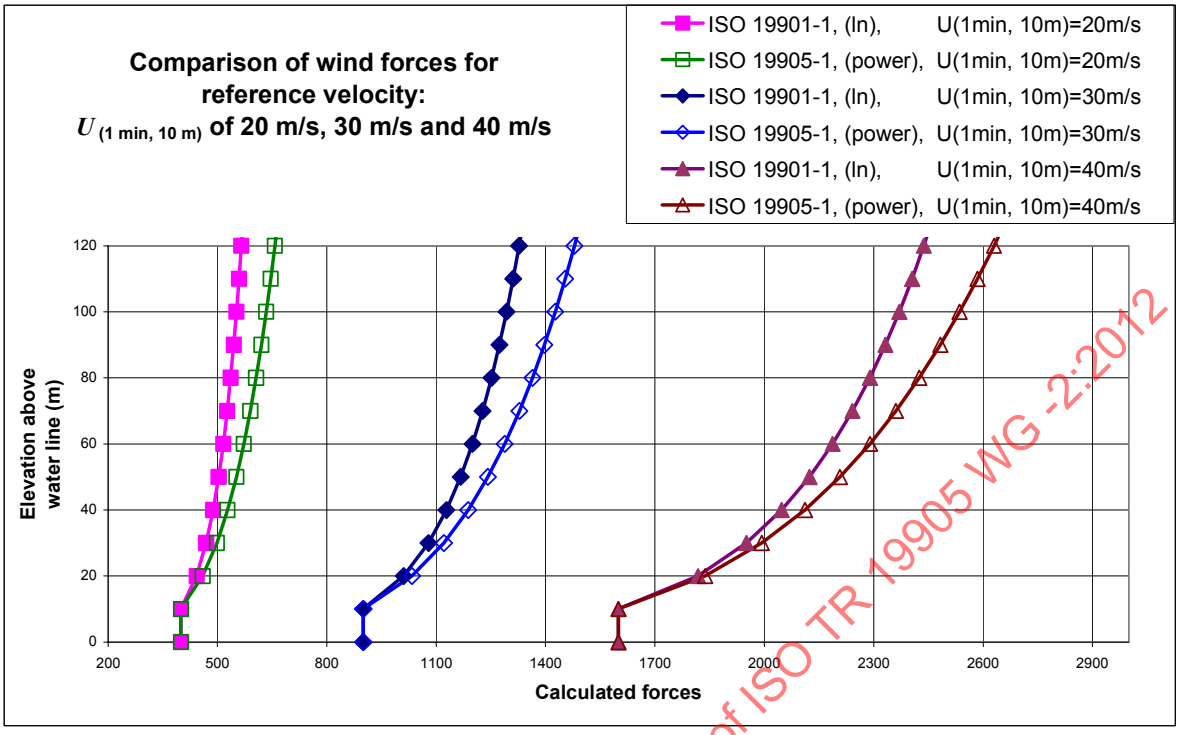

Figure TR.6.4.5-2 — Comparison of wind forces for different $U_{(1min,10m)}$ reference velocities

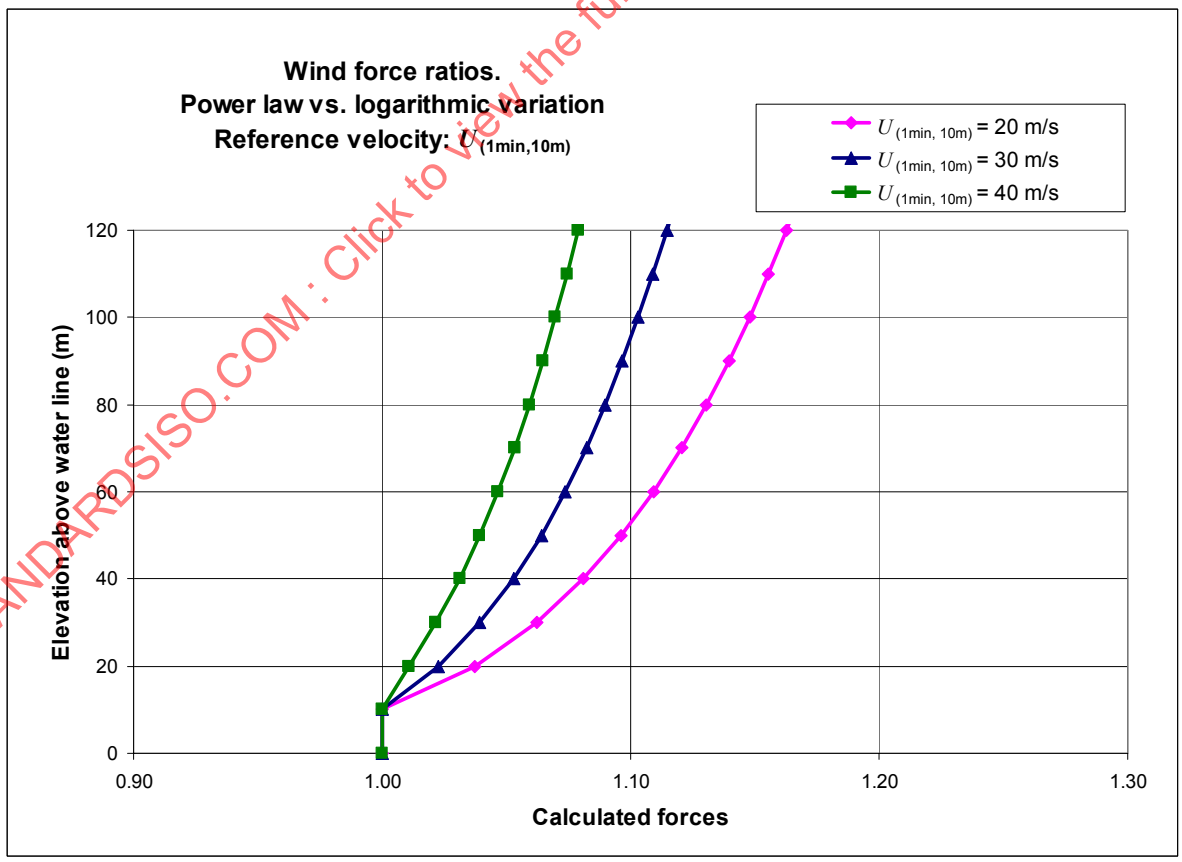

Figure TR.6.4.5-3 — Wind force ratios of power law vs. logarithmic variation for different $U_{(1min,10m)}$ reference velocities

7 Commentary to ISO 19905-1:2012, Clauses 7 and A.7

TR.7.1 Scope

The main objective of Clause 7 is to provide documentation of the numbers, methods and formulations of ISO 19905-1:2012, A.7.

Clause 7 is limited to considering wind loading on legs and hulls and hydrodynamic forces acting on the legs and appurtenances under the action of waves and current. Typical jack-up leg designs consist of legs with an open lattice frame structure with typical member dimensions of 0,25 m to 1,0 m in diameter, although some may be composed of larger diameter tubular legs. A special feature of most jack-ups is the racks fitted to the chord elements for jacking purposes. The fact that jack-ups are mobile limits marine growth build-up generally, except when jack-ups are deployed in long-term assignments (see ISO 19905-1:2012, Clause 11).

The models, methods and coefficients for computing the forces were considered together in the development of ISO 19905-1:2012, A.7, and represent a consistent method such that the whole clause should be considered in its entirety. This means that no coefficients should be taken from this clause or ISO 19905-1:2012, A.7 unless the corresponding method is applied.

Clause 7 is organized such that the main subclauses have the same numbers as the corresponding subclause in ISO 19905-1. This means that subclause TR.7.2 in this report corresponds to ISO 19905 1:2012, A.7.2 and so on.

TR.7.3.2 Hydrodynamic model

TR.7.3.2.1 General

The hydrodynamic modelling of the leg of a jack-up can be carried out by utilizing either “detailed” or “equivalent” techniques. In both cases the geometric orientation of the elements are accounted for. The hydrodynamic properties are then found as described here.

TR.7.3.2.1.1 Length of members

Lengths of members are normally to be taken as the node-to-node distance of the members, in order to account for small non-structural items.

TR.7.3.2.1.2 Spudcan

A criteria for considering the spudcan is suggested such that the effect of the wave and current forces on the spudcan may normally be neglected at deep water or deep penetrations. However, there may be special cases, e.g. with large spudcans in combination with high currents, that should be considered also outside the suggested criteria.

TR.7.3.2.1.3 Shielding and solidification

Shielding is normally neglected for computations of the hydrodynamic model as presented herein. The shielding is dependent on KC- and Re-numbers. Since it is difficult to quantify shielding, and shielding in waves is less than in constant flow[7-1],[7-2], shielding is neglected. The same criteria are used for solidification as for shielding such that both effects should be considered if advantage is taken due to shielding in wave and current loads.

According to Reference [7-3], shielding should be neglected for $S/D \leq 4$ for an array of elements, where S is the outer diameter of the array and D is the diameter of individual elements. This is also considered in Reference [7-1].

If information on shielding is obtained from experiments, care should be taken to distinguish between shielding and the effect discussed in ISO 19905-1:2012, A.7.3.3.4. These effects are different but could possibly be confused in tests on small models in large tanks.

Solidification is an increase of wave forces due to interference from objects "side by side" in the flow field. This is normally not included in the hydrodynamic coefficient formulation for jack-ups since shielding is also neglected. Jack-up rigs are usually space frame structures with few parallel elements in close proximity so that this effect is usually not important.

In Reference [7-1] solidification effects are quantified for two elements and for a group of elements. The drag coefficient may increase 100 % if two tubulars are placed side by side, or be reduced for a group of elements, e.g. a conductor array, where shielding is also present.

The effect is less than 10 % in the worst direction and it is therefore suggested that it be omitted in ISO 19905-1, when:

$$A_s/A_t < 0{,}5 \qquad \text{(TR.7.3-1)}$$

where

A_s is the sum of projected areas for all members in the considered plane;

A_t is the total projected envelope area of the considered plane.

Solidification should be considered if shielding is included.

TR.7.3.2.2 "Detailed" leg model

All relevant members are modelled with their own unique descriptions for the Morison term values and with correct orientation to determine v_n , $\dot{u}_n$ and $\ddot{r}_n$ and the corresponding drag coefficient times diameter $C_D D = C_{Di} D_i$ and inertia coefficient times sectional area $C_M A = C_{mi} \pi D_i^2/4$, as defined in ISO 19905-1:2012, A.7.3.2.4.

TR.7.3.2.3 "Equivalent" leg model

The hydrodynamic model of a bay is comprised of one "equivalent" vertical tubular to be located at the geometric centre of the actual leg. The corresponding (horizontal) v_n , $\dot{u}_n$ and $\ddot{r}_n$ are to be applied with equivalent $C_D D = \sum C_{De} D_e$ and $C_M A = \sum C_{Me} A_e$, given in ISO 19905-1:2012, A.7.3.2.3. The model should be varied with elevation, as necessary, to account for changes in dimensions, marine growth thickness, etc.

TR.7.3.2.3.1 Equivalent drag coefficient

In order to comprise the information on drag forces for individual members of a lattice leg into an equivalent vertical member over the bay length s, a fixed diameter and a directional dependent drag coefficient is specified. This model accounts for the geometrical orientation of the individual members. In this model the principle of no shielding and no blockage is assumed.

The equivalent diameter is recommended such that the inertia coefficient normally follows without any further computations. The equivalent value of the drag coefficient, C_{De}, times the equivalent diameter, D_e, is specified. If another reference diameter D_e is preferred, the product of $C_{De} D_e$ should in any case be equal to that specified in ISO 19905-1:2012, A.7.3.2.3. The expression for C_{Dei} may be simplified for horizontal and vertical members as follows:

— vertical member (e.g. a chord) : $C_{Dei} = C_{Di} (D_i/D_e)$ (TR.7.3-2)

— horizontal member : $C_{Dei} = \sin^3 \alpha_i \; C_{Di} (D_i l_i / D_e s)$ (TR.7.3-3)

TR.7.3.2.3.2 Equivalent inertia coefficient

The equivalent value of the inertia coefficient, C_{Me}, and the equivalent area, A_e, to be used in ISO 19905-1:2012, A.7.3.3.2, represent the C_{MA} chosen as:

C_{Me} may normally be taken as equal to 2,0 when using A_e

= 1,0 for flat plates (brackets);

A_e is the equivalent area of leg per unit height = $(\Sigma A_i l_i)/s$;

A_i is the equivalent area of element = $\pi D_i^2/4$;

D_i is the reference diameter as defined in ISO 19905-1:2012, A.7.3.2.4.

The reference diameters D_i and corresponding area of member A_e are chosen such that the use of an inertia coefficient C_{Me} = 2,0 or C_{Me} = 1,0 is consistent with the inertia forces for chords and brackets respectively. A conservatism is present since the inertia coefficient for rough tubulars is set to 1,8 and there is no reduction of forces for inclined members. For normal lattice leg designs the conservatism will not play any significant role as the drag forces are dominant. The inertia force will also be dominated by chords due to their larger diameter, such that the conservatism is judged to be insignificant for extreme wave forces.

If, however, a more accurate model is wanted, an alternative is given using the individual member inertia coefficients, as specified in ISO 19905-1:2012, A.7.3.2.4, and including the effect of inclined members. The equivalent inertia coefficient C_{Me} is then determined by the summation shown in ISO 19905-1:2012, A.7.3.2.3. This model is in closer agreement with the “detailed model”. It should be stressed that the coefficients must be defined together with their reference dimensions D_i.

As comments to this formulation the following may be observed:

— for horizontal members with flow along the length axis, the inertia coefficient is:

C_{Mei} = 1,0

— for a vertical rough tubular, the inertia coefficient will be:

C_{Mei} = 1,8

— for other vertical members, the inertia coefficient will be:

C_{Mei} = 2,0

— for other flat plates (brackets), the inertia coefficient will be:

C_{Mei} = 1,0

TR.7.3.2.4 Drag and inertia coefficients

TR.7.3.2.4.1 General

The coefficients determined herein are based on tests where the particle velocities and accelerations are measured simultaneously with the forces, usually in a controlled environment. This is the logical way to determine the loading coefficients. However, the important result in engineering is the overall forces predicted by the Morison's equation over the jack-up legs. Since some wave theory has to be applied, which does not perfectly predict the wave particle motions in all cases, additional scaling is suggested in ISO 19905-1:2012, A.6.4.2 (see also Appendix TR.7.B). This is important to consider when reading this chapter as the stated coefficients can differ from those applied in other recommendations or classification rules.

TR.7.3.2.4.2 Hydrodynamic coefficients for tubulars

TR.7.3.2.4.2.1 General

There exists a wealth of data on hydrodynamic coefficients (drag and inertia coefficients) for tubulars, mainly from model tests. A number of model tests have been performed in wind tunnels, others in oscillating water environments or in steady water flow, while (to our knowledge) only a few model tests have been performed in a wave environment. In addition, a few full-scale tests have been reported.

In the following section an overview is given of the literature that has been applied for the purpose of recommending values for the hydrodynamic coefficients of jack-up platforms.

Before choosing the appropriate hydrodynamic coefficients for tubular parts of jack-up platforms, the following questions have to be answered:

— Are the coefficients to be used for a fatigue analysis or an ultimate strength analysis?

— Are the tubular parts smooth or rough and, if they are rough, what is the roughness to be applied?

The parameters to be considered in determining the hydrodynamic coefficients are as follows:

Keulegan-Carpenter number $$KC = \frac{U_m T}{D} \quad \text{(TR.7.3-4)}$$

Reynolds number $$Re = \frac{UD}{\nu} \quad \text{(TR.7.3-5)}$$

Relative roughness $$= \frac{k}{D} \quad \text{(TR.7.3-6)}$$

where

k is the roughness height;

D is the diameter;

U_m is the maximum orbital particle velocity;

T is the wave period;

U is the flow velocity at the depth of the considered element;

ν is the kinematic viscosity of water ($\nu \approx 1{,}4 \times 10^{-6}$ m^2/s, t = 10°C).

Concerning the first question above, it is important to determine the range of Reynolds numbers and Keulegan-Carpenter numbers of interest. Both the drag coefficient C_D and the inertia coefficient C_M are dependent on the Reynolds number and the Keulegan-Carpenter number. In the ultimate strength case one is interested in the C_D and C_M coefficients in relatively long and steep waves, i.e. wave steepness $S = H_s/\lambda$ in the range 1/10-1/15. A typical ultimate strength case may be, for example, a tubular with diameter D = 0,3 m standing in a seastate with average zero-upcrossing period T_z = 10 s (λ = 156 m) and significant wave height H_s = 13,0 m. The representative water particle velocity for this wave will be:

$$U_W = \frac{H_s \pi}{T_z} = 4{,}1 \text{ m/s.}$$

Assuming a current velocity U_C of about 1,0 m/s, the total water particle velocity will be $U = U_W + U_C$ = 5,1 m/s. This results in the following Reynolds number and Keulegan-Carpenter numbers (close to the water surface):

$$Re = \frac{UD}{\nu} = 1{,}1 \times 10^6 \qquad KC = \frac{UT_z}{D} = 170$$

This means that in the ultimate strength case we are dealing with high KC-numbers and post-critical Re-numbers. Sarpkaya (see for example Reference [7-4]) uses a parameter $\beta = Re/KC$ to describe the test environment. In the ultimate strength environment described above, the value of β is approximately 6 500.

A typical fatigue case may, for example, be the same tubular in a seastate with T_z = 6 s. (λ = 56 m) and H_s = 5,6 m. In this case the representative water particle velocity will be $U_W = H_s\pi/T_z$ = 2,9 m/s. In the fatigue case, current is not part of the water particle velocity which is to be applied. This results in the following Reynolds number and Keulegan-Carpenter number (close to the water surface):

$$Re = 0{,}62 \times 10^6 \qquad KC = 58$$

This means that post-critical Re-numbers and relatively high KC-numbers are also to be dealt with in the fatigue case. Sarpkaya's β-parameter has a value β = 10 860 for the described fatigue case.

It may be concluded that, in general, for jack-up tubulars, the following ranges of Re-numbers and KC-numbers will be of interest:

— Re-numbers: ultimate strength, roughly from $Re \approx 1{,}0 \times 10^6$ to $4{,}5 \times 10^6$

fatigue, roughly from $Re \approx 0{,}5 \times 10^6$ to $1{,}0 \times 10^6$

— KC-numbers: ultimate strength, $KC > 100$

fatigue, $KC \approx$ 25 to 60

Since quite a large amount of the literature survey is dealing with papers written by Sarpkaya, the following range of Sarpkaya's β-parameter may be regarded to be of interest: $\beta \approx$ 6 000 to 20 000 (depending on the KC-number).

The answer to the second question concerning the roughness of the tubulars depends largely on the type of paint used and the smoothness of the steel surface, whether the tubular is new or has been in the water for quite some time (marine growth), or whether the tubular mainly stays in air, etc.

Smooth cylinders are defined as cylinders having a roughness of k/D < 0,000 1, while rough cylinders are assumed to have a roughness of k/D > 0,004 (i.e. highly rusted steel $k/D \approx$ 0,005 to 0,01). Marine roughness due to marine growth implies a roughness in the range $k/D \approx$ 0,01 to 0,15.

TR.7.3.2.4.2.2 Literature survey and recommended values

Table TR.7.3.2.4-1 presents the result of a survey of relevant literature with respect to inertia coefficients (C_M) and drag coefficients (C_D) for tubulars. Of course, there exists more relevant literature than that presented in Table TR.7.3.2.4-1, but it should give a reasonably representative overview.

Table TR.7.3.2.4-1 — Survey of relevant literature on C_M and C_D values for tubulars

Source	Geometric shape	Re-number	KC-number	C_D	C_M	Comments
Keulegan Carpenter 1958[7-5]	Smooth Cylinder	0,1-0,3 10^5 0,1 10^5	25-50 >100	1,3-1,5 1,0-1,2	1,3-1,8 2,4-2,6	Sub-Critical and Critical Flow. Low Re-numbers.
Sarpkaya 1976[7-6]	Smooth Cylinder	>0,5 10^6 >0,7 10^6	20-40 60-100	0,6-0,7 0,6-0,7	1,7-1,8 1,7-1,9	Post-Crit. Oscillating Flow.
Sand Roughened	Rough Cylinders k/D = 0,005 k/D = 0,01 k/D = 0,02	>0,5 10^6	20-40	1,5-1,7 1,6-1,8 1,7-1,9	1,2-1,4 1,2-1,4 1,1-1,3	Post-Crit. Oscillating Flow.
Sand Roughened	Rough Cylinders k/D = 0,005 k/D = 0,01 k/D = 0,02	>0,5 10^6	60-100	1,4-1,6 1,5-1,6 1,6-1,7	1,5-1,7 1,4-1,6 1,4-1,6	Post-Crit. Oscillating Flow.
Hogben et al. 1977[7-7] Survey Paper State of the Art	Smooth Cylinder Rough Cylinders k/D = 0,000 2 k/D = 0,002 k/D = 0,01 k/D = 0,05	>1,0 10^6 >1,0 10^6 >0,5 10^6 >0,5 10^6 >0,1 10^6	>25 >25 >25 >25 >25	≈0,6 0,6-0,7 ≈1,0 ≈1,0 ≈1,25	≈1,5	Post-Crit. Flow. Post-Crit. Flow.
Sarpkaya et al. 1982[7-4]	Smooth Cylinder Rough Cylinder k/D = 0,01	>0,1 10^6 >0,1 10^6	25-40 25-40	0,6-0,8 1,5-1,7	1,5-1,7 1,0-1,2	Critical - Super-Crit. Oscillating Flow. β = 4 000.
Sarpkaya et al. 1984[7-8]	Smooth Cylinder Rough Cylinder k/D = 0,01	≈0,1 10^6 ≈0,15 10^6 ≈0,1 10^6 ≈0,15 10^6	25-40 60 25-40 60	0,7-0,8 0,6-0,65 1,4-1,5 1,4-1,5	1,5-1,7 1,5-1,6 1,4-1,6 1,5-1,6	Critical - Super-Crit. Oscillating Flow. β = 2 500.
Sarpkaya et al. 1985[7-9]	Rough Cylinder k/D = 0,01	0,1-0,2 10^6 ≈0,21 10^6	25-40 50	1,4-1,5 1,4-1,5	1,0-1,3 1,2-1,3	Critical - Super-Crit. Oscillating Flow. β = 4 200.
According to Sarpkaya, available data with current and oscillatory flow substantiate the fact that drag coefficients obtained from tests at sea in general will be smaller than those obtained under laboratory conditions.						
Sarpkaya 1985[7-10]	Smooth Cylinder	0,2-0,3 10^6	20-25	0,6-0,7	1,6-1,8	Super-Crit. Oscillating Flow. β = 11 240.

Source	Geometric shape	Re-number	KC-number	C_D	C_M	Comments
Sarpkaya 1985[7-11], 1986[7-12], Survey Articles	Smooth Cylinder	>0,5 10^6 >0,5 10^6	25-40 >50	0,6-0,8 0,6-0,7	1,5-1,8 1,6-1,8	Post-Crit. Oscillating Flow.
	Rough Cylinder k/D = 0,02	>0,5 10^6 >0,5 10^6	25-40 >50	1,4-1,8 1,4-1,6	1,2-1,4 1,3-1,5	
Nath 1982[7-13]	Smooth Cylinder	≈0,5 10^6	∞	0,4-0,5		Super-Crit. Steady Flow.
	Rough Cylinder k/D = 0,02	≈0,5 10^6	∞	0,9-1,0		Post-Crit. Steady Flow.
	k/D >0,1	≈0,5 10^6	∞	1,0-1,2		
	Smooth Cylinder	0,15-0,2 10^6	15-25	0,3-0,6	0,8-1,4	Super-Crit. Oscillating Flow.
	Rough Cylinder k/D = 0,02	0,15-0,2 10^6	15-25	0,6-1,0	0,4-1,0	
	k/D >0,1	0,15-0,2 10^6	15-25	1,0-2,0	0,8-2,3	
There is very large scatter in the data presented by Nath.						
Bearman et al. 1985[7-14]	Smooth Cylinder	0,15-0,5 10^6	≈20	0,6-0,7	1,4-1,5	Super/Post-Crit. Flow, Regular Waves.
The authors present results for random waves as well, but it is difficult to draw any conclusion from these results.						
Kasahara et al. 1987[7-15]	Smooth Cylinder	0,5-1,0 10^6	20-40	0,5-0,6	1,6-1,8	Post-Crit. Oscillating Flow.
	Rough Cylinder k/D = 0,008 3	0,5-1,0 10^6	20-40 ≈50	1,1-1,4 1,1-1,2	1,3-1,7 1,6-2,3	Large Scatter in C_M-values.
	k/D = 0,004 2	0,5-1,0 10^6	20-40 ≈50	0,9-1,3 0,9-1,1	1,3-2,1 1,6-2,1	
Chaplin 1988[7-16]	Smooth Cylinder	≈0,2 10^6	≈20	0,6-0,7	1,4-1,5	Super/Post-Crit. Oscillating Flow.
Davies et al. 1990[7-17]	Smooth Cylinder	>0,5 10^6	≈20	0,6-0,7	1,5-1,6	Post-Crit. Flow, Reg. Waves.
	Smooth Cylinder	>0,5 10^6	≈18	0,5-0,7	1,5-1,7	Post-Crit. Flow. Random Waves.
The authors conclude that for smooth cylinders and KC > 4, drag and inertia coefficients in periodic waves may be used to represent average C_D and C_M values in random waves						

Source	Geometric shape	Re-number	KC-number	C_D	C_M	Comments
Rodenbusch et al. 1983[7-18]	Smooth Cylinder Rough Cylinder k/D = 0,02	>1,0 10^6 >1,0 10^6	∞ ∞	≈0,6 0,9-1,1		Post-Crit. Steady Flow (Steady Tow).
	Smooth Cylinder Rough Cylinder k/D = 0,02	>1,0 10^6 >1,0 10^6	>30 >30	0,6-0,7 1,4-1,5	1,6-1,7 1,1-1,3	Post-Crit. Oscillating Flow (Forced Motion).
	Smooth Cylinder Rough Cylinder k/D = 0,02	>1,0 10^6 >1,0 10^6	20-40 20-40	0,6-0,8 1,0-1,8	1,4-2,0 1,0-1,9	Post-Crit. Random Flow (Forced Motion).
	Smooth Cylinder Rough Cylinder k/D = 0,02	>1,0 10^6 >1,0 10^6	60-90 60-90	0,6-0,8 1,1-1,4	1,5-1,7 1,0-1,4	Post-Crit. Random Flow (Forced Motion).
The random tests show a relatively large spread, especially for the lower KC-numbers (20-40).						
Rodenbusch et al. 1986[7-19]	Smooth Cylinder Rough Cylinder k/D >0,000 5	>1,0 10^6 >0,5 10^6	>60 >60	0,65-0,75 1,1-1,3	1,5-1,7 1,1-1,5	Post-Crit. Random Flow (ForcedMotion).
Theophanatos et al. 1989[7-20]	Rough Cylinder k/D = 0,005 k/D = 0,0095 k/D = 0,025	>0,8 10^6		0,95-1,05 1,0-1,1 1,15-1,25	=>	Post-Crit. Steady Flow (Steady Tow). Sand Rough.
	k/D = 0,049 k/D = 0,098			1,15-1,25 1,3-1,4	=>	Pyramids
	k/D = 0,067			1,2-1,3	=>	Mussels
Klopman et al. 1990[7-21]	"Rough" Cylinder k/D = 0,000 12	≈0,5 10^6	≈15	0,6-0,9	1,3-1,6	Post-Crit. Random Waves.
Heideman et al. 1979[7-22]	Smooth Cylinder	>0,2 10^6 >0,2 10^6	15-30 >30	0,5-1,2 0,6-0,8	1,2-1,9	Post-Crit. Random Waves. Ocean Test Structure.
	Rough cylinder k/D ≈0,03-0,05	>0,2 10^6 >0,2 10^6	15-30 >30	0,9-1,8 0,8-1,3	0,9-1,7	
Large spread for lower KC-numbers (<30). Authors state that for large KC-numbers (>30), smooth cylinder C_D approaches an asymptote C_D = 0,68, while rough cylinder C_D approaches an asymptote C_D = 1,0. Tests performed in an ocean environment.						
Nath 1988[7-23]	Rough Cylinder Barnacles: k/D = 0,073 k/D = 0,104		∞ ∞	0,95 0,98-1,2		Post-Crit. Steady Flow. .

Source	Geometric shape	Re-number	KC-number	C_D	C_M	Comments
Wolfram & Theophanatos 1990[7-24]	Artificial Hard Fouling: k/D = 0,078		∞	0,98-1,2		Post-Crit. Steady Flow.
	Rough Cylinder Mussels: k/D = 0,075 k/D = 0,085		∞ ∞	1,22 1,26		Post-Crit. Steady Flow.
	Mixed Hard Fouling: k/D = 0,076		∞	1,11		
	Kelp: k/D = 1,25 k/D = 2,5		∞ ∞	1,51 1,69		
	Sea Anemones: k/D = 0,16		∞	1,35		
Roshko 1961[7-25]	Smooth Cylinder	>3,5 10^6	∞	0,65-0,75		Post-Crit. Steady Flow Wind Tunnel.
Miller 1976[7-26]	Smooth Cylinder	>3,0 10^6	∞	0,60-0,65		Post-Crit. Steady Flow Wind Tunnel.
	Rough Cylinder					
Sand Roughened	k/D = 0,000 4	>3,0 10^6	∞	≈0,80		Post-Crit. Steady Flow Wind Tunnel
	k/D = 0,000 9		∞	0,8-0,9		
	k/D = 0,001 4		∞	0,8-0,9		
	k/D = 0,002 1			0,9-1,0		
	k/D = 0,003 1			1,0-1,1		
	k/D = 0,005 0			1,0-1,1		
Pearl Barley	k/D = 0,015	>0,5 10^6		≈1,1		
	k/D = 0,023			≈1,1		
	k/D = 0,044			1,1-1,2		
Dried Peas	k/D = 0,042	>0,5 10^6		1,1-1,2		
	k/D = 0,063			1,2-1,4		
Pearcey et al. 1982[7-27]	Smooth Cylinder	>3,5 10^6	∞	≈0,6		Post-Crit. Steady Flow Wind Tunnel
	Rough Cylinder					
	k/D = 0,000 4	>2,0 10^6	∞	≈0,8		
	k/D = 0,001 4			≈0,88		
	k/D = 0,0028			≈0,92		

In addition to the literature review presented in Table TR.7.3.2.4-1, an interesting and useful overview of existing literature is presented in a survey report prepared by Advanced Mechanics Engineering Limited for the Health and Safety Executive[7-28].

The literature review presented in Table TR.7.3.2.4-1 shows that the test results at different facilities agree reasonably well with respect to the drag coefficients for smooth cylinders in post-critical flow. The majority of tests show C_D values between 0,6 and 0,7, both for the lower KC range for fatigue (25 to 60) and the higher KC range for ultimate strength. The suggested C_D value for smooth tubular elements (k/D < 0,000 1) in post-critical flow is therefore chosen to be C_D = 0,65.

For rough cylinders, the spread between the individual tests with respect to C_D values is considerably larger. Especially Sarpkaya[7-6] operates with very high post-critical C_D values for rough cylinders. It should be noted that none of the values obtained by the other authors referenced in Table TR.7.3.2.4-1 support the Sarpkaya values in the post-critical region. The differences between individual tests may partly be due to the different types of post-critical flow (different test conditions) and to the non-uniform definition of roughness used by the different authors.

One should also bear in mind that the wave particle velocities decrease with increasing depth below the water surface, which might mean a transition from the post-critical regime to the super-critical or even critical regime. This will result in a reduction in C_D values for smooth cylinders (although in the lower Re-number part of the critical regime it may result in an increase in C_D values, but here the water particle velocities are so low that the resulting contribution to the overall drag force will be significantly smaller than the contributions higher up on the cylinder). For rough cylinders the critical regime occurs at lower Re-numbers and there is no reduction in the drag coefficient in the super-critical regime. For large roughnesses an increase in the drag coefficient has in fact been reported in this regime[7-7],[7-35].

Based on the literature survey presented in Table TR.7.3.2.4-1 and the discussion above, the drag coefficient for rough cylinders (roughness k/D > 0,004) is chosen as equal to C_D = 1,0, both for the ultimate strength and the fatigue cases.

TR.7.3.2.4.2.3 Marine growth dependence

Rust and hard marine growth has been found to behave in essentially the same manner as artificial hard roughness, but a surface with hard marine growth behaves quite differently from a surface with soft marine growth. Another point of consideration is that different types of marine growth on a submerged tubular may dominate at different depths below the sea surface.

The use of anti-fouling coating will at least delay the development of marine growth but after a few years the anti-fouling coating becomes less effective. Regular cleaning of the tubulars is another possible way to limit the development of marine growth. In ISO 19905-1:2012, A.7.3.2, Table A.7.3-3, it is assumed that severe marine growth is not allowed. This is in accordance with the operational profile of mobile jack-up rigs, with cleaning of legs at intervals preventing severe marine growth.

The main contribution to forces is in the surface region, such that the extension of the marine growth below the surface zone is not important for the overall forces. The paint will in addition be somewhat roughened when exposed to the salt water for a longer period. Above the marine growth region, the use of values for a smooth cylinder has been recommended. This is mainly based on the fact that the marine growth will be limited to the region below MSL + 2 m, limiting the roughness above this region.

In addition, measurements also indicate that the wave forces in ocean waves are less than predicted by use of a constant C_D [7-30],[7-31]; see also Figure TR.7.3.2.4-1

Based on this, it is recommended that the value C_D for a smooth surface (C_D = 0,65) generally be used for the legs above MSL + 2 m and the value for a rough surface below MSL + 2 m (C_D = 1,0), as stated in ISO 19905-1:2012, Table A.7.3-2.

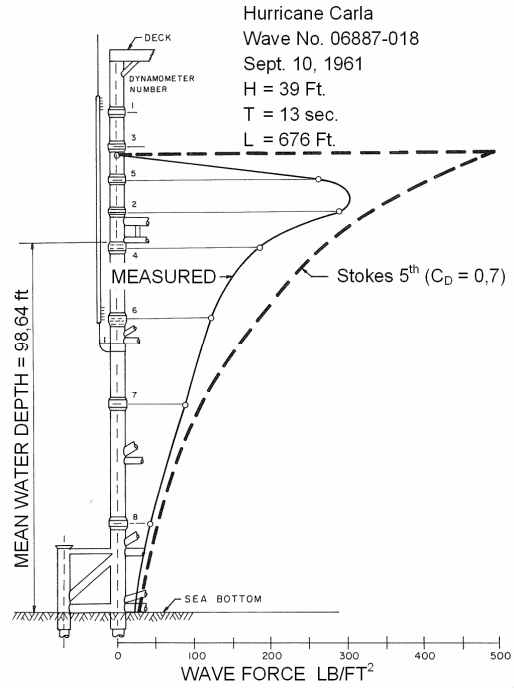

Figure 1 — TR.7.3.2.4-1 Comparison between measured and computed forces on a pile up to free surface[7-30],[7-31]

TR.7.3.2.4.2.4 Definition of relevant parameters

The drag coefficient (C_D) for tubulars may be considered as a function of roughness (k/D), Keulegan-Carpenter number (KC) and Reynolds number (Re) as an alternative to ISO 19905-1:2012, Table A.7.3-2. This explicit dependence is intended to be used in cases where there is more detailed knowledge, first of all on the roughness and in addition on the flow conditions around the members at a specific site. A definition of these governing parameters are included in subclause TR.7.3.2.4.2.

TR.7.3.2.4.2.5 Dependence on roughness

The roughness may be accounted for explicitly if the roughness is documented to be of an intermediate value compared with the smooth and rough k/D values assumed above. Recommended values for the roughness, k, may be found from Table TR.7.3.2.4-2.

Table TR.7.3.2.4-2 — Recommended roughness values for tubulars[7-1]

Surface	k (m)
Steel, new uncoated	5,0E-5
Steel, painted	5,0E-6
Steel, highly rusted	3,0E-3
Marine growth	5,0E-3 to 5,0E-2

Several authors have presented, in graphical form, the C_D dependence on the relative roughness k/D at post-critical Re-numbers. Figure TR.7.3.2.4-2 presents a graph from Miller[7-26], showing the variation of C_D with varying k/D based on several model experiments at post-critical Re-numbers. Figure TR.7.3.2.4-3 and Figure TR.7.3.2.4-4 show similar graphs presented by, respectively, Wolfram et al[7-24] and Pearcey et al[7-32]. Based on the available data with respect to the dependence of C_D on k/D, the expressions presented in Equation (TR.7.3-7) have been proposed to describe this dependence for the purposes of ISO 19905-1. The drag coefficient C_{Di} may then be obtained from Equation (TR.7.3-7):

$$C_{Di(k/D)} = \begin{cases} C_{Dsmooth} = 0{,}65 & ; \quad k/D < 0{,}000\,1 \\ C_{Dsmooth} = 0{,}65\left[2{,}36 + 0{,}34\,\log_{10}(k/D)\right] & ; \quad 0{,}000\,1 < k/D < 0{,}004 \\ C_{Drough} = 1{,}0 & ; \quad 0.004 < k/D \end{cases} \qquad \text{(TR.7.3-7)}$$

A graphic representation of Equation (TR.7.3-7) is shown in Figure TR.7.3.2.4-5. With respect to the inertia coefficients for smooth cylinders, all the references from Table TR.7.3.2.4-1 report post-critical C_M values lower than the asymptote C_M = 2,0. The C_M values lie mainly in the range 1,6 to 1,7. However, the question is whether (in general) some inertia contribution has been included in the drag forces used for the C_D determination. This would mean that the C_D values are slightly overestimated and the C_M values slightly underestimated. At the same time, since both fatigue and ultimate strength imply Keulegan-Carpenter numbers > 25, it is the drag dominated region which is of most interest and the chosen C_M values are not really critical. Based on this argument, the inertia coefficient for smooth cylinders in the post-critical regime is set equal to the asymptotic value C_M = 2,0.

The C_M values for rough cylinders, are in general reported to be slightly lower than the C_M values for smooth cylinders. Based on the same argument as used for the smooth cylinders, the inertia coefficient for rough cylinders in the post-critical regime is set equal to C_M = 1,8.

A summary of the recommended values for the hydrodynamic coefficients for tubulars is given in Table TR.7.3.2.4-3.

Table TR.7.3.2.4-3 — Recommended hydrodynamic coefficients for tubulars

Tubular	C_{Di}	C_{Mi}
Smooth (k/D<0,000 1)	0,65	2,0
Rough (k/D>0,004)	1,00	1,8
Intermediate k/D	Equation 4.7.1	2,0

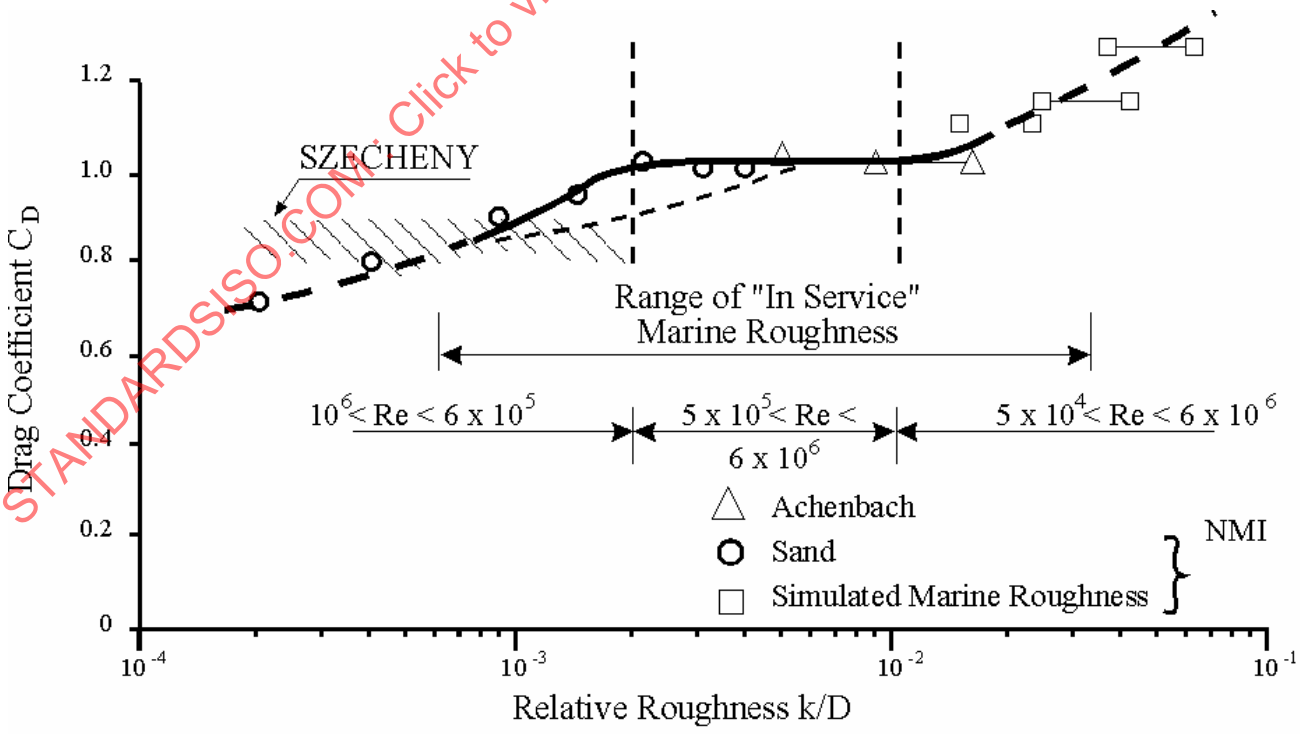

Figure TR.7.3.2.4-2 — Drag coefficient for rough cylinders at high Reynolds number[7-26]

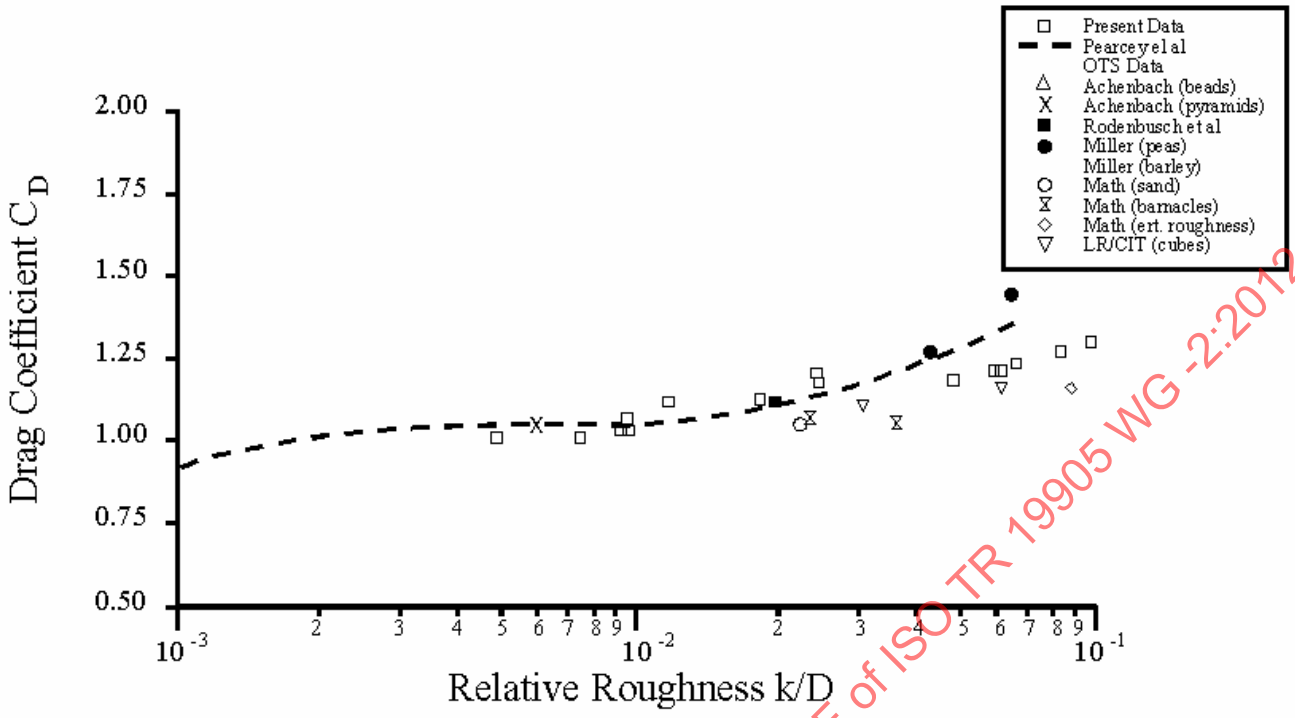

Figure TR.7.3.2.4-3 — Drag coefficient for post critical Reynolds numbers for rough cylinders[7-24]

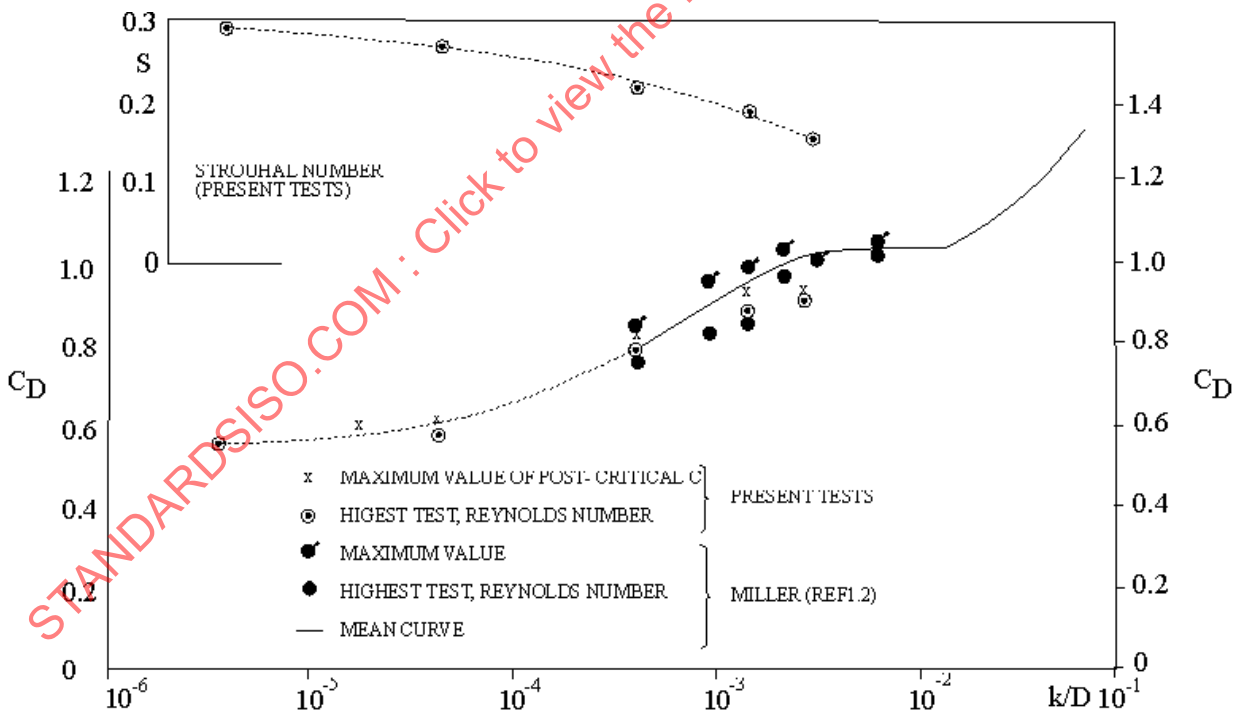

Figure TR.7.3.2.4-4 — Effect of roughness on drag coefficient and vortex shedding frequency for post-critical Reynolds numbers[7-32]

$$C_{Di}(k/D) \begin{cases} C_D \text{ smooth} = 0.65 & ; 1/10000 > k/D \\ C_D \text{ smooth} * (2.36 + 0.34 \, \mathrm{Log}_{10}(k/D)) & ; 1/250 > k/D > 1/10000 \\ C_D \text{ rough} = 1.0 & ; k/D > 1/250 \end{cases}$$

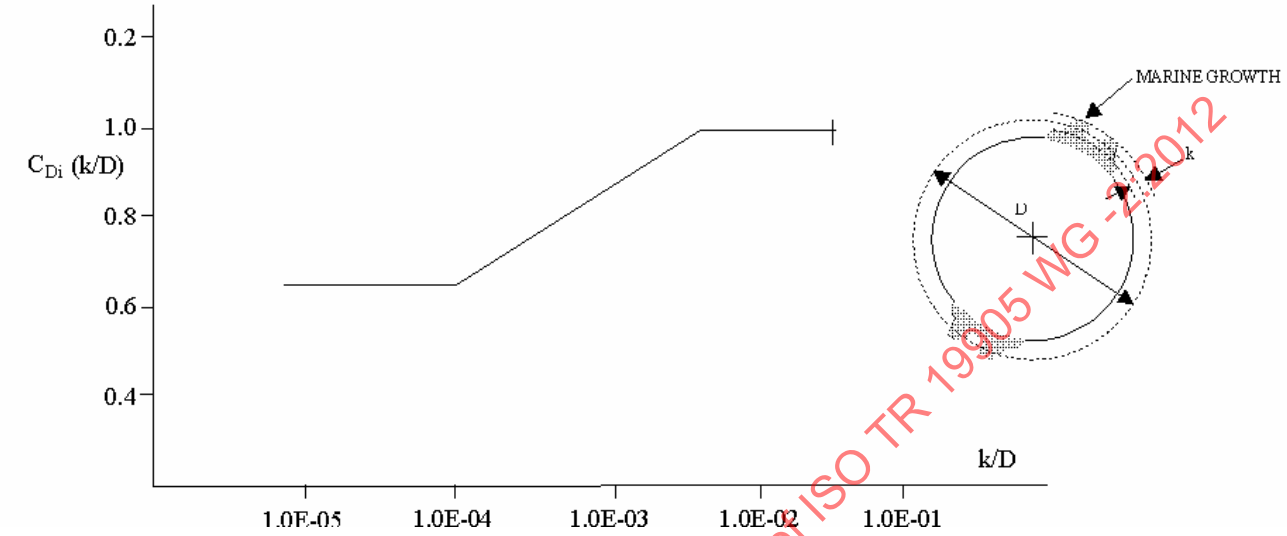

Figure TR.7.3.2.4-5 — Recommended values for the drag coefficient as function of relative roughness

TR.7.3.2.4.2.6 Keulegan-Carpenter number dependence

In post-critical conditions, for KC-numbers lower than approximately 30 to 40, there seems to be some dependence of the drag coefficient on the KC-number, at least for rough cylinders. For smooth cylinders this KC-dependence is more uncertain. The Christchurch Bay Tower (CBT) results for a clean cylinder reported by Bishop[7-33], for example, show this dependence for smooth cylinders, and so do the results reported from the Ocean Test Structure (OTS)[7-22], Wolfram and Theophanatos[7-24], and the SSPA results reported by Rodenbusch and Gutierrez[7-18], do not show this dependence for smooth cylinders.

For rough cylinders in post-critical conditions, the KC-dependence of the drag coefficient for KC-numbers lower than approximately 30 to 40 seems to be a more generally observed trend, as in References [7-18], [7-22] and [7-34] amongst others.

It must be emphasized that for decreasing KC-numbers (< 30) the (post-critical) conditions will gradually be more inertia dominated and less drag dominated, implying an increasing uncertainty in the reported C_D values.

Figure TR.7.3.2.4-6 shows C_D as a function of the KC-number for cylinders in waves from Reference [7-35]. In a similar way, Figures TR.7.3.2.4-7 and TR.7.3.2.4-8 show C_D as a function of KC-number for, respectively, a clean cylinder and a rough, barnacle-covered cylinder of the Ocean Test Structure (OTS)[7-22] as presented in Reference [7-28].

Based on the discussion above and the results reported in the literature, the explicit KC-dependence presented in Equation (TR.7.3-8) may be included in the computations in addition to the roughness dependence:

$$C_{Di(KC,k/D)} = C_{Di(k/D)} * \begin{cases} 1{,}45 & ; \quad KC < 10 \\ 2/(KC - 5)^{0,2} & ; \quad 10 < KC < 37 \\ 1{,}0 & ; \quad 37 < KC \end{cases} \qquad \text{(TR.7.3-8)}$$

A graphic representation of Equation (TR.7.3-8) is given in Figure TR.7.3.2.4-9.

Equation (TR.7.3-8) should also be used for smooth cylinders, in spite of the uncertainty with respect to the KC-dependence. However, for low KC-values the choice of C_D-value is less critical due to the transition to inertia-dominated conditions. Furthermore, using Equation (TR.7.3-8) for the entire roughness range (from smooth to rough) results in a more uniform and easier handling of the KC-dependence.

An inertia coefficient C_M = 2,0 for smooth cylinders and C_M = 1,8 for rough cylinders is suggested for use if KC-dependence is used for the drag coefficients at low KC-numbers.

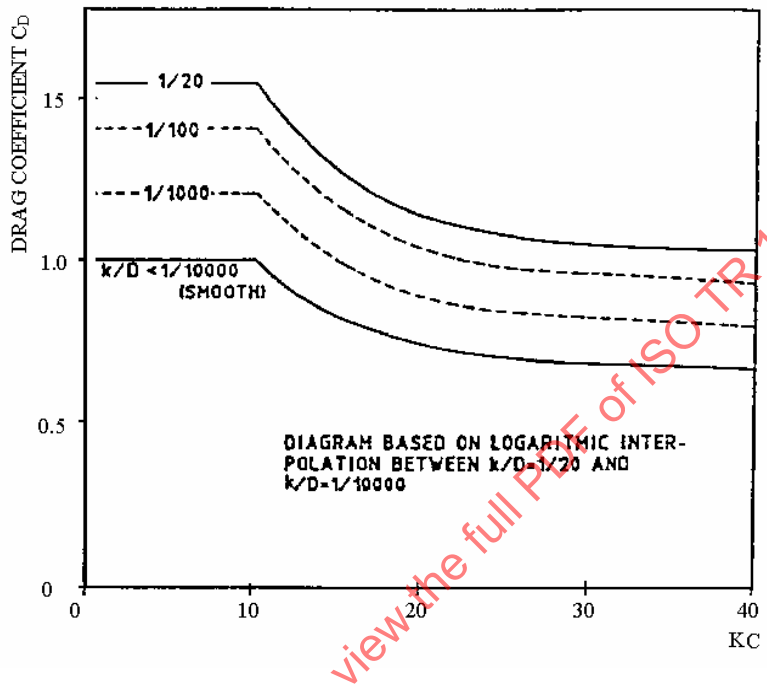

Figure TR.7.3.2.4-6 — Drag coefficient dependence on KC-number[7-35]

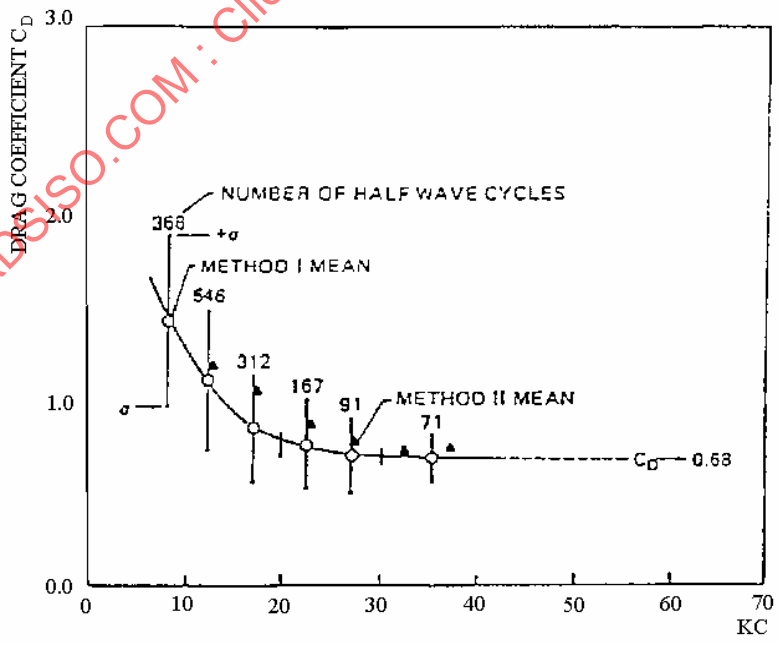

Figure TR.7.3.2.4-7 — Drag coefficient dependence on KC-number for clean cylinders of the Ocean Test Structures[7-22], [7-28]

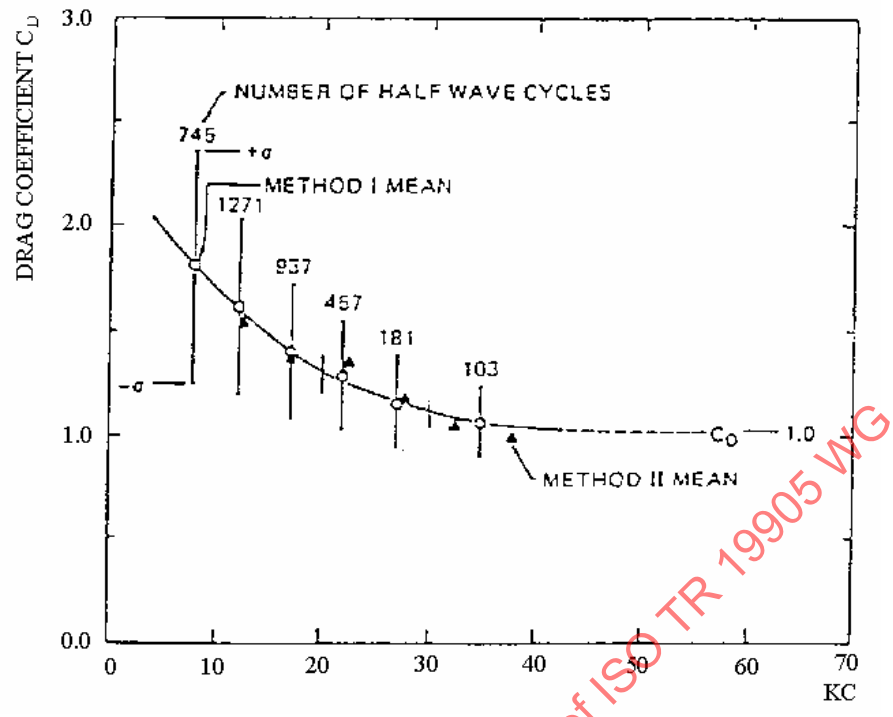

Figure TR.7.3.2.4-8 — Drag coefficient dependence on KC-number for barnacle-covered cylinders of the Ocean Test Structure[7-22], [7-28]

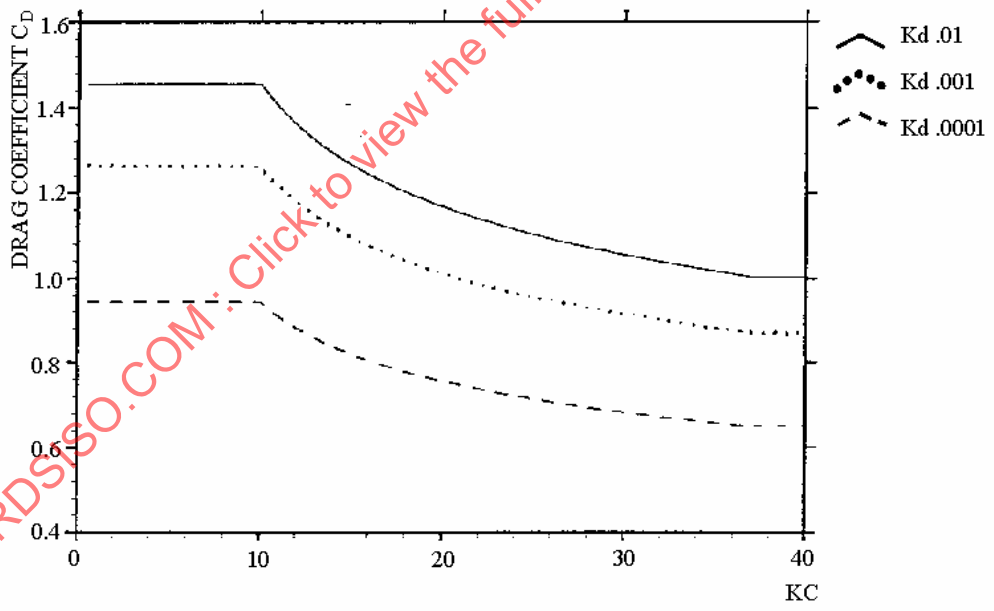

Figure TR.7.3.2.4-9 — Recommended drag coefficient dependence on KC-number for cylinders in waves, at high Reynolds numbers

TR.7.3.2.4.2.7 Reynolds number dependence

As previously discussed, the drag coefficient is dependent on the Re-number and this has been reported by several authors[7-7], [7-29] (Figures TR.7.3.2.4-11 and TR.7.3.2.4-12) and is reflected in some guidance on load computations, e.g. References [7-36] and [7-37] (Figure TR.7.3.2.4-10).

However, the use of test results reducing C_D in the critical region is not relevant for practical purposes as the roughness k/D < 1/100 000 implied in the curve for smooth cylinders is not applicable for jack-up structures.

The change in the Reynolds dependence with respect to roughness is quite large and it is therefore not possible to recommend one single curve for this dependence. The recommended set of curves shown in Figure TR.7.3.2.4-13 are mainly based on a functional fit to the test results presented in Reference [7-29] and in addition the drag coefficient in the critical regime is set to a minimum of C_D = 0,45. Test results have indicated lower C_D values, but only in the ideal conditions of test facilities. A recommended set of curves are given in Figure TR.7.3.2.4-13, complying with the roughness dependence of Figure TR.7.3.2.4-5 at large Reynolds numbers. Using the curve for roughness k/D = 0,01, there is no reduction below C_D = 1,0 for Reynolds numbers above 105, which supports the use of a constant C_D in ISO 19905-1.

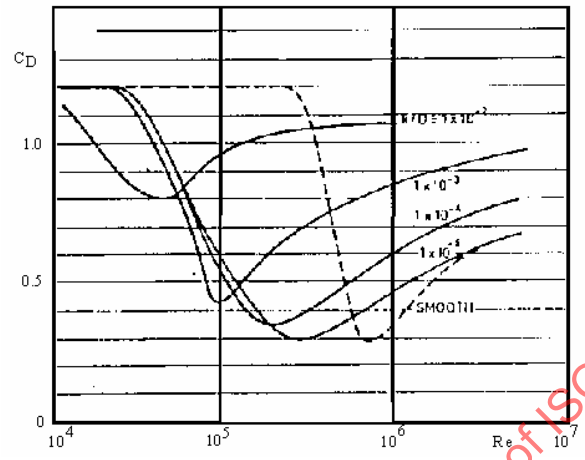

Figure TR.7.3.2.4-10 — Suggested Reynolds dependence in existing guidance[7-37]

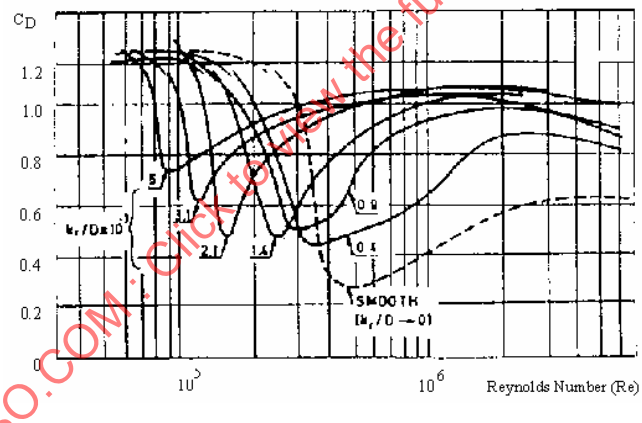

Figure TR.7.3.2.4-11 — Reynolds dependence of drag coefficient in test results[7-7]

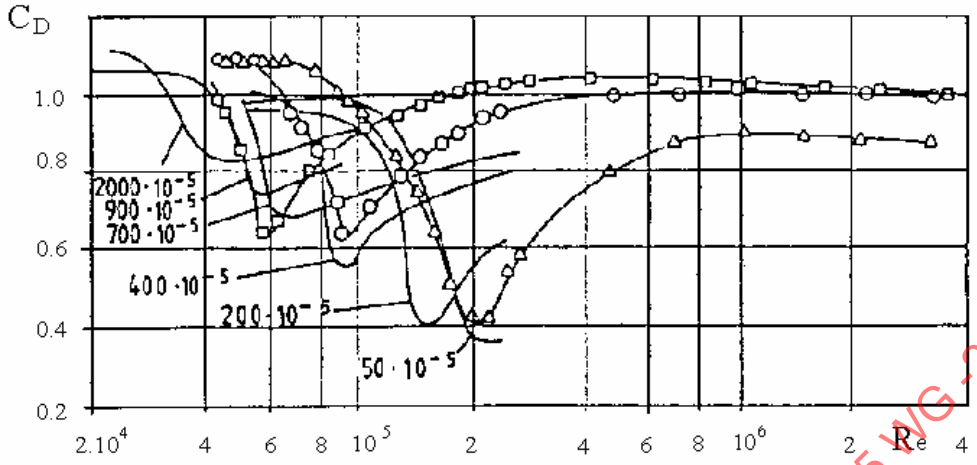

Drag coefficient C_D of rough circular cylinders in steady incident flow for different surface roughness values k/D (k = average height of surface roughness, D = cylinder diameter, $Rn = U_\infty D/\nu$, U_∞ = incident flow velocity.) Δ, $k/D = 110 \cdot 10^{-5}$; ○, $k/D = 450 \cdot 10^{-5}$; □, $k/D = 900 \cdot 10^{-5}$; ——, Fage & Warsap (1929), (Achenbach, 1971).

Figure TR.7.3.2.4-12 — Reynolds dependence of drag coefficient[7-29]

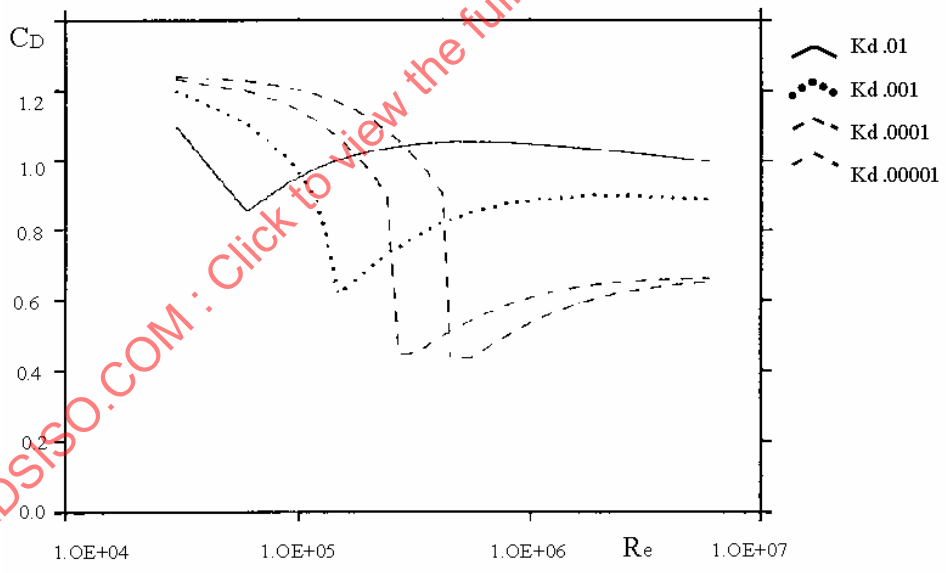

Figure TR.7.3.2.4-13 — Recommended values for Reynolds dependence for different values of relative roughness, KC > 40

TR.7.3.2.4.3 Hydrodynamic coefficients for gussets

Gussets are treated as flat plates implying that a C_{Di} = 2,0 and C_{Mi} = 1,0 is to be applied (considering the area associated with C_M as that of the circumscribed circle). For convenience, ISO 19905-1 proposes that gussets are included as equivalent horizontal members in the hydrodynamic model to assure proper directional dependence of forces. Shielding may be considered according to ISO 19905-1:2012, Figure A.7.3-2.

TR.7.3.2.4.4 Hydrodynamic coefficients for chords

TR.7.3.2.4.4.1 Split tube chords

With respect to the test results for split tube chord data, the following aspects are considered:

— The tests are almost always performed with a smooth cylinder section.

— Most of the tests are performed in stable current or wind conditions.

The first aspect is the most important, also indicated by the test results evaluation of the tubulars presented in TR.7.3.2.4.2. The drag coefficient for smooth tubulars is about $C_{Dsmooth}$ = 0,65, while for rough cylinder this increases to C_{Drough} = 1,0.

The second aspect on stable flow conditions should not affect the results very much as the KC values are very high in extreme load evaluations. However, the test result in Reference [7-38] showed higher values in waves than in stable current. This has not yet been fully explained, but comparisons made in Reference [7-28] indicates that test results in waves from flume experiments overpredict the drag forces. A number of test results[7-2] have been considered, from wind tunnel tests and towing in water, when evaluating hydrodynamic coefficients for split tube chords.

The drag coefficient is first estimated for the directions 0° and 90° as defined in Figure TR.7.3.2.4-14. The drag coefficients for 0° are dominated by the tubular part and no particular effect of the rack on the drag coefficient is seen from the tests. That is, for typical dimensions of the tubular diameter and rackplate thickness t, D_i/t >> 1,0, tests show values of about $C_D \approx 0{,}65$. This indicates that the drag coefficients chosen for the tubular are also valid for the split tube chord for the 0° direction. In order to be consistent with the roughness dependence of the drag coefficient for tubulars, the drag coefficient in the marine growth region is increased due to roughness to C_{Drough} = 1,0 for θ = 0°.

NOTE For the 90° direction the drag coefficient should be similar to that of a flat plate for large W/D_i ratios, C_{Dplate} = 2,0. However, test results seem to indicate that the C_D values for this direction referring to the mean rack width W, are, on average, about 1,8, see Figure TR.7.3.2.4-15. The suggested drag coefficient in ISO 19905-1 is therefore set to be 1,8 for small W/D_i ratios, increasing to 2,0 for large W/D_i ratios. The interpolation between these two numbers is based on engineering judgment.

The drag coefficient for the wave flow normal to the rack, related to the rack width W, is recommended as:

$$C_{D1} = \begin{cases} 1{,}8 & W/D_i < 1{,}2 \\ 1{,}4 + W/3D_i & 1{,}2 < W/D_i < 1{,}8 \\ 2{,}0 & 1{,}8 < W/D_i < 2{,}0 \end{cases} \qquad \text{(TR.7.3-9)}$$

For the interpolation between the directions 0° and 90°, a number of formulations are available, but since there were a number of test results available, a best fit of a new formulation was decided.

The following interpolation formula was found to fit the data best (see Appendix TR.7.C) and at the same time be flexible with respect to the drag coefficient for rough and smooth surfaces at 0°:

$$C_{Di} = \begin{cases} C_{Do} & \theta < 20° \\ C_{Do} + (C_{D1}W/D_i - C_{Do})\sin^2[(\theta - 20°)9/7] & 20° < \theta < 90° \end{cases} \qquad \text{(TR.7.3-10)}$$

where

C_{Do} is the drag coefficient for the chord at θ = 0° and is to be taken as that of a tubular with appropriate roughness, see TR.7.3.2.4.2, i.e. C_{Do} = 0,65 above MWL + 2,0 m and C_{Do} = 1,0, below MWL + 2,0 m; possible dependence on KC and Re numbers as for a tubular;

C_{D1} is the drag coefficient for flow normal to the rack (θ = 90°), related to the projected diameter (the rack width W). Explicit dependence on KC may be taken according to Figure TR.7.3.2.4-9, but is normally not relevant for extreme loading conditions. Dependence on k/D or Re may normally be neglected.

The above formulation was derived based on the assumption that the chord behaves like a tubular up to a direction where the rack enters the flow field, and from there and up to 90° the chord acts as a flat plate.

In addition to the above formulation, two other formulations were tested as shown in Figure TR.7.3.2.4-16. Equation (TR.7.3-10) gave an excellent fit with the observed drag coefficients for a smooth tubular and is therefore recommended for use with split tube chords.

Interpolation formulae similar to those used in References [7-36] and [7-49] are compared in Figure TR.7.3.2.4-17 with Equation (TR.7.3-10), for a regular wave analysis. There is some difference in the direction close to 90°, but the number of test results behind the formulation in ISO 19905-1 is believed to justify the change.

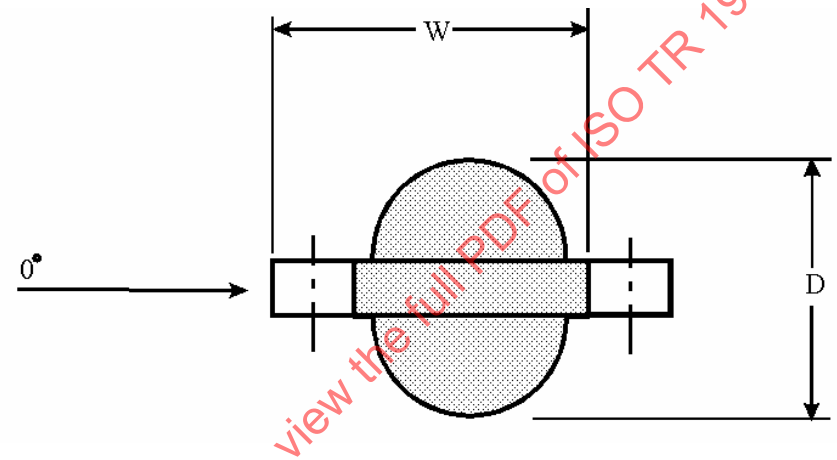

Figure TR.7.3.2.4-14 — Definition of directions and dimensions for a split tube chord

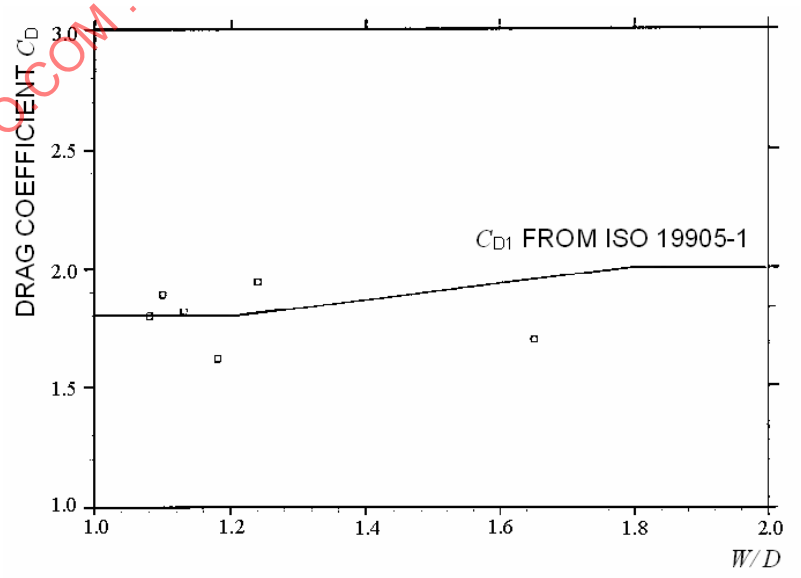

Figure TR.7.3.2.4-15 — Drag coefficient at 90° related to rack width W

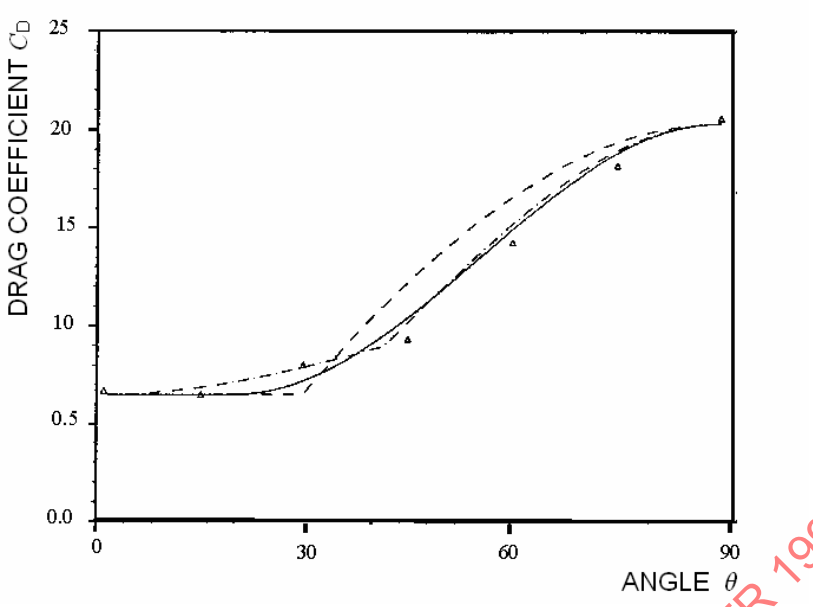

Figure TR.7.3.2.4-16 — Alternative interpolation formulations fit to data

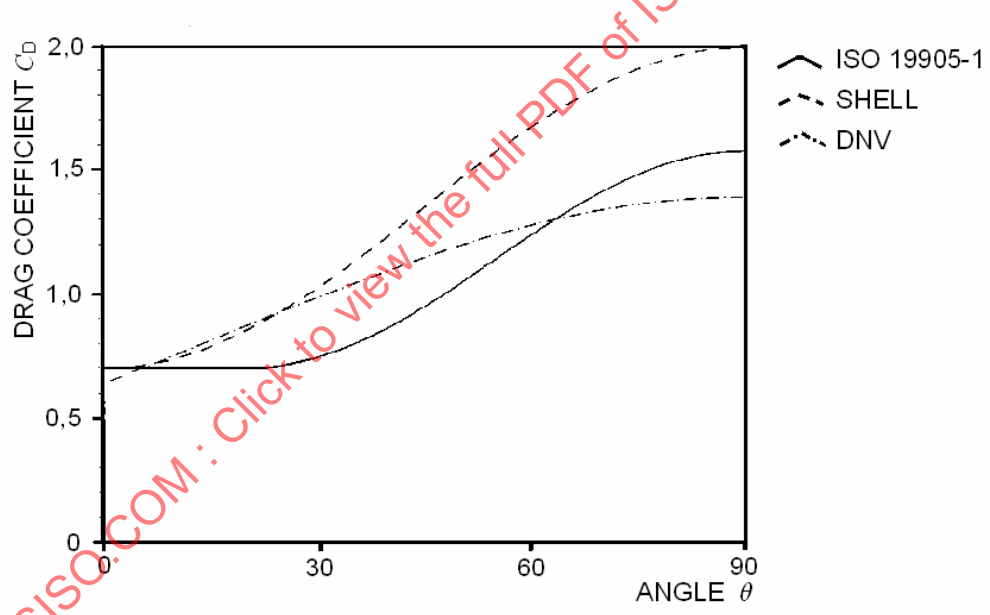

Figure TR.7.3.2.4-17 — Comparison with some current practices for regular wave analysis[7-36], [7-39]. W/D = 1,24 and the scaling regular/irregular = 0,7, valid below MWL + 2,0 m

For the inertia coefficient, the theory[7-29] indicates C_M = 2,0 for a smooth tubular related to the projected diameter and C_M = 1,0 for an isolated flat plate. However, when the plate is considered in conjunction with the split tube sections, C_M = 2,0 is appropriate for the combined section. For a rough tubular as indicated in ISO 19905-1:2012, Table A.7.3-2, the inertia coefficient should be about 1,8 in the marine growth region. However, since the inertia forces will not contribute much to the extreme forces on the legs, the inertia coefficient was set to 2,0 related to the width of the chord measured over the tubular, i.e. at 0°. This is a simple solution and will be conservative in the direction of the tubular for a rough surface and unconservative in the direction of the rack and on average correct. This formulation will also be consistent with the simplified modelling of the leg section where the reference diameter D_i is the dimension D and using C_{Me} = 2,0.

For large rack to diameter ratios W/D, it may however be considered appropriate to modify (reduce) the inertia coefficient such that it accounts more correctly for the combination of the contributions from the flat plate and tubular components.

TR.7.3.2.4.4.2 Triangular chords

For triangular chords (Figure TR.7.3.2.4-18), little test data are available. Some currently applied formulae for drag coefficients of more basic sections were therefore used in addition to the test results to improve the background for the actual chosen values. Drag coefficients related to two typical shapes are given in Reference [7-1], as shown in Figure TR.7.3.2.4-19, for a triangular box section and two plates mounted normally on each other. A triangular chord is a combination of these cross-sections. The numbers at different directions are compared in Table TR.7.3.2.4-4. The drag coefficients were determined by vectorial summation of drag forces in direction 1 and 2 according to Figure TR.7.3.2.4-19.

To relate the drag coefficient to a fixed dimension $D_i = D$ the back plate width is chosen. A fixed dimension and directional dependent drag coefficient is convenient for modelling purposes. The drag coefficient related to this fixed diameter may be computed as:

$$C_{Di} = C_{Dpr}(\theta) * D_{pr}(\theta) / D_i \qquad \text{(TR.7.3-11)}$$

where

$CD_{pr}(\theta)$ is the drag coefficient referenced to the projected diameter;

$$= \begin{cases} 1{,}70 & ; \quad \theta = 0° \\ 1{,}95 & ; \quad \theta = 90° \\ 1{,}40 & ; \quad \theta = 105° \\ 1{,}65 & ; \quad \theta = 180° - \theta_o \\ 2{,}00 & ; \quad \theta = 180° \end{cases}$$

$D_{pr}(\theta)$ is the projected diameter of the chord determined as:

$$D_{pr}(\theta) = \begin{cases} D\cos(\theta) & ; \quad 0 < \theta < \theta_o \\ W\sin(\theta) + D/2\left|\cos(\theta)\right| & ; \quad \theta_o < \theta < 180 - \theta_o \\ D\left|\cos(\theta)\right| & ; \quad 180 - \theta_o < \theta < 180 \end{cases}$$

θ_o is the angle where half the backplate is hidden behind the rackplate, determined as $\theta_o = \tan^{-1}(D/2W)$.

Table TR.7.3.2.4-4 — Comparison of drag coefficients for simple sections and chord C_{Dpr} evaluated from tests

	θ	⊥ /45/	Δ /45/	ISO 19905-1
C_{Dpr}:	0	1,7	1,3	1,70
	45	2,5	1,8	1,825
	90	2,2		1,95
	135	1,5	1,3	1,50
	180	2,0	1,8	2,00

(W/D = 1,1)

As a basis for the suggested drag coefficients the results available from TEES[7-40] and DHL[7-41], [7-2] were considered together with the recommendations in Reference [7-39]. The drag coefficients recommended in ISO 19905-1 are compared with the TEES test results in Figure TR.7.3.2.4-20.

The inertia coefficient C_{Mi} = 2,0 may be applied for all directions, related to the equivalent volume of $\pi D_i^2/4$ per unit length, where $D_i = D$, the backplate dimension. This assumes that the outline cross-sectional area is approximately $\pi D_i^2/4$. If the rack width is not of similar size to the backplate dimension, a more detailed consideration of the inertia coefficient should be made if the loadings on the leg are not drag dominated, i.e. if the results are sensitive to the choice of inertia coefficient.

Explicit dependence on KC may be taken according to Figure TR.7.3.2.4-9, but it is normally not relevant for extreme loading conditions. Dependence on k/D or Re may normally be neglected.

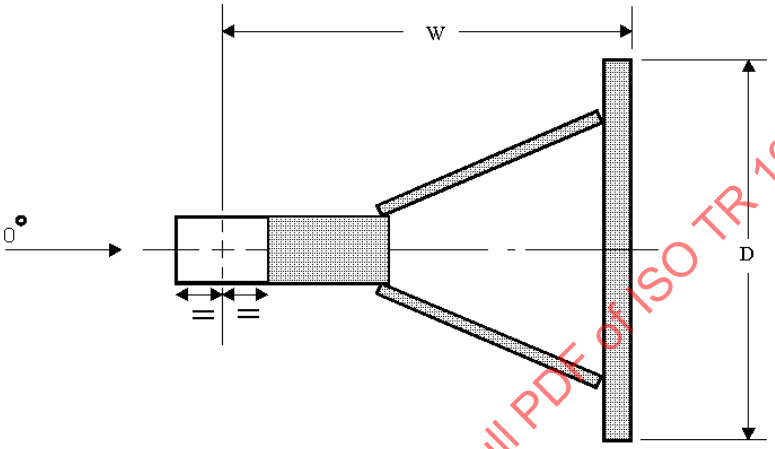

Figure TR.7.3.2.4-18 — Definition of dimensions and angles for a triangular chord

TR.7.3.2.4.5 Other shapes

For other shapes, or groups of elements, see for example Reference [7-1].

Table C1 Shape coefficient for irregular cross sections.

Profile	α (deg.)	C_{S1}	C_{S2}
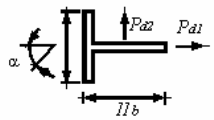	0 45 90 135 180	2.0 1.2 -1.6 -1.1 -1.7	0 0.9 2.2 -2.4 0
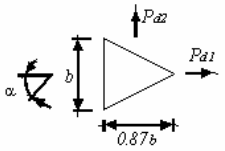	0 80	1.8 -1.3	0 0

Figure TR.7.3.2.4-19 — Drag coefficients for basic sections in uniform flow[7-1]

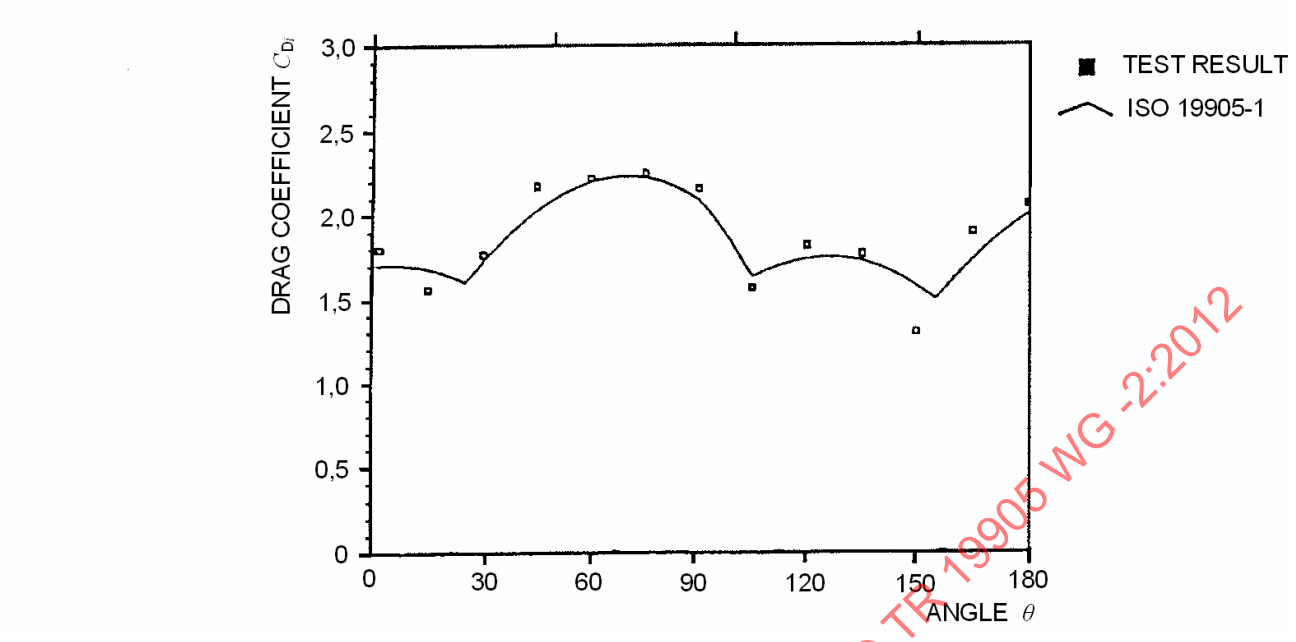

a) Marathon LeTourneau 116C

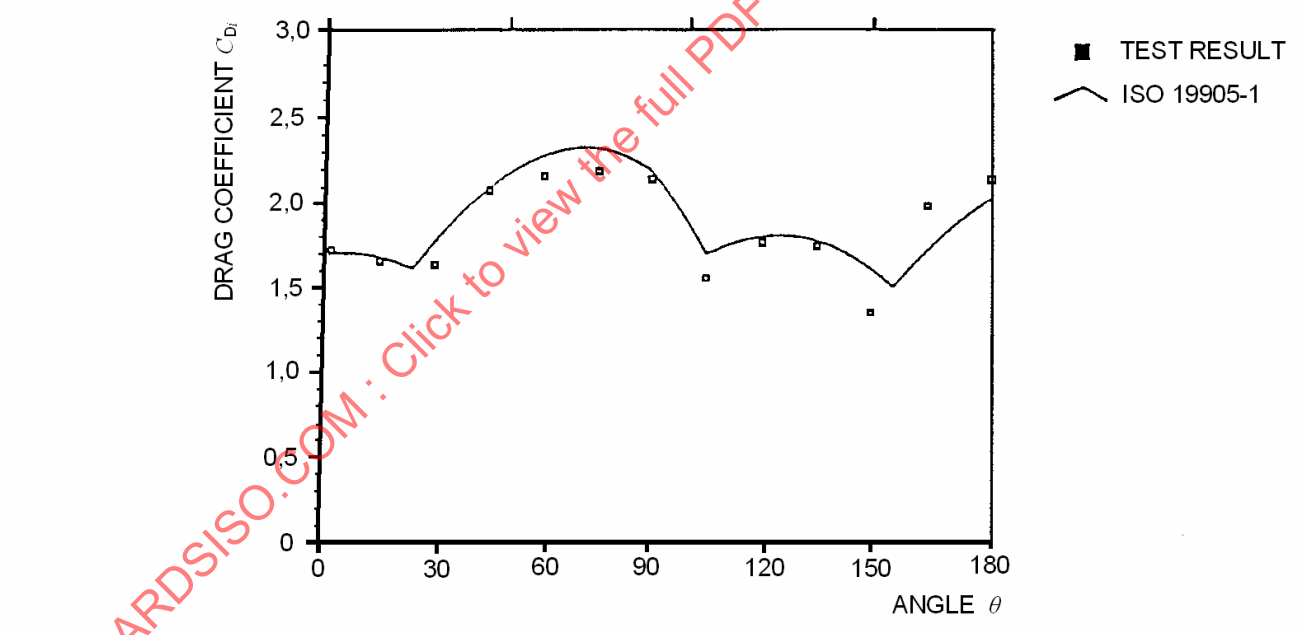

b) Marathon LeTourneau Gorilla

Figure TR.7.3.2.4-20 — Comparison between TEES test results[7-40] and the formulation in ISO 19905-1

TR.7.3.2.5 Marine growth

In addition to the effect on the roughness, the effective diameter should be increased to account for marine growth. Here it is recommended to increase the radius by 12,5 mm (i.e. diameter increased by 25 mm) over the full water depth for tubulars.

TR.7.3.3 Wave and current actions

TR.7.3.3.2 Hydrodynamic actions

Jack-up leg sections are complex structures, usually made of slender members. The best engineering tool available for computation of hydrodynamic forces is Morison's equation. However, the limitations of Morison's equation should be recognized. For single large-diameter members/legs, which may be an alternative to lattice legs, more appropriate theories and formulations for the hydrodynamic forces can be applied.

Hydrodynamic coefficients for large diameter members may be calculated according to TR.7.3.2.4 and TR.7.3.2.5, or based on references such as ISO 19902:2007[4], A.9.5.2.3, Reference [7-12] or Reference [7-42]. However, care should be taken in using coefficients from other standards and references within the context of the overall assessment process presented within this document. Factors may have been implicitly incorporated into the coefficient which may or may not be consistent with those used in the development of this assessment practice (e.g. spreading factor).

TR.7.3.3.2.1 Morison equation

A limitation on the application of Morison's equation to predict wave loads is implemented. The limitation is set to:

$$\lambda > 5D_i \qquad \text{(TR.7.3-12)}$$

where

λ is the wave length and

D_i is the reference dimension of individual leg members (within a lattice leg).

The above limitation implies that the members should be small compared with the waves.

Morison's equation[7-43] is an empirical relation given by a drag term plus an inertia force term as:

$$\Delta F = \Delta F_{drag} + \Delta F_{inertia} = 0{,}5\rho\ C_D\, D\, |u_x|\, u_x + \rho\, C_M\, (\pi D^2/4)\ \dot{u}_x \qquad \text{(TR.7.3-13)}$$

where

C_D is the drag coefficient;

C_M is the inertia coefficient;

$u_x, \dot{u}_x$ are the horizontal water particle velocity and acceleration;

D is the tubular diameter;

ρ is the density of fluid surrounding the tubular.

The above equation was established to be used for vertical circular cylinders in waves, but has later been modified and generalized to account for current, inclined members and relative velocity and acceleration. These extensions are further defined for use in ISO 19905-1 and discussed in the following subclauses.

TR.7.3.3.2.2 Drag action

For the drag part of the equation, the extension from Morison's original formula is made as:

$$\Delta F_{drag} = 0{,}5\ \rho\, C_D\, D\, |v_n|\, v_n \qquad \text{(TR.7.3-14)}$$

where v_n is now introduced as the relative particle velocity normal to the local member axis including current, taken as:

$$v_n = u_n + V_{Cn} - \alpha \dot{r}_n \quad \text{(TR.7.3-15)}$$

where

$u_n + V_{Cn}$ is the combined particle velocity from wave and current by vectorial summation normal to the member considered;

$\dot{r}_n$ is the velocity of the considered member normal to its axis and in the direction of the combined particle velocity;

α = 0, if an absolute velocity is to be applied, i.e. neglecting the structural velocity;

=1, if relative velocity is to be included; may only be used for stochastic/random wave force analyses if:

$U_{red} = uT_n/D_i \geq 20.$

where

u is the particle velocity;

T_n is the first natural period of surge or sway motion;

D_i is the reference diameter of a chord.

In the above definition of combined velocity, current is included. This should be acceptable as the member does not distinguish between the velocity due to current or wave motions. The backflow of the wake is different in combined wave and current fields (KC dependence), but this has a small influence on the prediction of the largest force in an extreme wave for single members of diameters typical for jack-ups; see TR.7.3.2.4.

For inclined members the above definition implies that the procedure to arrive at the force components is first to determine the particle velocity component normal to the member axis, then to determine the force normal to the member axis and thereafter to determine the force components in the global directions. This implies that the force component along the member is neglected.

On the inclusion of the relative velocity there has been some reluctance to directly accept the extension to the original Morison's equation. Intuitively the extension should be correct using the same argument as for current forces as the member only experiences the flow field passing locally. However, the displacements of the members are quite small and there have been few data to support such an extension as pointed out in Reference [7-44]. In Reference [7-45] the test results show that for small amplitude motions the damping may be overpredicted when the relative velocity is included. However, for a typical jack-up, with member diameters less than 1 m and natural periods around 5,0 s, the sensitivity to member displacement is not large because the parameter $U_{red} = uT_n/D_i \approx 20$ or more in an extreme sea state; see Figure TR.7.3.3.2-1. In addition, the Christchurch bay test results show that the relative velocity formulation gives good prediction of the in-line loading[7-46], "correctly predicting the important hydrodynamic damping at the resonant frequency". From this it may be concluded that the relative velocity formulation is probably applicable for jack-up structures. A limitation is introduced to avoid any significant overprediction of damping.

The reduced velocity U_{red} may be computed for a wave height equal to the significant wave height and using the first natural period normally corresponding to the fixed condition soil parameters. In practical cases it is suggested to evaluate U_{red} for a majority of members close to the sea surface, and to include relative velocity for either all or no members.

The relative velocity formulation is in effect similar to the inclusion of damping reaction forces. All predictions of damping are uncertain, and compared with other damping estimates the relative velocity formulation is

judged to be reasonably well estimated. This additional damping from the relative velocity formulation should be considered when choosing the structural/proportional damping coefficient. A low structural damping should be considered when the relative velocity is included.

A procedure to combine the forces on several individual members into one member with equivalent diameter and drag coefficient to be used with the horizontal water particle velocities is discussed in ISO 19905-1:2012, A.7.3.2.3.

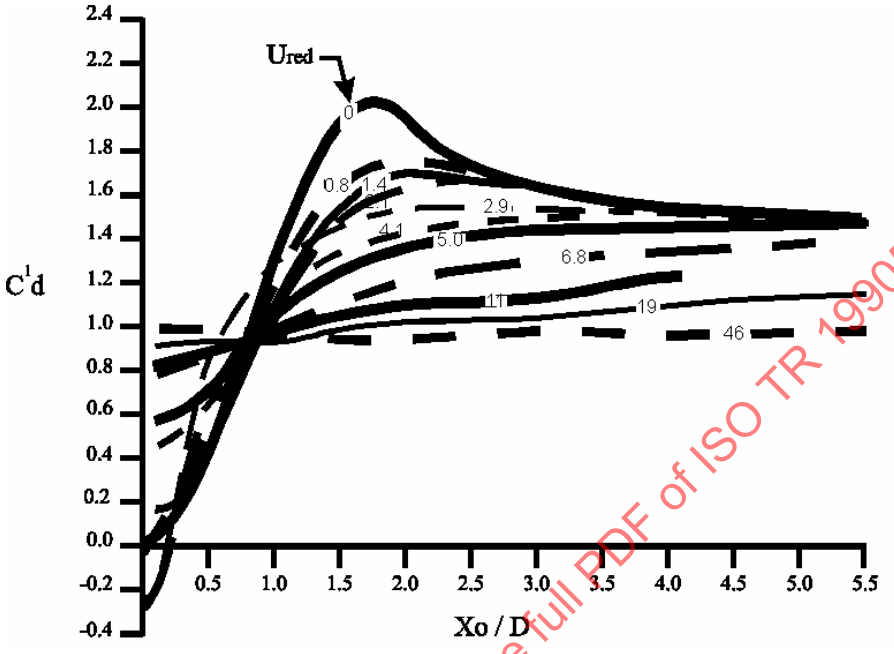

Figure TR.7.3.3.2-1 — Oscillating drag coefficient vs. motion amplitude to diameter ratio X_o/D for given reduced velocities[7-45]

TR.7.3.3.2.3 Inertia actions

These actions are not dominant for extreme loads of typical jack-up lattice legs. A more comprehensive model could be applied to include relative accelerations (noting that in this case the added mass should not be included in the structural model).

In ISO 19905-1 the formulation is given as:

$$\Delta F_{\text{inertia}} = \rho\, C_M\, A\, \dot{u}_n - \rho\, C_A\, A\, \ddot{r}_n \qquad \text{(TR.7.3-16)}$$

where

$\Delta F_{\text{inertia}}$ is the normal force per unit length of member (in this case the member is vertical and the force horizontal);

ρ is the density of fluid surrounding the tubular;

C_M is the inertia coefficient;

A is the cross-sectional area of member;

$\dot{u}_n$ is the water particle acceleration normal to the member;

C_A is the added mass coefficient, $C_A = C_M - 1$;

$\ddot{r}_n$ is the acceleration of the considered member, normal to the member axis and in the direction of the combined particle acceleration.

The last term in Equation (TR.7.3-16) is not included in a deterministic analysis. The term should be included in a stochastic analysis representing the added mass force due to the member acceleration.

$$m_a \ddot{r}_n = \rho C_A A \ddot{r}_n$$

where

m_a is the added mass contribution (per unit length) for the member.

This implicitly defines how to treat inclined members. However, for inclined members the horizontal force may alternatively be determined by accounting for the inclination on the added mass part of the inertia force, but not on the Froude-Krylov part of the force. The horizontal inertia force is hence computed as:

$$\Delta F_{inertiaH} = \rho \pi D^2/4 \, [(C_M - 1)\sin^2\beta_i + 1] \, \dot{u}_n \qquad \text{(TR.7.3-17)}$$

where β_i is the angle between the particle acceleration and the element orientation as defined in Figure A.7.3-1. It should be noted that the vertical particle acceleration will also provide a horizontal component on inclined braces. For global force calculations this will generally be unimportant as the loadings on different braces at different angles will tend to cancel out.

TR.7.3.3.3 Wave models

In general there are two different computational methods with corresponding suitable wave theories;

— deterministic regular wave analysis, and

— stochastic irregular or random wave analysis.

For the deterministic regular wave analysis all formulated wave theories may be chosen from a mathematical point of view. For shallow waters however, the choice of wave theory is limited to those properly predicting wave asymmetry and the corresponding change in wave kinematics.

For the stochastic irregular wave analysis, linear Airy wave theory or variations of Airy theory are suitable. Airy wave theory does not fully describe the wave kinematics behaviour since this wave theory implies symmetric waves, which are not always applicable for shallow water. This will limit the application of this type of analysis to deeper and intermediate water depths and is considered further in ISO 19905-1:2012, A.6.4.2.6; see also Appendix TR.7.B.

TR.7.3.3.3.1 Deterministic waves

Currently there are a number of wave theories that are applied in the analysis of jack-up platforms. In most cases the deterministic computations are performed using Stokes fifth order[7-47] or Dean Stream function[7-48]] theories. The Dean Stream function theory shows the best fit to test results[7-48], [7-49] for shallow water waves. The difference in overall forces from these two wave theories will, however, be small at large to intermediate water depths and for low wave steepnesses.

Figure TR.7.3.3.3-1 is included in ISO 19905-1 in a linear scale to guide the selection of the appropriate wave theory for deterministic analyses. Only the Dean stream and Stokes wave theory are recommended here in order to limit the range of possible choices, reducing the scatter in wave force predictions.

TR.7.3.3.3.2 Stochastic waves

For stochastic wave analysis, Airy's wave theory is the traditional choice using the principle of sum of independent wave components as implied in time domain simulation and frequency domain solutions for

standard irregular seas. For both the Dean Stream and Stokes wave theories there are implicit phase dependencies between wave components at different frequencies.

To account for changes in wetted surface a modification of the Airy wave theory is required, introducing the surface elevation as a parameter in the kinematics. A number of such stretching methods have been proposed in literature. One simple method, the Wheeler stretching method[7-50], compares well with test results in model tank measurements[7-51]. Even for the Wheeler stretching method there exist different variations. The chosen definition is that originally suggested in Reference [7-50], to substitute the true elevation at which the kinematics are required with one which is at the same proportion of the mean water depth. This can be expressed by:

$$z' = \frac{z - \zeta}{1 + \zeta/d} \qquad \text{(TR.7.3-18)}$$

where

z is the elevation at which the kinematics are required (coordinate measured vertically upward from the mean water surface);

z' is the modified coordinate to be used in particle velocity formulation;

ζ is the instantaneous water level (same axis system as z);

d is the still or undisturbed water depth (positive).

This method causes the kinematics at the surface to be evaluated from linear theory expressions as if they were at the still water level.

If a frequency domain analysis is to be applied in extreme response predictions, it is recommended to use linearization with respect to a finite wave height, H_{max}, defined in A.6.4.2.2; however, damping should be linearized using a lower wave height. Stochastic linearization implies the use of a unit wave height and, when combined with the assumption of Gaussian statistics, the extreme response may be underpredicted; see Figure TR.7.3.3.3-3. For fatigue computations stochastic linearization is recommended[7-52] as fatigue damage is not dominated by the extreme wave heights; however, consideration should be given to local loads arising from the finite wave height.

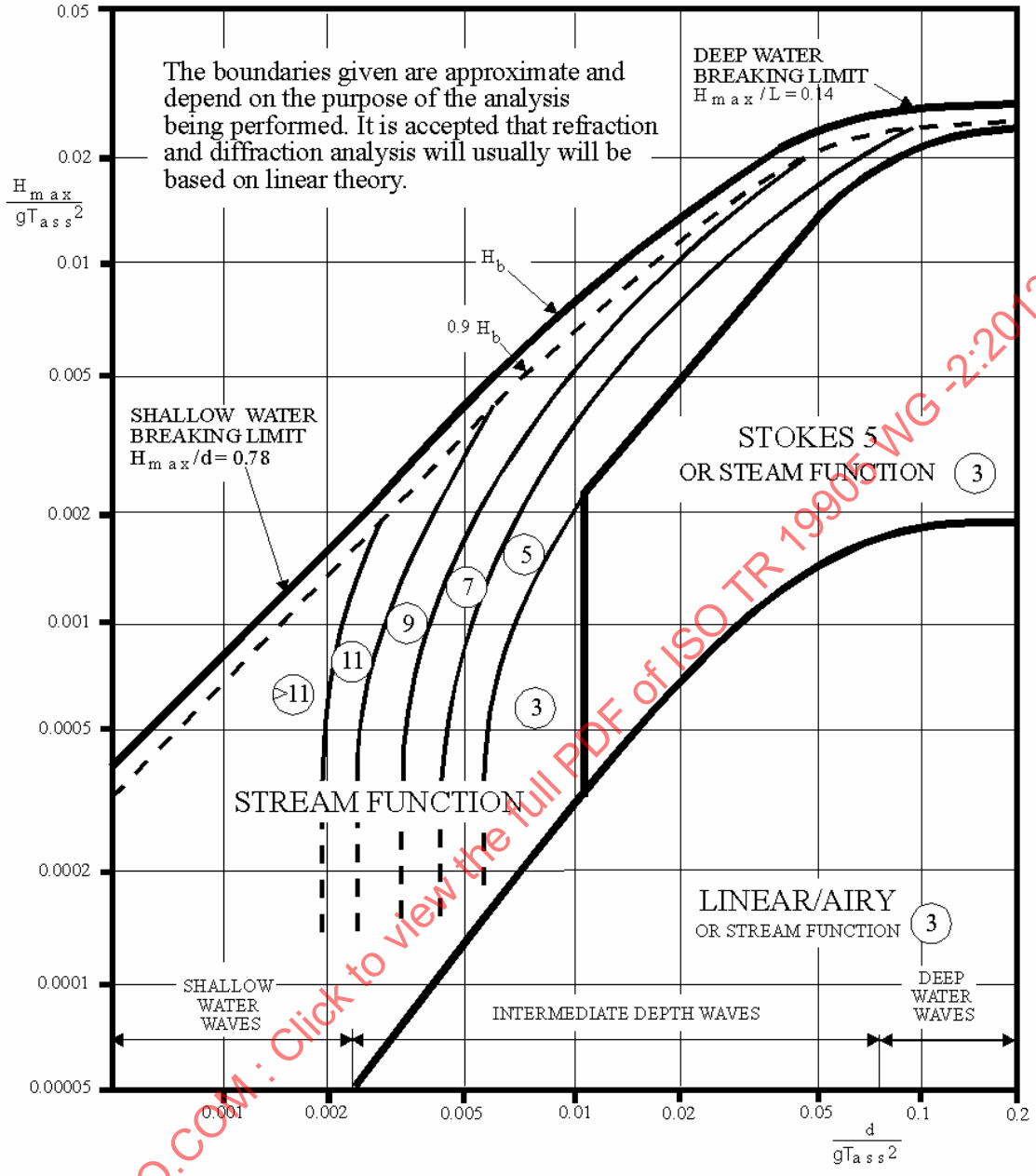

Notes

1) None of these theories is theoretically correct at the breaking limit.
2) Wave theories intended for limiting height waves should be referenced for waves higher than 0,9H_b when stream function theory may underestimate the kinematics.
3) Stream function theory is satisfactory for wave loading calculations over the remaining range of regular waves. However, stream function programs may not produce a solution when applied to near breaking waves or deep water waves.
4) The order of stream function theory likely to be satisfactory is circled. Any solution obtained should be checked by comparison with the results of a higher order solution.
5) The error involved in using Airy theory outside its range of applicability is discussed in the background document.

Nomenclature

H_{max}/gT_{ass}^2	=	Dimensionless wave steepness
d/gT_{ass}^2	=	Dimensionless relative depth
H_{max}	=	Wave height (crest to trough)
H_b	=	Breaking wave height
d	=	Mean water depth
T_{ass}	=	Wave period
L	=	Wave length (distance between crests)
g	=	Acceleration due to gravity

Figure TR.7.3.3.3-1 — Range of validity of different wave theories[7-53]

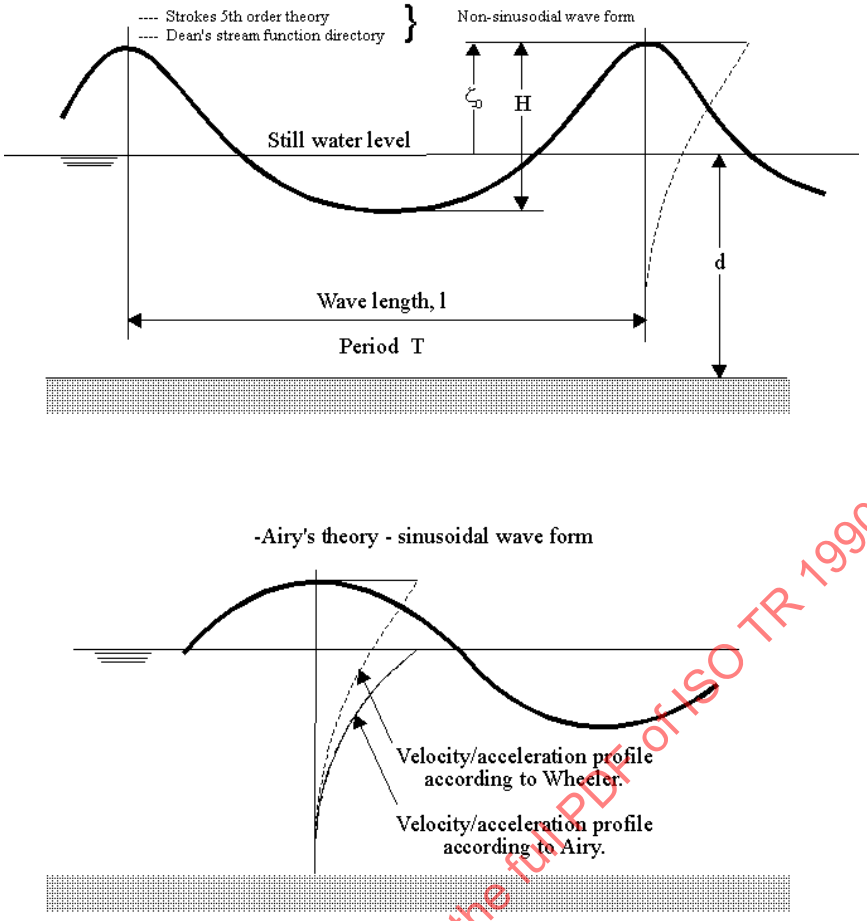

Figure TR.7.3.3.3-2 — Surface elevation, and velocity profiles for deterministic regular waves

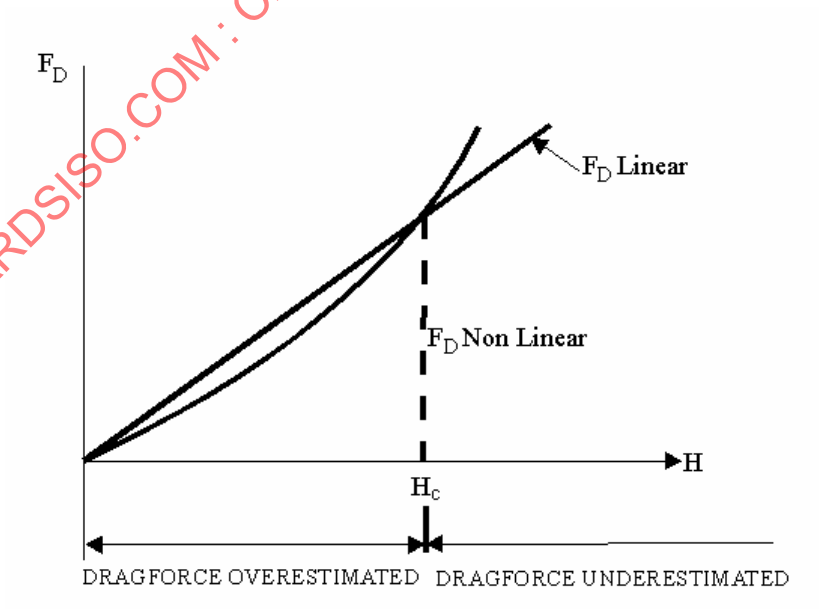

Figure TR.7.3.3.3-3 — Linearization with respect to wave height[7-54]

TR.7.3.3.4 Current

TR.7.3.3.4.1 - General

The current specified for a specific site is intended to be included as specified in ISO 19905-1:2012, A.6.4.3. Interpolation between the data points may be required and linear interpolation is recommended for simplicity.

TR.7.3.3.4.2 Combination with wave particle velocities

It should be emphasized that the wave and current velocities are intended to be treated together, as a sum of separate force contributions will significantly underestimate the hydrodynamic actions.

TR.7.3.3.4.3 Reduction of current by the actuator disc formula

The current velocity will be reduced due to the presence of the structure in the current flow field. An estimate of the reduction of the steady flow velocity may be found from[7-55]:

$$V_C/V_f = [1 + \Sigma(C_{Di}D_i)/4W]^{-1} \geq 0,7 \qquad \text{(TR.7.3-19)}$$

where

V_C is the reduced current velocity to be used in analysis;

V_f is the observed far field current;

C_{Di} is the drag coefficient of an element i;

D_i is the element diameter of element i;

W is the width of the structure.

Several limitations of the above relation are discussed in References [7-55] and [7-3] and a lower limit to the reduction of the current velocity is suggested to be 0,7.

The above equation contains a sum of C_{Di} and diameters D_i, but is not explicit with respect to inclined members. The summation $\Sigma C_{Di}D_i$ is similar to the computation of the equivalent drag coefficient and diameter, $C_{De}D_e$, in ISO 19905-1:2012, A.7.3.2, where member inclination is accounted for. Since the equation should be considered for separate groups of elements[7-55], it suggested to apply the formula for each leg and use the following format:

$$V_C = V_f [1 + C_{De}D_e/(4D_F)]^{-1} \qquad \text{(TR.7.3-20)}$$

where

V_C is the current velocity to be used in the hydrodynamic model; V_C should not be taken as less than $0,7V_f$;

V_f is the far field (undisturbed) current;

C_{De} is the equivalent drag coefficient, as defined in ISO 19905-1:2012, A.7.3.2.3;

D_e is the equivalent diameter, as defined in ISO 19905-1:2012, A.7.3.2.3;

D_F is the face width of leg, outside dimensions.

For structures where the hydrodynamic geometry varies significantly with depth, the blockage factors can be computed for different depths. In view of the reduced drag above MSL (due to lack of marine growth) it may be appropriate to calculate current blockage for the stretched part of the current above MSL separately.

TR.7.3.3.4.4 Current stretching

It is suggested to let the profile follow the surface elevation by changing the coordinate system similarly to that of the Wheeler stretching defined by Equation (TR.7.3-20). The current profile is recommended in ISO 19905-1:2012, A.6.4.3.

TR.7.3.4 Wind actions

The wind force acting on each block of the jack-up is obtained by multiplying the pressure (which accounts for the elevation and shape of the block; see ISO 19905-1:2012, A.6.4.6.2 and ISO 19905-1:2012, A.7.3.4.2 respectively) by the projected area. The total wind force and overturning moment on the jack-up can then be obtained by summing the wind forces over all the blocks accounting for their respective elevations. Where a block has a vertical extent of more than 15 m, it is recommended that it be subdivided and the appropriate height coefficients applied to each part of the block.

The wind speed varies with height since the boundary layer friction (which is increased by the roughness of the sea surface) retards the wind near the sea surface. The lower layers then retard those above them, resulting in increasing velocity above the sea level, until the retarding forces reduce to zero.

A wind profile is normally used to represent the variation of wind speed with respect to height. A power law of 10 (N = 10) to represent the wind is generally appropriate unless site-specific data indicate otherwise as discussed in ISO 19905-1:2012, A.6.4.6.2. The wind speed measured at 10 m above the mean sea level is normally used as the reference in defining the wind speed profile.

The shape coefficients for various typical components of a jack-up are given in the table in ISO 19905-1:2012, A.7.3.4.2. Items with “solid” faces are treated as individual blocks. A different approach is used for open lattice structures, such as derricks, crane booms, helideck support structures, flare booms and raw water towers, etc. Here the table in ISO 19905-1:2012, A.7.3.4.2 recommends the use of 50 % of the total projected profile area of the item (e.g. 50 % of the product of the derrick width overall and the vertical extent of block under consideration) in association with the appropriate shape coefficient for the isolated shapes comprising the lattice.

For leg structures, the equivalent hydrodynamic coefficients on lattice legs may be taken from ISO 19905-1:2012, A.7.3.2.3. These will generally be the same as those for clean legs in large velocities and long waves and hence the smooth values are generally recommended.

TR.7.8 Other considerations

For the most critical individual leg members the possibility of local vortex induced vibrations should be evaluated. This check will normally be covered at the design stage. However, if the site conditions of wind or current and/or wave height exceed those used for design, such a check may be required. This is because vortex induced vibrations may lead to very high local stresses and a major contribution to fatigue loading.

Vortex induced resonance will not normally occur if:

$S > 0{,}2$ for tubulars (TR.7.3-21)

$S > 0{,}145$ for flat plates (TR.7.3-22)

where

S is the Strouhal number; $S = [(f_i\, D_i)/v_n]$;

v_n is the flow velocity normal to the member;

D_i is the diameter of the member;

f_i is the fundamental vibration frequencies of the member (in Hz).

Further information and bounds for S above at which vortex shedding will not occur may be found in References [7-1] and [7-56].

Guidance regarding vortex shedding can also be found in References [7-57] and [7-42].

APPENDIX TR.7.A : Example of equivalent model computations

Dimensions in millimetres

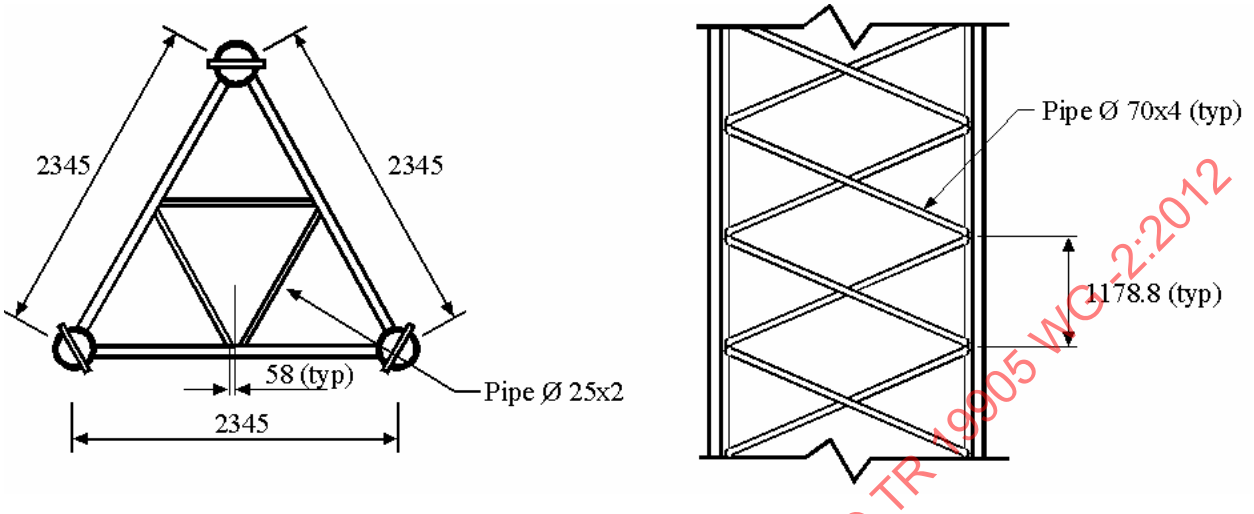

Figure TR.7.A-1 — Model of a bay for test purposes

Table TR.7.A-1 — Computations of equivalent model for heading 0° to be used in site assessment for z < MWL + 2 m, chord WD = 1,13

	i	α_i	β_i	cos…*	C_{Di}	D_i	l_i	$C_{Di}*D_i*l_i$*cos…
Chords	1	(30)	90,0	1,0	1,0	0,65	5,0	3,25
	2	(30)	90,0	1,0	1,0	0,65	5,0	3,25
	3	(90)	90,0	1,0	2,124	0,65	5,0	6,90
Inclined braces	4	–30	26,7	0,25	1,0	0,30	11,2	0,84
	5	–30	–26,7	0,25	1,0	0,30	11,2	0,84
	6	30	26,7	0,25	1,0	0,30	11,2	0,84
	7	30	–26,7	0,25	1,0	0,30	11,2	0,84
	8	90	26,7	1,0	1,0	0,30	11,2	3,36
	9	90	–26,7	1,0	1,0	0,30	11,2	3,36
Span breakers	10	–30	0,	0,125	1,0	0,10	5,0	0,06
	11	30	0,	0,125	1,0	0,10	5,0	0,06
	12	90	0,	1,0	1,0	0,10	5,0	0,50
								$\Sigma C_{Di}*D_i*l_i$*cos = 24,10

* Geometric factor = $[\sin^2\beta_i + \cos^2\beta_i \sin^2\alpha_i]^{3/2}$
see ISO 19905-1:2012, A.7.3.2.3

s = 5,0 m

$C_{De}*D_e = \sum C_{Di} D_i l_i / s$ = 4,82

$D_e = \sqrt{(\sum D_i^2 l_i / s)}$ = 1,58

C_{De} = 4,82/1,58 = 3,05

C_{Me} = 2,0

} Equivalent model

Table TR.7.A-2 — Computations of equivalent model for heading 0° to be compared with model test results, chord WlD = 1,13, model scale = 1:4,264

	i	α_i	β_i	cos…*	C_{Di}	D_i	l_i	$C_{Di}*D_i*l_i*$cos…
Chords	1	(30)	90	1,0	0,65	0,152	1,178	0,116 4
	2	(30)	90	1,0	0,65	0,152	1,178	0,116 4
	3	(90)	90	1,0	2,124	0,152	1,178	0,380 3
Inclined braces	4	–30	26,7	0,25	0,65	0,07	2,628	0,028 99
	5	–30	–26,7	0,25	0,65	0,07	2,628	0,028 99
	6	30	26,7	0,25	0,65	0,07	2,628	0,028 99
	7	30	–26,7	0,25	0,65	0,07	2,628	0,028 99
	8	90	26,7	1,0	0,65	0,07	2,628	0,119 57
	9	90	–26,7	1,0	0,65	0,07	2,628	0,119 57
Span breakers	10	–30	0,	0,125	0,65	0,025	1,173	0,002 38
	11	30	0,	0,125	0,65	0,025	1,173	0,002 38
	12	90	0,	1,0	0,65	0,025	1,173	0,019 06
							$\Sigma C_{Di}*D_i*l_i*$cos =	0,992

* Geometric factor = $[\sin^2\beta_i + \cos^2\beta_i \sin^2\alpha_i]^{3/2}$
see ISO 19905-1:2012, A.7.3.2.3

$s = 1{,}178$
$C_{De} * D_e = 0{,}842$
$D_e = \sqrt{\sum D_i{}^2 1_i / s} = 0{,}370$
$C_{De} = 0{,}842 / 0{,}370 = 2{,}277$
$C_{Me} = 2{,}0$
} equiv. model (model scale)

$C_{De} * D_e = 3{,}59$
$D_e = 1{,}58$
$C_{De} = 2{,}277$
$C_{Me} = 2.0$
} equiv. model (full scale)

Table TR.7.A-3 — Computations of equivalent model for heading 30° to be compared with model test results, chord W/D = 1,13, model scale = 1:4,264

	i	α_i	β_i	cos…*	C_{Di}	D_i	l_i	$C_{Di}*D_i*l_i*$cos…
Chords	1	(60)	90	1,0	1,663	0,152	1,178	0,297 8
	2	(60)	90	1,0	1,663	0,152	1,178	0,297 8
	3	(30)	90	1,0	0,65	0,152	1,178	0,116 4
Inclined braces	4	0	26,7	0,091	0,65	0,07	2,628	0,010 88
	5	0	–26,7	0,091	0,65	0,07	2,628	0,010 88
	6	60	26,7	0,716	0,65	0,07	2,628	0,085 61
	7	60	–26,7	0,716	0,65	0,07	2,628	0,085 61
	8	30	26,7	0,254	0,65	0,07	2,628	0,030 37
	9	30	–26,7	0,254	0,65	0,07	2,628	0,030 37
span breakers	10	60	0,	0,650	0,65	0,025	1,173	0,012 39
	11	60	0,	0,650	0,65	0,025	1,173	0,012 39
	12	30	0,	0,125	0,65	0,025	1,173	0,002 38
								$\Sigma C_{Di}*D_i*l_i*$cos = 0,992 9

* Geometric factor = $[\sin^2\beta_i + \cos^2\beta_i \sin^2\alpha_i]^{3/2}$
see ISO 19905-1:2012, A.7.3.2.3

s = 1,178
$C_{De} * D_e$ = 0,843
$D_e = \sqrt{\sum D_i{}^2 1_i / s}$ = 0,370
C_{De} = 0,843 / 0,370 = 2,278
C_{Me} = 2,0
} equiv. model (model scale)

$C_{De} * D_e$ = 3,59
D_e = 1,58
C_{De} = 2,278
C_{Me} = 2,0
} equiv. model (full scale)

Dimensions in millimetres

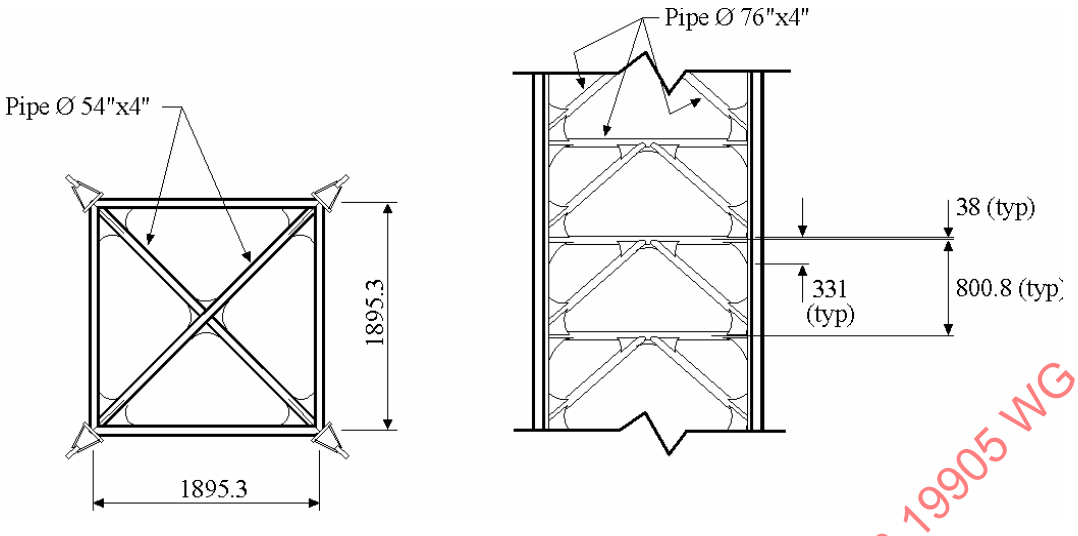

Figure TR.7.A-2 — Square bay with triangular chords

Table TR.7.A-4 — Square bay with triangular chords, equivalent model to be used in site assessment
z < MWL + 2 m

	i	α_i	β_i	cos…*	C_{Di}	D_i	l_i	$C_{Di}*D_i*l_i*$cos…
Chords	1	45	90	1,0	1,65	0,71	3,4	3,983
	2	45	90	1,0	1,65	0,71	3,4	3,983
	3	135	90	1,0	1,79	0,71	3,4	4,321
	4	135	90	1,0	1,79	0,71	3,4	4,321
Inclined braces	5	0	40,2	0,268 9	1,0	0,32	10,6	0,912
	6	90	40,2	1,0	1,0	0,32	10,6	3,392
	7	90	40,2	1,0	1,0	0,32	10,6	3,392
	8	0	40,2	0,268 9	1,0	0,32	10,6	0,912
Side Horiz.	9	0	0,	0,091	1,0	0,32	11,2	0,0
	10	90	0,	1,0	1,0	0,32	11,2	3,584
	11	90	0,	1,0	1,0	0,32	11,2	3,584
	12	0	0,	0,091	1,0	0,32	11,2	0,0
Span breakers	13	45	0,	0,354	1,0	0,23	11,4	2,622
	14	45	0,	0,354	1,0	0,23	11,4	2,622
Brackets	15	90,	0,	1,0	2,0	0,98	0,98	1,921
							$\Sigma C_{Di}*D_i*l_i*$cos…	= 39,550

* Geometric factor = $[\sin^2\beta_i + \cos^2\beta_i \sin^2\alpha_i]^{3/2}$
see ISO 19905-1:2012, A.7.3.2.3

s = 3,4

$C_{De} * D_e$ = 11,63

D_e = $\sqrt{(\sum D_i^2 l_i / s)}$ = 2,30

C_{De} = 11,63/2,30 = 5,06

C_{Me} = 2,0

} equivalent model

Table TR.7.A-5 — Square bay with triangular chords, Equivalent model to be used in comparison with test results, model scale 1:4,256

	i	α_i	β_i	cos…*	C_{Di}	D_i	l_i	$C_{Di}*D_i*l_i*$cos…
Chords	1	45	90	1,0	1,65	0,167	0,800 8	0,220 7
	2	45	90	1,0	1,65	0,167	0,800 8	0,220 7
	3	135	90	1,0	1,79	0,167	0,800 8	0,298 9
	4	135	90	1,0	1,79	0,167	0,800 8	0,298 9
Inclined braces	5	0	40,2	0,268 9	0,65	0,076	2,481	0,033 0
	6	90	40,2	1,0	0,65	0,076	2,481	0,122 6
	7	90	40,2	1,0	0,65	0,076	2,481	0,122 6
	8	0	40,2	0,268 9	0,65	0,076	2,481	0,033 0
Side Horiz.	9	0	0,	0,091	0,65	0,076	2,628	0,0
	10	90	0,	1,0	0,65	0,076	2,628	0,129 8
	11	90	0,	1,0	0,65	0,076	2,628	0,129 8
	12	0	0,	0,091	0,65	0,076	2,628	0,0
Span breakers	13	45	0,	0,354	0,65	0,054	2,680	0,033 3
	14	45	0,	0,354	0,65	0,054	2,680	0,033 3
Brackets	15	90,	0,	1,0	2,0	0,231	0,231	0,107 0
							$\sum C_{Di}*D_i*l_i*$cos… =	1,783 6

* Geometric factor = $[\sin^2\beta_i + \cos^2\beta_i \sin^2\alpha_i]^{3/2}$
see ISO 19905-1:2012, A.7.3.2.3

s = 0,8008
$C_{De} * D_e$ = 2,227
$D_e = \sqrt{\sum D_i{}^2 1_i / s}$ = 0,542
C_{De} = 2,227/0,542 = 4,109
C_{Me} = 2,0
} equiv. model (model scale)

$C_{De}*D_e$ = 9,48
D_e = 2,307
C_{De} = 4,109
C_{Me} = 2,0
} equiv. model (full scale)

APPENDIX TR.7.B: Comparison cases to assess implications of the ISO 19905-1 formulation

Computations are performed on a “simplified model” with no mass. The irregular and regular wave results are computed according to ISO 19905-1:2012, A.6.4 and A.7. These computations are made to asses the implications of changes made concerning drag coefficients and wave kinematics formulations compared with previous practices.

The significant wave height is chosen as judged realistic for the two water depths investigated:

Water depth 30 m:
significant wave height H_{srp} = 10 m

Water depth 90 m:
significant wave height H_{srp} = 14 m

The period range specification is taken from ISO 19905-1:2012, A.6.4.2:

$$\sqrt{(11{,}8H_s)} < T < \sqrt{(19{,}5H_s)}$$
$$3{,}5\sqrt{(H_s)} < T_Z < 3{,}6\sqrt{(H_s)}$$

The current and current profile is often site dependent. Here the current is set to be constant over the water depth, extrapolated to sea surface.

The example design for the computations is defined by:

Three legs, split tube chords

Diameter chord (tubular)	D_c	=	0,7 m
Rack width	W	=	0,8 m
Diameter of braces	D_b	=	0,3 m
Length of braces per m. height	l_b	=	13,44 m
Leg spacing	x_{leg}	=	50 m
Leg diameter	D_1	=	10 m

The following table gives particulars for two existing practices and ISO 19905-1.

Practice I:

Irregular waves:

	C_D	D	l	cos	
Tubular	1,0	*0,3	*13,44	*0,6	= 2,419
Chord 1	2,114	*0,7	*1,0	*1,0	= 1,479
Chord 2,3	1,279	*0,7	*2,0	*1,0	= 1,790
$C_{De}D_e$					5,688

Kinematics according to:
Delta stretching

Regular waves: Stokes' fifth

	C_D	D	l	cos	
Tubular	0,7	*0,3	*13,44	*0,6	= 1,693
Chord 1	1.486	*0,7	*1,0	*1,0	= 1,040
Chord 2,3	0,896	*0,7	*2,0	*1,0	= 1,245
$C_{De}D_e$					3,989

No shielding assumed

Practice II:

Regular waves : Stokes' fifth

Tubular	0,64	*0,3	*13,44	*0,6	= 1,548
Chord 1	1,307	*0,7	*1,0	*1,0	= 0,915
Chord 2,3	0,973	*0,7	*2,0	*1,0	= 1,362
$C_{De}D_e$					3,825

Irregular waves: Airy with constant stretching

$C_{De}D_e$	=	3,825 * 1,3	= 4,973

ISO 19905-1:

	C_D	D	l	cos	
Tubular	1,0	*0,3	*13,44	*0,6	= 2,419
Chord 1	2,057	*0,7	*1,0	*1,0	= 1,440
Chord 2,3	1,056	*0,7	*1,0	*2,0	= 1,478
z < 1,5 m					5,338
z > 1,5 m					4,491

Kinematics according to:
Wheeler stretching

Regular waves: Stokes' fifth

No shielding for waves
Reduction of current by a factor:
$1/[1 + C_{De}D_e/(4D_1)] = 0,88$

Table TR.7.B.1 — Comparison including wave height scaling
Water depth = 30 m, H_{srp} = 10 m

Case	Environment H/T H_s/T_z m and s	Current m/s	Base shear MN	Overturning moment MNm
Regular waves Practice I $H = H_{max} = 1{,}86\ H_{srp}$	18,6/14,0	0,0 1,0	5,58 8,03	143 197
Regular waves Practice II $H = H_{max} = 1{,}86\ H_{srp}$	18,6/14,0	0,0 1,0	5,42 7,70	139 189
Irregular waves Practice II $H_s = H_{srp}$	10,0/11,0	0,0 1,0	3,18 6,89	108 145
Regular waves ISO 19905-1 $H = H_{det} = 0{,}86\ H_{max}$	16,5/14,0	0,0 0,88	4,90 6,96	115 157
Irregular waves ISO 19905-1 H_s = [1+,5exp(-d/25)]*H_{srp}	11,84/11,0	0,0 0,88	5,95 7,88	122 154

Table TR.7.B.2 — Comparison including wave height scaling
Water depth = 90 m, H_{srp} = 14,0 m

Case	Environment H/T H_s/T_z m and s	Current m/s	Base shear MN	Overturning moment MNm
Regular waves Practice I $H = H_{max} = 1{,}86\ H_{srp}$	18,6/16,5 26,0/16,5	0,0 0,5	9,82 12,30	668 819
Regular waves Practice II $H = H_{max} = 1{,}86\ H_{srp}$	18,6/16,5 26,0/16,5	0,0 0,5	9,41 11,79	641 785
Irregular waves Practice II $H_s = H_{srp}$	14,0/13,0 14,0/13,0	0,0 0,5	11,22 13,11	747 859
Regular waves ISO 19905-1 $H = H_{det} = 0{,}86\ H_{max}$	23,14/16,5 23,14/16,5	0,0 0,44	8,90 11,20	578 709
Irregular waves ISO 19905-1 H_s = [1+,5exp(-d/25)]*H_{srp}	14,34/13,0 14,34/13,0	0,0 0,44	9,12 10,80	573 671

The results for both the 30 m and 90 m water depth cases in Tables TR.7.B-1 and TR.7.B-2 show improved agreement between regular and irregular wave force calculations for ISO 19905-1 methodology as compared to Practice II.

The main differences between Practice II and ISO 19905-1 are as follows:

— ISO 19905-1 uses a reduced wave height for regular wave analysis in this comparative study instead of a reduced drag coefficient;

— ISO 19905-1 includes a shallow water wave height correction to be applied to the significant wave height used in irregular wave analysis.

The shallow water wave height correction term is described and justified in TR.6.4.2.6. The effect of wave asymmetry in shallow water in Practice II is included only by a conservative kinematics model above the mean water level for an irregular wave analysis. Other practices give no consideration to shallow water effects in irregular wave analysis.

The agreement between regular and irregular wave forces is better at the 90 m water depth case than for the 30 m water depth case. However, the correction term for shallow water cases is justified as compared to the Practice II results.

APPENDIX TR.7.C: Comparison of test results for chords

Split tube chords compared in the following:

	rack ratio W/D
F&G	1,08
NKK	1,10
MLMC	1,13
MSC	1,19
MLMC	1,24

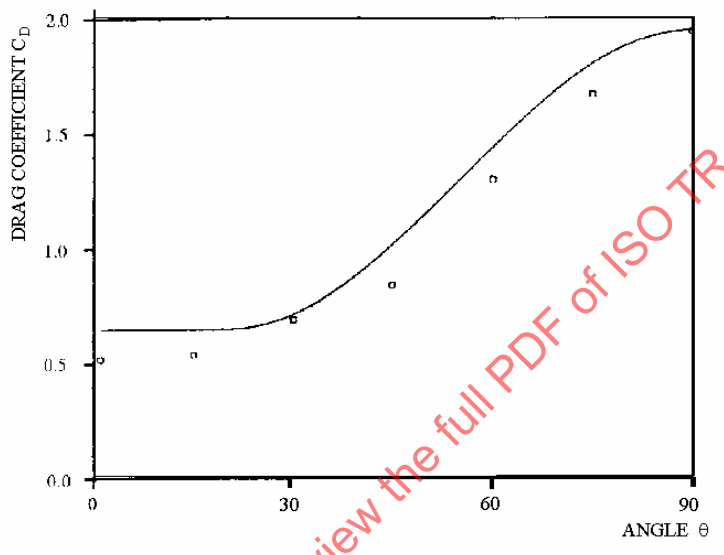

Figure TR.7.C-1 — Comparison of the ISO 19905-1 formulation with model tests, ratio W/D = 1,08[7-58]

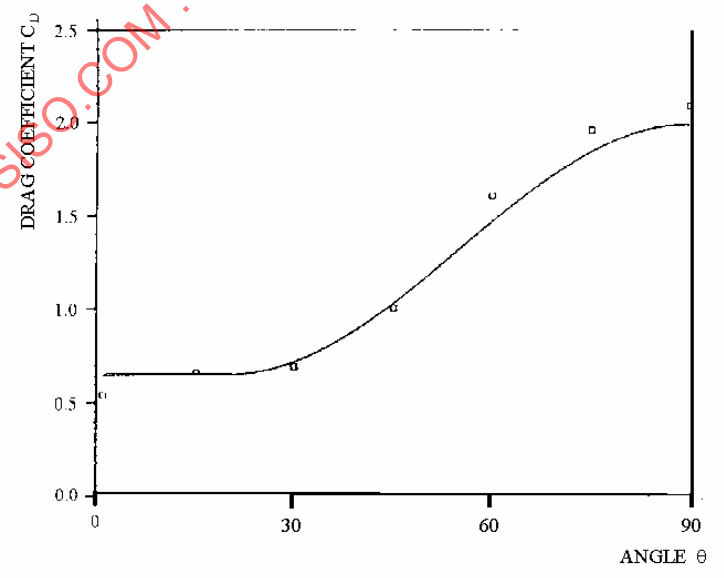

Figure TR.7.C-2 — Comparison of the ISO 19905-1 formulation with model tests, ratio W/D = 1,10[7-59]

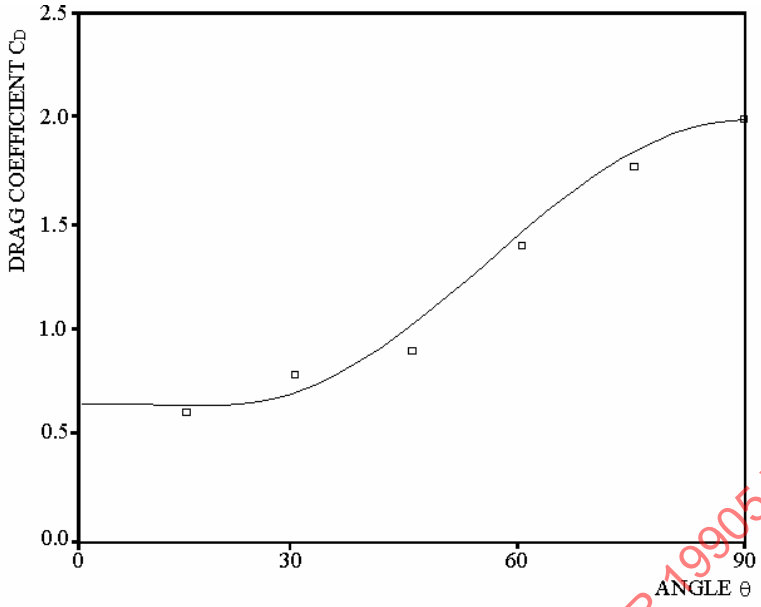

Figure TR.7.C-3 — Comparison of the ISO 19905-1 formulation with model tests, ratio WlD = 1,13[7-60]

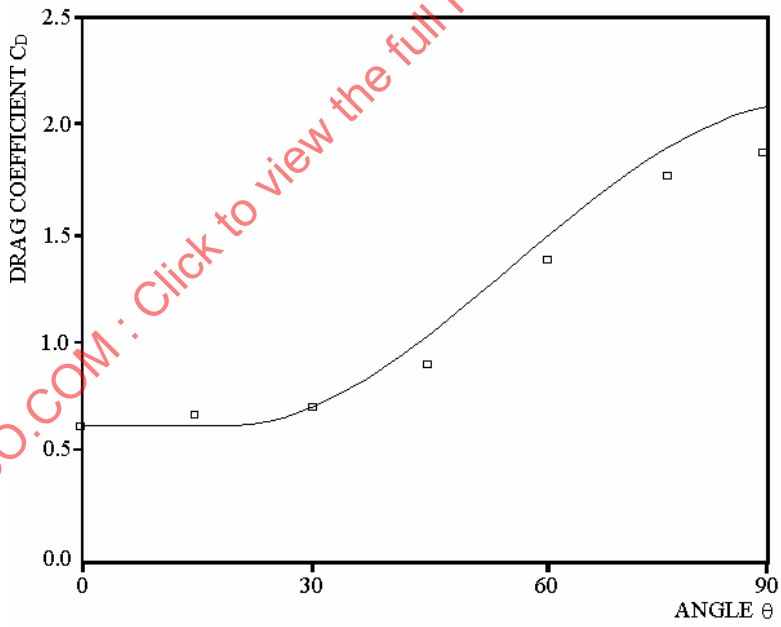

Figure TR.7.C-4 — Comparison of the ISO 19905-1 formulation with model tests, rack WlD = 1,19[7-2]

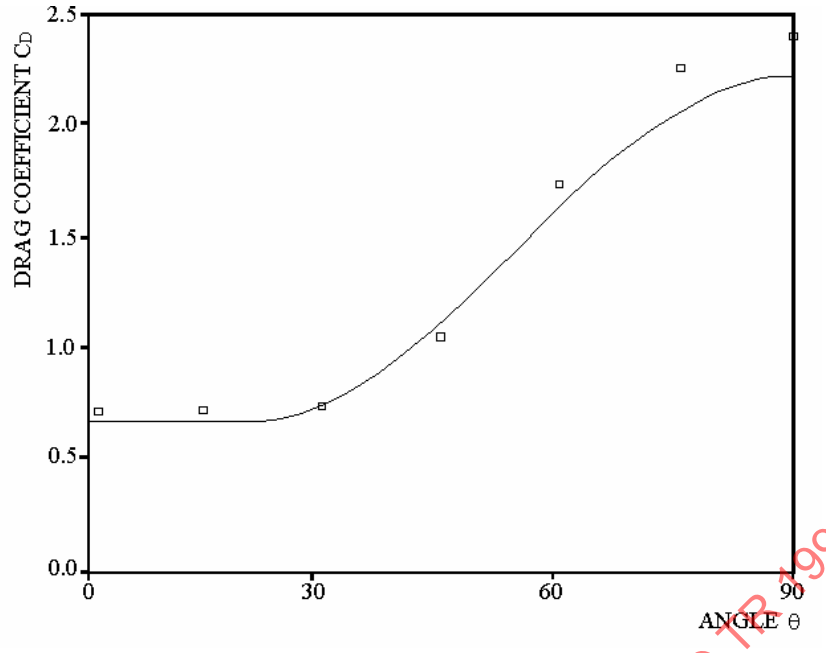

Figure TR.7.C-5 — Comparison of the ISO 19905-1 formulation with model tests, rack W/D = 1,24[7-60]

8 Commentary to ISO 19905-1:2012, Clauses 8 and A.8

TR A.8.8.6 Derivation of the alternative simplified negative stiffness correction term for P-Δ effects

TR A.8.8.6.1 Summary

The method described below allows a simple procedure for incorporating P-Δ effects in a jack-up structural analysis by means of a negative stiffness. The advantage of this simple procedure is the ability to include such effects without the necessity to adopt the iterative procedures required by other methods. This method is accurate in determining the global response parameters, including hull displacement and base overturning moment. It is also accurate in determining the leg moment below the lower guide (usually the most critical part of the leg). In its simplest form the procedure will conservatively predict the shear in the legs (by roughly 10 %). However, leg shear is rarely a controlling factor in structural assessments; therefore, this difference is insignificant.

TR A.8.8.6.2 Description of the method

The incorporation of P-Δ effects in the structural analysis is accomplished by including a correction term in the global stiffness matrix of the structure. When an analysis is performed with the correction term included, the resulting deflections, etc. will include P-Δ effects. Note that since the global stiffness matrix is modified before the analysis, no subsequent changes to the matrix are required (i.e. no iterations are required in the solution).

The correction term to the global stiffness matrix is determined by a simple hand calculation and is:

$$-P_g/L$$

where

P_g is the effective hull gravity load (includes hull weight and weight of the legs above the hull);

L is the distance from the spudcan point of rotation to the hull centre of gravity.

This single (negative) value is then incorporated into the global stiffness matrix of the jack-up structural model. This can be accomplished in various ways depending on the software in use. Typically, an orthogonal pair of horizontal translational earthed spring elements can be attached to a node representing the hull centre of gravity, and the negative value is entered for each of the spring constants. Some software packages allow direct matrix manipulation.

The effect of the negative stiffness is to produce an additional overturning load at the hull. The overturning moment produced by this lateral load about the base is equal to the overturning moment caused by the vertical load (of hull and legs above the hull) times the deflection of the hull. Thus, the effect of the translation of the vertical load is incorporated as a lateral force couple.

TR A.8.8.6.3 Basis for the method

The P-Δ effect is a consideration of the displacement of the structure under the applied loads. In its most general form, the solution considers the displacements of each element of the structure under loading. This is typically called a 'large displacement' solution. In this general procedure, the deflections of the structure are used to reform the stiffness matrix, which is then used to recalculate the displacements. While this is analytically correct, there is a requirement to resolve the stiffness matrix several times for each loading condition.

If the overall structural displacements are not very large, approximate solutions may be used. Typically, approximate solutions are valid if $\tan\theta \approx \theta$, where θ is the rotation of the structure about its base. These approximate solutions are known as “geometric stiffness” solutions. The classical column moment magnification or “Euler amplification” term is an example. The negative spring method is another example, which allows a simple procedure to incorporate P-Δ effects in a jack-up structural analysis. The advantage of

this simple procedure is the ability to include such effects without the necessity to adopt the iterative procedures required by other methods.

The P-Δ effect for jack-up structures is manifested as a change in lateral stiffness of the individual legs, given a change in the axial load in each leg. For jack-ups the change in axial load in each leg is caused by the application of the gravity loading and environmental loading. The net effect on the P-Δ of the axial load changes in each leg due to the environmental loading cancels out. Thus, for overall structural response, only the gravity load need be considered in the calculation of P-Δ effects. The reduced stiffness then affects the response to environmental loadings.

The derivation of this simple method and a comparison of this simple method with an "exact" solution are presented below.

TR A.8.8.6.4 Derivation of the simplified correction term

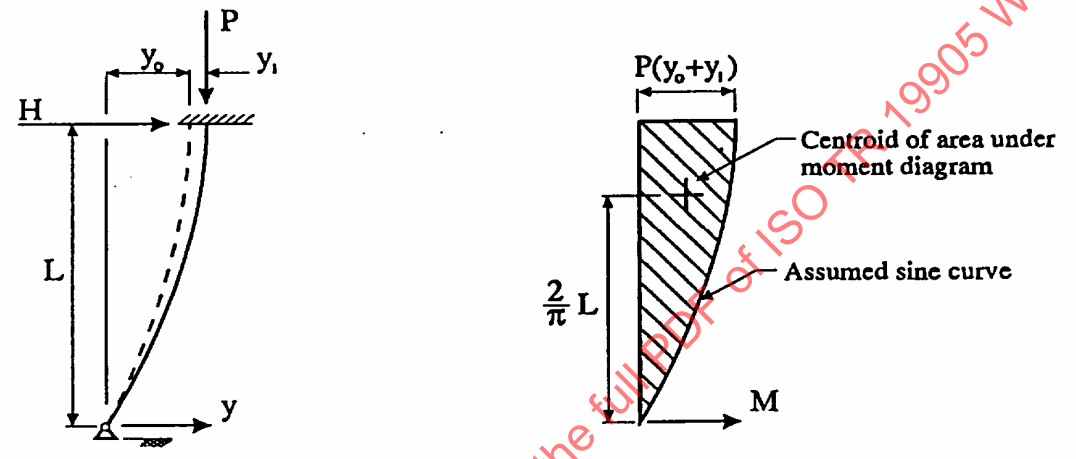

a) Beam deflection

b) Moment diagram
(due to secondary bending only)

Ref.: Salmon and Johnson, *Steel Structures*, p 620.

y_0 is the deflection without axial load, P

y_1 is the additional lateral deflection due to axial load, P

To calculate y_1, take moment of M/EI diagram between support and midspan

$$y_1 = \frac{P(y_0 + y_1)}{EI}\left\{\frac{2L}{\pi}\right\}\left\{\frac{2L}{\pi}\right\}$$

Centroid of area under moment diagram
Area under moment diagram

Rearranging:

$$y_1 = (y_0 + y_1)\frac{4PL^2}{\pi^2 EI}$$

using:

$$P_E = \frac{\pi^2 EI}{(kL)^2} \quad \text{(with } k = 2\text{)}$$

$$y_1 = (y_0 + y_1)\frac{P}{P_E}$$

$$y_1 = y_0\left\{\frac{P/P_E}{1-P/P_E}\right\}$$

Total lateral deflection: $y_{max} = y_0 + y_1$

$$y_{max} = y_0 + y_0\left\{\frac{P/P_E}{1-P/P_E}\right\}$$

$$= y_0\left\{\frac{1}{1-P/P_E}\right\}$$

"Euler amplification" term

Determine effect on stiffness:

Define $K_o = \frac{H}{y_0}$ Lateral stiffness without axial load, P

$$= \frac{3EI}{L^3}$$

Define $K_1 = \frac{H}{y_{max}}$ Lateral stiffness with axial load, P

$$= \frac{H}{y_0}\left\{1-\frac{P}{P_E}\right\}$$

$$= K_o\left\{1-P\left[\frac{4L^2}{\pi^2 EI}\right]\right\}$$

$$= K_o - P\left\{\frac{3EI}{L^3}\right\}\left\{\frac{4L^2}{\pi^2 EI}\right\}$$

$$= K_o - \left\{\frac{12}{\pi^2} * \frac{P}{L}\right\}$$

Conclusion: Effective lateral stiffness reduced by $-\frac{12P}{\pi^2 L}$

where

P is the axial load in one leg.

NOTE This is based on assuming a sine curve for deflection.

Repeat calculations assuming a linear deflection (rather than a sine curve):

$$y_1 = \frac{P(y_0 + y_1)}{EI}\left\{\frac{L}{2}\right\}\left\{\frac{2L}{3}\right\}$$

Centroid of area under moment diagram
Area under moment diagram

Rearranging:

$$y_1 = (y_0 + y_1)\frac{PL^2}{3EI}$$

$$y_1 = y_0\left\{\frac{PL^2 / 3EI}{1 - PL^2 / 3EI}\right\}$$

$$y_{max} = y_0 + y_1$$

$$y_{max} = y_0\left\{\frac{1}{1 - PL^2 / 3EI}\right\}$$

Amplification for linear assumption

Determine effect on stiffness:

Define $K_o = \frac{H}{y_0}$ Lateral stiffness without axial load, P

$$= \frac{3EI}{L^3}$$

Define $K_1 = \frac{H}{y_{max}}$ Lateral stiffness with axial load, P

$$= \frac{H}{y_0}\left\{1 - \frac{PL^2}{3EI}\right\}$$

$$= K_o\left\{1 - \left[\frac{PL^2}{3EI}\right]\right\}$$

$$= K_o - \frac{P}{L}$$

Conclusion: Based on linear deflection assumption, lateral stiffness is reduced by $-P/L$ term. This is the usual approximation of geometric stiffness.

Effect on total jack-up stiffness:

$K_E = K_{e1} + K_{e2} + K_{e3}$ sum of individual leg stiffnesses (neglects hull rotation)

For each leg:

$$P = P_{gravity} + P_{environment}$$

$$K_E = [k_{01} - \frac{12}{\pi^2}\frac{1}{L}(P_{g1} + P_{e1})] + [k_{02} - \frac{12}{\pi^2}\frac{1}{L}(P_{g2} + P_{e2})] + \ldots$$

$$= (k_{01} + k_{02} + k_{03}) - \frac{12}{\pi^2}\frac{1}{L}(P_{g1} + P_{g2} + P_{g3}) - \frac{12}{\pi^2}\frac{1}{L}(P_{e1} + P_{e2} + P_{e3})$$

Assume net vertical environmental load $(P_{e1} + P_{e2} + P_{e3}) = 0$

$K_E = (\Sigma K_{0i}) - \frac{12}{\pi^2}\frac{P_G}{L}$, where P_G is total gravity load only

If linear deflection assumption is made:

$$K_E = (\Sigma K_{0i}) - \frac{P_G}{L}$$

TR A.8.8.6.5 Verification against an "exact" solution

Verification of this simple procedure was made against an "exact" solution. In this case, the "exact" solution was performed using analysis software which accounts for large displacements. In this procedure, the displaced configuration of the structure is used to update the stiffness matrix, and iteration is used to converge on a given solution.

Verification was performed using a jack-up structural model as shown in Figure TR.A.8.8.6-1. The leg chord, horizontal and diagonal members are modelled as individual elements. The hull (in this case) is assumed to act as a rigid body. The hull to leg connection included leg clamping devices. These were modelled along with the leg guides. For the purpose of this verification, the detailing of the hull and leg/hull connection is not important. The spudcans were modelled as "pinned".

Loading of the model was accomplished as shown on Figure TR.A.8.8.6-2. Loadings due to wave and wind (and dynamic inertial) were considered separately to verify the behaviour under the two separate types of loading. The loading direction was towards the bow in both cases. For each case, a vertical load was applied at the hull centre of gravity. It is interesting to note that the vertical load is necessary for solution using "exact" large displacement methods, but is not needed to obtain a solution using the simple method.

A summary of the comparison results is given in Tables TR.A.8.8.6-1 (wave load) and TR.A.8.8.6-2 (wind load). Verification with these two load cases was done separately, since the loading occurs on different parts of the structure. The level of loading is arbitrary. Values assumed here are greater than used in the site assessment of this particular jack-up.

Discussion of the individual response parameters from Tables TR.A.8.8.6-1 and TR.A.8.8.6-2 is given below.

a) Global response parameters

The fundamental response quantities of deck displacement and overturning moment agree to within 1%. The base shear for the simple method is not correct since it includes the additional (fictitious) lateral force applied to the hull. The difference between the total applied force and the base shear is the additional lateral force applied at the hull. In theory, the moment due to the vertical load (P-Δ moment) should be replaced by a lateral force couple, i.e. lateral loads at the hull and base. Reduction of the base shear (in global axes) by this additional lateral force at the hull will equate the global base shear with the applied load.

b) Windward and leeward leg parameters

The values for individual leg axial load and moment at the lower guide agree to within 1%. These quantities are the most critical parameters for structural assessments.

The distribution of global base shear among the individual legs is not as accurately matched by the simple method. For each leg, the lateral stiffness is decreased by increasing axial load. Thus, the distribution of global base shear will depend on the axial load present in each leg. The simple method, since it lumps the effects of all legs into one correction term, cannot accurately predict the shear re-distribution among the legs.

This lack of re-distribution of global base shear loading is not generally important to a structural assessment. The amount will depend on the level and type of loading (wave or wind). For the two cases given, 1% and 5% of the total base shear load (in global axes) is shifted from the leeward leg to the windward legs.

When the leg base shears are not corrected, the simple method conservatively over-predicts the shear in the legs. Since shear force is not as critical as the leg bending moment this conservatism is not very restrictive.

If a correction is desired, the added lateral load at the hull can be subtracted in equal fractions from the leg spudcan reactions (in global axes). Note that, in the case of the windward leg, this will slightly under-predict the "correct" global shear reaction.

Table TR.A.8.8.6-1 — Verification of simple procedure for P-Δ effect with exact solution — Wave loading case

	No P-Δ	**Simple method**	**Exact solution**
Global response parameters			
Hull displacement (inches)	21.6	24.5	24.7
Base OTM (Kip-ft $\times$ 10^3)	227.	253.	251.
Base Shear (kips)	711.	780.	711.
(Added lateral load at hull, kips)		(69.)	
Windward leg parameters			
Axial force (kips)	3 638.	3 524.	3 534.
Shear at spudcan (kips)	250.	272.	254.
(Corrected by 69/3 =23 kips)		(249.)	
Moment at lower guide(Kip-ft $\times$ 10^3)	48.	56.	56.
Leeward leg parameters			
Axial force (kips)	5 477.	5 706.	5 685.
Shear at spudcan (kips)	212.	235.	204.
(Corrected by 69/3 =23 kips)		(212.)	
Moment at lower guide(Kip-ft $\times$ 10^3)	57.	65.	65.
Shear transferred from leeward leg to windward leg due to P-Δ (kips)		0.	8.

Table TR.A.8.8.6-2 — Verification of simple procedure for P-Δ effect with exact solution — Wind loading case

	No P-Δ	Simple method	Exact solution
Global response parameters			
Hull displacement (inches)	44.9	51.0	51.4
Base OTM (Kip-ft $\times$ 10^3)	490.	545.	541.
Base Shear (kips)	1 055.	1 198.	1 055.
(Added lateral load at hull, kips)		(143.)	
Windward leg parameters			
Axial force (kips)	2 538	2 300.	2 318.
Shear at spudcan (kips)	352.	399.	375.
(Corrected by 143/3 = 48 kips)		(351.)	
Moment at lower guide(Kip-ft $\times$ 10^3)	124.	141.	141.
Leeward leg parameters			
Axial force (kips)	7 803.	8 279.	8 242.
Shear at spudcan (kips)	352.	400.	305.
(Corrected by 143/3 = 48 kips)		(352.)	
Moment at lower guide(Kip-ft $\times$ 10^3)	124.	141.	140.
Shear transferred from leeward leg to windward leg due to P-Δ (kips)		0.	47.

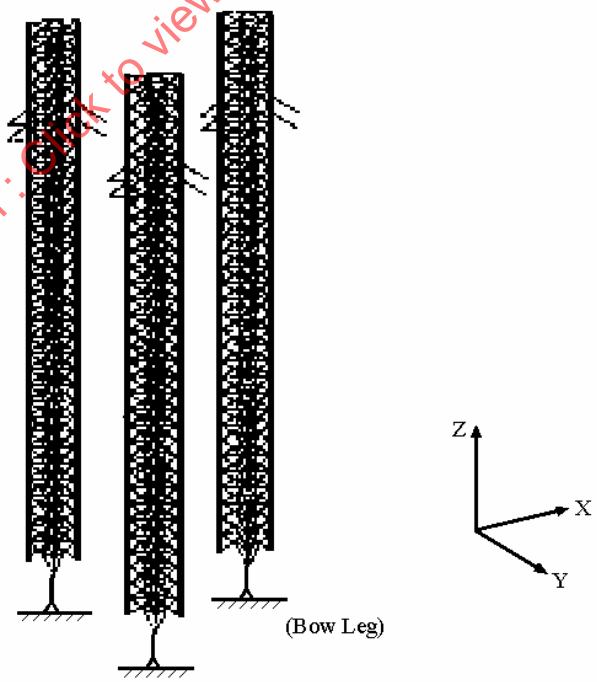

Figure TR.A.8.8.6-1 — Analysis model

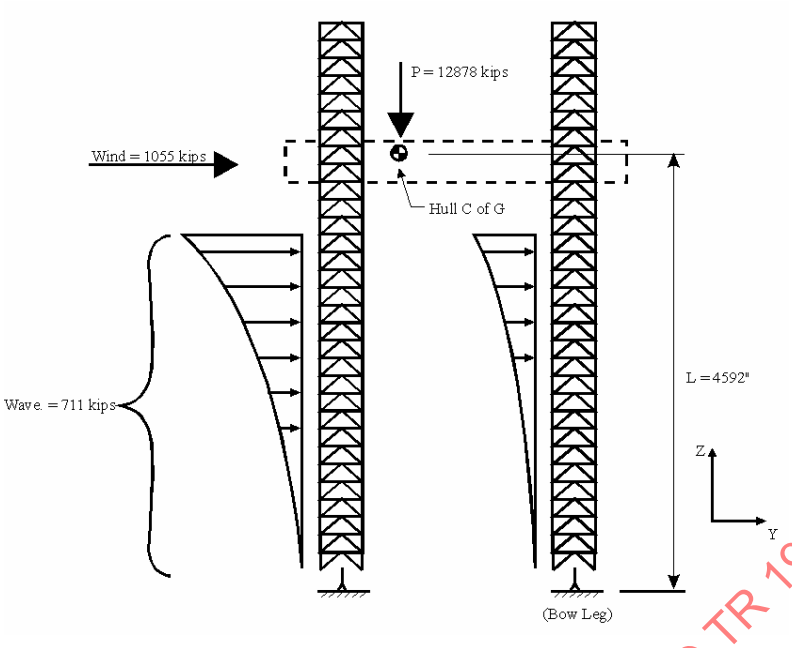

Figure TR.A.8.8.6-2 — Load application

9 Commentary to ISO 19905-1:2012, Clauses 9 and A.9

TR.9.3.6.2 Derivation of the limiting horizontal reaction given in ISO 19905-1:2012, Table A.9.3.7

When F_M = 0 the yield surface equation, ISO 19905-1:2012, Equation (A.9.3-30), can be rearranged to give:

$$\left[\frac{F_H}{Q_H}\right]^2 = 16(1-a)\left[\frac{F_V}{Q_V}\right]^2\left[1-\frac{F_V}{Q_V}\right]^2 + 4a\left[\frac{F_V}{Q_V}\right]\left[1-\frac{F_V}{Q_V}\right] \quad (9\text{-}1)$$

where

a is the depth interpolation parameter;

F_H is the horizontal force applied to the spudcan due to the assessment load case;

F_V is the gross vertical force acting on the soil beneath the spudcan due to the assessment load case;

Q_V is the gross ultimate vertical foundation capacity.

If the preload resistance factor, $\gamma_{R,PRE}$ =1,1, the term $\frac{F_V}{Q_V}$ can be express as follows:

$$\frac{F_V}{Q_V} = \frac{\frac{V_{Lo}}{1,1} + W_{BF} - B_S}{Q_V}$$

$$= \frac{\frac{V_{Lo} + 1,1W_{BF} - 1,1B_S}{1,1}}{Q_V}$$

$$= \frac{V_{Lo} + W_{BF} - B_S + 0,1(W_{BF} - B_S)}{1,1Q_V}$$

$$= \frac{Q_V + 0,1(W_{BF} - B_S)}{1,1Q_V}$$

$$= \frac{Q_V + 0,1(Q_V - V_{Lo})}{1,1Q_V}$$

$$= \frac{1,1Q_V - 0,1V_{Lo}}{1,1Q_V}$$

where

B_S is the soil buoyancy of spudcan below bearing area, i.e. the submerged weight of soil displaced by the spudcan below D, the greatest depth of maximum cross-sectional spudcan bearing area below the sea floor;

V_{Lo} is maximum vertical reaction under the spudcan considered required to support the in-water weight of the jack-up during the entire preloading operation (this is not the soil capacity);

W_{BF} is the submerged weight of the backfill.

Hence:

$$\frac{F_V}{Q_V} = 1 - \frac{0,1V_{Lo}}{1,1Q_V} \tag{9-2}$$

$$1 - \frac{F_V}{Q_V} = \frac{0,1V_{Lo}}{1,1Q_V} \tag{9-3}$$

Substituting Equations (9-2) and (9-3) into Equation (9-1):

$$\left[\frac{F_H}{Q_H}\right]^2 = 16(1-a)\left[1 - \frac{0,1V_{Lo}}{1,1Q_V}\right]^2\left[\frac{0,1V_{Lo}}{1,1Q_V}\right]^2 + 4a\left[1 - \frac{0,1V_{Lo}}{1,1Q_V}\right]\left[\frac{0,1V_{Lo}}{1,1Q_V}\right]$$

$$= 16(1-a)\left[\frac{0,1^2V_{Lo}{}^2}{1,1^2Q_V{}^2} - 2\frac{0,1^3V_{Lo}{}^3}{1,1^3Q_V{}^3} + \frac{0,1^4V_{Lo}{}^4}{1,1^4Q_V{}^4}\right] + 4a\left[\frac{0,1V_{Lo}}{1,1Q_V} - \frac{0,1^2V_{Lo}{}^2}{1,1^2Q_V{}^2}\right] \quad \text{“Exact” solution} \tag{9-4}$$

For a = 0:

$$\left[\frac{F_H}{Q_H}\right]^2 = 16\left[1 - \frac{0,1V_{Lo}}{1,1Q_V}\right]^2\left[\frac{0,1V_{Lo}}{1,1Q_V}\right]^2$$

$$\frac{F_H}{Q_H} = 4\left[1 - \frac{0,1V_{Lo}}{1,1Q_V}\right]\left[\frac{0,1V_{Lo}}{1,1Q_V}\right] \tag{9-5}$$

For $\gamma_{R,PRE}$ = 1,1, Equation (9-5) yields a nearly linear curve which can be approximated by the following linear relationship:

$$\frac{F_H}{Q_H} \approx 0{,}33\frac{V_{Lo}}{Q_V}$$

Similarly, for a = 0 and $\gamma_{R,PRE}$ = 1,15:

$$\frac{F_H}{Q_H} = 4\left[1-\frac{0{,}15V_{Lo}}{1{,}15Q_V}\right]\left[\frac{0{,}15V_{Lo}}{1{,}15Q_V}\right] \quad (9\text{-}6)$$

Equation (A.9-6) yields a nearly linear curve which can be approximated by the following linear relationship:

$$\frac{F_H}{Q_H} \approx 0{,}45\frac{V_{Lo}}{Q_V}$$

10 Commentary to ISO 19905-1:2012, Clauses 10 and A.10

TR.10.4.2.1 Natural period — General

It is anticipated that most site assessments of jack-ups will use computer-based structural models to determine the unit's natural period. The following discussion is given, however, to help the analyst better understand the contribution of the different components of mass, compliance and stiffness on the natural period. Due to the fact that the mass of the hull dominates the mass distribution of a jack-up, the global dynamic behaviour can be determined from an idealized single degree-of-freedom system. Thus the fundamental mode period can be estimated from a system described by:

— an equivalent mass representing the mass of the jack-up and its distribution (see ISO 19905-1:2012, 10.4.2.3). The equivalent mass is equal to the mass of the hull plus a contribution from the mass of the legs, including added mass, and is located at the centre of gravity of the hull.

— an equivalent spring representing the combined effect of the overall (global) structural stiffness. This includes stiffness contributions from: leg bending, leg shear deformation, axial straining of the legs, the leg to hull connections, the hull and the spudcan-foundation interface (if applicable).

The period is determined from the following equation applied to one leg:

$$T_n = 2\pi\sqrt{(M_e / K_e)} \quad (10\text{-}1)$$

where

T_n is the highest (or first mode) natural period;

M_e is the effective mass associated with one leg;

$$= \frac{M_{hull}}{N} + M_{la} + \frac{M_{lb}}{2} \quad (10\text{-}2)$$

M_{hull} is the full mass of hull including maximum variable load;

N is the number of legs;

M_{la} is the mass of leg above lower guide (in the absence of a clamping mechanism) or above the centre of the clamping mechanism;

M_{lb} is the mass of leg below the point described for M_{la}, including added mass for the submerged part of the leg ignoring spudcan; the added mass may be determined as $A_e\rho(C_{Me} - 1)$ per unit length of one leg (for definitions of A_e and C_{Me}, see ISO 19905-1:2012, A.7.3.2.3); ρ = mass density of water.

K_e is the effective stiffness associated with one leg (for derivation, refer to TR.10.4.2.2).

$$= \frac{3EI}{L^3} \frac{\left[1-\frac{P}{P_E}\right]}{\left[1-\frac{\frac{3L}{4}-\frac{12F_gI}{AF_vY^2}\left\{\frac{EI}{K_{rs}}+\frac{L}{2}\right\}-\frac{3(EI)^2}{F_rLK_{rs}K_{rh}}}{\left\{\frac{EI}{K_{rs}}+L+\frac{EI}{F_rK_{rh}}\right\}}+\frac{7.8I}{A_sF_hL^2}\right]} \quad (10\text{-}3)$$

When the soil rotational stiffness K_{rs} at the spudcan-foundation interface is zero this may be re-written:

$$K_e = \frac{3EI}{L^3} * \frac{\left[1-\frac{P}{P_E}\right]}{\left[1+\frac{12F_gI}{AF_vY^2}+\frac{3EI}{F_rLK_{rh}}+\frac{7,8I}{A_sF_hL^2}\right]} \quad (10\text{-}4)$$

K_{rs} is the rotational spring stiffness at spudcan-foundation interface;

K_{rh} is the rotational stiffness representing leg to hull connection stiffness (see below);

F_r is the factor to account for hull bending stiffness

$$= \frac{1}{\left\{1+\frac{YK_{rh}}{2EI_H}\right\}} \quad (10\text{-}5)$$

I_H is the representative second moment of area of the hull girder joining two legs about a horizontal axis normal to the line of environmental action;

E is Young's modulus for steel;

A is the axial area of one leg (equals sum of effective chord areas, including a contribution from rack teeth; see ISO 19905-1:2012, A.8.3.3, Note);

A_s is the effective shear area of one leg (see ISO 19905-1:2012, Figure A.8.3-1);

I is the second moment of area of the leg (see ISO 19905-1:2012, Figure A.8.3-2), including a contribution from rack teeth (see ISO 19905-1:2012, 8.3.5);

Y is the distance between the centre of one leg and the line joining the centres of the other two legs (3 leg jack-up)

is the distance between windward and leeward leg rows for the direction under consideration (4 leg jack-up);

F_g is the geometric factor;

= 1,125 (3 leg jack-up), 1,0 (4 leg jack-up);

F_v is a factor to account for vertical soil stiffness, K_{vs}, and vertical leg-hull connection stiffness, K_{vh} (see below)

$$= \frac{1}{\left\{1+\frac{EA}{LK_{vs}}+\frac{EA}{LK_{vh}}\right\}} \quad (10\text{-}6)$$

F_h is a factor to account for horizontal soil stiffness, K_{hs}, and horizontal leg-hull connection stiffness, K_{hh} (see below)

$$= \frac{1}{\left\{1+\frac{EA_s}{2{,}6LK_{hs}}+\frac{EA_s}{2{,}6LK_{hh}}\right\}} \quad (10\text{-}7)$$

L is the length of leg from the seabed reaction point (see A.8.6.2) to the point separating M_{la} and M_{lb} (see above);

P is the mean force due to vertical fixed load and variable load acting on one leg;

$$= \frac{M_{hull}g}{N} \quad (10\text{-}8)$$

g is the acceleration due to gravity;

P_E is the Euler buckling force of one leg

$$= \alpha 2EI \quad (10\text{-}9)$$

α is the minimum positive non-zero value of αL satisfying:

$$\tan(\alpha L) = \left\{\frac{(K_{rs}+K_{rh})\alpha EI}{(\alpha EI)^2-(K_{rs}K_{rh})}\right\} \quad (10\text{-}10)$$

Thus:

— when K_{rs} = 0 and K_{rh} = ∞, αL = π/2 and hence:

$$P_E = \frac{\pi^2 EI}{4L^2} \quad (10\text{-}11a)$$

— when K_{rs} = ∞ and K_{rh} = ∞, αL = π and hence

$$P_E = \frac{\pi^2 EI}{L^2} \quad (10\text{-}11b)$$

The hull to leg connection springs, K_{rh}, K_{vh} and K_{hh} represent the interaction of the leg with the guides and supporting system and account for local member flexibility and frame action. They should be computed with respect to the point separating M_{la} and M_{lb}, as described above. The following approximations may be applied:

K_{hh} = ∞

K_{vh} is the effective stiffness due to the series combination of all vertical pinion or fixation system stiffnesses, allowing for combined action with shock-pads, where fitted.

Jack-up with fixation system:

K_{rh} is the combined rotational stiffness of fixation systems on one leg;

$$= F_n h^2 k_f \qquad (10\text{-}12a)$$

where

F_n = 0,5 (three chord leg); = 1,0 (four chord leg);

h is the distance between chord centres;

k_f is the combined vertical stiffness of all fixation system components on one chord.

Jack-up without fixation system:

K_{rh} is the rotational stiffness allowing for pinion stiffness, leg shear deformation and guide flexibility;

$$= F_n h^2 k_j + \frac{k_u d^2}{1+(2{,}6 k_u d/EA_s)} \qquad (10\text{-}12b)$$

where

h is the distance between chord centres (opposed pinion chords) or pinion pitch points (single rack chords);

k_j is the combined vertical stiffness of all jacking system components on one chord;

d is the distance between upper and lower guides;

k_u is the total lateral stiffness of upper guides with respect to lower guides;

A_s is the effective shear area of leg.

The above equations for estimating the fundamental natural period are approximate and ignore the following effects:

— more realistic representation of possible fixity at the spudcan-foundation interface in the form of (coupled) horizontal, vertical and rotational spring stiffnesses;

— three dimensional influences of the system as compared with the two-dimensional single leg model.

TR.10.4.2.2 Derivation of K_e, effective stiffness used to calculate the jack-up natural period

To determine K_e, the effective stiffness associated with one leg, given in Equation (10-3) above, which can be used in conjunction with a proportioned equivalent jack-up mass to calculate a natural period, the following effects which cause hull lateral deflections are considered:

a) bending of the legs, leg-soil and leg-hull rotational stiffness;

b) shear deformation of the legs;

c) axial deformation of the legs;

d) hull bending deformation;

e) horizontal soil and leg-hull connection stiffness;

f) vertical soil and leg-hull connection stiffness;

g) second order P-Δ or Euler amplification.

Effects d), e) and f) can readily be considered by means of modifications to terms in the stiffness equation that can be derived for effects a), b) and c). Taking each effect in turn:

a) Bending of the legs, leg-soil and leg-hull rotational stiffness

Consider one leg as shown in the following figure:

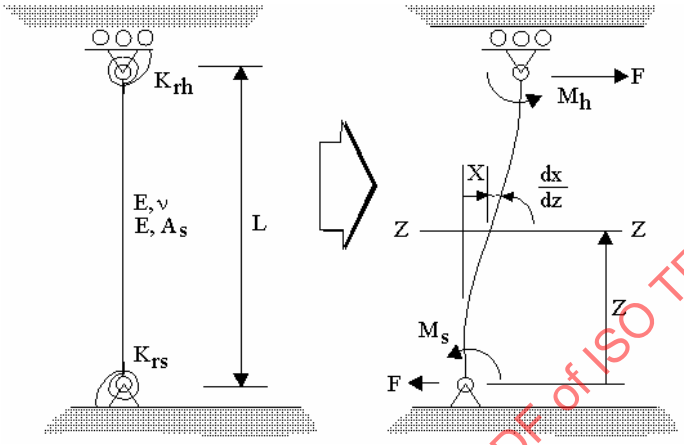

F is the shear transmitted from the hull;

E is Young's modulus;

ν is Poisson's ratio;

I is the second moment of area of leg;

A_s is the effective leg shear area;

L is the length considered;

K_{rh} is the leg-hull connection rotational stiffness;

K_{rs} is the leg-soil connection rotational stiffness;

M_h is the moment on leg-hull spring;

M_s is the moment on leg-soil spring.

The bending equation may be written for any section z-z as:

$$M_{zz} = Fz - M_s$$

Substituting the general equation of flexure:

$$EI\frac{\partial^2 x}{\partial z^2} = -M_{zz} = M_s - F.z$$

Hence:

$$EI\frac{\partial x}{\partial z} = -M_s z - F\frac{z^2}{2} + A \qquad (10\text{-}13)$$

$$EIx = M_s\frac{z^2}{2} - F\frac{z^3}{6} + A.z + B$$

Apply the boundary condition: z = 0, x = 0, $\frac{\partial x}{\partial z} = \frac{M_s}{K_{rs}}$

Hence: B = 0 and $A = \frac{EIM_s}{K_{rs}}$

The deflection at any point is then given by:

$$EIx = \frac{M_s z^2}{2} - \frac{Fz^3}{6} + \frac{M_s zEI}{K_{rs}}$$

To determine M_s, apply the boundary condition: $z = L$, $M_h = FL - M_s$, $\frac{\partial x}{\partial z} = \frac{M_h}{K_{rh}}$.

Also from Equation (10-13):

$$\frac{\partial x}{\partial z} = \frac{M_s.z}{EI} - \frac{F.z^2}{2EI} + \frac{M_s}{K_{rs}}$$

Thus when $z = L$:

$$\frac{\partial x}{\partial z} = \frac{M_s.L}{EI} - \frac{F.L^2}{2EI} + \frac{m_s}{K_{rs}} = \frac{M_h}{K_{rh}} = \frac{F.L - M_s}{K_{rh}}$$

Rearranging:

$$M_s = \frac{\left\{\frac{FL}{K_{rh}} + \frac{FL^2}{2EI}\right\}}{\left\{\frac{1}{K_{rs}} + \frac{1}{K_{rh}} + \frac{L}{EI}\right\}} \qquad (10\text{-}14)$$

The deflection x_{LB} at $z = L$ due to bending is [from Equation (10-13)]:

$$x_{LB} = \frac{M_s L^2}{2EI} + \frac{M_s L}{K_{rs}} - \frac{FL^3}{6EI}$$

Rearranging and substituting from Equation (10-14), the effective bending stiffness, $K_B = F/xL$B, at $z = L$ is obtained thus:

$$x_{LB} = F\left\{\frac{\left\{\left\{\frac{L}{K_{rh}}+\frac{L^2}{2EI}\right\}\left\{\frac{L^2}{2EI}+\frac{L}{K_{rs}}\right\}\right\}}{\left\{\frac{1}{K_{rs}}+\frac{1}{K_{rh}}+\frac{L}{EI}\right\}} - \frac{L^3}{6EI}\right\}$$

$$K_B = \left\{\frac{\left\{\left\{\frac{L}{K_{rh}}+\frac{L^2}{2EI}\right\}\left\{\frac{L^2}{2EI}+\frac{L}{K_{rs}}\right\}\right\}}{\left\{\frac{1}{K_{rs}}+\frac{1}{K_{rh}}+\frac{L}{EI}\right\}} - \frac{L^3}{6EI}\right\}^{-1}$$

After rearrangement and manipulation:

$$K_B = \frac{3EI/L^3}{1-\left\{\frac{\frac{3L}{4}-\frac{3(EI)^2}{LK_{rs}K_{rh}}}{\frac{EI}{K_{rs}}+L+\frac{EI}{K_{rh}}}\right\}} \qquad (10\text{-}15)$$

b) Shear deformation of the legs

Considering that the shear force at any section zz is constant, the deflection x_{zzS} due to shear is:

$$x_{zzS} = F.z/(A_s.G)$$

but:

$G = E/\{2(1 + \nu)\}$ and, for steel, $\nu = 0{,}3$

hence:

$$x_{zzS} = 2{,}6Fz/(A_sE) \qquad (10\text{-}16)$$

and the shear stiffness, K_S, when $z = L$, is:

$$K_S = \frac{F}{x_{LS}} = \frac{A_sE}{2{,}6L} \qquad (10\text{-}17)$$

c) Axial deformation of the legs

1) Consider a 3-leg jack-up, and assume that the legs are placed at the vertices of an equilateral triangle. The shear applied to the hull is $3F$, i.e. F acting on each leg.

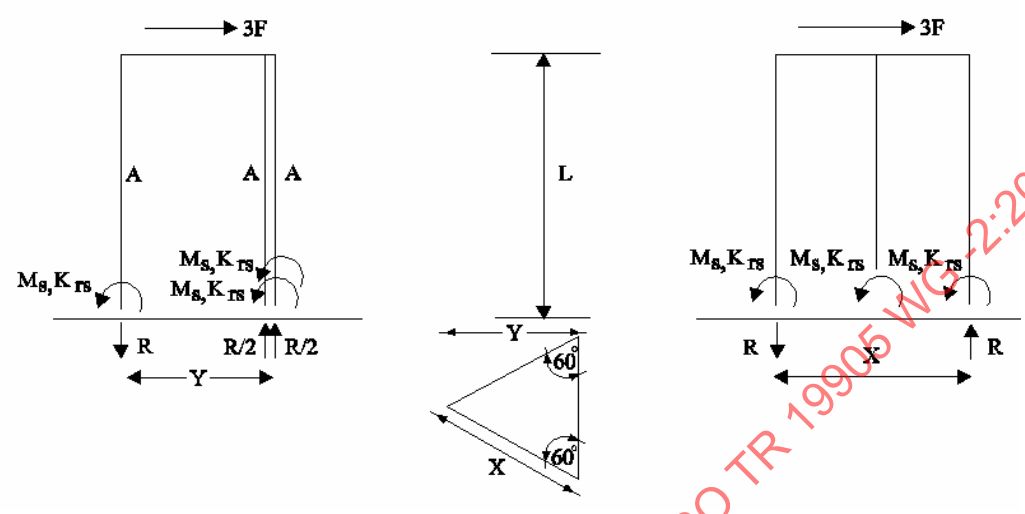

Case 1

$$3FL - 3M_s - RY = 0$$

thus:

$$R = \frac{3(FL - M_s)}{Y}$$

applying Hook's law:

$$\delta_{axial} = \frac{3(FL - M_s)L}{AEY}$$

The resulting hull rotation is:

$$\theta_{hull} = 3.\delta_{axial}/(2.Y) = \frac{9(FL - M_s)L}{2AEY^2}$$

and the horizontal hull deflection is:

$$\Delta_{horz} = \theta_{hull}.L = \frac{9(FL - M_s)L^2}{2AEY^2}$$

Case 2

$$3FL - 3M_s - RX = 0$$

thus:

$$R = \frac{3(FL - M_s)}{X}$$

$$\delta_{axial} = \frac{3(FL - M_s)L}{AEX}$$

$$\theta_{hull} = 2.\delta_{axial}/X = \frac{6(FL - M_s)L}{AEX^2}$$

$$\Delta_{horz} = \theta_{hull}.L = \frac{6(FL - M_s)L^2}{AEX^2}$$

If $X = Y/\cos 30 = \frac{Y\sqrt{3}}{2}$

$$\Delta_{horz} = \frac{9(FL - M_s)L^2}{2AEY^2}$$

i.e. assuming an equilateral hull, the two loading directions yield the same horizontal displacement at the hull:

$$\Delta_{\text{horz}} = \frac{9(FL - M_s)L^2}{2AEY^2} \tag{10-18}$$

2) Consider an N-leg jack-up where N = 4, and assume that the legs are placed in two parallel rows. The shear applied to the hull is NF, i.e. F acting on each leg.

Applying similar methods as above:

$$\Delta_{\text{horz}} = \frac{4(FL - M_s)L^2}{AEY^2} \tag{10-19}$$

where Y is the distance between the windward and leeward leg rows.

Comparing Equations (10-18) and (10-19), it can be seen that Equation (10-18) is a factor, F_g, of:

F_g = (9/2)/4 = 1,125

larger than Equation (10-19).

The effective horizontal stiffness due to axial deformation, K_A, rearranging Equation (10-19), including F_g and substituting for M_s from Equation (10-14), is:

$$K_A = \frac{F}{\Delta_{\text{horz}} F_g}$$

$$= \frac{AEY^2 / 4F_g L^2}{L - \dfrac{\left\{\dfrac{L}{K_{rh}} + \dfrac{L^2}{2EI}\right\}}{\left\{\dfrac{1}{K_{rs}} + \dfrac{1}{K_{rh}} + \dfrac{L}{EI}\right\}}}$$

$$= \frac{AEY^2 / 4F_g L^3}{\dfrac{\left\{\dfrac{EI}{K_{rs}} + \dfrac{L}{2}\right\}}{\left\{\dfrac{EI}{K_{rs}} + L + \dfrac{EI}{K_{rh}}\right\}}} \tag{10-20}$$

d) Hull bending deformation

Assume that the hull can be represented by equivalent beams joining the legs, of typical bending stiffness I_H:

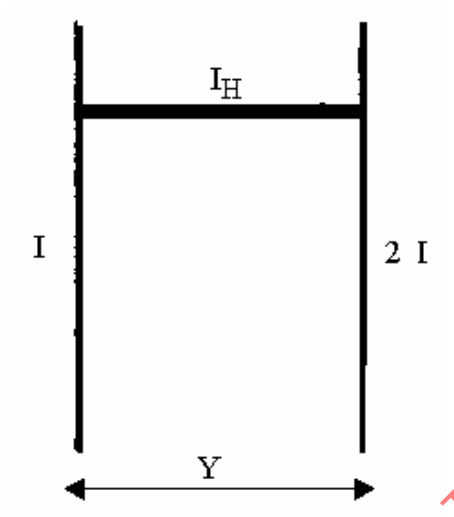

If it is assumed that the hull deflects in double-curvature under the influence of the moments transmitted by the leg-hull connection springs, and that the rotational deflections at the two sides are equal (the side with higher stiffness has two legs acting on it) we can write, for one half of the beam:

$$\theta = \frac{M(Y/2)}{EI_H}$$

Hence the hull rotational stiffness, K_{hull}, = $M/\theta = 2EI_H/Y$.

If this stiffness is considered as acting in series with the leg-hull connection spring K_{rh}, the modified stiffness is:

$$K_{rh}' = 1/\left(\frac{1}{K_{rh}} + \frac{1}{K_{hull}}\right)$$

Rearranging, and substituting for K_{hull}, gives:

$$K_{rh}' = K_{rh}/(1 + \frac{Y.K_{rh}}{2E.I_H})$$

Hence the modification factor F_r, to be applied to the leg-hull connection stiffness, K_{rh}, to account for hull flexibility is:

$$F_r = \frac{1}{\left\{1 + \frac{YK_{rh}}{2EI_H}\right\}} \qquad (10\text{-}21)$$

e) Horizontal soil leg-hull connection stiffness

The horizontal soil and leg-hull connection stiffnesses, K_{hs} and K_{hh}, can be considered to act in series with the lateral stiffness due to leg shear deformation ($A_S G/L$). The combined stiffness is then:

$$K_S' = 1/\left(\frac{L}{A_S G} + \frac{1}{K_{hs}} + \frac{1}{K_{hh}}\right)$$

Rearranging gives:

$$K_S' = (A_S G/L)/(1 + \frac{A_S G}{LK_{hs}} + \frac{A_S G}{LK_{hh}})$$

$$= (A_S G/L)(1 + \frac{A_S E}{2{,}6LK_{hs}} + \frac{A_S E}{2{,}6LK_{hh}})$$

If it is considered that the modified leg deformation stiffness K_s' is linked to the unmodified value by a factor F_h:

$$F_h = \frac{1}{\left\{1 + \frac{A_s E}{2{,}6LK_{hs}} + \frac{A_s E}{2{,}6LK_{hh}}\right\}} \quad (10\text{-}22)$$

f) Vertical soil and leg-hull connection stiffness

The vertical soil and leg-hull connection stiffnesses, K_{vs} and K_{vh}, can be considered to act in series with the axial stiffness due to leg axial deformation (AE/L). The combined stiffness is then:

$$K_A' = 1/\left(\frac{L}{AE} + \frac{1}{K_{vs}} + \frac{1}{K_{vh}}\right)$$

Rearranging:

$$K_A' = (AE/L)/\left(1 + \frac{AE}{LK_{vs}} + \frac{AE}{LK_{vh}}\right)$$

If it is considered that the modified leg deformation stiffness K_A' is linked to the unmodified value by a factor F_v:

$$F_v = \frac{1}{\left\{1 + \frac{AE}{L.K_{vs}} + \frac{AE}{L.K_{vh}}\right\}} \quad (10\text{-}23)$$

g) Second order P-Δ or Euler amplification

The deflection will (approximately) be amplified by a factor (1 – [P/P_E]) due to second order effects. The Euler load, P_E, can be derived as follows, accounting for the soil and leg-hull connection rotational springs:

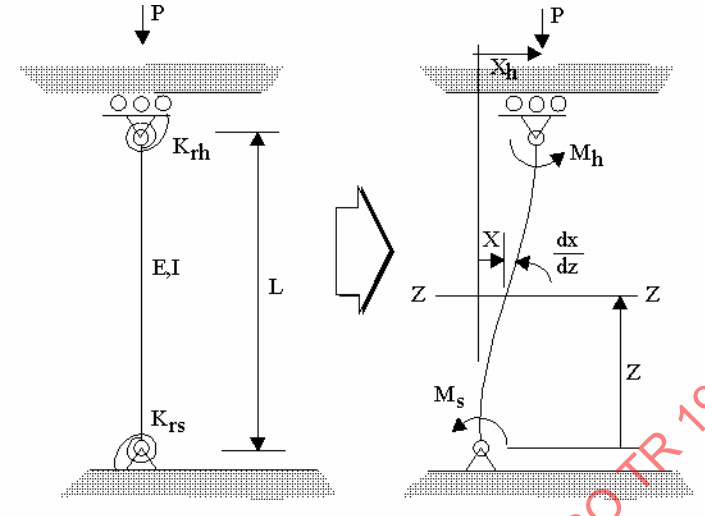

P is the axial load in leg;

E is Young's modulus;

I is the second moment of area of leg;

L is the length considered;

K_{rh} is the leg-hull connection rotational stiffness;

K_{rs} is the leg-soil connection rotational stiffness;

M_h is the moment on leg-hull spring;

M_s is the moment on leg-soil spring;

x_h is the hull deflection.

The bending equation may be written for any section z-z as:

$$M_{ZZ} = Px - M_S$$

Substituting the general equation of flexure:

$$EI\frac{\partial^2 x}{\partial z^2} = -M_{zz} = M_s - Px$$

hence:

$$\frac{\partial^2 x}{\partial z^2} + \frac{Px}{EI} = \frac{M_s}{EI}$$

Let $\mu^2 = P/(EI)$

hence:

$$\frac{\partial^2 x}{\partial z^2} + \mu^2 (x - \frac{M_s}{P}) = 0 \quad (10\text{-}24)$$

The solution to Equation (10-24) is:

$$x = A.\cos\mu z + B.\sin\mu z + \frac{M_s}{P} \quad (10\text{-}25)$$

differentiating Equation (10-25):

$$\frac{\partial x}{\partial z} = -\mu A.\sin\mu z + \mu B.\cos\mu z \quad (10\text{-}26)$$

When $z = 0$, $x = 0$ and hence, from Equation (10-25), $A = -M_s/P$

When $z = 0$, $\frac{\partial x}{\partial z} = \frac{M_s}{K_{rs}}$ and hence, from Equation (10-26), $B = M_s/(\mu.K_{rs})$

Thus: $x = \frac{-M_s}{P}.\cos\mu z + \frac{M_s}{\mu K_{rs}}.\sin\mu z + \frac{M_s}{P}$ (10-27)

and: $\frac{\partial x}{\partial z} = \frac{\mu M_s}{P}\sin\mu z + \frac{M_s}{K_{rs}}\cos\mu z$ (10-28)

Apply boundary conditions at leg-hull interface to derive the equation yielding the Euler load:

When $z = L$, $\frac{\partial x}{\partial z} = \frac{M_h}{K_{rh}}$ (10-29)

and: $x = x_h$ (10-30)

also: $M_h = Px_h - M_s$ (10-31)

From Equations (10-28) and (10-29):

$$\frac{M_h}{K_{rh}} = \frac{\mu M_s}{P}\sin\mu L + \frac{M_s}{K_{rs}}\cos\mu L \quad (10\text{-}32)$$

From Equations (10-27) and (10-30):

$$x_h = \frac{M_s}{P}\cos\mu L + \frac{M_s}{\mu K_{rs}}\sin\mu L + \frac{M_s}{P} \quad (10\text{-}33)$$

Substituting Equation (10-33) into Equation (10-31) gives:

$$M_h = -M_s\cos\mu L + \frac{P.M_s}{\mu K_{rs}}\sin\mu L$$

hence: $\frac{M_h}{M_s} = \frac{P}{\mu K_{rs}}\sin\mu L - \cos\mu L$ (10-34)

Rearranging Equation (10-32) gives:

$$\frac{M_h}{M_s} = \frac{\mu K_{rh}}{P}\sin\mu L + \frac{K_{rh}}{K_{rs}}\cos\mu L \qquad (10\text{-}35)$$

Equating Equations (10-34) and (10-35):

$$\sin\mu L\left\{\frac{P}{\mu K_{rs}} - \frac{\mu K_{rh}}{P}\right\} = \cos\mu L\left\{1 + \frac{K_{rh}}{K_{rs}}\right\}$$

or: $$\tan\mu L = \frac{\left\{1 + \frac{K_{rh}}{K_{rs}}\right\}}{\left\{\frac{P}{\mu K_{rs}} - \frac{\mu K_{rh}}{P}\right\}}$$

$$= \frac{\mu K_{rs}.P + \mu K_{rh}P}{P^2 - \mu^2 K_{rs}K_{rh}}$$

By definition $P = \mu^2 EI$, so:

$$\tan\mu L = \frac{(K_{rs} + K_{rh})\mu EI}{(\mu EI)^2 - (K_{rs}K_{rh})} \qquad (10\text{-}36)$$

NOTE 1 When $K_{rs} = 0$, and $K_{rh} = \infty$, Equation (10-36) reduces to $\tan\mu L = \infty$

i.e. $\mu L = \pi/2, 3\pi/2, 5\pi/2, \ldots$

The smallest finite value satisfying Equation (10-36) is $\pi/2$, thus $\mu L = \pi/2$ and $\mu^2 = P/(EI)$ hence:

$$P_E = \pi^2 EI / (4L^2)$$

NOTE 2 When $K_{rs} = \infty$, and $K_{rh} = \infty$, Equation (10-36) reduces to $\mathrm{Tan}\mu L = 0$

i.e. $\mu L = 0, \pi, 2\pi, 3\pi, \ldots$

Rejecting the first value ($\mu L = 0$), as this gives $P_E = 0$, the smallest value satisfying Equation (10-36) is:

$$\mu L = \pi$$

hence:

$$P_E = \pi^2 EI / L^2$$

NOTE 3 For finite values of K_{rs} and K_{rh} the Euler load may be determined using a graphical solution. For example:

$K_{rs} = 2{,}65 \times 10^{10}$ Nm/rad

$K_{rh} = 5{,}30 \times 10^{10}$ Nm/rad

$E = 2{,}10 \times 10^{11}$ N/m^2

$I = 7{,}45$ m^4

$L = 100$ m

From Equation (10-36) the LHS = $\tan\mu L$ = $\tan 100\mu$ (note μ is in radians per metre)

the RHS $= \dfrac{(K_{rs} + K_{rh})\mu EI}{(\mu EI)^2 - (K_{rs}K_{rh})}$

$= \dfrac{124{,}4\mu}{2\,448\mu^2 - 1{,}404\,5}$

Plotting these as shown in Figure C7.A.1, the smallest non-zero value in the example is:

μ_1 = 0,018 248

Thus the Euler crippling load is:

$P_E = (0{,}018\,248)^2 EI$

or, in the more general form:

$P_E = 0{,}337\,389\pi^2 EI / L^2$

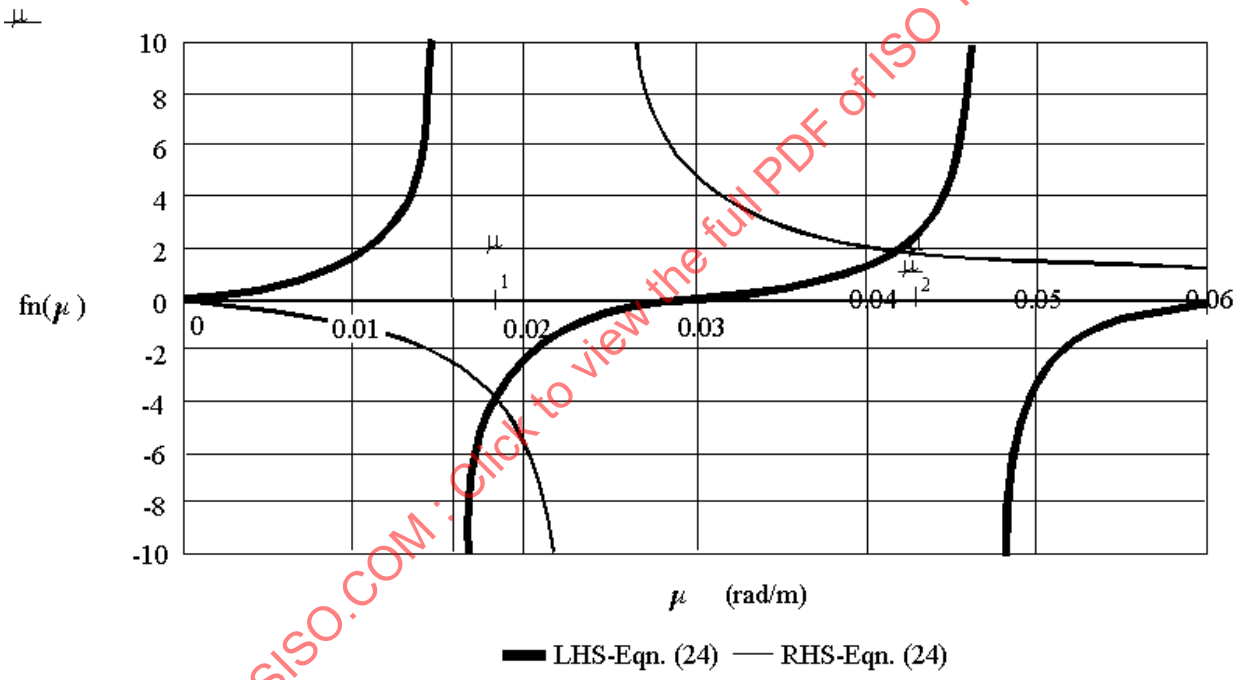

Figure C7.A.1 — Graphical solution of Equation (10-36)

Combining effects a) to g) above:

For the leg under consideration, all the effects can be combined by considering the components as springs in series, thus K_e, the effective spring stiffness for one leg, is deduced from:

$$\frac{1}{K_e} = \frac{1}{K_B} + \frac{1}{K_S} + \frac{1}{K_A}$$

where the stiffness terms K_B, K_S and K_A are derived in Equations (10-15), (10-17) and (10-20).

Rearranging and including the Euler amplification effect:

$$K_e = \frac{\left[1-\frac{P}{P_E}\right]}{\frac{1}{K_B}+\frac{1}{K_S}+\frac{1}{K_A}}$$

$$= \frac{\left[1-\frac{P}{P_E}\right]}{1-\left\{\frac{\frac{3L}{4}-\frac{3(EI)^2}{LK_{rs}K_{rh}}}{\frac{EI}{K_{rs}}+L+\frac{EI}{K_{rh}}}\right\}}{3EI/L^3}+\frac{2{,}6L}{A_sE}+\frac{\left\{\frac{\frac{EI}{K_{rs}}+\frac{L}{2}}{\frac{EI}{K_{rs}}+L+\frac{EI}{K_{rh}}}\right\}}{AEY^2/4F_gL^3}$$

$$= \frac{\frac{3EI}{L^3}\left[1-\frac{P}{P_E}\right]}{1-\left\{\frac{\frac{3L}{4}-\frac{3(EI)^2}{LK_{rs}K_{rh}}}{\frac{EI}{K_{rs}}+L+\frac{EI}{K_{rh}}}\right\}+\frac{7{,}8I}{A_sL^2}+\frac{4F_gL^3}{AEY^2}\left\{\frac{\frac{3(EI)^2}{L^3K_{rs}}+\frac{3EI}{2L^2}}{\frac{EI}{K_{rs}}+L+\frac{EI}{K_{rh}}}\right\}}$$

$$= \frac{\frac{3EI}{L^3}\left[1-\frac{P}{P_E}\right]}{1-\left\{\frac{\frac{3L}{4}-\frac{4F_gL^3}{AEY^2}\left\{\frac{3(EI)^2}{K_{rs}L^3}+\frac{3EI}{2L^2}\right\}-\frac{3(EI)^2}{LK_{rs}K_{rh}}}{\frac{EI}{K_{rs}}+L+\frac{EI}{K_{rh}}}\right\}+\frac{7{,}8I}{A_sL^2}}$$

$$= \frac{\frac{3EI}{L^3}\left[1-\frac{P}{P_E}\right]}{1-\left\{\frac{\frac{3L}{4}-\frac{12F_gI}{AY^2}\left\{\frac{EI}{K_{rs}}+\frac{L}{2}\right\}-\frac{3(EI)^2}{LK_{rs}K_{rh}}}{\frac{EI}{K_{rs}}+L+\frac{EI}{K_{rh}}}\right\}+\frac{7{,}8I}{A_sL^2}}$$

If the correction terms to K_{rh}, A_s and A, which are F_r, F_h, and F_v as defined in Equations (10-21), (10-22) and (10-23) respectively, are included:

$$K_e = \frac{\frac{3EI}{L^3}\left[1-\frac{P}{P_E}\right]}{1-\left\{\frac{\frac{3L}{4}-\frac{12F_gI}{F_vAY^2}\left\{\frac{EI}{K_{rs}}+\frac{L}{2}\right\}-\frac{3(EI)^2}{F_rLK_{rs}K_{rh}}}{\frac{EI}{K_{rs}}+L+\frac{EI}{F_rK_{rh}}}\right\}+\frac{7{,}8I}{F_hA_sL^2}}$$

If the foundation is effectively pinned, and K_{rs} = 0, the equation can be simplified as follows (multiply top and bottom of central term in denominator by K_{rs}, and then set K_{rs} = 0):

$$K_e = \frac{\frac{3EI}{L^3}\left[1-\frac{P}{P_E}\right]}{1+\frac{12F_gI}{F_vAY^2}+\frac{3EI}{F_rLK_{rh}}+\frac{7{,}8I}{F_hA_sL^2}}$$

If the foundation and leg-hull connection are effectively encastré, and K_{rs} = K_{rh} = ∞, the equation can be simplified as follows (note that the F_r term to incorporate hull stiffness has vanished, as its definition relies on a finite value of K_{rh}; if an alternative definition were applied, its effect could be retained).

$$K_e = \frac{\frac{12EI}{L^3}\left[1-\frac{P}{P_E}\right]}{1+\frac{24F_gI}{F_vAY^2}+\frac{31{,}2I}{F_h.A_s.L^2}}$$

In the absence of any of the terms for effects other than bending (i.e. setting A and A_s to infinity), this further reduces to $12EI/L^3$, which is as expected for a beam, encastré at each end, with one end free to slide.

TR.10.4.3.3 Hysteretic damping

Soil material damping is typically small at small strains; in the absence of specific data, 2 % is considered to be a reasonable estimate. At larger strains, amplitude-dependent hysteretic damping will also occur. Where a non-linear foundation model is adopted for the dynamic response analysis, the hysteretic foundation damping is accounted for directly. Where a linear foundation model with stiffness reduction according to ISO 19905-1:2012, A.9.3.4.2.1 is adopted, the hysteretic damping may be added to account for the effects of foundation hysteretic damping. Hysteretic damping should be used only in combination with non-linear rotational stiffness reduction and should not be used in combination with the initial stiffness.

Foundation hysteretic damping is a consequence of the hysteretic behaviour of the foundation soils. Whenever significant foundation non-linearity is present, an additional damping component may be added to system damping to account for this phenomenon. This foundation hysteretic damping component can be included implicitly in a detailed non-linear dynamic analysis embodying hysteretic spudcan foundation elements, or it may be calculated explicitly in the case of a simpler quasi-static analysis. Templeton (2006)[10-1] recommended a method to accomplish this based on the application of Masing construction to non-linear load vs. displacement characterization of the jack-up system. The following is based on that method:

1) The entire structure should be modelled (e.g. via a bar stool model). The model should be linear except for the inclusion of foundation non-linearities (e.g. via the use of hysteretic spudcan foundation elements or progressive stiffness reduction) and P-Δ effects.

2) This model should be used to produce a force vs. deflection (backbone) curve for the horizontal force, F (equal to the amplitude of the extreme load cycle, including the effects of dynamic amplification), vs the horizontal deflection, x, both at the effective centre of combined storm and inertial loading.

3) The hysteretic damping, D_{hyst}, as a function of deflection should be developed from the F vs. x (backbone) curve according to the definition:

$$D_{hyst} = \frac{2}{\pi}\left[\frac{2}{Fx}\left(\int_0^x F\mathrm{d}x\right)-1\right]$$

with the limits of integration zero to x, the (single amplitude) of the extreme load cycle, including the effects of dynamic amplification, which may require multiple or iterative analysis to determine consistent values of x and D_{hyst}.

4) The hysteretic damping D_{hyst} (a fraction of critical damping) should be added to the small-strain soil material damping used in determining the SDOF DAF.

5) The hysteretic damping should be determined for each loading direction to be considered in the assessment for which a substantially different stiffness reduction is used.

Further details and examples for each of these steps are provided by Templeton and Lewis[10-2], who also provide further details of a procedure to apply this method and examples for application to a case of hurricane loading as well as comparisons to field data.

TR.10.4.3.4 Vertical radiation damping in earthquake analysis

Guidance on the frequency dependence of stiffness and damping for jack-ups under earthquake excitation is presently under development for inclusion in the next edition of this Technical Report.

TR.10.5.3.4 / C.2.4 Guidance on the fourth method of ISO 19905-1:2012, Table A.10.5.1 — Application of the drag-inertia method

Details on the background to, and limitations of, this method can be found in Annex B.

11 Commentary to ISO 19905-1:2012, Clauses 11 and A.11

No commentary is offered.

12 Commentary to ISO 19905-1:2012, Clauses 12 and A.12

TR.12.6.2.2 Nominal bending strength

The calculations of nominal bending strength for compact and non-compact sections require knowledge of the plastic moment capacity of the section. For a section composed of uniform material this is given by:

$$M_p = F_y Z$$

where

F_y is the yield strength, in stress units, taken as the minimum of the yield strength and 90 % of the ultimate tensile strength (UTS; see ISO 19905-1:2012, A.12.2.2);

Z is the plastic section modulus.

For hybrid sections there is more than one set of material properties to consider. Standard techniques are recommended for evaluation of M_p and an example is provided below.

TR.12.6.2.2.1 Example

Consider the simplified problem of a square rack section (component 1) of properties:

F_{y1} = minimum of yield strength of 700 MN/m^2 and 0,9 ultimate strength of 766 MN/m^2

F_{y1} = 766 x 0,9 = 690 MN/m^2

connected to a solid square chord section (component 2) of properties:

F_{y2} = minimum of yield strength of 345 MN/m^2 and 0,9 ultimate strength of 485 MN/m^2

F_{y2} = 345 MN/m^2

as shown in Figure TR.12.3-1 below.

Dimensions are as marked.

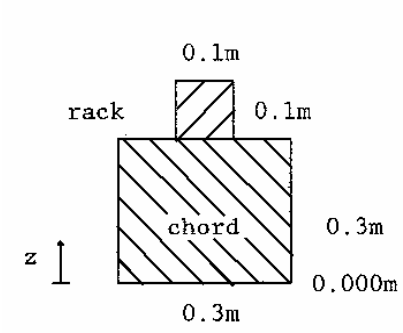

Figure TR.12.3-1 — Example hybrid chord section

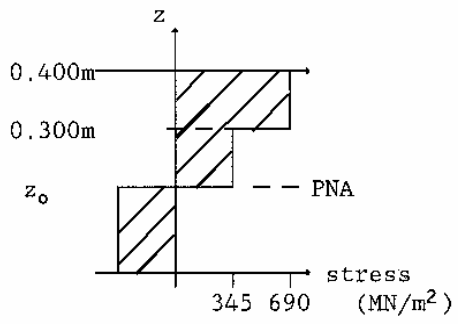

Figure TR.A.12.3-2 — Fully plastic stress distribution

On the assumption that the strain for component 1 to be loaded to its nominal strength is not sufficient to lead to fracture of component 2, the plastic stress distribution for pure bending is as shown in Figure TR.12.3-2. The plastic neutral axis is a distance z_o from the back face of the chord component, such that:

$$345 \times 0{,}3 \times z_o = 345 \times 0{,}3 \times (0{,}3 - z_o) + 690 \times 0{,}1 \times 0{,}1$$

i.e.

$$z_o = 0{,}183 \text{ m}$$

The section plastic moment is then:

$$M_p = 345 \times 0{,}3 \times 0{,}183 \times (0{,}183/2)$$
$$+ 345 \times 0{,}3 \times 0{,}117 \times (0{,}117/2)$$
$$+ 690 \times 0{,}1 \times 0{,}100 \times (0{,}117 + 0{,}100/2) = 3{,}59 \text{ MNm}$$

TR.12.6.3.2 Background for η in interaction equation approach

The treatment of biaxial bending in AISC LRFD tends to be conservative for beam-columns. The linear addition of the x- and y-axis bending components of the utilization check is conservative for all practical non-rectangular cross-sections. This is most apparent when assessing a circular tubular member. While ISO 19905-1 does not use the AISC formulation for circular tubulars, the following discussion is informative and is indicative of the problem with all cross-sections. The bending strength of the circular tube must be the same in all directions, but this is not reflected in the AISC LRFD equations. For example, a circular tubular member subject to bending in a plane at 45° to the x-axis has in the AISC LRFD code a nominal strength of 71 % of that for uniaxial bending in the x- or y- planes, i.e. the calculated utilization ratio depends on the local axis of bending, which is illogical.

The problem is not confined to circular tubulars, as most sections would have a reduction in nominal strength on account of this linear addition. It was considered appropriate to address this reduction in strength in the general interaction equations in ISO 19905-1.

In deriving a suitable form, the problem for the circular tubular was considered first. Clearly, since the circular tubular has equal bending strength in all directions, the correct actual bending moment should be the vectorial sum of the x- and y-axis bending moments. Expressed as a utilization equation for bending only:

$$\left[\left\{\frac{\gamma_{R,Pb} M_{uay}}{M_{by}}\right\}^2 + \left\{\frac{\gamma_{R,Pb} M_{uaz}}{M_{bz}}\right\}^2\right]^{\frac{1}{2}} \leq 1{,}0$$

and with the addition of axial load (for $P_u/\phi_a P_n$ > 0,2)

$$\frac{\gamma_{R,Pa} P_u}{P_p} + \frac{8}{9}\left[\left\{\frac{\gamma_{R,Pb} M_{uay}}{M_{by}}\right\}^2 + \left\{\frac{\gamma_{R,Pb} M_{uaz}}{M_{bz}}\right\}^2\right]^{\frac{1}{2}} \leq 1,0$$

Since most jack-up chords are closed sections with high torsional stiffnesses similar to tubulars, the logical step was to formulate a similar equation which had the ability to account for sections not exhibiting circular symmetry. This was carried out by using a generalized exponent η to form the equations given in ISO 19905-1. One of the equations is given below as an example (for $\gamma_{R,Pa} P_u / P_p$ > 0,2).

$$\frac{\gamma_{R,Pa} P_u}{P_p} + \frac{8}{9}\left[\left\{\frac{\gamma_{R,Pb} M_{uay}}{M_{by}}\right\}^\eta + \left\{\frac{\gamma_{R,Pb} M_{uaz}}{M_{bz}}\right\}^\eta\right]^{\frac{1}{\eta}} \leq 1,0$$

With η = 1,0, the equations revert to the standard AISC LRFD equations, and hence a conservative assessment can be made. However, if a less conservative assessment is required, it is necessary to determine the value for η (see ISO 19905-1:2012, F.2).

If the nominal bending strengths M_{by} and M_{bz} are the same and η = 2,0, then this would imply that the section has equal bending strength in all directions. Favourable interaction between, for example, the $-M_{uay}$ and $+M_{uaz}$ moments acting on triangular chords with a single rack cannot be reproduced by the above equation. In such cases recourse to the section-specific interaction surface is recommended (see ISO 19905-1:2012, A.12.6.3.3 and F.3).

13 Commentary to ISO 19905-1:2012, Annex C

TR.C.2.4 Guidance on the fourth method of ISO 19905-1:2012, Table A.10.5.1 — Application of the drag-inertia method

Details on the background to, and limitations of, the drag-inertia method can be found in Annex B.

Annex A
(informative)

Detailed example calculation

A.1 Introductory comments

A.1.1 General points

This detailed example calculation serves to blaze a trail through the analysis methods in ISO 19905-1:2012. These methods have been applied to a hypothetical jack-up, the “typical jack-up”, and this annex provides a set of engineer's notes on the analysis. Most of the options available have been covered. It is intended that an engineer endeavouring to perform an analysis of a unit according to ISO 19905-1 can look up the relevant section(s) of this annex to find sample calculations. Details of the “typical jack-up” unit that would normally be provided by, or available from, the designer are provided in A.13, Appendix A.B.

A.1.2 How to use this annex

The flow chart of ISO 19905-1:2012, Figure 5.2-1 (the FLOW CHART) shows the general analysis route, and provides the basic structure of the detailed example calculation. This is reproduced at the appropriate part of the calculation sequence.

By following each box in the FLOW CHART, the detailed example calculation is conveniently sub-divided. To address any one item in a FLOW CHART box, the user can flick through the text until coming to a reproduction of the relevant box, and start to follow the calculations from there. It is not recommended that the user picks up calculations from other points in the middle of the text.

While the order of the FLOW CHART is obeyed, the route through ISO 19905-1 to complete each FLOW CHART item is in order of convenience. Where alternative paths are available to complete an action, these are marked and placed one after the other.

Throughout this annex, roadsign-like symbols have been added to assist the user in navigating the analysis options. The detailed example calculation is intended to be read with ISO 19905-1 open for reference.

A.1.3 Navigation within this annex

The detailed example calculation begins with the first section of ISO 19905-1 and proceeds to the point at which the FLOW CHART is encountered. Each subsequent calculation step begins with a reproduction of the relevant FLOW CHART box, which is often accompanied by a few explanatory comments. In most cases, this is followed by a “local route card”, in the following form:

WIND ACTIONS - route

Introduction	(7.3.4)
Wind actions calculations	(A.7.3.4.1-2)
or Model tests	(A.7.3.4.3)

The local route card is a more detailed list of the sections to be followed when completing an item of the FLOW CHART, and shows the major choices available. Similar cards appear at other points in the text as considered beneficial.

At key points “high level” instructions are given, for example advising the user when an item is complete and the next FLOW CHART entry should be started. These are identified by the upturned triangle:

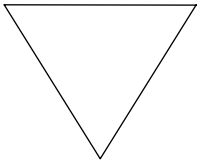

Within the items of the FLOW CHART there can be a choice of routes through the analysis; these have been followed, one after the other, with a road sign like format adopted to show the points where routes diverge, and to label the turn-off points for each option.

Examples include:

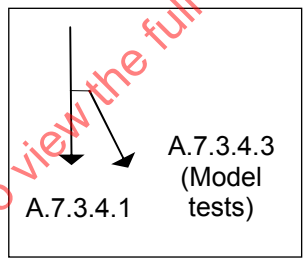

followed by:

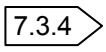

Once all the options have been discussed, a convergent route sign of similar form is given. Smaller labels are provided for minor route choices and short turn-offs.

Whereas the major FLOW CHART items are tackled in an obedient order, the actions within each item are tackled in the most appropriate order at the time.

A few other symbols are used, as referenced by the following key to symbols.

A.1.4 Key to symbols

The following types of symbol appear in the detailed example calculation document.

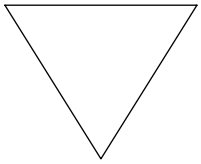

Top level navigational instruction, for example showing where an item in the overall assessment has been completed, or where a level of assessment has been concluded.

"Local route sign" showing the general route(s) available to achieve an item in the overall FLOW CHART:

Introduction	(7.3.4)
Wind actions calculations	(A.7.3.4.1-2)
or Model Tests	(A.7.3.4.3)

7.3.4 Reference to an entry in the route card above.

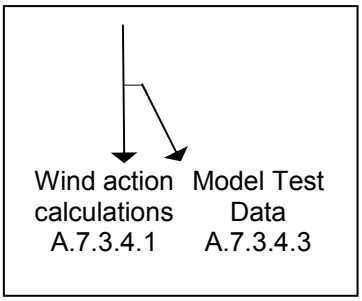

Point at which the analysis route divides into options which are separately labelled within ISO 19905-1.

A.7.3.4.3 Indicator of start of a separately labelled option, as directed by the signpost immediately above. Option terminates at the next similar sign, or at the following sign:

4.7 Reference to an entry in the route card which continues on an identified option.

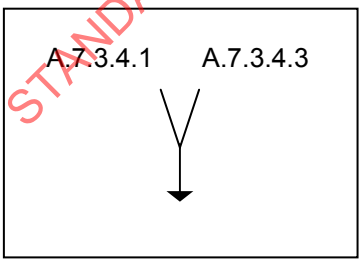

Point at which separately labelled options converge onto the same route again.

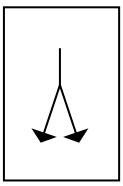

Point at which a minor division in the analysis route occurs. This is usually within a subclause.

OPTION Minor option in the route as introduced by the above sign. Terminated either by a similar sign, or by the convergent sign shown below:

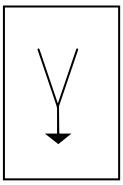

Point at which minor route divisions re-converge.

i
A.7.3.3.3.1

Reference to source of further information in ISO 19905-1.

A.2 Initial steps in the analysis of the "typical jack-up"

A.2.1 Initial route, introduction and overall considerations

Read Introduction & Scope	1
If unfamiliar with ISO 19905-1, note:	
Normative references	2
Terms and definitions	3
Abbreviated terms and symbols	4
(not comprehensively covered herein)	
Overall considerations	5
Follow FLOW CHART	Fig 5.2-1

1 Introduction & Scope

ISO 19905-1, which was developed from SNAME Technical & Research Bulletin 5-5A, states the general principles and basic requirements for the site-specific assessment of mobile jack-ups; it is intended to be used for assessment and not for design.

Site-specific assessment is normally carried out when an existing jack-up unit is to be installed at a specific site. The assessment is not intended to provide a full evaluation of the jack-up; it assumes that aspects not addressed in ISO 19905 have been addressed using other practices and standards at the design stage. In some instances, the original design of all or part of the structure could be in accordance with other standards in the ISO 19900 series, and in some cases different practices or standards could have been applied. It is, however, a pre-requisite that the jack-up holds a valid classification society certification from a recognized classification society (RCS) (see ISO 19905-1:2012, Clause 1 and 3.52), or can be shown to meet the same requirements.

The purpose of the site assessment is to demonstrate the adequacy of the primary structure of the jack-up and its foundations for the assessment situations and defined limit states, taking into account the consequences of failure. It is important that the results of a site-specific assessment be appropriately recorded, e.g. using the recommended contents list of ISO 19905-1:2012, Annex G or similar, and communicated to those persons required to know or act on the conclusions and recommendations. According to the Introduction to the ISO, alternative approaches to the site-specific assessment can be used, provided that they have been shown to give a level of structural reliability equivalent, or superior, to that implicit in ISO 19905-1.

5 Overall considerations

5.1 ISO 19905-1 includes the following general requirements and recommendations:

5.1.1 Assessments undertaken in accordance with ISO 19905-1 shall be performed only by persons competent through education, training and experience in the relevant disciplines.

5.1.2 Adequate planning of the assessment condition shall be undertaken before a site-specific assessment is started.

5.1.3 The assessment shall normally include both extreme storm and operational assessments because the critical mode of operation is not always obvious. (*For the purpose of this detailed example calculation a single extreme storm event has been assessed.*)

5.1.4 The assessor should prepare a report summarizing the inputs, assumptions and conclusions of the assessment. A recommended contents list is given in ISO 19905-1:2012, Annex G.

5.1.5 Country-specific rules and regulations must be considered and addressed. [*For the purpose of this detailed example calculation it is assumed that there is no need to satisfy any country-specific requirements (as given in ISO 19905-1:2012, Annex H).*]

5.2 The assessment of the jack-up can be carried out at various levels of complexity as expanded in a), b) and c) (in order of increasing complexity). The objective of the assessment is to show that the acceptance criteria of ISO 19905-1:2012, Clause 13 are met. If this is achieved at a certain complexity level there is no requirement to consider a higher complexity level. In all cases, ISO 19905-1 requires the adequacy of the foundation to be assessed to level b) or c).

a) Compare assessment situations with design conditions or other existing assessments determined in accordance with ISO 19905-1.

b) Carry out appropriate calculations according to the simpler methods (e.g. pinned foundation, SDOF dynamics) given in ISO 19905-1. Where possible, compare results with those from existing more detailed/complex (e.g. secant or yield interaction foundation model, time domain dynamics) calculations.

c) Carry out appropriate detailed calculations according to the more complex methods (e.g. secant, yield interaction or continuum foundation model, time domain dynamics) given in ISO 19905-1:2012.

For the purpose of this detailed example calculation it is assumed that case c) applies and that recourse to ISO 19905-1 is necessary to justify the safe use of the unit.

FIGURE 5.2-1

It is now appropriate to start using the FLOW CHART in ISO 19905-1:2012, Figure 5.2-1, as reproduced overleaf.

A.2.2 Overall analysis FLOW CHART as given in ISO 19905-1:2012, Figure 5.2-1

NOTE Cross-references in the figure refer to ISO 19905-1:2012.

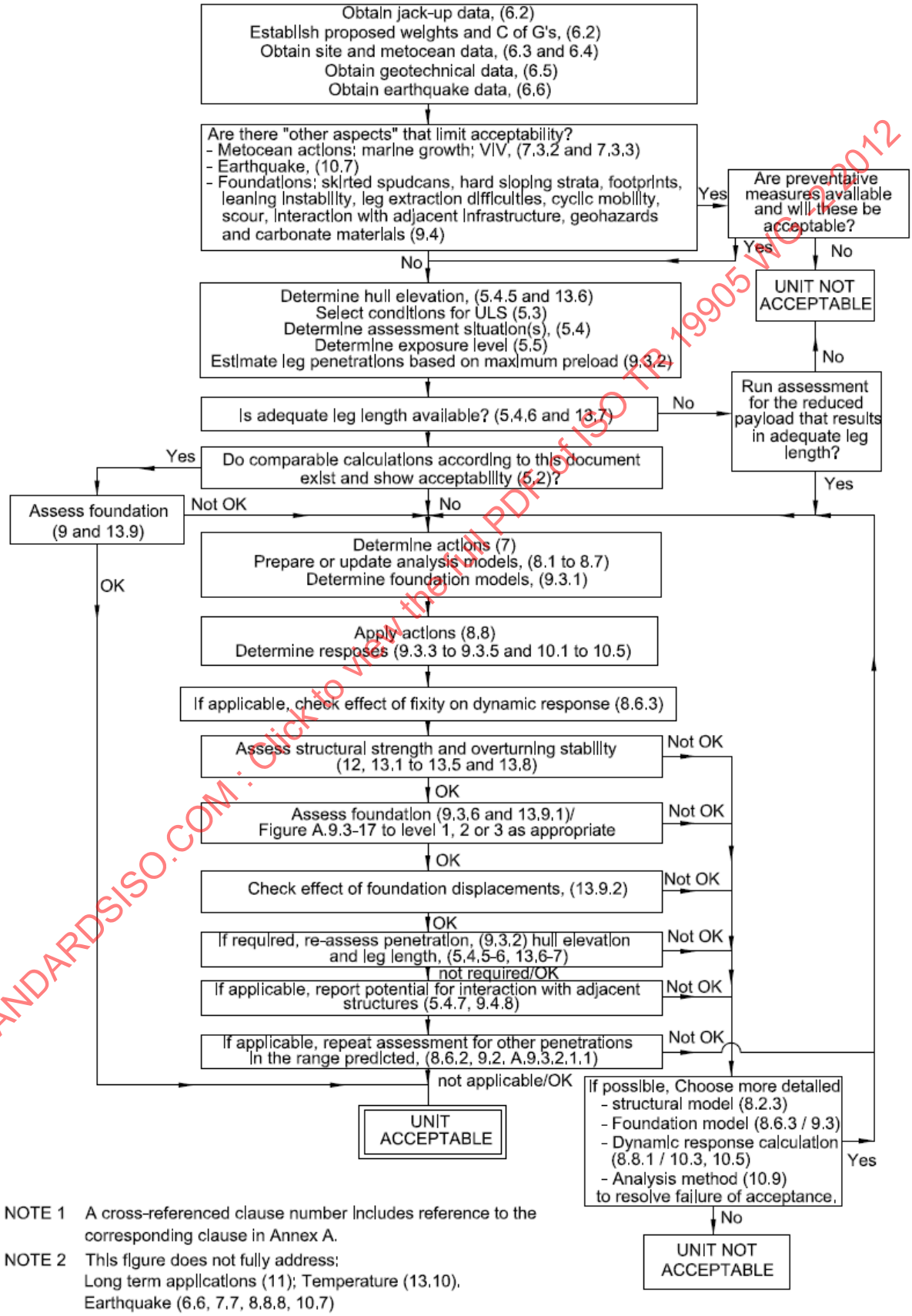

NOTE 1 A cross-referenced clause number includes reference to the corresponding clause in Annex A.

NOTE 2 This figure does not fully address: Long term applications (11); Temperature (13.10), Earthquake (6.6, 7.7, 8.8.8, 10.7)

A.3 Data assembly

6 Data to assemble for each site

Obtain jack-up data , (see also Annex G)	(6.2)
Establish proposed weights and C of Gs,	(6.2)
Obtain site and metocean data,	(6.3 & 6.4)
Obtain geotechnical data,	(6.5)
Obtain earthquake data,	(6.6)

The first item in the FLOW CHART involves data collection. The references are well itemized, and so no local route sign is required.

A.3.1 Obtain jack-up data

6.2 Jack-up data

The jack-up data used as a basis for the example calculations is summarized:

Rig type:	"typical jack-up"
Installed leg length:	174,9 m
Spudcan area:	243 m^2
Spudcan height:	8,5 m
Drawings operations manual:	held and used as reference
Elevating system:	electric opposed-pinion elevating system (four high)
Holding system	rack-chock fixation system
Leg-hull connection details:	see data sheets appended to this annex

Establish proposed weights and centre of gravity

It is assumed that this study represents a survival assessment.

Maximum elevated weight: (100 % variable load)	19 394 t
Minimum elevated weight: (50 % variable load)	17 289,5 t

The weight distribution can be deduced from plans and the original data package.

For the assessed condition the survival centre of gravity is at the leg centroid:

LCG:	19,2 m	fwd. of aft legs centres
TCG:	0,0 m	port of longitudinal CL
Tolerance:	± 0,0 m	either way

Information is not specifically presented for substructure and derrick position, nor hook, rotary or setback loads, however the above centre of gravity incorporates the substructure and derrick.

Weight of one leg excluding can:	1 870,4 t
Weight of footing spudcan:	570,3 t
Total leg weight including spudcan:	2 440,8 t

Determine buoyancy of legs and can:

Buoyancy per unit length	= displaced weight of one bay / length of one bay = (1,025 × enclosed volume of one bay) ÷ 10,21 m = 3,232 t/m

Obtain buoyant upthrust on can. Assume can is flooded.

Mass of can:	570,3 t
For steel of density 7,856 t/m^3:	
Volume of steel in can	= 570,3 / 7,856 (displaced volume of water) = 72,6 m^3
So buoyant upthrust:	= 1,025 × 72,6 = 74,4 t

To meet an overturning requirement it is permitted that ballast water can be added to the hull weight. This is not considered herein, as the overturning check is not the limiting assessment parameter.

Preload/predrive capability

The “typical jack-up” being considered for the purpose of the detailed example calculation preloads by filling ballast tanks with water to temporarily increase the weight of the unit to proof test the foundations during installation.

Preload capability	15 876 t preload footing reaction

It is understood from the operations manual that this is also the limiting bearing pressure for the spudcan.

Design parameters/ deviations:	none
Relevant modifications:	none

A.3.2 Obtain site and metocean data

6.3 Site and operational data

The “typical jack-up” is considered at two locations for the purpose of the detailed example calculation:

Location 1 — Sand foundation condition

Location coordinates:	arbitrary test location 1 — “sand”
Seafloor topography:	assumed flat and undisturbed
Waterdepth:	121,9 m referenced to lowest astronomical tide (LAT)
Platform location:	N/A for arbitrary test location
Airgap requirements:	operating airgap of 20,9 m from LAT to keel
Rig heading:	N/A, omni-directional assessment
Platform interface:	N/A for arbitrary test location

Location 2 — Clay foundation condition

Location coordinates:	arbitrary test location 2 — “clay”
Seafloor topography:	assumed flat and undisturbed
Waterdepth:	85,0 m referenced to lowest astronomical tide (LAT)
Platform location:	N/A for arbitrary test location
Airgap requirements:	minimum safe airgap (19,7 m from LAT to keel; see ISO 19905-1:2012, 13.6)
Rig heading:	N/A, omni-directional assessment
Platform interface:	N/A for arbitrary test location

6.4 Metocean data

Metocean data for the extreme storm event (ULS assessment) is considered on an omni-directional basis for the purpose of these detailed example calculations based on the 50-year independent extremes.

Waterdepth (LAT or CD); see also A.6.4.4:

Location 1 (sand):

Waterdepth: 121,9 m referenced to lowest astronomical tide (LAT)

Location 2 (clay):

Waterdepth: 85,0 m referenced to lowest astronomical tide (LAT)

Wind, wave and current act in the same direction, and at the same time as the extreme water level. No directional data is to be used here.

A.6.4.2 Waves

Waves based on the 50-year independent extreme for the purpose of the detailed example calculation:

A.6.4.2.2 Extreme wave height

Location 1 (sand):

Maximum wave height H_{max}: 26,8 m

and based on H_{max} = 1,86 H_{srp} (for non-cyclonic areas)

Significant wave height H_{srp}: 14,4 m

Location 2 (clay):

Maximum wave height H_{max}: 26,8 m

and based on H_{max} = 1,86 H_{srp} (for non-cyclonic areas)

Significant wave height H_{srp}: 14,4 m

A.6.4.2.3 Deterministic waves

The wave kinematics factor κ, assumed to be 0,86 for detailed example calculations (for comparative purposes to SNAME). Formulae are based on latitude, waterdepth, waveheight and leg-spacing; see ISO 19905-1:2012, Equation (A.6.4-3).

Associated wave period T_{ass}: 16,6 s for both assessment cases (assumed to be intrinsic)

Check: $3{,}44\sqrt{H_{srp}} < T_{ass} < 4{,}42\sqrt{H_{srp}}$

$13{,}05 < T_{ass} < 16{,}8$

Therefore within bounds of ISO 19905-1:2012, Equation (A.6.4-8)

A.6.4.2.4 Wave crest elevation

Wave crest elevation calculated using in-house software using Stokes 5th wave theory based on a deterministic wave:

Wave crest elevation H_{crest}: 15,1 m

i
A.7.3.3.3.1

A.6.4.2.5 Wave spectrum

A JONSWAP spectrum has been specified and in-house software caters for this spectrum.

A.6.4.2.7 Peak and zero upcrossing periods

Peak wave period T_p (intrinsic): 16,6 s
(no additional data specified for arbitrary test case)

Check using T_z: $3{,}2\sqrt{H_{srp}} < T_z < 3{,}6\sqrt{H_{srp}}$

$12{,}1 < T_z < 13{,}7$

Check gamma for range of T_z using JONSWAP:

T_p / T_z lowerbound: 1,37 (within range for JONSWAP)

T_p / T_z upperbound: 1,22 (within range for JONSWAP)

Therefore within bounds of ISO 19905-1:2012 Equation (A.6.4-10)

A.6.4.2.8 Short crestedness

Not considered if following the wave-kinematics approach.

A.6.4.2.9 Maximizing the wave/current response

Where the natural period of the jack-up is such that it can respond dynamically to waves (see ISO 19905-1:2012, A.10.4.1), the maximum dynamic response can be caused by waves or sea states with periods outside the ranges given in ISO 19905-1:2012, A.6.4.2.3 and A.6.4.2.7. Such conditions should also be investigated to ensure that the maximum (dynamic plus quasi-static) response is determined by considering sea states with different combinations of significant wave height and spectral period, or deterministic waves with different combinations of individual wave height and period.

It is assumed that the case being considered addresses the worst combined loading condition.

If dynamics is significant, care should be taken to ensure that the maximum (dynamic plus quasi-static) response is assessed, possibly for seastates with a smaller wave-height if the wave period is close to the rig natural period and the worst loading condition reported.

A.6.4.3 Current

The specified linearized current profile for this assessment is as follows:

Surface current: 1,49 m/s

Near bottom current: 0,82 m/s at 1 m above seabed

This supersedes the use of ISO 19905-1:2012 Equations (A.6.4-12) and (A.6.4-13).

In the presence of waves the current profile should be stretched/compressed such that the surface component remains constant. This can be achieved by substituting the elevation as described in ISO 19905-1:2012, A.7.3.3.3.2.

Note: In the assessment calculations the current velocity may be reduced to account for interference from the structure.

i
A.7.3.3.4

A.6.4.4 Waterdepth

Location 1 (sand):

Still water level (LAT)	121,9 m

Assessment is based on a combined tidal rise and storm surge of 2,44 m

For these detailed example calculations the following split is assumed:

Tidal rise (MHWS):	1,22 m (mean high water spring)
Storm surge:	1,22 m
Extreme still water level (SWL):	LAT + MHWS + storm surge 124,4 m
Mean sea level (MSL):	122,5 m

Location 2 (clay):

Still water level (LAT)	85,0 m

Assessment is based on a combined tidal rise and storm surge of 2,44 m

For these detailed example calculations the following split is assumed:

Tidal rise (MHWS):	1,22 m (mean high water spring)
Storm surge:	1,22 m
Extreme still water level (SWL):	LAT + MHWS + storm surge 87,4 m
Mean sea level (MSL):	85,6 m

A.6.4.5 Marine growth

No site-specific data are given; default values per ISO 19905-1:2012, A.7.3.2.5 will be included

A.6.4.6 Wind

Wind speed based on the 50-year independent extreme for the purpose of the detailed example calculation:

1-minute sustained design wind at 10 m above sea level is 51,5 m/s.

Formulations for the calculation of wind actions are given in ISO 19905-1:2012, A.7.3.4.

A.6.4.6.2 Wind Profile

In the absence of a site-/area-specific wind profile, the logarithmic function, approximated by a power law should be applied per ISO 19905-1:2012, Equation (A.6.4-14):

i
A.7.3.4

A.3.3 Obtain geotechnical data

6.5 **Geophysical and geotechnical information**

It is assumed that the unit is to operate in areas for which there is site-specific geotechnical data which has been gathered in accordance with ISO 19905-1:2012, 6.5. For the present detailed example calculations two locations are to be considered, with interpreted soil conditions of 1) shallow penetration in homogeneous medium dense sand and 2) deep penetration in clay whose strength increases with depth, as described below:

Location 1 — Sand:

submerged unit weight	γ'	=	11,0 kN/m^3
triaxial friction angle	ϕ	=	34,0°
relative density	D_R	=	60 %
Poisson's ratio	ν	=	0,2

Location 2 — Clay:

submerged unit weight varies linearly between:

from	γ'	=	4,0 kN/m^3 at surface
to	γ'	=	5,8 kN/m^3 at depth of 19,0 m
to	γ'	=	5,8 kN/m^3 at depth of 36,5 m
to	γ'	=	8,0 kN/m^3 at depth of 45,0 m

undrained cohesive shear strength varies linearly:

from	s_u	=	2,40 kN/m^2 at surface
to	s_u	=	27,33 kN/m^2 at depth of 19,0 m
to	s_u	=	40,46 kN/m^2 at depth of 29,0 m
to	s_u	=	50,30 kN/m^2 at depth of 36,5 m
to	s_u	=	67,00 kN/m^2 at depth of 45,0 m

shear modulus varies linearly:

from	G	=	0,0 MN/m^2 at surface
to	G	=	23,1 MN/m^2 at depth of 19,0 m
to	G	=	31,6 MN/m^2 at depth of 29,0 m
to	G	=	37,9 MN/m^2 at depth of 36,5 m
to	G	=	62,8 MN/m^2 at depth of 45,0 m

overconsolidation ratio is as follows:

R_{OC} = 1,4 at surface to 19,0 m

R_{OC} = 1,2 from 19,0 to 29,0 m

R_{OC} = 1,0 from 29,0 to 36,5 m

R_{OC} = 1,1 from 36,5 to 45,0 m

R_{OC} = 1,2 below 45,0 m

soil undrained shear strength sensitivity:

$s_{u,a}/s_u$ = 2,7

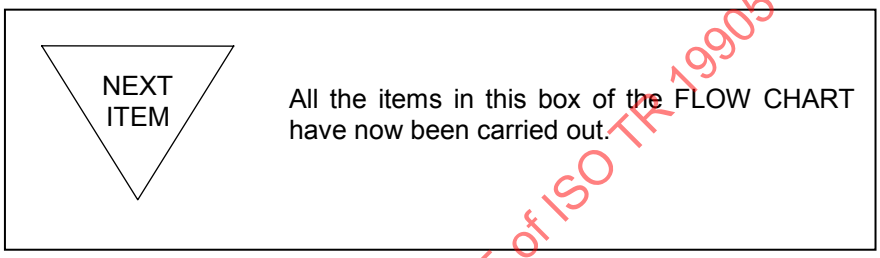

A.4 Other limiting aspects

The first item in the FLOW CHART involves data collection. The references are well itemized, and so no local route sign is required.

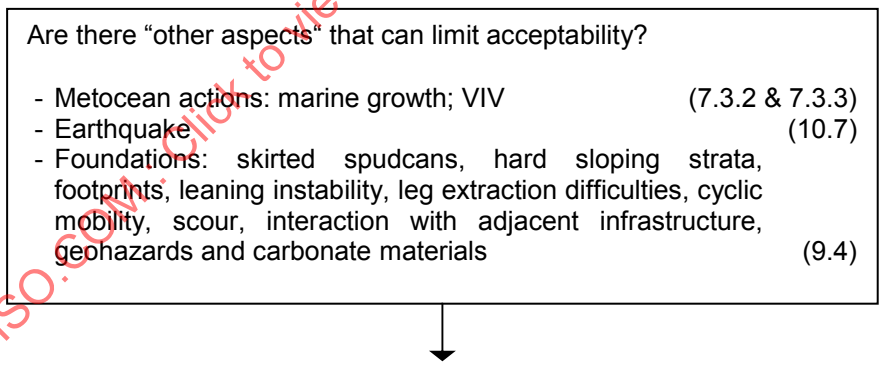

ISO 19905-1 requires an initial review of the data available at this stage to determine if there are any “other aspects”, generally outside the scope of ISO 19905-1 that may need to be considered from the outset.

These, however, are outside the scope of this annex and so are not considered further. The following analysis assumes that these aspects are not limiting and the assessment can proceed.

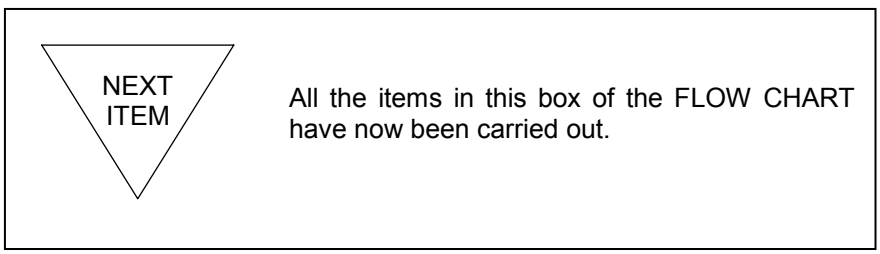

A.5 Establish assessment configuration and situation(s)

5 Determine hull elevation configuration and penetration

Determine hull elevation	(5.4.5 & 13.6)
Select conditions for ULS	(5.3)
Determine assessment situation(s)	(5.4)
Determine exposure level	(5.5)
Estimate leg penetrations based on maximum preload	(9.3.2)

The actions in this item of the main FLOW CHART concern leg length demands. Their completion is straightforward and so no local route sign is required.

A.5.1 Determine hull elevation

The hull elevation used in the assessment shall comply with the requirements specified in ISO 19905-1:2012, 13.6. Generally this is the larger of that required to maintain adequate clearance with:

— adjacent structures, such as a fixed platform, and

— the wave crest.

13.6 Hull elevation — Minimum airgap requirements

Check that a minimum of 1,5 m clearance exists between the assessment return period extreme wave crest elevation and the underside of the hull:

Test location 1 —Sand

Determine minimum airgap above LAT:

Lowest astronomical tide:	121,9 m above sea bed
Tidal rise (MHWS): (mean high water spring)	1,22 m
Storm surge:	1,22 m
Extreme still water level (SWL)	LAT + MHWS + storm surge 124,4 m above seabed
Wave crest elevation H_{crest}:	15,1 m
Clearance	1,5 m
Minimum airgap	MHWS + storm surge + H_{crest} + 1,5 m 1,22 + 1,22 + 15,1 + 1,5 19,04 m
Specified airgap:	20,9 m from LAT to keel > 19,04 m

Therefore satisfies minimum airgap requirements for test location 1 — sand.

Test location 2 — Clay

Determine minimum airgap above LAT:

Lowest astronomical tide:	85,0 m above sea bed.
Tidal rise (MHWS): (mean high water spring)	1,22 m
Storm surge:	1,22 m
Extreme still water level (SWL):	LAT + MHWS + storm surge 82,4 m above seabed
Wave crest elevation H_{crest}:	15,8 m
Clearance	1,5 m
Minimum airgap	MHWS + storm surge + H_{crest} + 1,5 m 1,22 + 1,22 + 15,8 + 1,5 19,74 m
Specified airgap:	None specified at location 2

Therefore unit assessed at minimum airgap of 19,74 m for test location 2 — clay.

A.5.2 Select conditions for ULS

5.3 Selection of limit states

Normally only the ultimate limit states (ULS) need be assessed in a jack-up site-specific assessment.

For the purpose of the detailed example calculations, the site-specific assessment includes evaluation of the ULS for the assessment situations including extreme combinations of metocean actions defined in ISO 19905-1:2012, 6.4 and the associated storm mode gravity actions based on the data summarized in ISO 19905-1:2012, Annex G. The applicable partial action and resistance factors for the ULS and exposure level are summarized in ISO 19905-1:2012, Annex B.

It is noted that when the ULS metocean conditions are less severe than those defined for changing to the elevated storm configuration, ISO 19905-1 requires that this ULS situation be assessed with the jack-up in the most critical operating configuration (increased variable load, cantilever extended and unequal leg loads).

Similarly, for jack-ups where the operations manual permits increases in, or redistribution of, the variable load with reduced metocean conditions (operating configuration, nomograms, etc.), ISO 19905-1 requires that the assessor perform the ULS assessment using the operational metocean conditions with the associated operating mode gravity actions and configuration. Where nomograms are used, a representative selection of situations applicable to the site shall be assessed (e.g. the extreme storm event and one or more less severe metocean conditions).

NOTE The situations above are often found in benign areas where the ULS metocean conditions are within the defined serviceability limit states (SLS) limits for the jack-up and do not exceed the limits for changing the jack-up to the elevated storm configuration. For the purpose of the detailed example calculations the ULS assessment case is assumed to be the most critical.

A.5.3 Assessment situation

5.4 Determine assessment situation(s)

5.4.1 General

For the purpose of this assessment the unit is assumed to be able to achieve an equal leg loading condition and has been assessed for the storm survival condition only.

It is noted that where the assessment results indicate that an assessment situation does not meet the appropriate acceptance criteria, the assessment configuration may be adjusted to achieve acceptability, providing that any resulting deviations from the standard operating procedure of the jack-up are practically achievable, are documented and are communicated by the jack-up owner to his offshore personnel and, if relevant, to the operator. Alternatively, metocean data applicable to the season(s) of operation may be considered.

5.4.2 Reaction point and foundation fixity

The reaction point at the spudcan is detailed in ISO 19905-1:2012, 9.3. Noting that the assumption of pinned footings is a conservative approach for the bending moment in the leg in the way of the leg-to-hull connection (see ISO 19905-1:2012, 8.6.3), this assessment has allowed for a foundation restraint condition based on the inclusion of foundation fixity; see ISO 19905-1:2012, 9.3.

5.4.3 Extreme storm event approach angle

This assessment has considered sufficient storm approach angles to ensure the critical directions for each of the various checks are covered.

5.4.4 Weights and centre of gravity

Weight and centre of gravity details for the assessed condition are summarized in the tables taken from ISO 19905-1:2012, Annex G.

5.4.5 Hull elevation

The unit is assumed to be installed at a specified airgap of 20,9 m at the sand location, and the minimum safe airgap of 19,74 m at the clay location; see ISO 19905-1:2012, 13.6.

5.4.6 Leg length reserve

In this assessment the leg reserve above the upper guide will be checked against the minimum requirement of 1,5m. Leg reserve calculations are detailed in ISO 19905-1:2012, 13.7.

A larger reserve can be required due to:

— strength limitations of the top bay;

— the increase in the proportion of the leg bending moment carried by the holding system due to the effective reduction in leg stiffness at the upper guide;

— additional settlement due to scour.

5.4.7 Adjacent structures

The potential interaction of the jack-up with any adjacent structures is not considered herein.

In the event of the unit being installed next to a structure (e.g. platform), aspects requiring consideration by the operator include the effects of the jack-up's spudcans on the foundation of the adjacent structure and the effects of relative motions on well casing, drilling equipment and well surface equipment (risers, connectors, flanges, etc.).

5.4.8 Other

The assessment is based on the best estimate of the conditions at the site.

ISO 19905-1 requires that the validity of the assessment be confirmed once the jack-up has been installed if the actual conditions are inconsistent with the assumptions made, e.g. penetration, eccentricity of spudcan support, orientation, leg inclination. Factors such as large guide clearances and sensitivity to RPD cannot be properly quantified prior to installation.

A.5.4 Exposure level

5.5 **Determine exposure level**

It is assumed that the unit is to operate manned and non-evacuated, an 'L1' exposure level based on ISO 19905-1:2012, Table 5.5-1, and should therefore be assessed for either the 50 year independent extremes with partial action factor of 1,15 (as considered herein) or for the 100 year joint probability metocean data with partial action factor of 1,25.

i
5.5 &
Table 5.5-1

A.5.5 Estimate leg penetrations

Leg penetration calculations are undertaken here to determine the anticipated depth of spudcan penetration during preloading.

A.9.3.2 **Prediction of footing penetration during preloading**

The objective of this calculation is to determine the penetration depth at which the gross bearing capacity equals the applied structural spudcan reaction applied during preloading after consideration of the appropriate soil buoyancy and weight of backfill on top of the spudcan.

A.9.3.2.1.2 Modelling the spudcan

The profile of the equivalent spudcan diameter is first determined from the spudcan drawings supplied for the jack-up unit in question. For the present detailed example calculations, the resulting spudcan data is given below:

Actual spudcan:	Equivalent axi-symmetric footing
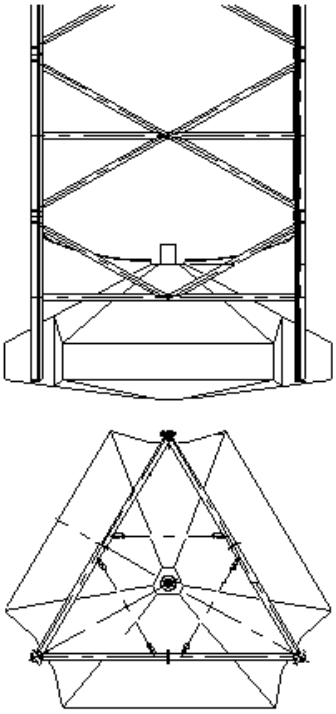	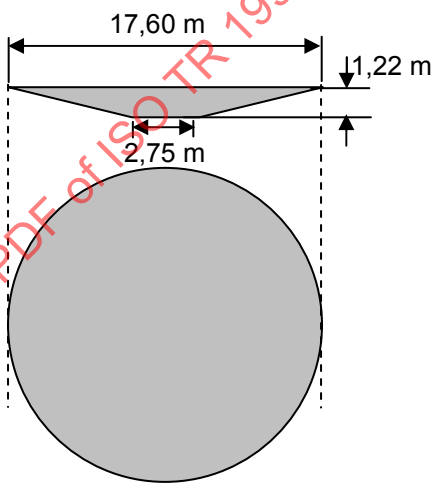

β =	164°
Maximum $\pi B^2/4$ =	243,21 m^2
Total spudcan volume =	1 164,83 m^3
A_s =	99,4 m^2
Tip to maximum plan area distance =	1,22 m

ISO 19905-1:2012, A.9.3.2 to A.9.3.2.6.6 provides methods for deriving the vertical footing capacity for a range of soil types and profiles. For the purposes of the present calculations the two locations considered here in detail are homogeneous silica sand, and clay whose undrained shear strength increases with depth.

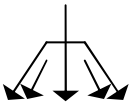

A.9.3.2.2 Penetration in clays

For an undrained clay foundation as defined earlier (Location 2):

submerged unit weight varies linearly between:

from	γ'	=	4,0 kN/m^3 at surface
to	γ'	=	5,8 kN/m^3 at depth of 19,0 m
to	γ'	=	5,8 kN/m^3 at depth of 36,5 m
to	γ'	=	8,0 kN/m^3 at depth of 45,0 m

undrained cohesive shear strength varies linearly:

from	s_u	=	2,40 kN/m^2 at surface
to	s_u	=	27,33 kN/m^2 at depth of 19,0 m
to	s_u	=	40,46 kN/m^2 at depth of 29,0 m
to	s_u	=	50,30 kN/m^2 at depth of 36,5 m
to	s_u	=	67,00 kN/m^2 at depth of 45,0 m

For the present clay example, deep penetrations are anticipated due to the relatively soft soils at the sea floor. Consequently backflow is anticipated to occur during preloading, hence the $W_{BF,0}$ and B_S terms are included in the bearing capacity equation [Equation (A.9.3-1)] in accordance with ISO 19905-1:2012, A.9.3.2.1.4.

The undrained vertical bearing capacity for preloading the clay foundation (allowing for backflow and displaced soil) is given by Equation (A.9.3-1) as:

$$V_L = Q_V - W_{BF} + B_S$$

where:

$Q_V = (s_u N_c s_c d_c + p_o') \pi B^2/4$ from ISO 19905-1:2012, Equation (A.9.3-7)

$W_{BF} = W_{BF,omin} + W_{BF,A} = \gamma'[(\pi B^2/4)(D - H_{cav}) - (V_{spud} - V_D)]$
(assuming no infill occurs after preloading operations, i.e. $W_{BF,A}$=0)

Using the spudcan geometry:

V_{spud} = 1 164,83 m^3

V_D = 116,7 m^3

For the particular soil profile considered in this detailed example calculation, the normalized rate of increase in undrained shear strength with depth $\rho B/s_{um}$ = 9,6, which is greater than the maximum value of 5,0 for which bearing capacity factors are presented in ISO 19905-1:2012, E.1. Consequently, for this particular case, the profile of $N_c s_c d_c$ with depth, D, is calculated using 6,0 at the seafloor and the d_c relationship provided in ISO 19905-1:2012, A.9.3.2.2, and an average s_u value between D and $D + B/2$ below the spudcan, also in accordance with ISO 19905-1:2012, A.9.3.2.2.

The value of p_o' is calculated from $\gamma' D$, where the variation of γ' is provided in the geotechnical input data. The same variation of γ' is used for determination of the backfill weight during preloading, $W_{BF,omin}$.

However, the bulk unit weight used to determine the spudcan buoyancy, B_S, is taken as the γ' value at the lowest depth of the spudcan's maximum plan area for a given spudcan tip penetration depth.

Using the above equations, the spudcan penetration resistance profile, i.e. V_L versus spudcan tip penetration depth, can be computed in order to calculate the spudcan penetration resistance curve.

The cavity depth, beyond which spudcan backflow is initiated, can be calculated using the methodology described in ISO 19905-1:2012, A.9.3.2.1.4. As the rate of increase of undrained shear strength with depth is constant for relatively large ranges of depths, H_{cav} has been determined using ISO 19905-1:2012, Equation (A.9.3-3):

$$H_{cav}/B = S^{0,55} - 0,25S$$

where S is defined in ISO 19905-1:2012, Equation (A.9.3-5) as:

$$S = [s_{um} / (\gamma' B)]^{(1-\rho/\gamma')}$$

H_{cav} has been calculated for each soil layer and the minimum value of H_{cav} has been used to define the depth at which soil backflow will occur during penetration of the spudcan into the example soil profile, calculated here as being 4,6 m.

Using the above information and equations, V_L can be determined for various depths in order to produce the spudcan penetration resistance curve as shown below:

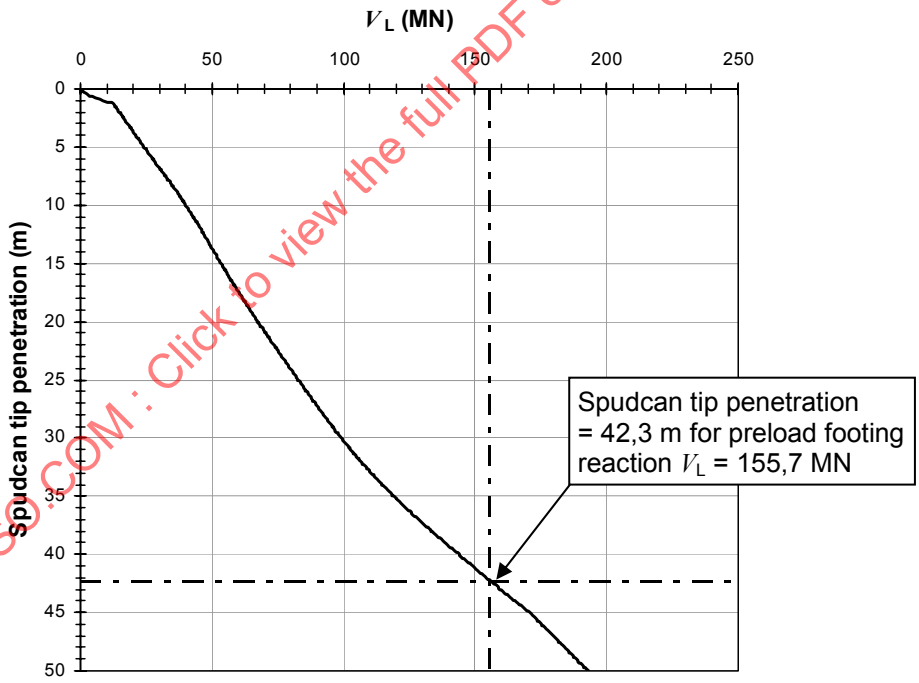

Here the penetration resistance has been calculated using depth intervals of 0,1 m, resulting in a predicted spudcan tip penetration of 42,3 m for a preload footing reaction of 155,7 MN.

The calculation of V_L for this particular spudcan tip penetration depth will now be demonstrated:

$$V_L = Q_V - W_{BF} + B_S$$

where:

$$Q_V = (s_u N_c s_c d_c + p_0')\pi B^2/4$$

$$W_{BF} = W_{BF,o} + W_{BF,A}$$

Assuming no backfill occurs after preloading operations, i.e. $W_{BF,A} = 0$, and $W_{BF,o} = W_{BF,omin}$, then according to ISO 19905-1:2012, Equation (A.9.3-2):

$$W_{BF} = \gamma'[A(D - H_{cav}) - (V_{spud} - V_D)]$$

$$B_S = \gamma' V$$

where:

D = 41,0 m (the depth of the lowest elevation of the maximum spudcan plan area)

B = 17,6 m

$\pi B^2/4$ = A = 243,21 m^2

H_{cav} = 4,6 m

Average s_u between D and $D + B/2$ below the spudcan = 67,8 kPa

$N_c s_c$ = 6,0

d_c = 1,47

p_0' = 203,8 kPa at D = 41,0 m (calculated using the variation of γ' with depth provided in the geotechnical input data)

γ' = 5,8 kN/m^3 at D = 40,8 m for use in calculation of B_S

Average γ' of backflowed material = 5,1 kN/m^3 between H_{cav} and D

V_{spud} = 1 164,83 m^3

V_D = 112,1 m^3

Therefore:

Q_V = 194,6 MN

W_{BF} = 39,8 MN

B_S = 0,65 MN

V_L = 155,5 MN

The reason for this being slightly lower than V_{Lo} is due to the use of a depth increment of 0,1 m; V_L = 155,9 for D = 41,1 m.

A.9.3.2.3 Penetration in soils with partial drainage (silts)

Refer to guidance provided in ISO 19905-1:2012, A.9.3.2.3 (outside of the scope of this annex).

A.9.3.2.4 Penetration in silica sands

The soil properties for the silica sand location (Location 1) are characterized by:

$\phi'_{triaxial}$ = 34,0°

γ' = 11,0 kN/m^3

To calculate the vertical bearing capacity of the spudcan in the sand, the apparent friction angle mobilized during spudcan penetration has been estimated as 29,0° in order to account for the effects described in ISO 19905-1:2012, E.2.

The ultimate vertical bearing capacity for a circular footing (allowing for backflow and displaced soil) can be calculated from:

$$V_{Lo} = Q_V - W_{BF,o} + B_S \quad \text{(A.9.3-1)}$$

where

$$Q_V = \gamma' N_\gamma \pi B^3/8 + p'_o N_q \pi B^2/4 \quad \text{(A.9.3-8)}$$

where the terms are obtained as follows.

In this case the calculation will show that the spudcan is partially embedded in the sea floor (i.e. the maximum plan area of the spudcan is not in contact with the sea floor surface), hence no backflow occurs, and consequently:

p_o' = 0,0

$W_{BF,0}$ = 0,0

For the present detailed example calculations, the small spudcan soil buoyancy term, B_S, has not been incorporated. The bearing capacity equation stated above therefore simplifies to:

$$Q_V = \gamma' N_\gamma \pi B^3/8$$

In accordance with ISO 19905-1:2012, A.9.3.2.1.2 the equivalent cone angle, β, for the presently considered spudcan geometry is 162°. In this instance one could interpolate the bearing capacity factor $N\gamma$ given in ISO 19905-1:2012, E.2 using the values for ϕ = 25° and 30° for β = 150° and 180°. However, for the purposes of the present example, $N\gamma$ has been selected from ISO 19905-1:2012, Table A.9.3-3 for ϕ' = 29°:

N_γ = 12,8

The spudcan penetration resistance curve can now be calculated. If the predicted penetration curve indicated that penetrations greater than those required to mobilize the full spudcan area were required to support the preload footing reaction, then the spudcan soil buoyancy and weight of backfill should be incorporated into the calculation.

The spudcan penetration resistance curve is shown for the present example below:

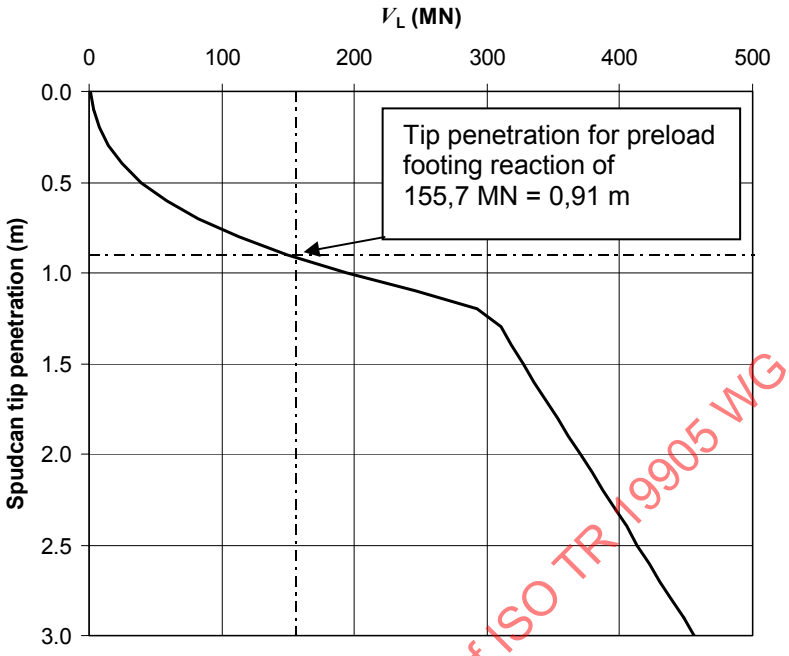

For the present preload footing reaction, V_{LO} = 155,7 MN, the corresponding tip penetration is 0,91 m, corresponding to partial spudcan penetration into the soil with an equivalent spudcan-soil contact diameter, B, of 14,1 m.

A.9.3.2.5 Penetration in carbonate sands

This is not a mainstream calculation and therefore not considered in the scope of this annex.

A.9.3.2.6 Penetration in layered soils

Performing penetration calculations in layered soils is often a complex undertaking and considered outside of the scope of this annex.

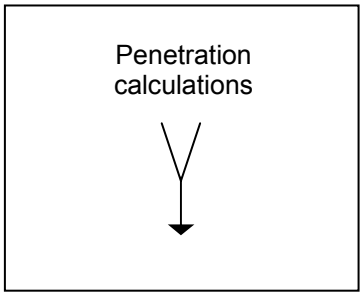

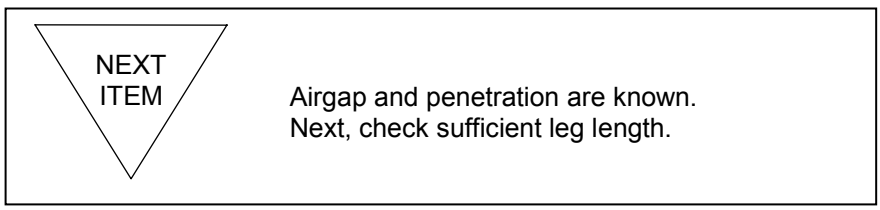

A.6 Assessment of leg length

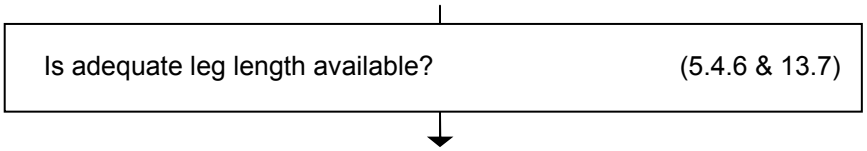

The foregoing calculation of penetration and airgap will determine how much leg reserve there is for a given water depth. The availability of leg length should be checked against this, and if there is insufficient reserve the unit is not recommended for use. In some such cases it may be possible to refine the penetration analysis, or use less preload so that the calculated leg length reserve can be made acceptable.

Is adequate leg length available?

13.7 Leg length reserve

Referring to ISO 19905-1:2012, 13.7, the leg length reserve above the upper guides should account for the uncertainty in the prediction of leg penetration and account for any settlement. ISO 19905-1 specifies that the leg length reserve shall be at least 1,5 m. The greater the uncertainty, the larger the leg length reserve that should be available. A larger reserve can also be required due to:

— strength limitations of the top bay;

— the increase in the proportion of the leg bending moment carried by the holding system due to the effective reduction in leg stiffness at the upper guide.

For this unit:

	Location 1 (Sand)	Location 2 (Clay)
Fixed factors (keel to U.G.):	26,0 m	26,0 m
Airgap above LAT:	20,9 m	19,7 m
Water depth (LAT):	121,9 m	85,0 m
Tip penetration:	0,9 m	42,3 m
Total length used:	169,7 m	173,0 m
Leg length:	174,9 m	174,9 m
Reserve:	5,2 m	1,9 m

The unit has sufficient leg reserve for the sand assessment case: 5,2 m > 1,5 m therefore satisfies the requirements of ISO 19905-1.

The unit has sufficient leg reserve for the clay assessment case: 1,9 m > 1,5 m therefore satisfies the requirements of ISO 19905-1.

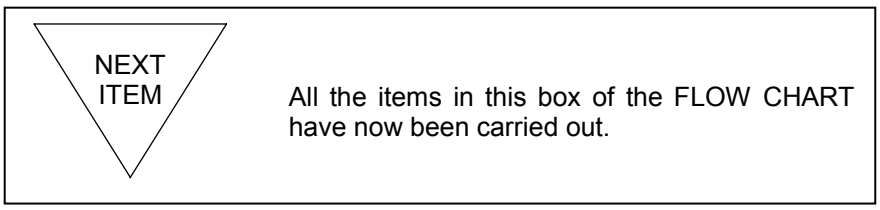

A.7 Review existing calculations

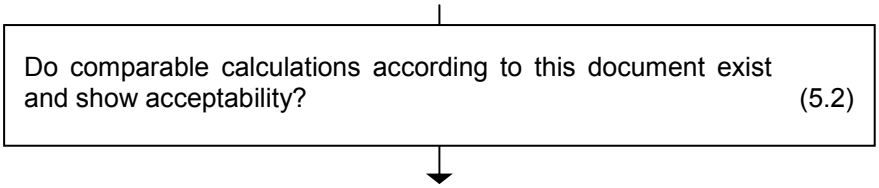

If the assessment situation is comparable with design conditions or other existing assessments determined in accordance with ISO 19905-1 then it may be appropriate to draw conclusions from these for the current assessment. This is the lowest level of application of ISO 19905-1 as mentioned in 5.2.

There have been no analyses of this unit at this location according to ISO 19905-1. Therefore, acceptability cannot be demonstrated at this stage.

Had there been a previous study according to ISO 19905-1 in which the foundation conditions, metocean conditions, waterdepth, airgap and penetration had been as severe, or more severe, and for which the unit had been acceptable for the relevant assessment checks, then no further analysis would have been necessary and the unit would have been acceptable. Site-specific foundation assessment must always be completed as part of this comparison. Because this was not so, a higher level of complexity must be carried out. All the following items in the flow chart apply to either the “simple” (b) or the “detailed” (c) methods of ISO 19905-1:2012, 5.2.

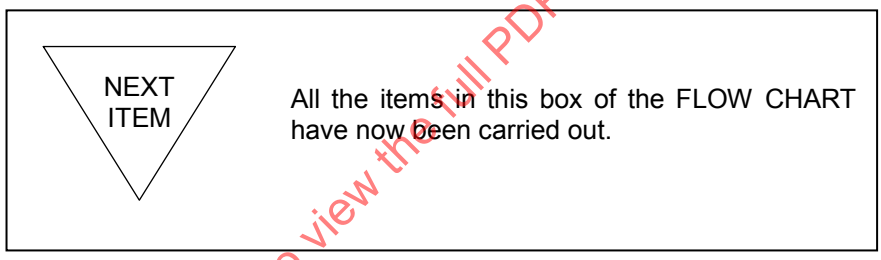

A.8 Establish actions, prepare analysis and foundation models

The top-level route is:

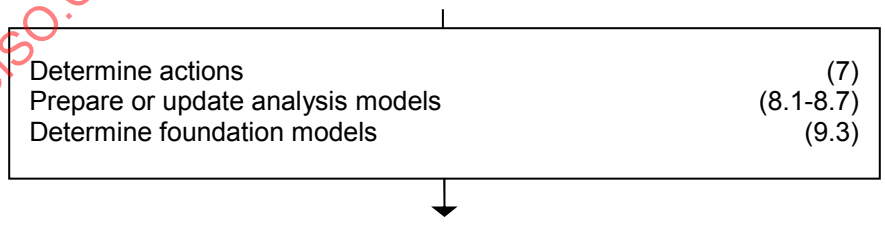

This item of the FLOW CHART contains sizable pieces of work and is split into local route flow charts. It is therefore presented in three parts. Here the actions, including hydrodynamic coefficients and wind loads, are tackled.

A.8.1 Establish actions

7 Determine actions

Local route

General	(7.2)
Metocean actions	(7.3 & A.7.3)
Functional loads	(7.4 & A.7.4)
Displacement dependant effects	(7.5)
Dynamic effects	(7.6)
Earthquakes	(7.7)
Other actions	(7.8)

7.2 General

The example calculations detailed herein cover the following aspects.

a) Metocean actions:

1) actions on legs and other structures from wave and current, plus

2) actions on hull and exposed areas (e.g. legs) from wind.

b) Functional actions:

1) fixed actions, plus

2) actions from variable load.

c) Indirect actions resulting from responses:

1) displacement dependent effects, plus

2) accelerations from dynamic response.

The example calculations do not address the following:

— earthquake actions;

— other actions

7.3 Metocean actions

7.3.1 General

The wave/current actions on the legs and other structures and the wind actions on the hull, legs and other structures detailed herein are considered to act simultaneously and from the same direction and are based on the 50 year return period individual extremes.

It is noted that whilst the directionality of wind, wave and current may be considered when it can be demonstrated that such directionality is applicable, this has not been considered for the purpose of the example calculations detailed herein. Likewise, use of 100-year joint probability metocean data is permitted.

i
A.7.3.1.1

A.7.3.2.1 Methods for the determination of actions

The example calculations detailed herein follow a deterministic assessment approach developing static metocean actions and an inertial loadset based on a dynamic amplification factor (DAF).

The action calculation follows the steps outlined in ISO 19905-1:2012, Table A.7.3-1 (Metocean action calculation procedures).

7.3.2 Hydrodynamic model

The use of model tests to establish coefficients is permitted as an option within ISO 19905-1:2012, A.7.3.2.1.

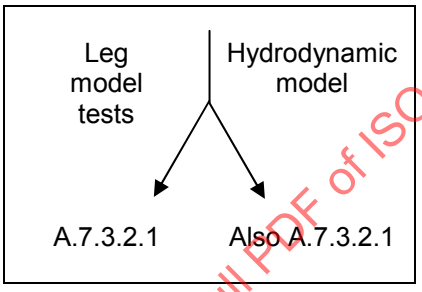

A.7.3.2.1 Model tests for hydrodynamic coefficients

Applicable test results may be used to select the coefficients for non-circular members (and not the complete leg), but must consider:

— roughness;

— Keulegan-Carpenter number dependence;

— Reynolds number dependence.

Model tests and analytical studies for complete legs are difficult to interpret and are unlikely to give results that are consistent with the methodology used here. This is particularly true for legs in which tubular members contribute significantly to the total drag coefficient because of Reynolds number dependency.

For the purposes of this annex it is not appropriate to carry this option further.

A.7.3.2.1 Leg hydrodynamic model

The hydrodynamic modelling of the jack-up leg can be carried out by utilizing “detailed” or “equivalent” techniques and is dependant on the modelling technique being used for assessment. In both cases details of all the leg members are considered in the hydrodynamic calculations.

Member lengths are normally taken as the node-to-node distance of the members (that point where two member axes intersect) in order to account for small non-structural items (e.g. anodes, jetting lines of less than 4 inches nominal diameter). Larger non-structural items such as raw water pipes and ladders are to be included in the model. Free standing conductors and raw water towers are to be considered separately from the leg hydrodynamic model.

The jack-up unit being considered has two raw water pipes/caissons on the bow and one on the port leg, but there are no non-structural items identified for the legs of this unit. No details of ladders or other free-standing pipes or caissons are included in the data package being used for assessment; these would have been sought and included were this not an example calculation.

Shielding and solidification effects are not normally considered (see ISO 19905-1:2012, A.7.3.2.1, Note 2). Current blockage is applied to the current velocity, as detailed later under the flag for A.7.3.3.4.

i
Table A.7.3-5, A.7.3.4 & ISO/TR 19905-2 7.3.2.4 & 7.3.2.5

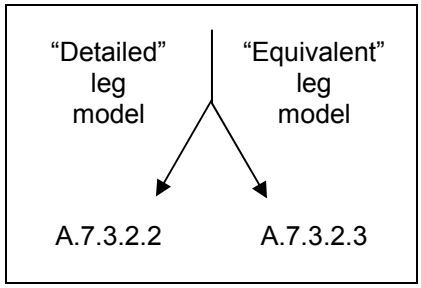

A.7.3.2.2 "Detailed" leg model

Summary of leg member details for hydrodynamic calculations:

Lower part of legs — up to 42 m above spudcan tip:

horizontal braces:

length = 16,15 m

outer diameter = 0,406 m

diagonal braces:

length = 9,28 m

outer diameter = 0,406 m

angle to horizontal = 30°

internal spanbreakers:

length = 7,34 m

outer diameter = 0,229 m

Upper part of legs — above 42 m above spudcan tip:

horizontal braces:

length = 16,15 m

outer diameter = 0,356 m

diagonal braces:

length = 9,28 m

outer diameter = 0,356 m

angle to horizontal = 30°

internal spanbreakers:

length = 7,34 m

outer diameter = 0,229 m

Lower and upper leg section brace offsets:

Vertical offset = 1,07 m

Horizontal offset = 0,30 m

(both stated as full offset values)

Raw water caisson details:

Bow leg (two caissons):

length = 16,2 m below MSL

outer diameter = 0,46 m

Port leg (one caisson):

length = 16,2 m below MSL

outer diameter = 0,46 m

Starboard leg — no raw water caissons

Gusset plates:

The “typical jack-up” being considered has no gusset-plating on the legs.

i
A.7.3.2.4

A.7.3.2.4 Drag and inertia coefficients

Base hydrodynamic coefficients for all of the above tubular members; see ISO 19905-1:2012, Table A.7.3.2:

Smooth C_D (above MSL + 2 m) = 0,65

Smooth C_M (above MSL + 2 m) = 2,00

Rough C_D (below MSL + 2 m) = 1,00

Rough C_M (below MSL + 2 m) = 1,80

From A.6.4.4 we have the following MSL conditions:

Location 1 (sand): MSL = 123,1 m

Location 2 (clay): MSL = 86,2 m

The unit is assumed not to have operated in deeper water depths; had this been the case, and the fouled legs not cleaned, the surface would be taken as rough for wave actions above MSL + 2 m.

The chords of this unit are covered by ISO 19905-1:2012, Figure A.7.3-3 and subsequent equations, with reference dimensions:

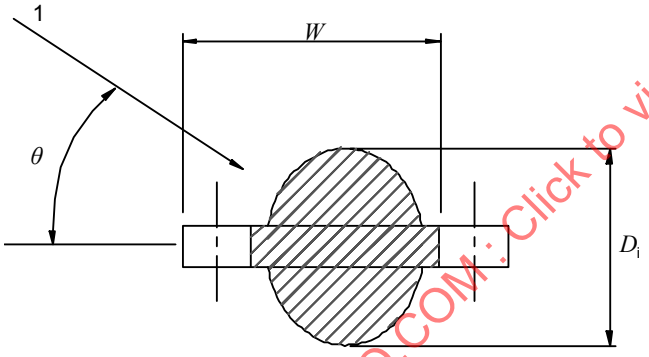

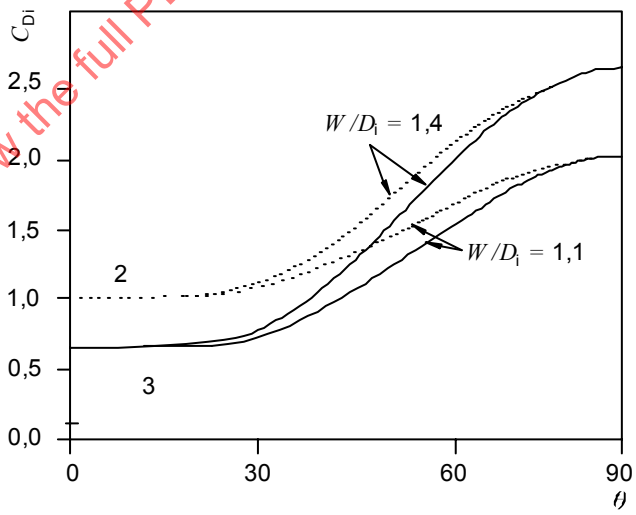

Key

1 flow direction
2 rough
3 smooth

C_{Di} drag coefficient to be used with D_i
D_i reference dimension of chord i
W average width of the rack
θ angle between flow direction and plane of rack (degrees)

Split-tubular chord dimensions:

Chord width (W) (tooth root to opposite tip) = 0,792 m

Chord depth (D) = 0,749 m

A.7.3.2.5 Marine growth

No anti-fouling measures have been included in this analysis of the “typical jack-up”, and no site-specific information on marine growth thickness. Therefore a default marine growth thickness of 12,5 mm (i.e. total of 25 mm across the diameter of a tubular member) is to be applied to all members below MSL + 2 m.

For a split tube chord as shown in ISO 19905-1:2012, Figure A.7.3-3, the rough drag coefficient $C_{Di,}$ is related to the reference dimension:

$$D_i = D + 2t_m$$

where:

t_m = marine growth thickness

therefore:

D_i = 0,749 + 0,025

= 0,774 m

Based on ISO 19905-1:2012, Equations (A.7.3-7) and (A.7.3-8), the chord member drag coefficients are calculated as follows:

Angle	**Rough** (below MSL+2 m)		**Smooth** (above MSL +2 m)	
θ (°)	D_i (m)	CD_i	D_i (m)	CD_i
0	0,774	1,000	0,749	0,650
15		1,000		0,650
30		1,042		0,712
45		1,238		1,005
60		1,515		1,416
75		1,750		1,767
90		1,842		1,903
105		1,750		1,767
120		1,515		1,416
135		1,238		1,005
150		1,042		0,712
165		1,000		0,650
180		1,000		0,650

Rough values include the effect of marine growth, smooth values do not.

For all headings the chord C_{Mi} = 1,8 below MSL + 2 m, and 2,0 above MSL + 2 m. This does not change for marine growth.

All leg members are now covered.

NEXT ITEM

The necessary calculation for the detailed leg is now complete. If required, the information can be combined in an equivalent leg model as described in the option below. Instructions applicable to both cases follow the equivalent leg model.

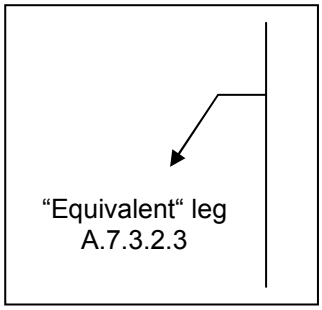

A.7.3.2.3 "Equivalent" leg model

An equivalent leg model comprising a single tubular with effective hydrodynamic properties may be constructed from the detailed member hydrodynamic information. For each different type of bay, overall parameters are derived as follows:

Equivalent diameter of leg: $D_e = \sqrt{\Sigma D_i^2 l_i / s}$

Equivalent drag coefficient: $C_{De} = \Sigma\, C_{Dei}$

where:

$$C_{Dei} = [\, \sin^2\beta_i + \cos^2\beta_i \sin^2\alpha_i \,]^{3/2}\, C_{Di}\, \frac{D_i l_i}{D_e s} \qquad \text{(A.7.3-2)}$$

The above expression for C_{Dei} may be simplified for horizontal and vertical members as follows:

Vertical members (e.g. chords):

$$C_{Dei} = C_{Di}\,(D_i/D_e) \qquad \text{(A.7.3-3)}$$

Horizontal members:

$$C_{Dei} = \sin^3\alpha_i\, C_{Di}\, \frac{D_i l_i}{D_e s} \qquad \text{(A.7.3-4)}$$

Equivalent inertia coefficient:

$$C_{Me}\, A_e = A_e\, \Sigma\, C_{Mei} \qquad \text{(A.7.3-5)}$$

where:

$$C_{Mei} = [1 + (\sin^2\beta_i + \cos^2\beta_i \sin^2\alpha_i)(C_{Mi} - 1)]\, \frac{A_i\, l_i}{A_e s} \qquad \text{(A.7.3-6)}$$

with

s = bay height

α_i = angle in horizontal plane of member axis from flow direction

β_i = angle of member axis from horizontal.

A_e = effective area of leg = $\pi D_e^2/4$

and other symbols as defined above.

Equivalent leg hydrodynamic coefficients were determined using the above relationships with summary results presented below for a single section.

For the "typical jack-up" being considered the leg has triangular symmetry, and a zero-degree heading is defined as perpendicular to the plane of the rack.

Rough coefficients below MSL + 2 m

Lower leg section (up to 42 m above spudcan tip): All legs have 16-inch diameter bracing and no raw water structure.

Heading (°)	D_e (m)	CD_e	A_e (m^2)	CM_e	$CD_e.D_e$	$CM_e.D_e^2$
0	2,202	2,995	3,809	1,664	6,594	8,070
30		3,058			6,735	
45		3,029			6,671	
60		2,995			6,594	

Upper leg section (above 42 m above spudcan tip): All legs have 14-inch diameter bracing.

No raw water caissons — all legs up to 12,2 m below MSL:

Heading (°)	D_e (m)	CD_e	A_e (m^2)	CM_e	$CD_e.D_e$	$CM_e.D_e^2$
0	2,050	3,025	3,301	1,694	6,203	7,121
30		3,061			6,337	
45		3,091			6,276	
60		3,025			6,203	

Two 18-inch diameter raw water caissons from 12,2 m below MSL (bow leg)

Heading (°)	D_e (m)	CD_e	A_e (m^2)	CM_e	$CD_e.D_e$	$CM_e.D_e^2$
0	2,161	3,317	3,667	1,705	7,167	7,958
30		3,379			7,301	
45		3,351			7,241	
60		3,317			7,167	

One 18-inch diameter raw water caisson from 12,2 m below MSL (port leg)

Heading (°)	D_e (m)	CD_e	A_e (m^2)	CM_e	$CD_e.D_e$	$CM_e.D_e^2$
0	2,106	3,174	3,484	1,700	6,685	7,540
30		3,238			6,819	
45		3,209			6,759	
60		3,174			6,685	

Starboard leg — no raw water caisson fitted (see data above).

Smooth coefficients above MSL + 2 m

Legs below hull:

Bow leg — fitted with two 18-inch diameter raw water caissons.

Heading (°)	D_e (m)	CD_e	A_e (m^2)	CM_e	$CD_e.D_e$	$CM_e.D_e^2$
0	2,048	2,446	3,293	1,792	5,004	7,513
30		2,516			5,152	
45		2,485			5,086	
60		2,443			5,004	

Port leg — fitted with one 18-inch diameter raw water caisson.

Heading (°)	D_e (m)	CD_e	A_e (m^2)	CM_e	$CD_e.D_e$	$CM_e.D_e^2$
0	1,996	2,358	3,129	1,781	4,706	7,095
30		2,432			4,855	
45		2,401			4,792	
60		2,358			4,706	

Starboard leg — no raw water caisson fitted.

Heading (°)	D_e (m)	CD_e	A_e (m^2)	CM_e	$CD_e.D_e$	$CM_e.D_e^2$
0	1,943	2,269	2,965	1,769	4,409	6,677
30		2,346			4,558	
45		2,313			4,495	
60		2,269			4,409	

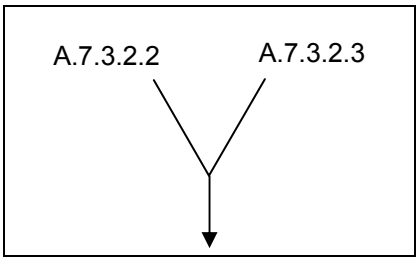

Leg hydrodynamic coefficients have now been calculated.

7.3.3.4 Current

Current velocities for this analysis have been defined as a linear profile passing through two points (A.6.4.3); the intermediate current values are linearly interpolated between these points by the software.

The current induced drag actions are determined in combination with the wave actions. This is carried out by the vectorial addition of the wave and current induced particle velocities prior to the drag action calculations.

The current induced drag forces are determined in combination with the wave actions as required by ISO 19905-1:2012, A.7.3.3.4, with allowance made for reduction in current velocity to account for interference per ISO 19905-1:2012, Equation (A.7.3-19):

$$V_C = V_f\,[1 + C_{De}D_e/(4D_F)]^{-1} \qquad \text{(A.7.3-19)}$$

where:

V_f is the far field (undisturbed) current velocity;
surface 1,49 m/s

C_{De} is the equivalent drag coefficient of the leg as defined in ISO 19905-1:2012, A.7.3.2 (leg section-specific);
e.g. 3,317 for 0-degree loading on bow leg including two 18” raw water casings
(see ‘equivalent leg’ calculations detailed herein)

D_e is the equivalent diameter of the leg, as defined in ISO 19905-1:2012, A.7.3.2 (leg section-specific);
e.g. 2,161 on bow leg (including two 18” raw water casings)

D_F is the face width of leg, outside dimensions, orthogonal to the flow direction;
16,9 m for 0-degree loading onto bow leg

therefore

V_C is the current velocity to be used in the hydrodynamic model,
e.g. = 0,90 V_f based on the example values above, and is consistently 0,90 to 0,91 for all leg sections.

Check that V_C is not less than 0,7V_f as specified in ISO 19905-1. This is satisfied.

i
see Reference [A.7.3-5] and
ISO TR 19905-2 A.7.3.3.3.1

7.3.4 Establish wind loads

Wind actions are computed using wind velocity, wind profile and exposed areas. Wind velocities and wind profiles presented in A.6.4.6 are used.

Generally block areas are used for the hull, superstructures and appurtenances.

These actions can be calculated using appropriate formulae and coefficients or can be derived from applicable wind tunnel tests.

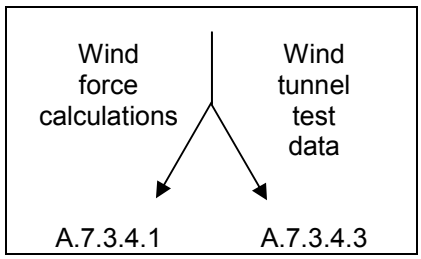

A.7.3.4.1 Wind force calculations

Wind force calculations on the structure above MSL are split into:

— wind load on legs below the hull,

— wind load on the hull (including all superstructure and appurtenances),

— wind load on legs above the hull.

This subclause gives a method for deriving the wind force on the block areas (of no more than 15 m vertical extent) used to represent the hull, superstructure or appurtenances of the unit above.

The wind area of the hull and associated structures (excluding derrick and legs) can normally be taken as the projected area viewed from the direction under consideration.

Note that “shielding effects are not normally included in the calculation”. This is because a profile area viewed from the direction under consideration is to be used.

The wind force is determined using the following equation:

$$F_{wi} = P_i A_{Wi} \quad \text{(A.7.3-21)}$$

where:

P_i = the pressure at the centre of the block;

A_{Wi} = the projected area of the block considered.

The pressure P_i is computed using the following equation:

$$P_i = 0{,}5\ \rho\ V_{zi}^2\ C_s \quad \text{(A.7.3-22)}$$

where:

ρ = density of air (1,2224 kg/m^3);

V_{zi} = the specified wind velocity at centre of each block (see A.6.4.6.2);

C_s = shape coefficient (see ISO 19905-1:2012, Table A.7.3-4).

Wind force on hull

The effective area of the hull is calculated from the projected area "blocks" making up the hull structure. The following procedure is applied here.

— Identify major blocks in the hull structure. The descriptions in ISO 19905-1:2012, Table A.7.3-4 should be used with outboard profiles and general arrangement drawings of the jack-up.

— Measure projected areas of blocks and their effective arms above the SWL for the elevated position.

— Apply shape coefficients (from ISO 19905-1:2012, Table A.7.3-4).

— Calculate wind velocity V_Z to be applied to each block (height dependant) from ISO 19905-1:2012, Equations (A.6.4-14) and (A.6.4-15).

— Calculate total of wind forces and moments from each block

Summary results for the "typical jack-up" hull being considered, for an airgap of 20,9 m from LAT to keel (Location 1 — sand) are:

Heading (°)	**Effective area** [a] (m^2)	**Wind force** [b] (kN)	**Effective arm above MSL** (m)
0	2 397	5 030	40,2
60	3 664	7 731	40,7
90	3 521	7 427	40,5
120	3 039	6 447	42,2
[a] Effective wind areas include shape coefficients appropriate to each "block". [b] Wind force does not include environmental load factor $\gamma_{f,E}$.			

Wind force on exposed leg sections

The procedure for calculating the wind forces on the exposed leg sections is identical to that for the hull structure, except that shape coefficient is based on C_{De} using smooth drag coefficients (ignoring marine growth); see ISO 19905-1:2012, Table A.7.3-4.

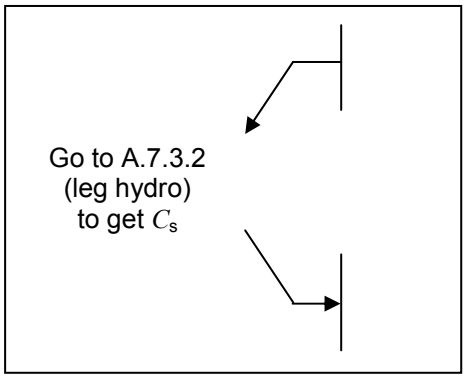

Example values presented for leg above hull (no raw water structure) — all legs:

Heading (°)	D_e (m)	C_{De}	$C_{De}.D_e$
0	1,943	2,269	4,409
60		2,346	4,558
90		2,313	4,495
120		2,269	4,409

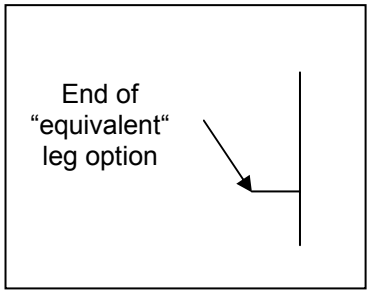

There is now sufficient information to calculate the wind loads on the exposed leg sections by use of an equivalent leg, using $C_s = C_{De}$ and projected width D_e.

A.7.3.4.3 Wind loads from wind tunnel (model tests)

Summary of leg member details for hydrodynamic calculations:

Wind pressures and resulting actions for the hull and associated structures can be determined from wind tunnel tests on a representative model. Care should be exercised when interpreting wind tunnel data for structures mainly comprised of tubular components, such as truss legs.

Use of model tests must consider:

— roughness;

— Keulegan-Carpenter number dependence;

— Reynolds number dependence.

This option is not explored further in this detailed example calculation.

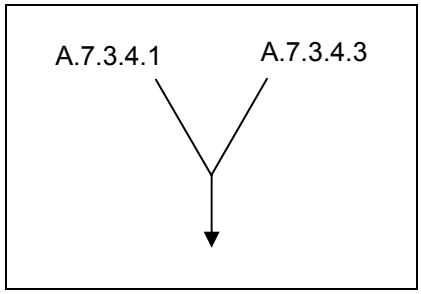

Leg hydrodynamic coefficients have now been calculated.

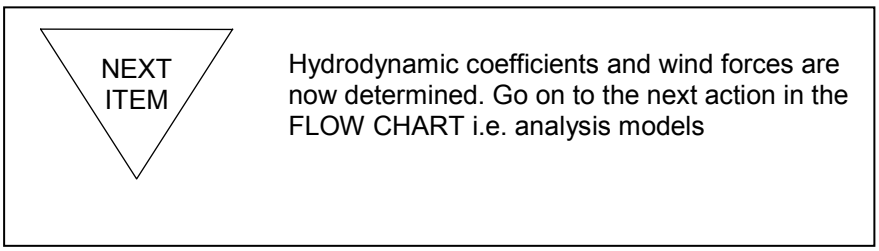

A.8.2 Prepare analysis models

The second action in this FLOW CHART box is now considered. The action refers to analysis models, but for the purpose of the example calculations only the structural models are prepared at this stage (sections A.8.1 to A.8.6) with the mass and load application (sections A.8.7 and A.8.8) covered in the response calculations.

8 **Structural models**

Local route

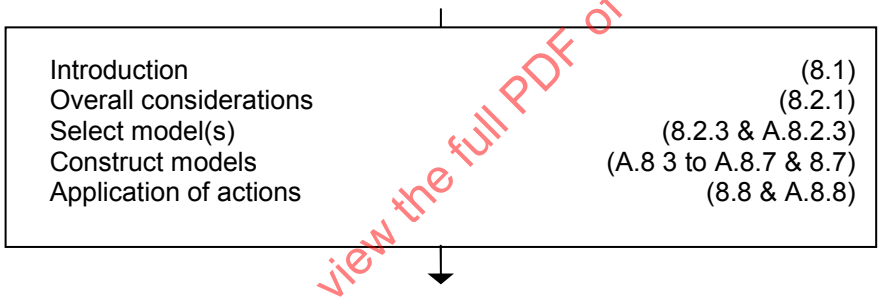

8.2.1 **Overall considerations**

Structural modelling of the jack-up is intended to achieve the following objectives for both the static and dynamic responses:

— realistic global response (e.g. displacement, base shear, overturning moment) for the jack-up under the applicable environmental and functional actions;

— suitable representation of the leg, leg-to-hull connection and the leg-foundation interaction, including non-linear effects as necessary; and

— adequate detail to enable realistic assessment of the leg structure, the structural/mechanical components of the jacking and/or fixation system and the foundation.

8.2.3 & A.8.2.3 **Select models**

For most jack-up configurations it is necessary to develop a finite element computer model including legs, leg-to-hull connection and hull. The choices regarding the level of complexity are as follows:

a) fully detailed model of all legs, leg-to-hull connections, with detailed or representative stiffness model of hull and, possibly, spudcan;

b) equivalent leg (stick model) and equivalent hull;

c) combined equivalent/detailed leg and hull, e.g. simplified lower legs and spudcans, detailed legs in way of the hull and leg-to-hull connections with detailed or representative stiffness model of the hull;

d) detailed single leg (or leg section) and leg-to-hull connection model.

The levels of modelling are expanded upon in ISO 19905-1:2012, A.8.2.3, with the limitations of each model outlined in Table A.8.2-1, reproduced below:

Table A 8.2-1 — Applicability of the suggested models

	Applicability						
Model type	I Base shear and overturning moment	II Overturning checks	III Foundation checks	IV Global leg forces	V Leg member forces	VI Jacking/ fixation system reactions	VII Hull element forces
a) Fully detailed leg	Yes	Yes	Yes	Yes	Yes	Yes	See note
b) Equivalent leg (stick model)	Yes	Yes	Yes	Yes	-	-	-
c) Combined equivalent/detailed leg and hull	Yes	Yes	Yes	Yes	Yes	Yes	See note
d) Detailed single leg and leg-to-hull connection model	-	-	-	-	Yes	Yes	-
NOTE Hull stresses are only available from more complex hull models.							

On the basis of the descriptions of the model types and the considerations in ISO 19905-1:2012, A.8.2.3, selection of appropriate analysis models can be made.

The following checks are required for this study: overturning, foundation, leg strength (chords and braces), and holdings system loads (pinions and rack chocks). The models which would satisfy these requirements are, from Table A.8.2-1:

— type a;

— type b combined with type d;

— type c.

Whilst model types a) and c) would be equally appropriate, it is considered that the most efficient models for this assessment are the equivalent 3-leg stick model (type b) for global loading, in conjunction with the single detailed leg model (type d) for leg and holding system strength checks.

It is appropriate to calibrate the leg properties in the 3-leg model against the characteristics of the detailed single leg model.

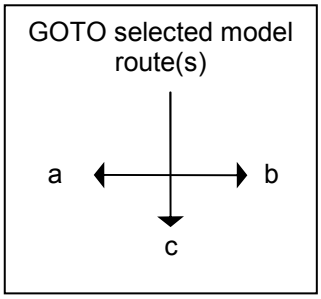

A.8.2.3 a) **Fully detailed 3 leg model — sub-route**

Detailed leg	(A.8.3.2)
Hull	(A.8.4)
Hull/leg connection	(A.8.5)
Spudcan	(A.8.6.1)

This modelling technique has not been used for this study. However, many of the notes for model types b and d are applicable, and appropriate reference is made to these.

A.8.3.2 **Detailed leg**

See notes for model type d (detailed leg model).

A.8.4 **Hull**

ISO 19905-1 requires that the hull structure be modelled so that the actions can be correctly transferred to the legs and the hull flexibility is represented accurately. The options are either a detailed hull model (ISO 19905-1:2012, A.8.4.2) generated using plate elements, or an equivalent hull model (ISO 19905-1:2012, A.8.4.3) — see hull modelling notes covered in model type b.

A.8.5 **Hull/leg connection**

See notes for model type d (detailed leg model). The leg-to-hull connections should be connected to either a detailed or a representative model of the hull instead of being earthed off in the single detailed leg model.

A.8.6.1 **Spudcan**

When modelling the spudcan, rigid beam elements are considered sufficient to achieve an accurate transfer of the seabed reaction into the leg chords and bracing.

Note: For a strength analysis of the spudcan and its connections to the leg, a detailed model of the spudcan and lower-leg, with appropriate boundary conditions, should be developed.

A.8.2.3 b) **Equivalent leg (stick model) — sub-route**

Equivalent leg	(A.8.3.3)
Hull	(A.8.4)
Hull/leg connection	(A.8.5)

The simple 3 leg model (type b) will be used to obtain global loads, such as spudcan reactions, and internal leg loads at the lower guide. For the detailed example calculation, detailed leg strength checks are to be performed; therefore the model type d will also be required.

In constructing the simple 3-leg model (type b), fairly detailed modelling of the hull/leg connection will be necessary to determine effective stiffnesses. If a type d detailed leg model is to be used later, it might also be used for this part of the calculation. Therefore, it would be more efficient to construct the type d model first.

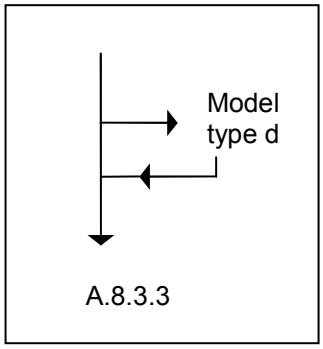

A.8.3.3 **Equivalent leg**

The appropriate leg sub-model is the “equivalent” leg, comprising a series of colinear beam elements as described in ISO 19905-1:2012, A.8.3.3.

The leg structure can be simulated by a series of colinear beams with the equivalent cross-sectional properties calculated using the formulae indicated in ISO 19905-1:2012, Tables A.8.3-1 and A.8.3-2 or derived from the application of suitable “unit” load cases to the “detailed leg”.

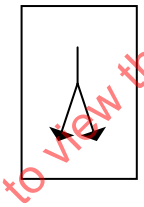

OPTION Apply formulae contained in ISO 19905-1:2012, Tables A.8.3-1 and A.8.3-2.

The unit has a split-cross braced design which can be modelled as type c (“X-brace”) with additional horizontals at the mid bays which have no effect on the shear area. Therefore, the equivalent shear area of one side is:

$$A_{Qi} = \frac{(1+\nu)sh^2}{\frac{d^3}{4A_D} - \frac{s^3}{12A_C}}$$

where

for the lower leg section:

ν = Poisson’s ratio for steel
= 0,3

S = bay height
= 10,21 m

h = chord spacing (centre to centre)
= 16,15 m

d = length of diagonal brace on face
= 18,56 m

A_D = area of brace diagonal
= 0,037 m^2

A_C = area of chord (inc. 10 % tooth per ISO 19905-1:2012, 8.3.5)
= 0,254 m^2

thus:

A_{Qi} = 0,082 m^2

for the upper leg section:

ν = Poisson's ratio for steel
= 0,3

S = bay height
= 10,21 m

h = chord spacing (centre to centre)
= 16,15 m

d = length of diagonal brace on face
= 18,56 m

A_D = area of brace diagonal
= 0,026 m^2

A_C = area of chord (inc. 10 % tooth ISO 19905-1:2012, per 8.3.5)
= 0,254 m^2

thus:

A_{Qi} = 0,057 m^2

The leg cross section is type A (triangular), and so:

A = 3 A_{Ci}
= 0,762 m^2 leg area

A_{Qy} = A_{Qz} equivalent shear area
= 3 A_{Qi}/2
= 0,122 m^2 lower leg shear area
= 0,086 m^2 upper leg shear area

I_y = I_z
= ½$A_{Ci}h^2$
= 33,12 m^4 leg 2nd moment of area

I_T = ¼$A_{Qi}h^2$
= 5,321 m^4 lower leg torsional moment of inertia
= 3,743 m^4 upper leg torsional moment of inertia

OPTION Determine cross sectional properties of the leg by application of “unit” load cases to a detailed leg model.

If a detailed leg model is available it is possible to use it to determine the equivalent leg cross-sectional properties. The technique is to rigidly restrain the leg model at the first point of lateral force transfer between the hull and leg, although it can be more convenient to use a different reference point, e.g. chock level or neutral axis of the hull, and to apply loads at, or near to, the spudcan (a known distance L). By comparing deflections with a simple beam model of the same length, under the same loads, effective beam properties can be deduced.

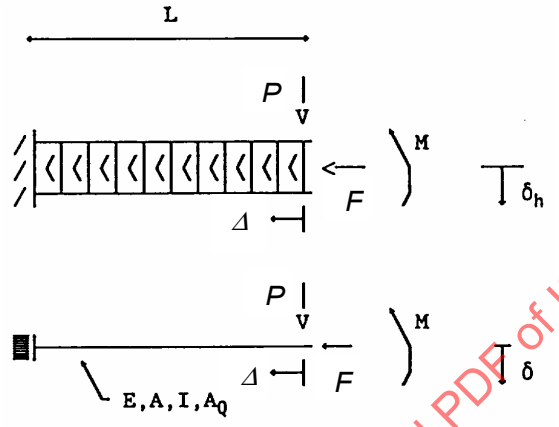

Calculations are presented for the sand assessment case only for the purpose of the detailed example calculations. Properties for the clay assessment case are calculated following the same process.

The following load cases should be considered, applied about the major and minor axes of the leg:

Axial “unit” load case

This is used to determine the axial area, A, of the equivalent beam according to standard beam theory:

$$\Delta = \frac{FL}{AE} \Rightarrow A = \frac{FL}{E\Delta}$$

where:

F = applied axial action
= 9,81x107 N (chosen to be representative of leg-load of this unit)

L = cantilevered length from the hull to seabed reaction point (A.8.6.2)
= 155,8 m for ‘sand’ assessment case

E = Young's modulus (steel = 205 000 N/mm^2)

Δ = axial deflection of cantilever at point of force application

From application of the loadcase, F, to the detailed leg model the following axial deflections, Δ, were calculated:

= 0,097 m for ‘sand’ assessment case

Therefore:

A = 0,765 m^2 for ‘sand’ assessment case

Pure moment load case

Applied either as a moment or a couple. This is used to derive the second moment of area (I) according to standard beam theory:

$$\delta = \frac{ML^2}{2EI} \Rightarrow I = \frac{ML^2}{2E\delta} \quad \text{and} \quad \theta = \frac{ML}{EI} \Rightarrow I = \frac{ML}{E\theta}$$

where

M = applied moment
= 1,603 × 10^9 N-m

δ = lateral deflection of cantilever at the point of moment application

θ = slope of cantilever at point of moment application

From application of the loadcase, M, to the detailed leg model the following lateral deflections, δ, and slope of cantilever, θ, at point of application were calculated:

δ = 2,858 m

θ = 0,037 radians

Therefore:

second moment of area (I) based on $ML^2/2E\delta$:

I = 33,20 m^4

second moment of area (I) based on $ML/E\theta$:

I = 33,21 m^4

ISO 19905-1 notes that the value of I resulting from the two equations can differ somewhat, understood to be dependent upon bracing configuration; the example case presented herein shows only a 0,05 % difference, but this would be expected to be significantly greater for K-braces configurations.

Pure shear

Pure shear, P, applied at the end of the leg, which can be used to derive I according to standard beam theory:

$$\theta = \frac{PL^2}{2EI} \Rightarrow I = \frac{PL^2}{2E\theta}$$

where

P = applied shear load
= 9,810 × 106 N-m

From application of the loadcase, P, to the detailed leg model the following lateral deflections, δ, and slope of cantilever, θ, at point of application were calculated:

δ = 2,11 m

θ = 0,017 radians

Second moment of area (I) based on $PL^2/2E\theta$:

I = 33,21 m^4

Using either this value of I, or a value obtained from the pure moment case, the effective shear area, A_s, can then be determined from:

$$\delta = \frac{PL^3}{3EI} + \frac{PL}{A_s G} \Rightarrow \quad A_s = \frac{7{,}8PLI}{3EI\delta - PL^3}$$

where

G = shear modulus = E/2,6 for Poisson's ratio of 0,3

A_s = 0,066 m^2

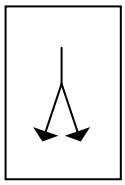

Comment on results: It is noted that the effective shear area A_s calculated from loads applied to the detailed leg model are lower than the equivalent shear area determined from the empirical formulae in ISO 19905-1:2012, Figure A.8.3-1 (for both the lower and upper leg sections). This may be due to the horizontal and vertical offsets between the brace node intersections such that s, h and d are not truly compatible with each other (i.e. d not exactly equal to $sqrt(s^2 + h^2)$ and the effect of the unbraced chord lengths at the spudcan.

8.7 & A.8.7 Mass modelling of leg

Although mass modeling is covered in ISO 19905-1:2012, 8.7 and A.8.7, the mass modeling of the leg is presented here for continuity purposes.

i
8.7 & A.8.7

Basic leg densities are covered in A.3.1 under the flag for 6.2, Jack-up data.

The weight of the raw water structure is added to the bow and port legs from 12,2 m below MSL to the keel level at 19,17 m above MSL.

Effective weight per unit lengths:

Bow	= 1,641 t/m
Port	= 0,821 t/m
Leg area	= 0,765 m^2,
Effective leg density	= 14,694 kg/m^3 (excluding RWS)

For the dynamic calculations, the added mass of the fluid entrained in, and surrounding, the leg should be accounted for (ISO 19905-1:2012, 8.7). This is calculated as follows:

added mass = $\rho A_e(C_{Me} - 1)$ [Note to Equation (A.7.3-6)]

where A_e is defined in A.7.3.2.3.

Added mass values for the “typical jack-up” being considered, accounting for marine growth, are as follows:

Added mass	**Bow leg** t/m	**Port leg** t/m	**Stbd leg** t/m
Lower leg section (up to 42 m above spudcan tip)	2,593	2,593	2,593
Up to 12,2 m below MSL	2,349	2,349	2,349
Up to MSL + 2 m	2,684	2,499	2,349

Using this information, the following table summarizes the leg density for each part of the leg accounting for leg properties, raw water structure and added mass with the total leg “effective” mass are shown at the bottom of the table.

It should be noted that the weight of water entrapped in the spudcan is included in the analyses but the added mass of water surrounding the spudcan is not in accordance with ISO 19905-1:2012, 8.7. The following densities and masses have been calculated for the sand case. The densities are exactly the same for the clay case, however, the masses are marginally different.

Leg densities for dynamic calculations

Leg densities		**Bow leg**	**Port leg**	**Stbd leg**
Spudcan (including 1 194 t of entrapped water)	Density (kg/m^3)	271 323		
	Length (m)	8,5		
	Mass (t)	1 764		
Lower leg section (up to 42 m above spudcan tip)	Density (kg/m^3)	18 083		
	Length (m)	33,50		
	Mass (t)	463,4		
Up to 12,2 m below MSL	Density (kg/m^3)	17 764		
	Length (m)	69,81		
	Mass (t)	948,7		
Up to MSL + 2 m	Density (kg/m^3)	20 300	19 032	17 764
	Length (m)	14,2	14,2	14,2
	Mass (t)	220,5	206,8	193,0
Up to keel level	Density (kg/m^3)	16 838	15 766	14 693
	Length (m)	17,71	17,71	17,71
	Mass (t)	228,1	213,6	199,1
Above keel	Density (kg/m^3)	14 693	14 693	14 693
	Length (m)	31,18	31,18	31,18
	Mass (t)	350,5	350,5	350,5
Total leg mass (t)		3 975	3 947	3 919

The spudcan is assumed flooded. It both carries a volume of water and displaces a volume of water. However, for the dynamic analyses the entrapped water in the spudcan is added to the mass of the spudcan.

Leg densities for gravity calculations

Leg densities		Bow leg	Port leg	Stbd leg
Spudcan	Density (kg/m^3)	76 266		
	Length (m)	8,5		
	Mass (t)	495,9		
Lower leg section (up to 42 m above spudcan tip)	Density (kg/m^3)	10 468		
	Length (m)	33,50		
	Mass (t)	268,3		
Up to 12,2 m below MSL	Density (kg/m^3)	10 468		
	Length (m)	69,81		
	Mass (t)	559,1		
Up to MSL + 2 m	Density (kg/m^3)	12 334	11 401	10 468
	Length (m)	14,2	14,2	14,2
	Mass (t)	134,0	123,9	113,7
Up to keel level	Density (kg/m^3)	16 838	15 766	14 693
	Length (m)	17,71	17,71	17,71
	Mass (t)	228,1	213,6	199,1
Above keel	Density (kg/m^3)	14 693	14 693	14 693
	Length (m)	31,18	31,18	31,18
	Mass (t)	350,5	350,5	350,5
Total leg weight (t)		2 035	2 011	1 986

These densities do not include added or entrapped mass but do include buoyancy.

A.8.4.3 Equivalent hull model

In an equivalent hull model, the deck, bottom, side shell and major bulkheads are modelled as a grillage of beams with properties chosen to represent the flexibilities of the hull.

ISO 19905-1 notes: “The axial and out-of-plane properties of the beams should be calculated based on the depth of the bulkheads, side-shell and the “effective width” of the deck and bottom plating. Beam elements should be positioned with their neutral axes at mid-depth of the hull. Due to the continuity of the deck and bottom structures and the dimensions of a typical hull box, the in-plane bending stiffness can be treated as large relative to the out-of-plane stiffness. The torsional stiffness should be approximated from the closed box-section of the hull and distributed between the grillage members.”

The first stage is to establish the geometry of the grillage. This is based on the plan of bulkheads and plate sides, and is shown in Figure A.8.2-1.

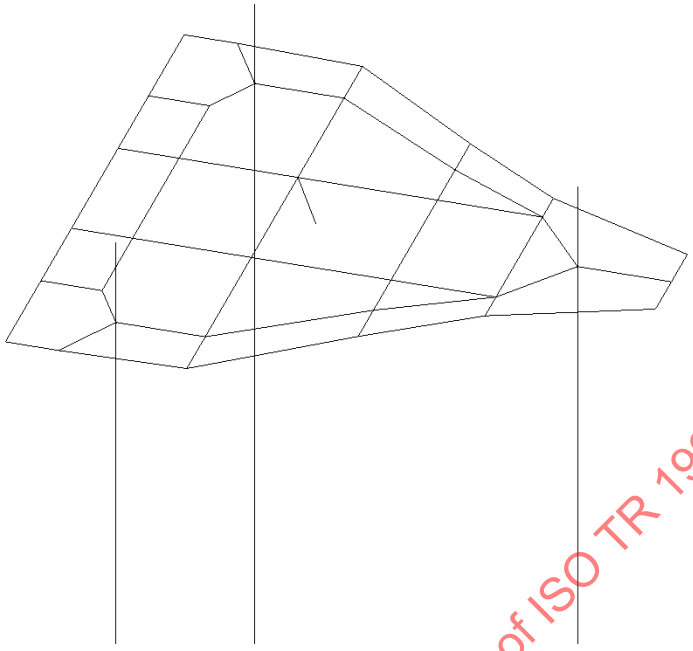

Figure A.8.2-1 — 3 stick leg model (showing hull beam grillage)

Next, properties are to be assigned to the equivalent beams. It is appropriate to assign sectional areas, second moments of area in plane and out of plane, and the torsional second moments of area. A typical calculation is as follows.

Assign long, beam-like portions of the structure, following a bulkhead or similar which can represent the web. An effective width of the beam-like component can be deduced from inspection of the plan, such that most of the plan area is assigned to beams with minimum overlap (see Figure A.8.2-2).

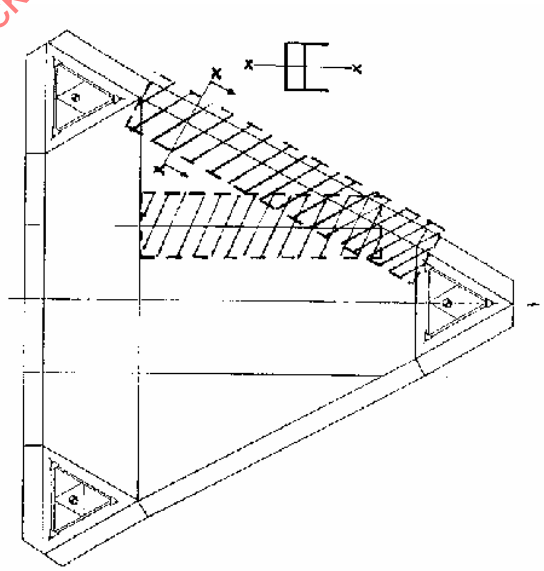

Figure A.8.2-2 — Example division of hull structure into equivalent beams (of different jack-up)

For example, a beam section to represent the sides of the unit is as follows:

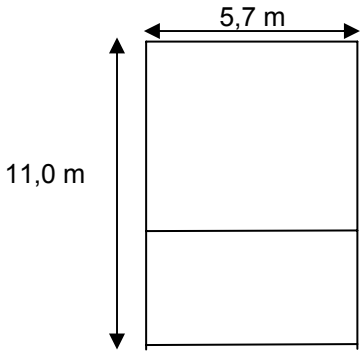

Plate thicknesses:

Main deck	=	25,4 mm
Machinery deck (Md)	=	12,7 mm
Bottom plate	=	25,4 mm
Sideshell:		
Below Md	=	14,3 mm
Above Md	=	12,7 mm
Legwell:		
Below Md	=	31,8 mm
Above Md	=	25,4 mm

NOTE Whilst stiffeners have been included in calculations below these are not detailed herein for simplification.

Area = 0,724 m^2
I_{XX} = 16,3 m^4
I_{YY} = 10,7 m^4 (see below)

Due to the continuity of the deck and bottom structures and the dimensions of a typical hull box, the in-plane bending I_{YY} stiffness can be treated as large relative to the out-of-plane stiffness, say 100 m^4.

The torsional stiffness should be approximated from the closed box section of the hull and distributed between the grillage members.

Transverse cross-section (taken through the leg centroid of the hull), considered typical torsional stiffness for hull beams:

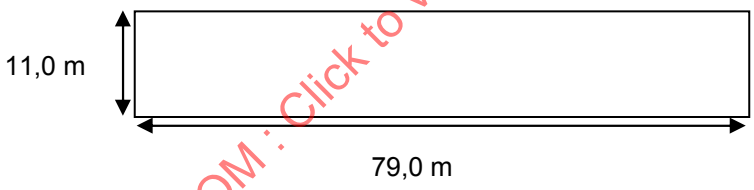

Main deck plate	=	19,5 mm
Bottom plate	=	14,3 mm
Sideshell plate	=	12,7 mm

Overall torsional stiffness of a box section — example calculation (formulation not given in ISO 19905-1:2012). It is assumed that the effect of any internal bulkheads can be ignorred because the shear flow in adjacent cells opposes and they therefore have minimal effect:

$I_t = \frac{4A^2}{\Sigma(b/t)}$ for plates of thickness t, width b and box enclosed area A.

Therefore for the above section, I_t = 263 m^4. This is apportioned equally between the six longitudinal beams, such that each has torsional second moment of area I_t = 43,9 m^4.

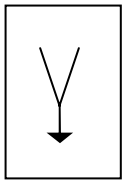

Performing the above calculations for each beam (not included herein) produces a hull model which matches the requirements of ISO 19905-1:2012, A.8.4.3.

8.5.7 Leg to hull connection stiffness

The determination of stiffnesses for the equivalent leg-to-hull connection model referred to in ISO 19905-1:2012, 8.5.7 can be accomplished by the following means of application of unit load cases to a detailed leg model in combination with a detailed leg-to-hull connection model in accordance with 8.3.2 and 8.5.

Unit load cases are applied, as described in ISO 19905-1:2012, A.8.3.3. In this instance the effective stiffness of the connection can be determined from the differences between the results from the detailed leg model alone (see the information reported under the flag for A.8.3.3 above) and those from the detailed leg plus leg-to-hull connection model as follows.

Axial "unit" load case

This is used to determine the vertical leg-to-hull connection stiffness, K_{vh}, from the axial end displacements of the detailed leg model, Δ, and the axial end displacements of the combined leg and leg-to-hull connection model, Δ_C, under the action of the same "unit" load case, F:

$$K_{vh} = F / (\Delta_C - \Delta) \qquad \text{(A.8.5-1)}$$

From application of the loadcase, F, to the detailed leg model with the leg-to-hull connection modelled as a series of spring and gap elements representative of the guides, pinions and rack chock system, the following axial deflections, Δ_C, were calculated:

$$\Delta_C = 0{,}106 \text{ m}$$

Therefore:

$$K_{vh} = 1{,}15 \times 10^{10} \text{ N/m}$$

Pure moment

Pure moment applied either as a moment or as a couple: This case is used to derive the rotational leg-to-hull connection stiffness, K_{rh} from either the end slopes, θ_M and θ_C, or the end deflections, δ and δ_C, of the two models under the action of the same end moment, M:

$$K_{rh} = M / (\theta_C - \theta) \text{ or } K_{rh} = ML / (\delta_C - \delta) \qquad \text{(A.8.5-2)}$$

From application of the loadcase, M, to the detailed leg model the following lateral deflections, δ_C, and slope of cantilever, θ_C, at point of application were calculated:

$$\delta_C = 3{,}287 \text{ m}$$
$$\theta_C = 0{,}039 \text{ radians}$$

Therefore:

Rotational connection stiffness, K_{rh}, based on $M / (\theta_C - \theta)$:

$$K_{rh} = 7{,}629 \times 10^{11} \text{ Nm/radian}$$

Rotational connection stiffness, K_{rh}, based on $ML / (\delta_C - \delta)$:

$$K_{rh} = 5{,}822 \times 10^{11} \text{ Nm/radian}$$

Note: Whereas the calculated leg second moment of areas calculated from the two equations based on pure moment load as shown under the flag for A.8.3.3 above were in good agreement, the rotational connection stiffness from the two equations based on pure moment load show some 31 % difference. Although not specifically referenced in ISO 19905-1:2012, this can additionally be derived from pure shear load in a similar manner (see below).

Pure shear

A pure shear loadcase can be used to determine the horizontal leg-to-hull connection stiffness, K_{hh}, in a similar manner, accounting for the rotational stiffness already derived. Normally the horizontal leg-to-hull connection stiffness can be assumed infinite.

The rotational connection stiffness, K_{rh} can additionally be calculated based on comparisons of end rotations, θ and θ_C, of the two models under the action of a pure shear load P:

$$K_{rh} = PL / (\theta_C - \theta)$$

From application of the loadcase, P, to the detailed leg model, the end rotation θ_C was calculated as 0,019 4 radians.

On this basis, K_{rh} is calculated as $8{,}217 \times 10^{11}$ Nm/radian, in better agreement with K_{rh} based on moment load and end rotations, θ, above and used hereafter throughout this assessment.

ISO 19905-1 warns that if the model contains non-linearities, e.g. due to the inclusion of gap elements, care should be taken to ensure that suitable magnitudes of “unit” load cases are applied to accurately linearize the connection for the final anticipated displacement including wind actions, etc. The difference in the rotational stiffness determined from θ's based on pure moment, and pure shear loads may be attributed to this.

No further investigation addressing the low rotational stiffness determined from δ's is covered herein.

A K_{rh} of $8{,}217 \times 10^{11}$ Nm/radian (determined from the pure shear case) is used going forward for the purpose of the detailed example calculations presented herein.

A.8.2.3 c) Combination leg (3-leg model) — sub-route

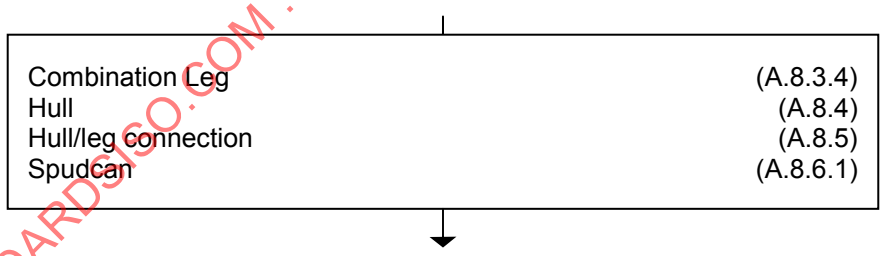

This modelling technique has not been used for this study. However, many of the notes for model types b and d are applicable, and appropriate reference is made to these. The notes on the hull sub-model and hull/leg connection sub-model as given for model type a also apply and are reproduced for this model type.

The plane of connection between the “detailed leg” and the “equivalent leg” should remain a plane and without shear distortion when the leg is bent. The connection should be composed of rigid elements that control local bending and shear distortion.

A.8.3.4 Combined detailed and equivalent leg

The combined detailed and equivalent leg model should be constructed with the areas of interest modelled in detail and the remainder of the leg modelled as an equivalent leg. To facilitate obtaining detailed stresses in the vicinity of the leg-to-hull connection (guides, fixation/jacking system, etc.), the detailed portion of the leg

model should extend far enough above and below this region to ensure that boundary conditions at the "detailed leg"/"equivalent leg" connection do not affect stresses in the areas of interest. Recommendation would be for a length extending from at least 4 bays below the lower guide to at least 4 bays above the upper guide, or the top of the leg (whichever comes first).

Care should be taken to ensure an appropriate interface and consistency of boundary conditions at the connections.

Construct a detailed leg sub-model as for the model type d, and equivalent leg with properties determined from type b.

Connections between the portions of detailed and equivalent leg sections should be made by rigid links from the three chords to the equivalent leg beam. Note that in these regions, spurious stresses may emerge from the response calculations.

A.8.4 Hull

ISO 19905-1 requires that the hull structure be modelled so that the actions can be correctly transferred to the legs and the hull flexibility is represented accurately. The options are either a detailed hull model (ISO 19905-1:2012, A.8.4.2) generated using plate elements, or an equivalent hull model (ISO 19905-1:2012, A.8.4.3); see hull modelling notes covered in model type b.

A.8.5 Hull/leg connection

See notes for model type d (detailed leg model). The leg-to-hull connections should be connected to either detailed or representative model of the hull instead of being earthed off in the single detailed leg model.

A.8.6.1 Spudcan structure

When modelling the spudcan, rigid beam elements are considered sufficient to achieve an accurate transfer of the seabed reaction into the leg chords and bracing.

Note: For a strength analysis of the spudcan and its connections to the leg, a detailed model of the spudcan and lower-leg, with appropriate boundary conditions, should be developed.

A.8.2.3 d) Single detailed leg — sub-route

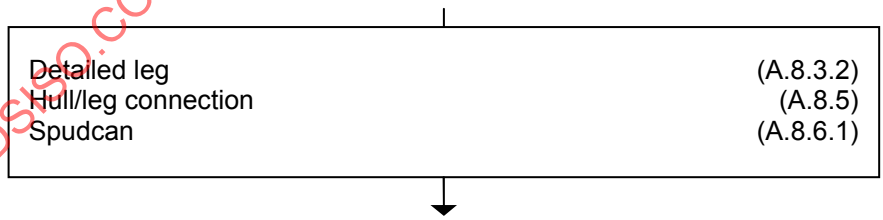

A.8.3.2 Detailed leg

Modelling should account for offsets between member work points and centroids, as omitting this detail can be unconservative. If member offsets are not included in the model, analysis of the relevant joints should consider their effect. Gusset plates are typically omitted in the structural leg model. However, their beneficial effects can be taken into account in the calculation of member and joint strength.

Guidelines on the construction of a leg model are noted as follows.

Model the following: chords,
horizontal braces,
diagonal braces and
internal braces.

Loads will be applied near the spudcan, so include some representation of this in the leg model.

Define joints coordinates as intersections of chord and brace centrelines. Simplify some intersections.

Set up mesh geometry

The leg consists of a single basic unit (one bay) repeated 16 times:

Side length of 16,15 m defined by horizontal intersects

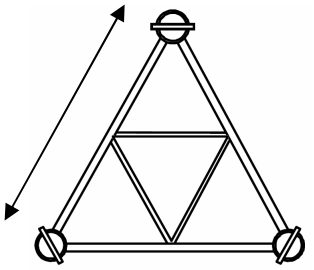

Component List:

3 chord sections
3 horizontal braces
4 half diagonal braces
3 internal span-breakers

Bay height of 10,21 m defined by the midpoint between chord/diagonal intersects.

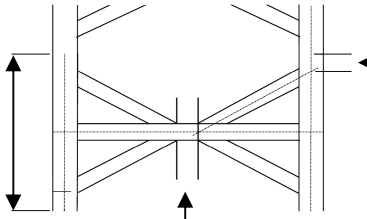

Total vertical brace offset of 1,07 m

Total horizontal brace offset of 0,30 m

Leg bracing begins at the bottom of the leg with a half bay, with complete bays starting at 11,43 m above the spudcan tip.

Properties of members

The leg chord section is uniform up the entire leg, but the horizontal and diagonal bracing members change at 42 m above spudcan tip.

Leg chord specification:

Area	(no tooth)	= 0,246 m^2
	(10 % tooth)	= 0,254 m^2
I_{yy}	(10 % tooth)	= 0,007 m^4
I_{zz}	(10 % tooth)	= 0,010 m^4
A_Q		= 0,106 m^2
I_{tors}		= 0,016 m^4

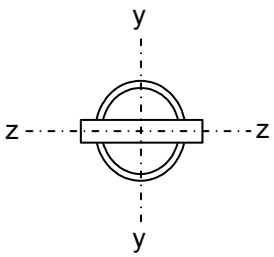

i
A.8.3.5 &
A.12.3

Bracing specification:

Horizontal braces (below 42 m above spudcan tip):

outer diameter = 0,406 m

wall thickness = 0,032 m

yield strength = 620,7 N/mm^2

Horizontal braces (above 42 m above spudcan tip):

outer diameter = 0,356 m

wall thickness = 0,025 m

yield strength = 586,3 N/mm^2

Diagonal braces (below 42 m above spudcan tip):

outer diameter = 0,406 m

wall thickness = 0,032 m

yield strength = 620,7 N/mm^2

Diagonal braces (above 42 m above spudcan tip):

outer diameter = 0,356 m

wall thickness = 0,025 m

yield strength = 586,3 N/mm^2

Internal spanbreakers:

outer diameter = 0,229 m

wall thickness = 0,010 m

Material properties:

Young's modulus (steel) = 205 000 N/mm^2

Density = 7 860 kg/m^3

Checklist for detailed leg	OK?
Chords included	y
Horizontal braces	y
Diagonal braces	y
Internal braces	y
Spudcan	no
Joints coordinates modelling	y
Gusset plates ignored	y

A.8.5 Construct hull / leg connection model

A specific jack-up design concept can be described by a combination of the following components:

a) with or without fixation system;

b) opposed or unopposed jacking pinions [see ISO 19905-1:2012, Figure A.8.5-2 a)];

c) pin and yoke jacking system [see ISO 19905-1:2012, Figure A.8.5-2 b)];

d) fixed or floating jacking system.

i
Figure C.1-1

The “typical jack-up” being considered is fitted with a fixation system (type a) and opposed jacking pinions (type b), with representative leg-to-hull connections shown in ISO 19905-1:2012, Figure A.8.5-3 c) (reproduced below):

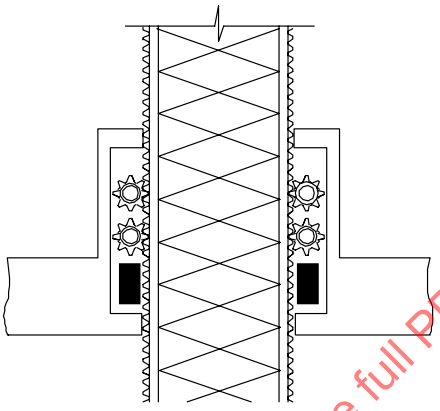

Figure A.8.5-3 c) — Representative leg-hull connection (fixed jacking with fixation system)

Guidance notes:

— jacking system to be properly modelled in terms of stiffness, orientation, clearance;

— consider effects of guide and support system clearances;

— consider effects of wear;

— consider effects of construction tolerances;

— consider effects of backlash at gear train and between pinion and rack.

A.8.5.2 Guide structure

The guide structures should be modelled to restrain the chord member horizontally only in directions in which guide contact occurs.

Upper and lower guides restrain movement parallel and perpendicular to the rack as shown. These can be represented by gaps in these directions. It is appropriate to set the gaps at the correct positions with respect to the chord beam position as constructed (as opposed to the chord centroid). Between chord beam and gaps place springs of stiffnesses derived below.

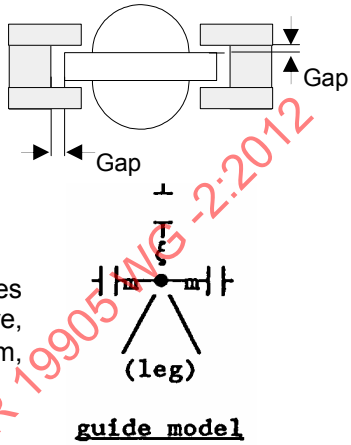

guide model

Guide simulation values would normally be provided by the designer; see the data sheet appended to this annex for details used for assessment of the “typical jack-up” being considered.

As a simplification or, in the absence of other data, the upper and lower guides can be considered to be relatively stiff with respect to the adjacent structure, such as jackcase, etc., so a nominally high spring stiffness, e.g. 1×10^6 kN/m, can be used in all directions since the gaps account for degrees of freedom.

Lower guide position

The nominal lower guide position relative to the leg can be derived using the sum of leg penetration, water depth and hull elevation. It is however recommended that, for this leg brace configuration, four lower-guide/ rack-chock positions are covered when assessing leg strength: one with the lower guide aligned at a nodal intersect (horizontal or diagonal) and the other at midspan above, or below, the horizontal. This is to allow for uncertainties in the prediction of leg penetration and possible differences in penetration between the legs.

Guide lengths

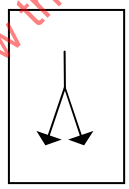

OPTION The finite lengths of the guides can be included in the modelling by means of a number of discrete restraint springs/connections to the hull. Care should be taken to ensure that such restraints carry reactions only in directions/senses in which they can act.

OPTION Alternatively the results from analyses ignoring the guide length can be corrected, if necessary, by modification of the local bending moment diagram to allow for the proper distribution of guide reaction; see ISO 19905-1:2012, Figure A.8.5-5.

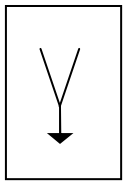

In this assessment, single connections are modelled at the centre of the guides.

A.8.5.3 Elevating system

Values typically provided by designer: vertical stiffness — 7,005 E+08 N/m per pinion for the “typical jack-up” unit being considered (see data sheet appended to this annex).

Opposed rack pinions resist deflection parallel with the rack.

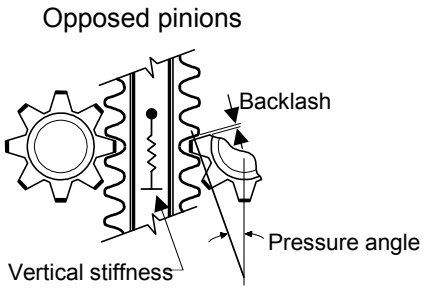

A linear spring or cantilever beam can be used to simulate the jacking pinion with a gap sized to represent the total clearance due to backlash, wear and tolerances.

Backlash (vertical component) = 0,002 m

No offset modelling is required in this instance.

A.8.5.4 Fixation system

The unit has a rack-chock fixation system; stiffness values typically provided by designer.

Vertical stiffness = $6{,}224 \times 10^9$ N/m (per chord)

Lateral stiffness = $1{,}3920 \times 10^9$ N/m (per chord)

It is important that the model can simulate the local moment strength of the fixation system arising from its finite size and the number and location of the supports. For the purpose of these calculations this is modelled as two sets of connections at positions located toward the top and bottom of the fixation system.

A.8.5.5 Shock pads — Floating jacking systems

The unit has no shock pads.

Were these present, the shock pad stiffness should be modelled by spring and gap elements to allow for load-reversal in a similar manner to the pinion stack. Spring stiffnesses should be based on the manufacturer effective shock pad stiffness accounting for any non-linear characteristics if known/available.

A.8.5.6 Jackcase and associated bracing

The stiffness of the jackcase and associated bracing should be modelled accurately since it can have a direct impact on the distribution of horizontal forces between the guides and the jacking system.

A representative beam structure has been modelled in the finite element software as shown in the figure below. The beam positions are such that the centroids of the jack posts are in the correct positions, as are the centroids of the horizontal and diagonal bracing members. Some approximation of beam positions at the top corners of the jackcase was used to fit in guide connections.

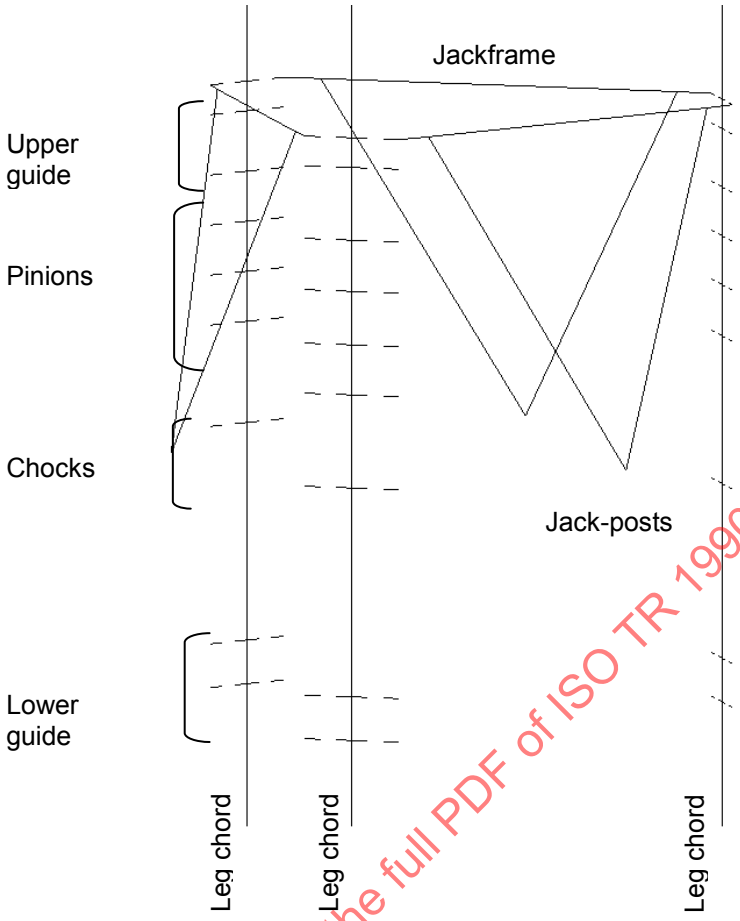

Finite element model of hull / leg interface

Beam properties are drawn from the plans:

Vertical jack post beams:

Area = 0,597 m^2

I_{yy} = 1,228 m^4

I_{zz} = 0,112 m^4

All other beams

Area = 0,077 m^2

I_{yy} = 0,008 m^4

I_{zz} = 0,006 m^4

Checklist for hull / leg	OK?
Jacking system stiffness	y
Orientation	y
Clearances	y
Guide, support clearances	y
Wear	y
Construction tolerances	y
Backlash	y

It is assumed here that the flexibility of the structure adjacent to the lower guide is incorporated in the lower guide connection springs.

The model is earthed at the base of the jackhouse, and at the lower guide connections.

A.8.6.1 Spudcan

The spudcan is modelled with rigid beam elements, or using very stiff beam properties to transfer the seabed reaction at the "effective penetration" (see ISO 19905-1:2012, A.8.6.2) into the leg chords and bracing. Spudcan nodes are linked to the bottom nodes of each leg chord by rigid links, or using very stiff beam properties.

It should be noted that, due to the sudden change in stiffness, the spudcan connections can cause artificially high stresses at the leg to spudcan connections. Hence the modelling and selection of element type should be carefully considered when an accurate calculation of leg member stresses is required in this area.

For a strength analysis of the spudcan and its connections to the leg, a detailed model with appropriate boundary conditions should be developed. This analysis can be performed on an independent model of the spudcan and a section of the lower leg.

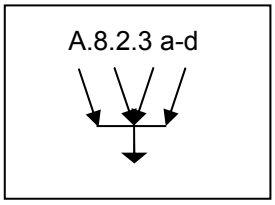

Modelling routes converge

A.8.3 Determine foundation models

The third action in this FLOW CHART box is now considered. The action refers to foundation models.

9.3 Foundation models

For the purpose of the detailed example calculations we are considering the inclusion of foundation fixity, and to determine the foundation capacities and stiffnesses the yield-interaction surface must be developed

Local route

Introduction	9.3.1
Define yield interaction surface	(A.9.3.3)
Foundation stiffness	(A.9.3.4.1 & A.9.3.4.3 / 4)
Stiffness modification	(A.9.3.4.2.1 & A.9.3.4.2.2)
Soil-leg interaction (optional)	(A.9.3.4.6)

9.3.1 Introduction

For the purpose of the detailed example calculation the yield interaction model approach adopts linear vertical, linear horizontal and secant rotational stiffness with iterative reduction of rotational stiffness to ensure compliance with the yield interaction surface.

A.9.3.3.2 Ultimate vertical/horizontal/rotational capacity interaction function.

The fundamental equation for the ultimate vertical/horizontal/rotational capacity interaction function for spudcans is given in Equation (A.9.3-16):

$$\left[\frac{F_H}{Q_H}\right]^2 + \left[\frac{F_M}{Q_M}\right]^2 - 16(1-a)\left[\frac{F_V}{Q_V}\right]^2\left[1-\frac{F_V}{Q_V}\right]^2 - 4a\left[\frac{F_V}{Q_V}\right]\left[1-\frac{F_V}{Q_V}\right] = 0 \qquad \text{(A.9.3-16)}$$

A.9.3.3.2 Location 1 (sand)

The ultimate bearing capacities are defined in ISO 19905-1:2012, A.9.3.3.2:

Q_V = 155,7 MN as above

Q_H = 0,12 Q_{Vnet} (A.9.3-26)

= 18,7 MN

Q_M = 0,075 B Q_{Vnet} (A.9.3-27)

= 164,8 MNm

The spudcan penetration at Location 1 has previously been calculated to be partially penetrated with a tip penetration of 0,91 m; consequently backfill and spudcan buoyancy do not need to be considered.

However, in this specific case, due to the partial penetration of the spudcan in the sand, the yield surface can be extended for F_V/Q_V > 0,5 in order to account for the increased moment capacity due to the increase in contact diameter resulting from further penetration, as described in ISO 19905-1:2012, A.9.3.3.4.

Using:

B = 14,1 m

B_{max} = 17,60 m

Q_V = F_V = 155,7 MN

Q_{Mps} = 0,075 B Q_{Vnet} $(B_{max}/B)^3$ (A.9.3-43)

= 2,06 Q_{Vnet}

Q_{Mpv} = 0,15 B Q_{Vnet} (A.9.3-44)

= 2,10 Q_{Vnet}

Consequently as Q_{Mps} < Q_{Mpv}:

Q_{Mp} = Q_{MPs} = 2,06 Q_{Vnet}

The corresponding unfactored yield interaction envelope in the F_V-F_H and F_V-F_M planes are given by:

	Unfactored capacities		
F_V/Q_V	F_V (MN)	F_H (MN)	F_M (MNm)
0,000	0,0	0,0	0,0
0,025	3,9	1,8	16,1
0,050	7,8	3,6	31,3
0,075	11,7	5,2	45,7
0,100	15,6	6,7	59,3
0,125	19,5	8,2	72,1
0,150	23,4	9,5	84,0
0,175	27,3	10,8	95,2
0,200	31,1	12,0	105,5
0,225	35,0	13,0	114,9
0,250	38,9	14,0	123,6
0,275	42,8	14,9	131,4
0,300	46,7	15,7	138,4
0,325	50,6	16,4	144,6
0,350	54,5	17,0	149,9
0,375	58,4	17,5	154,5
0,400	62,3	17,9	158,2
0,425	66,2	18,3	161,1
0,450	70,1	18,5	163,1
0,475	74,0	18,6	164,4
0,500	77,9	18,7	164,8
0,525	81,8	18,6	167,5
0,550	85,7	18,5	174,2
0,575	89,6	18,3	179,8
0,600	93,4	17,9	184,2
0,625	97,3	17,5	187,4
0,650	101,2	17,0	189,2
0,675	105,1	16,4	189,5
0,700	109,0	15,7	188,1
0,725	112,9	14,9	184,9
0,750	116,8	14,0	179,9
0,775	120,7	13,0	172,9
0,800	124,6	12,0	163,8
0,825	128,5	10,8	152,4
0,850	132,4	9,5	138,7
0,875	136,3	8,2	122,4
0,900	140,2	6,7	103,6
0,925	144,1	5,2	82,1
0,950	148,0	3,6	57,7
0,970	151,1	2,2	36,1
0,980	152,6	1,5	24,6
0,990	154,2	0,7	12,5
1,000	155,7	0,0	0,0

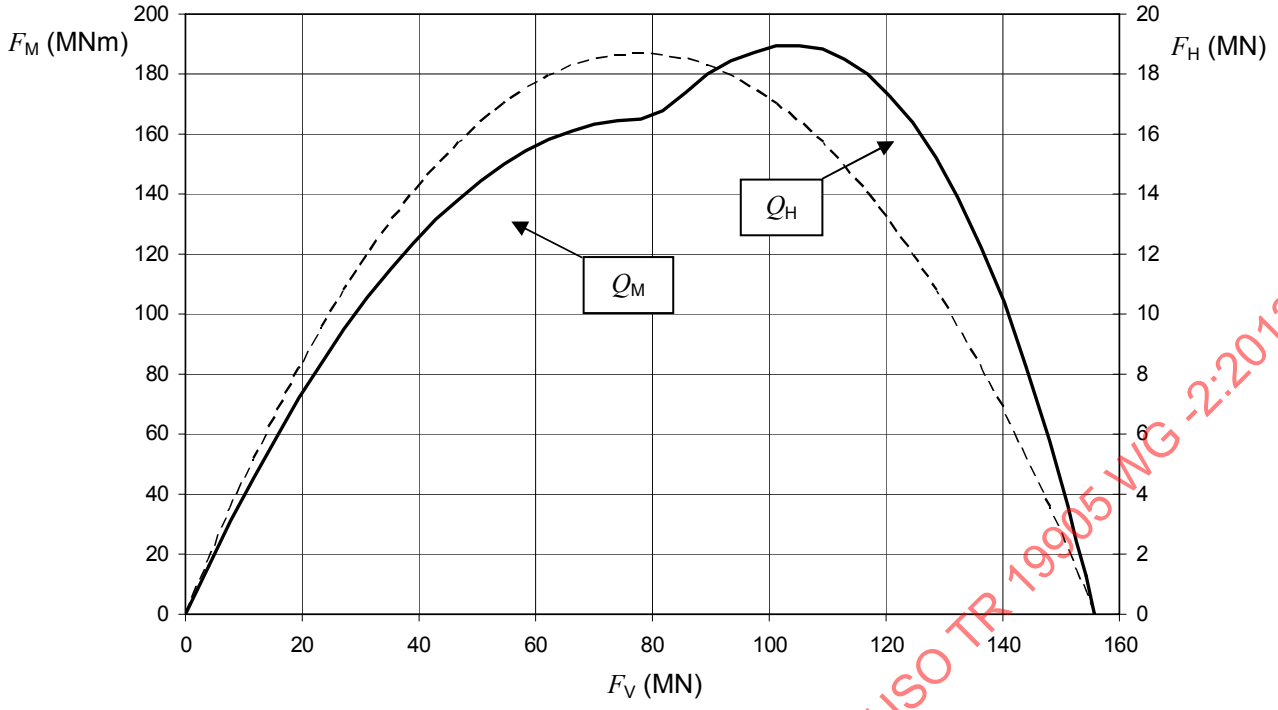

Unfactored bearing capacity envelope for Location 1 (sand) in the F_V-F_M and F_V-F_H planes.

A.9.3.3.2 Location 2 (clay)

The general yield surface equation, ISO 19905-1:2012, Equation (A.9.3-16), is used for a clay foundation; however, the maximum horizontal and moment capacities, Q_H and Q_M, are calculated using a different approach:

D = 41,0 m

$Q_H = C_H Q_{Vnet}$

As $D > B$, $C_H = C_{Hdeep}$ where:

$$C_{Hdeep} = [1,0 + (s_{u,a}/s_{uo})][0,11+0,39(A_s/A)] \quad \text{(A.9.3-25)}$$

As the soil sensitivity is given as 2,7 it is reasonable to assume that $s_{u,a}/s_{uo}$ = 1/2,7 = 0,37

A_s = 99,4m^2 and A = 243,2m^2, therefore:

$Q_H = 0,369\ Q_{Vnet}$

$$Q_{vnet} = (s_u N_c s_c d_c)\pi B^2/4 \quad \text{(A.9.3-22)}$$

At D = 41,0 m:

s_u = 67,8 kPa (averaged over D and $D + 0,5B$)

$N_c s_c d_c$ = 8,8

Hence:

Q_{vnet} = 145,0 MN

Q_H = 53,5 MN

To determine the maximum moment capacity, Q_M:

$$Q_{Mo} = (0,1 + 0,05a(1 + b/2))Q_{Vnet}B \quad \text{(A.9.3-19)}$$

$a = D/2,5B = 0,93$

$b = (D_b s_{u,a})/(D s_u)$

$D_b = D - H_{cav} = 41,0 - 4,6 = 36,4$ m

$s_{u,a} = s_u$ at D divided by soil sensitivity = 59,1 / 2,7 = 21,9 kPa

$s_u = 67,8$ kPa

Therefore:

$b = 0,33$

Hence:

$Q_M = 393,7$ MNm

However as Location 2 is a clay foundation, the bearing capacity envelope for $F_V < 0,5Q_V$ is calculated in accordance with ISO 19905-1:2012, A.9.3.3.3:

$$\left(\frac{F_H}{f_1 Q_H}\right)^2 + \left(\frac{F_M}{f_2 Q_M}\right)^2 - 1,0 = 0 \quad \text{(A.9.3-32)}$$

As suction can be relied upon in such a normally consolidated clay, $f_2 = f_1$ and full adhesion is assumed, i.e. $\alpha = 1,0$, as such, $f_1 = 1,0$. In this situation $m_\alpha = 0,0$, hence the horizontal and moment capacities for $F_V < 0,5Q_V$ are equal to those for $F_V = 0,5\ Q_V$ and:

$$\left(\frac{F_H}{Q_H}\right)^2 + \left(\frac{F_M}{Q_M}\right)^2 = 1,0$$

The corresponding unfactored yield interaction envelope in the FV-FH and FV-FM planes are given by:

F_V/Q_V	Unfactored capacities		
	F_V (MN)	F_H (MN)	F_M (MNm)
0,000	0,0	531,4	387,3
0,025	48,3	531,4	387,3
0,050	96,6	531,4	387,3
0,075	144,9	531,4	387,3
0,100	193,2	531,4	387,3
0,125	241,5	531,4	387,3
0,150	289,8	531,4	387,3
0,175	338,1	531,4	387,3
0,200	386,4	531,4	387,3
0,225	434,7	531,4	387,3
0,250	483,0	531,4	387,3
0,275	531,3	531,4	387,3
0,300	579,6	531,4	387,3
0,325	627,9	531,4	387,3
0,350	676,2	531,4	387,3
0,375	724,5	531,4	387,3
0,400	772,8	531,4	387,3
0,425	821,1	531,4	387,3
0,450	869,4	531,4	387,3
0,475	917,7	531,4	387,3
0,500	966,1	531,4	387,3
0,525	1 014,4	530,6	386,8
0,550	1 062,7	528,5	385,2
0,575	1 111,0	524,9	382,6
0,600	1 159,3	519,9	378,9
0,625	1 207,6	513,3	374,2
0,650	1 255,9	505,2	368,3
0,675	1 304,2	495,5	361,2
0,700	1 352,5	484,2	352,9
0,725	1 400,8	471,0	343,3
0,750	1 449,1	456,0	332,4
0,775	1 497,4	438,9	319,9
0,800	1 545,7	419,5	305,8
0,825	1 594,0	397,6	289,8
0,850	1 642,3	372,7	271,6
0,875	1 690,6	344,2	250,9
0,900	1 738,9	311,3	226,9
0,925	1 787,2	272,5	198,6
0,950	1 835,5	224,7	163,8
0,970	1 874,1	175,4	127,8
0,980	1 893,5	143,7	104,8
0,990	1 912,8	102,0	74,3
1,000	1 932,1	0,0	0,0

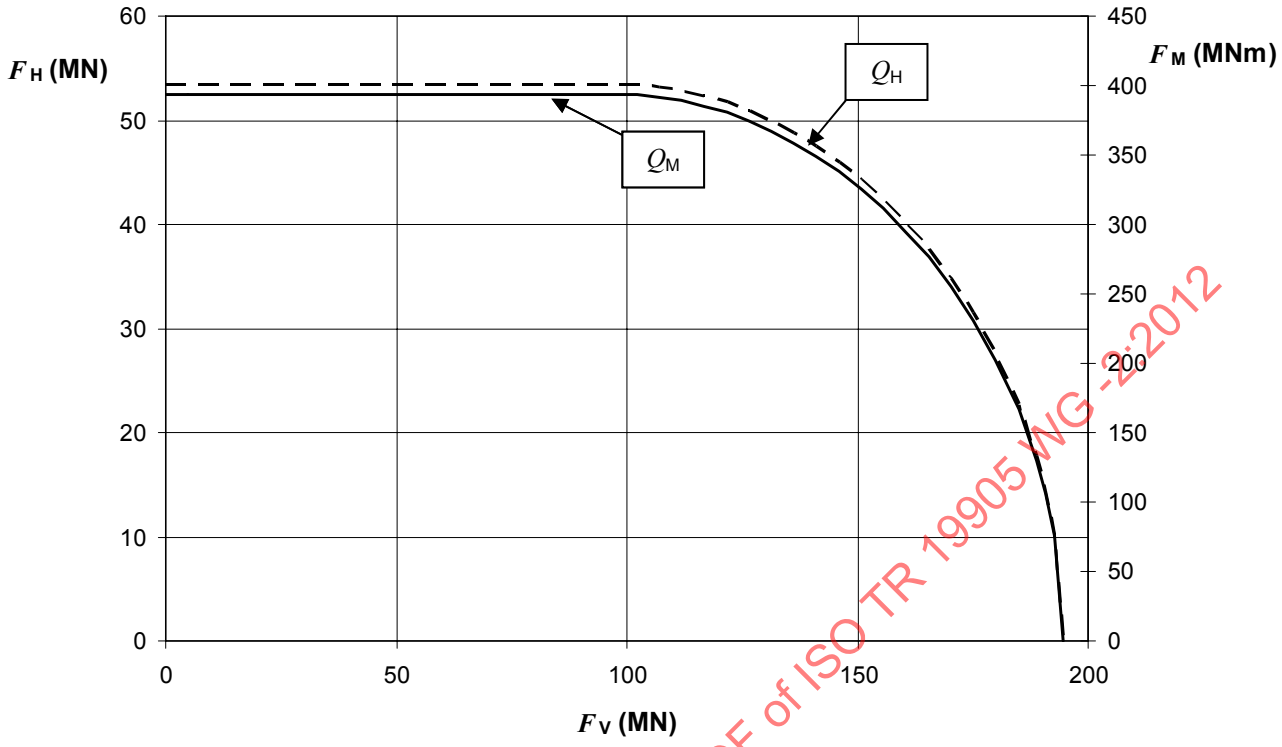

Unfactored bearing capacity envelope for Location 2 in the F_V-F_M and F_V-F_H planes.

A.9.3.4 Foundation stiffness

The initial elastic vertical, horizontal and rotational spudcan stiffnesses K_1, K_2 and K_3, are defined for all soil conditions by:

Vertical spring stiffness, K_1:

$$K_1 = K_{d1} \frac{2GB}{(1-\nu)} \quad \text{(A.9.3-46)}$$

Horizontal spring stiffness, K_2:

$$K_2 = K_{d2} \frac{16GB(1-\nu)}{(7-8\nu)} \quad \text{(A.9.3-47)}$$

Rotational spring stiffness, K_3:

$$K_3 = K_{d3} \frac{GB^3}{3(1-\nu)} \quad \text{(A.9.3-48)}$$

The appropriate shear modulus values for both example soil profiles are now calculated using ISO 19905-1:2012, A.9.3.4.3 and A.9.3.4.4 for the clay and sand soil profiles, respectively.

A.9.3.4.4 Selection of shear modulus, G, in sand

For Location 1 (sand):

The sand shear modulus, G, can be calculated using:

$$G/p_a = j\left(V_{sw}/Ap_a\right)^{0,5} \quad \text{(A.9.3-55)}$$

where:

p_a = atmospheric pressure = 101,3 kPa

$j = 230\left(0,9 + \frac{D_R}{500}\right)$

V_{sw} = 84,2 MN

A = 156,3 m^2 (the spudcan area in contact with the soil)

D_R = 60 % from geotechnical input data

Therefore:

j = 234,6

G = 54 444 kPa

A.9.3.4.3 Selection of shear modulus, G, in clay

G = 50 497 kPa — the shear modulus corresponding to that at the lowest depth of the maximum plan area (D = 41,0m) as interpolated from the geotechnical input data.

NOTE If G had not been specifically supplied, the corresponding shear modulus could be calculated according to ISO 19905-1:2012, A.9.3.4.3.

A.9.3.4.1 Initial elastic foundation stiffnesses

Location 1 (sand):

The spudcan is predicted to be partially penetrated into the soil (i.e. D = 0) with an equivalent spudcan diameter, B = 14,11m.

The Poisson ratio of the sand is provided in the geotechnical data as ν = 0,2.

As the spudcan is partially penetrated, no stiffness depth factors are applied; therefore:

$K_{d1} = K_{d2} = K_{d3}$ = 1,0

and

K_1 = 1 920 MN/m

K_2 = 1 821 MN/m

K_3 = 63 710 MNm/rad

Location 2 (clay):

The spudcan is predicted to be fully penetrated into the soil. The maximum depth of the lowest portion of the spudcan with maximum plan area, D, is 41,0 m. When combined with the spudcan diameter, B = 17,6m, the normalized spudcan embedment, $2D/B$ > 4,0. Furthermore, the earlier backfill calculations (see ISO 19905-1:2012, A.9.3.2.1.4) indicate that backfill is predicted to act on top of the spudcan. Consequently, stiffness depth factors are applied, in accordance with ISO 19905-1:2012, A.9.3.4.2, to the calculated initial elastic foundation stiffnesses using the data in Table A.9.3-6 for ν = 0,5:

K_{d1} = 1,69

K_{d2} = 1,91

K_{d3} = 2,16

Therefore:

K_1 = 7 109 MN/m

K_2 = 4 881 MN/m

K_3 = 442 091 MNm/rad

A.9.3.4.5 Selection of shear modulus in layered soils

(Outside the scope of this annex)

A.9.3.4.6 Soil-leg interaction

(Outside the scope of this annex)

NEXT ITEM

Foundation models are now set up.

Proceed to apply actions.

A.9 Apply actions and determine response

Apply actions	(8.8)
Determine responses	(9.3.3 to 9.3.5 and 10.1 to 10.5)

A.9.1 Application of actions

8.8 Apply actions

8.8.1.1 General

The assessment loadcase F_d is determined by the following generalized form where partial factors are applied before undertaking the structural response analysis.

$$F_d = \gamma_{f,G}\, G_F + \gamma_{f,V}\, G_V + \gamma_{f,E}\, [E_e + \gamma_{f,D}\, D_e] \quad (8.8\text{-}1)$$

Where the actions are defined as:

Fixed loads, G_F: Actions due to fixed load located at the appropriate position.

Variable loads, G_V: Actions due to max. or min. variable load positioned at the most onerous centre of gravity location applicable to the configurations under consideration.

Metocean loads, E_e: Actions due to metocean conditions during the extreme storm event (or zero for an earthquake assessment).

Inertia loads, D_e: Actions due to dynamic response (zero for stochastic storm assessment).

8.8.1.2 Two-stage deterministic storm analysis

The partial action factors applicable to the deterministic storm analysis addressed herein are given below:

$\gamma_{f,G}$ = 1,0
$\gamma_{f,V}$ = 1,0
$\gamma_{f,E}$ = 1,15 (applied to the 50 return period independent extreme metocean actions)
$\gamma_{f,D}$ = 1,0

8.8.1.3 Stochastic storm analysis

For stochastic storm analyses the partial action factors are all set to zero.

8.8.1.4 Earthquake analysis

Earthquake analyses are not covered by this detailed example calculation. For more information, see ISO 19905-1:2012, 8.8.1.4.

A.8.8.2 Functional actions due to fixed and variable loads

Fixed loads comprise weights. To model this, a gravitational acceleration is applied to the FE model, which shall have suitable masses and densities.

The hull dead weight plus 100 % of the variable load is 19 394 t and the hull dead weight plus 50 % variable is 17 289,5 t. The hull mass is represented by a combination of self-generated mass across the hull structure and point masses located at specific node points on the model which give the correct overall centre of gravity.

It should be noted that the gravity loadcase is only used to check the representative masses applied to the unit for the dynamic analysis are correct, and to determine the equivalent vertical forces to represent the unit weight in the final quasi-static analysis.

The centre of gravity of the dead load plus variable load is:

LCG: 19,2 m fwd. of aft legs centres.

TCG: 0,0 m towards port from longitudinal CL.

Tolerance: ± 0,0 m either way for the purpose of this assessment.

Note that centre of gravity tolerances would not usually be set to zero, and the most onerous of the extreme positions of a tolerance envelope or box would usually be considered for individual loading directions in the subsequent analyses.

The mass and weight modelling of the legs is presented above, under the flag where ISO 19905-1:2012, 8.7 and A.8.7 are discussed, and below with the total weight of each leg reported along with the total weight of the unit.

Analysis type	**Bow leg** (t)	**Port leg** (t)	**Stbd leg** (t)	**Total unit mass** (t) [c]
Sand assessment				
Dynamic [a] (inc. added mass / no buoyancy)	3 975,5	3 947,3	3 919,0	31 235,8
Static [b] (no added mass / inc buoyancy)	2 035,9	2 011,3	1 986,6	25 427,8
Clay assessment				
Dynamic [a] (inc. added mass / no buoyancy)	3 983,4	3 956,2	3 928,8	31 262,4
Static [b] (no added mass / inc buoyancy)	2 020,3	1 996,7	1 972,9	25 383,9

[a] The mass of the legs used for dynamic analyses includes structural mass, added mass, entrapped mass and excludes buoyancy.

[b] The mass of the legs for static analyses includes structural mass and buoyancy only.

[c] The total footing reaction includes the total hull (including 100 % variable) and the weight of all three legs.

The slight increase in weight for the clay dynamic assessment is due to more leg below the water and therefore increased added mass. The reduction in weight for the clay static assessment is due to the additional buoyancy associated with more leg being below the water.

The following table shows the pinned footing reactions for the maximum hull weight condition from application of a “gravity” loadcase to the “static” model, i.e. accounting for leg buoyancy but no environmental actions.

NOTE This loadcase was performed as a check only.

Assessment Case	Leg	F_x (kN) (Shear X)	F_y(kN) (Shear Y)	F_z (kN) (Vertical)
Sand	Bow	–126,6	0,00	83 381
	Port	61,3	–110,8	83 150
	Starboard	61,3	110,8	82 908
	Total	0,00	0,00	249 439
Clay	Bow	–123,6	0,00	83 228
	Port	61,8	–111,6	83 007
	Starboard	61,8	111,6	82 775
	Total	0,00	0,00	249 010

The total vertical reaction agrees with the total unit weight less leg buoyancy, confirming that the correct masses have been applied to the model.

Given the water depth and metocean conditions considered, the “typical jack-up” has been assessed in elevated storm mode only; no assessment of an operating condition has been considered.

A.8.8.3 Hull sagging

Hull sagging moments have been incorporated into the dynamic and final quasi-static analyses through application of moments at the leg-to-hull connection points.

These moments were calculated by applying a gravity loadcase to the model and clamping the leg-to-hull connection point on each leg. The mass of the hull was modelled by a combination of self-generated mass across the hull structure and point masses located at specific node points on the model which give the correct overall CoG

The reaction moments calculated at the leg to hull connection points are presented below, together with the reduced moments (reduced by 75 % as permitted by ISO 19905-1:2012) later applied to the dynamic and final quasi-static analyses.

Leg	Hull sagging moments		Hull sagging moments reduced by 75 %	
	M_x (MNm)	M_y (MNm)	M_x (MNm)	M_y (MNm)
Bow	0,0	–664,0	0,0	–166,0
Port	544,0	262,4	136,0	65,6
Stbd	–544,0	262,4	–136,0	65,6

A.8.8.4 Metocean actions

Wind loads can be applied as distributed forces, but for this assessment are applied as nodal point loads to the equivalent leg stick-model. The distribution is adequately covered by applying loads at three elevations.

— wind loads on the legs below the hull;

— wind loads on the hull;

— wind loads on the legs above the hull.

Care must be taken when following the nodal point load approach to ensure that not only the correct total shear is applied, but also that the point of application results in the correct overall overturning moment.

The wind areas and load calculations are covered above, under the flag where ISO 19905-1:2012, A.7.3.4 is discussed, with a summary of the winds loads and respective lever-arms presented below.

Storm direction	Force/arm		
	Leg below hull	Hull	Leg above hull
Sand assessment			
060°	141,3 kN / 140,6 m	8 890,8 kN / 163,8 m	170,6 kN / 171,9 m
090°	144,2 kN / 140,8 m	8 541,6 kN / 163,6 m	176,5 kN / 171,9 m
120°	142,2 kN / 140,8 m	7 414,4 kN / 165,3 m	170,7 kN / 171,9 m
Clay assessment			
060°	105,9 kN / 139,8 m	8 831,0 kN / 163,3 m	61,8 kN / 169,7 m
090°	109,9 kN / 140,5 m	8 484,7 kN / 163,1 m	64,7 kN / 169,7 m
120°	106,9 kN / 140,5 m	7 366,3 kN / 164,8 m	61,8 kN / 169,7 m

Wave/current actions should be applied to the leg and spudcan structures at the correct locations such that the correct shear and overturning loads are applied to each leg. The wave/current actions are defined in ISO 19905-1:2012, 7.3.3.

The in-house program FORCE-3 has been used to generate a distributed loadset on each of the legs to represent the hydrodynamic load distribution. The equivalent hydrodynamic leg model derived earlier is used in the equivalent leg (stick) model being used for this assessment. Wave/current forces from this stage of analysis are presented below.

Assessment	Storm direction[a]	Wave/current force (kN)	Wave/current moment (MN.m)
Sand[b]	060°	20 209	1 863,6
	090°	20 584	1 898,3
	120°	19 987	1 839,4
Clay[c]	060°	20 115	2 076,0
	090°	20 312	2 090,8
	120°	19 630	2 019,9

[a] Storm direction defined as positive anticlockwise from onto the bow, i.e. 0° is loading onto the bow.

[b] Moments taken about the effective penetration (0,46 m above the spudcan tip) for the “sand” assessment case.

[c] Moments taken about the effective penetration (4,25 m above the spudcan tip) for the “clay” assessment case.

As per the requirements of ISO 19905-1, the “apparent” wave period was used in the stochastic DAF analysis, with the “intrinsic” wave period used to determine the wave particle kinematics.

A.8.8.5 Inertial actions

For a deterministic analysis an inertial loadset must be determined in combination with the other actions. If the SDOF method is used, the inertial load should be applied through a point modelled at the centre of gravity of the unit. However, if a stochastic dynamic analysis is used, the loadset should match both the inertial base shear and inertial overturning moments.

Although an equivalent SDOF DAF has been calculated and presented herein for comparative purposes, this analysis is based on the stochastic dynamic DAFs and the loadset will therefore represent the appropriate overturning and shear contributions. Note that the calculation of an SDOF DAF would require the use of the "apparent" wave period in accordance with ISO 19905-1:2012, A.7.3.3.5/A.10.5.2.2.2.

For the purposes of this analysis no inertia loads are applied to the legs above the upper guide due to the very short length of leg above the jackframe. This should be judged on a case-by-case basis, and at locations where any significant length of leg remains above the upper guide ISO 19905-1 recommends that the appropriate inertia forces on the leg above the hull should be included.

The applied loadset matches both the inertial base shear and inertial overturning moment through application of lateral forces applied to the hull (to match the base shear) and a correcting moment applied as a vertical couple to adjust the inertial base shear.

A.8.8.6 Large displacement effects

Large displacement effects can be captured in a number of ways:

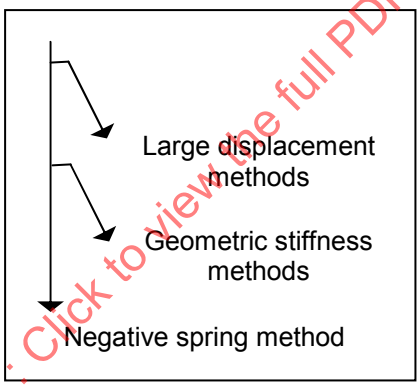

A.8.8.6.a Large displacement methods

The in-house FE package includes the large displacement optionand this is used to include the global "P-Δ" effects.

A.8.8.6.b Geometric stiffness methods

Incorporates a linear correction to the stiffness matrix based on the axial forces present in the elements. No guidance presented herein.

A.8.8.6.c Negative spring method

A simplified geometric stiffness approach which essentially applies an additional lateral force to the hull which is proportional to the structural deflection of the hull. No guidance presented herein.

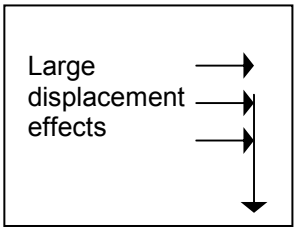

A.8.8.7 Conductor actions

The “typical jack-up” has been assessed without a conductor and no guidance is presented herein.

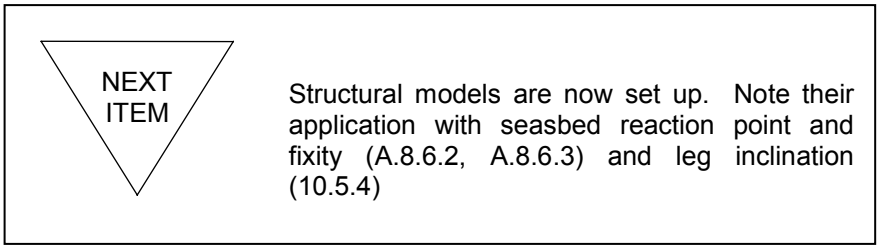

A.9.2 Determine responses — Foundation response

This covers the degredation of secant rotational foundation stiffness for loads acting on the foundation.

In this example the results from the 60° heading for the bow leg are used to calculate r_f for both the sand and clay cases:

For Location 1 (sand)

F_V = 165,1 MN

F_H = 9,1 MN

F_M = 0,0 MNm

The ultimate bearing capacities have been calculated above, under the flag where ISO 19905-1:2012, A.9.3.3.2 is discussed, as:

Q_V = 155,7 MN

Q_H = 18,7 MN

Q_M = 164,8 MNm

a = 0,0 (for shallow embedment)

then, from A.9.3.4.2.3, noting that a = 0, equation A.9.3-52 reduces to::

$$r_f = \frac{\left\{\left[\frac{F_H}{Q_H}\right]^2 + \left[\frac{F_M}{Q_M}\right]^2\right\}^{\frac{1}{2}}}{4\left[\frac{F_V}{Q_V}\right]\left[1-\frac{F_V}{Q_V}\right]}$$

r_f = 1,0 so the point lies on the yield surface

In this case f_r is zero as the point lies on the yield surface which means the foundation rotational stiffness has also degraded to zero / perfectly pinned foundation restraint condition.

For Location 2 (clay):

F_V = 202,9 MN

F_H = 8,7 MN

F_M = 0,0 MNm

The terms in the failure ratio equation have been calculated above, under the flag where ISO 19905-1:2012, A.9.3.3.2 is discussed, as:

Q_V = 194,6 MN

Q_H = 53,5 MN

Q_M = 393,8 MNm

a = 1,0 (as $D \geq 2{,}5B$)

f_1 = 1,0

f_2 = 1,0

then

$$r_f = \left\{ \left[\frac{F_H}{f_1 Q_H} \right]^2 + \left[\frac{F_M}{f_2 Q_M} \right]^2 \right\}^{\frac{1}{2}} \qquad \text{(A.9.3-53)}$$

r_f = 1,0 so the point lies on the yield surface

In this case f_r is zero as the point lies on the yield surface, which means the foundation rotational stiffness has also degraded to zero/perfectly pinned foundation restraint condition

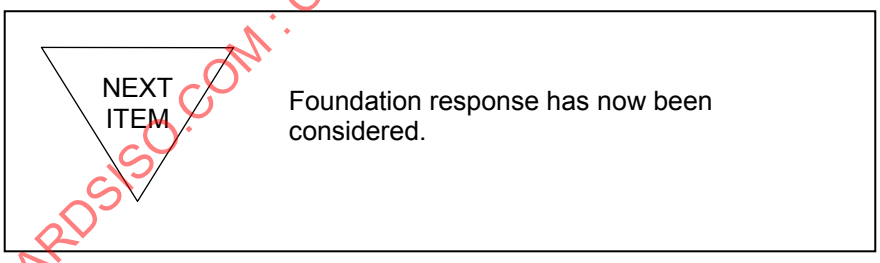

A.9.3 Determine responses — Structural response

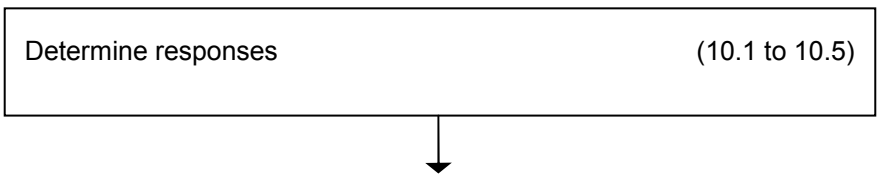

All the options for determining the unit response are considered in this section, including the SDOF method and time domain detailed dynamic approaches.

The hierarchy of modelling techniques is represented in ISO 19905-1:2012, Table 10.3-2, which can be referenced when a “more detailed response calculation” is required.

Local route

General	(10.2)
Types of analyses	(10.3)
Common parameters	(10.4)
- Natural periods	
- Mass	
- Damping	
- Foundations	
Storm analysis	(10.5)
- Two stage deterministic storm analysis	
- Stochastic storm analysis	

This annex is arranged to indicate a progress route considering all the options on the way, one after the other. ISO 19905-1 allows for repetition of stages of analysis, albeit at different levels of complexity, so that parts of this detailed example calculation may be encountered twice, especially for dynamic response calculation.

Reading through these sections provides a useful introduction to various aspects. Certain information is discussed which will be required during the calculation, whether using finite elements or not. It is logical to prepare this information now.

10.2 General considerations

The response of the jack-up refers to the internal forces of the leg members, overturning moments of the jack-up, horizontal deflections of the hull, reactions and displacements at the spudcans and forces in the holding system. The application of actions to the unit are discussed in ISO 19905-1:2012, 8.8 and A.8.8 and shown below:

10.3 Types of analyses

The extreme storm ULS response can be determined either by a two-stage deterministic storm analysis procedure using a quasi-static analysis that includes an inertial loadset or by a more detailed fully integrated (random) dynamic analysis procedure that uses a stochastic analysis.

ISO 19905-1:2012, Table 10.3-1 gives a list of some of the references used in an extreme storm response analysis. A common approach can be to start with a relatively simple analysis and to increase the level of complexity if the simple method shows the jack-up is unsuitable for the site.

Alternatively, an ultimate strength analysis of the jack-up structure can be performed where the collapse strength of the unit and its foundation is determined.

Detailed modelling for dynamic analysis may be preferred, but this is outside the scope of this annex.

10.4 Common parameters

The structural stiffness, hydrodynamic and wind actions are discussed in subclauses A.7 and A.8 of this annex. The following parameters relate to the dynamic characteristics and the characteristics of the wave/current excitation.

10.4.2 The natural period(s)

The natural period(s) may be determined either by a finite element structural model, or by equation.

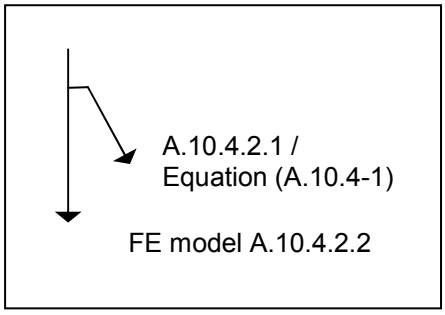

A.10.4.2.1 Natural period (from equation)

This approach uses equations given in Clause 10, TR.10.4.2.2. It is not recommended for use in analysis but is useful for demonstrating some of the factors that affect the natural period of a jack-up. No further guidance is given.

A.10.4.2.2 FE model approach

The three leg stick model is sufficient to meet the requirements of this paragraph.

For natural period calculations, non-linear effects are included in the analyses. The added mass of the model is built in by using the member densities of the appropriate sections of equivalent leg accounting for the added mass associated with the raw water structure (RWS), etc.; see above under the flag where ISO 19905-1:2012, 8.7 and A.8.7 are discussed. No buoyancy is included in the model other than in the P-Δ loadset used for large displacements.

The rig natural periods for sway and yaw are presented in the table below, with mode shapes presented in the subsequent figure.

Sand assessment natural periods

Assessment case	Mode	Linear frequency (Hz)	Linear period (s)	Non-linear frequency (Hz)	Non-linear period (s)
Sand	Pinned				
	Sway	0,103 4	9,67	0,093 0	10,75
	Yaw	0,129 5	7,72	-	-
	80 % Rotational fixity				
	Sway	0,127 5	7,84	0,124 3	8,04
	Yaw	0,152 6	6,55	-	-
	100 % Rotational fixity				
	Sway	0,133 7	7,48	0,128 6	7,78
	Yaw	0,159 6	6,26	-	-

Clay case

Assessment case	Mode	Linear frequency (Hz)	Linear period (s)	Non-linear frequency (Hz)	Non-linear period (s)
Clay	Pinned				
	Sway	0,104 3	9,59	0,097 1	10,30
	Yaw	0,130 6	7,66	-	-
	80 % Rotational fixity				
	Sway	0,165 7	6,04	0,161 8	6,18
	Yaw	0,189 5	5,28	-	-
	100 % Rotational fixity				
	Sway	0,168 2	5,94	0,164 7	6,07
	Yaw	0,192 1	5,21	-	-

NOTE Sway and surge have very similar periods; however, in this case sway is marginally longer.

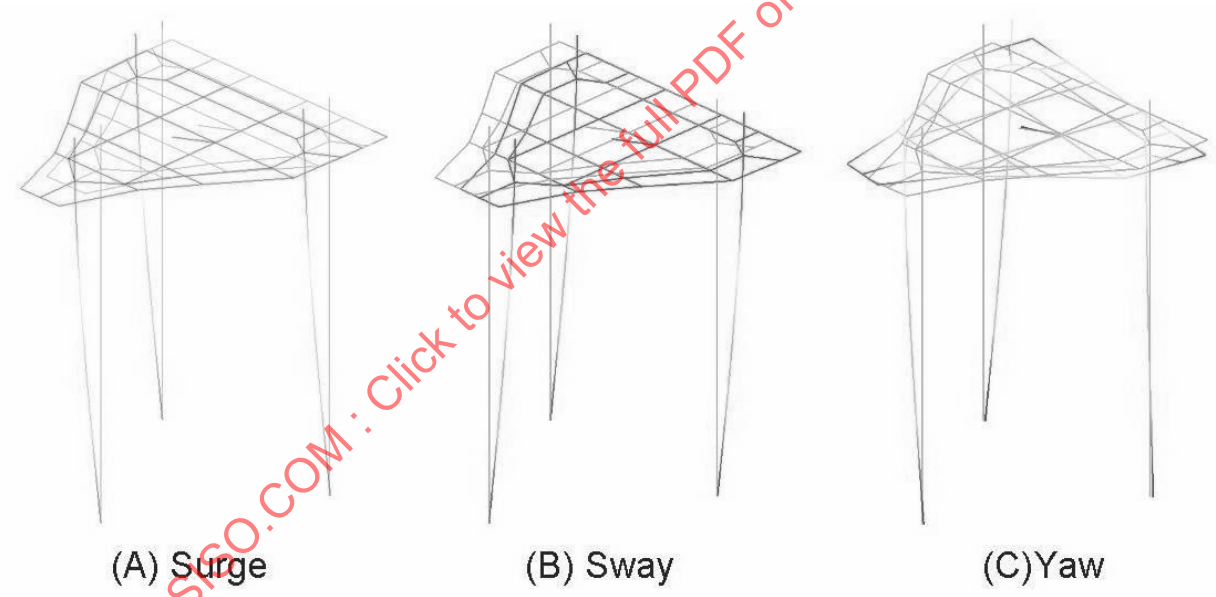

First 3 natural modes of vibration of unit

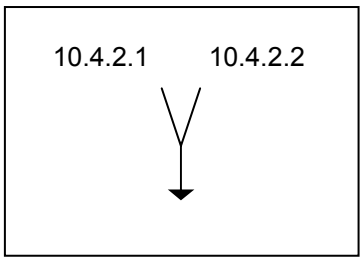

A.10.4.2.3 Mass

The masses used to calculate the natural periods are described in ISO 19905-1:2012, 8.7.

A.10.4.2.4 Variability in natural period

From ISO 19905-1:2012, Figure A.10.4-1, the first cancellation point occurs at around 8,8 s given a leg spacing of 57,61 m, with the second cancellation point at around 5,0 s. Given the wave period considered for the analysis is 16,6 s, it is not anticipated that cancellation effects will cause a problem for the SDOF method.

Since Ω is only marginally greater than 0,5 there is a relatively large separation between the natural period and the peak of the wave spectrum, so the SDOF method in this case should be reasonably accurate.

$T_n \approx 8{,}04$ s $\quad\quad \Omega = T_n/(0{,}9T_p) = 0{,}54$

$T_p \approx 16{,}60$ s

A.10.4.3 Damping

The primary damping components are foundation, hydrodynamic and structural, which can be modelled either linearly or non-linearly.

Structural and foundation damping is modelled linearly as a percentage of critical damping as a non-linear foundation model is not in use at this stage.

Hydrodynamic damping can be specified as a percentage of critical damping or accounted for using the relative velocity term in the drag force equations if:

$$\frac{uT_n}{D_i} \geq 20$$

where

u = 1,49 + ($\pi \times$ 14,46)/12,90 = 5,01

T_n = 8,04 s

D_i = 0,79

Therefore:

50,86 ≥ 20

So in this case relative velocity effects can be accounted for in the drag calculation which removes the need to specify additional damping. However, in some cases such as the “no mass” case required for calculation of the DAFs and for quasi-static analyses, relative velocity effects should not be used.

The applicable percentage critical damping for these analyses are:

structure, etc. 2 %

foundation 2 %

hydrodynamic 0 % with relative velocity
3 % without relative velocity

A.10.4.4 Foundations

The type of analysis chosen in ISO 19905-1:2012, 10.3 significantly affects how the foundations of the jack-up are assessed. In this case the deterministic two stage approach is taken; however, the requirements of both methods are shown below.

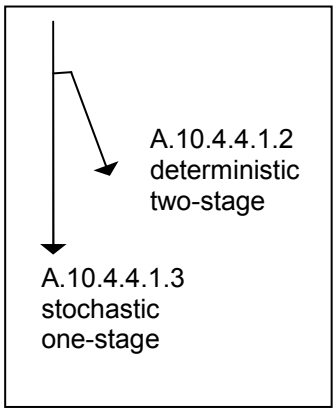

A.10.4.4.1.2 Deterministic two-stage

ISO 19905-1:2012, Figure A.10.5-2 illustrates the procedure schematically.

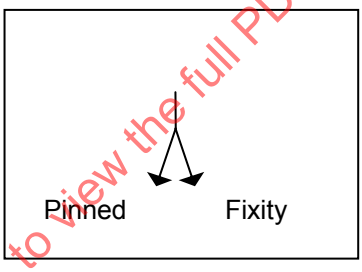

Pinned footing

From above, under the flag where ISO 19905-1:2012, A.8.6.2 is discussed, the reaction point is 0,45 m and 4,25 m above the spudcan tip for Location 1 (uniform sand) and Location 2 (clay) respectively. Simple supports are to be put into the finite element 3 leg stick model.

Fixity

If justifiable, include foundation fixity as a combination of horizontal, vertical and rotational springs. For the purposes of this annex fixity is justified and as such the flowing section will follow the fixity path.

(A.9.3.4.2.4) Include non-linear rotational, lateral and vertical soil springs.

(A.9.3.4.3) Upper and lower bound foundation stiffness values should be considered as appropriate for the areas of structure under consideration.

(A.9.3.6.5) Degree of fixity depends on:

— soil type

— spudcan characteristics

— maximum vertical footing load during installation

— foundation stress history

— structural stiffness of unit

— geometry of footings

— stress levels and load conditions under consideration

Apply springs at seabed reaction point. From the flag where ISO 19905-1:2012, A.8.6.2 is discussed, the reaction point is 0,45 m and 4,25 m above the spudcan tip for Location 1 (uniform sand) and Location 2 (clay) respectively.

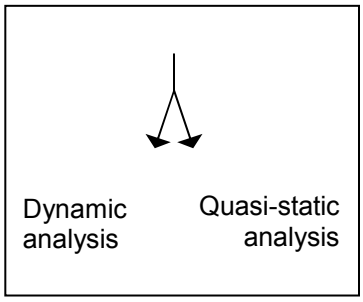

Dynamic analysis

This refers to the first stage of the two stage deterministic analysis approach. The dynamic analysis can include linearized foundation fixity but no non-linear fixity effects.

The rotational fixity can be taken as 80 % to 100 % of the value determined from ISO 19905-1:2012, A.9.3.4 and shown below. For the purposes of this annex, 80 % of the rotational fixity has been used for all dynamic analyses.

A.9.3.4 Foundation stiffness

The spudcan stiffnesses for the sand case were previously calculated above, under the flag where ISO 19905-1:2012, A.9.3.4.3 is discussed, and are summarized below:

K_1 = 1 920 MN/m

K_2 = 1 821 MN/m

K_3 = 63 710 MNm/rad

The spudcan stiffnesses for the clay case were previously calculated above, under the flag where ISO 19905-1:2012, A.9.3.4.3 is discussed, and are summarized below:

K_1 = 7 109 MN/m

K_2 = 4 881 MN/m

K_3 = 442 091 MNm/rad

Were a “pinned” assessment to be performed (which assumes the spudcan to be fixed but free to rotate, and hence has zero moment capacity), then the corresponding rotational spudcan stiffness, K_3, would be zero and the vertical and horizontal stiffnesses, K_1 and K_2, would be infinite.

Quasi-static analysis

The foundation for the quasi-static analysis can either be modelled using an elasto-plastic foundation model or a simple approach can be used to create moments on the spudcan by the inclusion of simple linear rotational springs. The moments thus induced on the spudcan are limited to a capacity based on the relationship between vertical force, horizontal force and moment. This procedure is defined below:

1. Include vertical, horizontal and rotational stiffnesses (linear springs) (see above under the flag where ISO 19905-1:2012, A.9.3.4 is discussed) in the analytical model. The loadset will include the factored functional and factored metocean actions along with the inertial actions calculated from the linearized dynamic analysis.

2. Calculate the yield interaction function value (see ISO 19905-1:2012, A.9.3.3 and the example below). Fixity is assessed by considering whether the footing load combination falls within the yield surface or not. The quantity r_f is a measure of whether the load combination falls within the surface or not, so that:

   $r_f \geq 1$ load combination lies outside the yield surface (no fixity)

   $r_f < 1$ load combination lies within the yield surface (fixity)

3. Because the degree of fixity will affect the footing loadset for a given environmental load condition, an iterative approach must be adopted to find the equilibrium position. If the moment is reduced to zero and the force combination still lies outside the yield envelope, a bearing failure is indicated.

4. If the force combination initially falls within the yield surface, the rotational stiffness should be further checked to satisfy the reduced stiffness conditions in ISO 19905-1:2012, A.9.3.4.2.

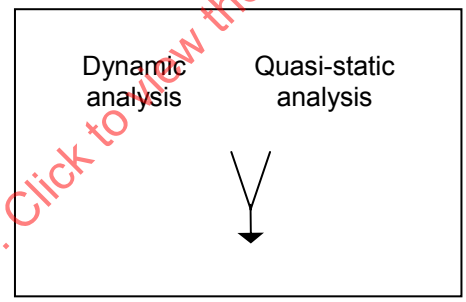

A.10.4.4.1.3 Stochastic one stage analysis

The stochastic one-stage analysis requires the use of a fully detailed non-linear time domain analysis which would take into account the elasto-plastic behaviour of the foundation. This procedure would incorporate the effects of non-linear foundation fixity in the dynamic response, with the potential for permanent plastic set and expansion of the current yield surface when it is transgressed. The metocean parameters (i.e. wind velocity, wave height and current velocity) are factored, see ISO 19905-1:2012, A.10.5.3.2.

As the dynamic response is influenced by the time history of the actions, a number of analyses would need to be performed for differing wave histories. The MPMEs would then need to be determined from a procedure described in ISO 19905-1:2012, A.10.5.3.4.

ISO 19905-1:2012, Figure A.10.5-4 illustrates the procedure schematically.

By its nature, this analysis would require a lot of processing and a full demonstration of this method is beyond the scope of this annex.

A.10.4.4.2 (Outside the scope of this annex)

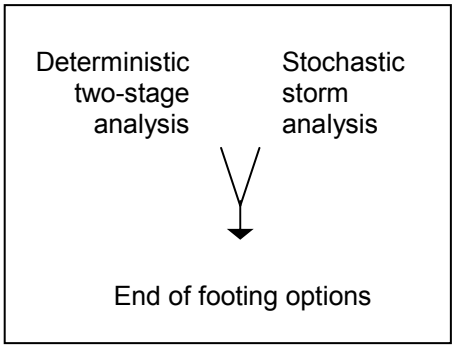

A.9.4 Determine dynamic response

10.5 **Storm analysis**

The first division in the route of the dynamic response calculation is between deterministic inertial loadset approaches and the detailed stochastic storm analysis approaches. The latter tend to be more complete but more complex.

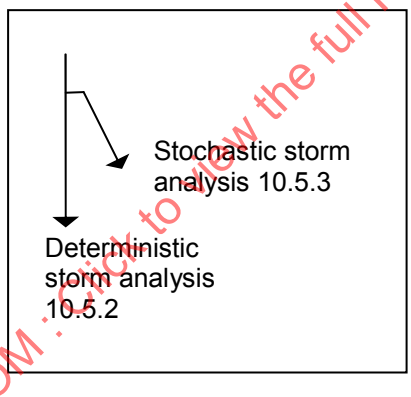

10.5.2 **Two stage deterministic storm analysis**
(Inertial loadset) Approaches (Stage 1)

In these approaches inertial loads are determined to represent the dynamic response. These are additional to the quasi-static loads determined earlier and are applied as a distributed loadset on both the hull and legs above the upper guide.

For the simple approach (single degree-of-freedom), go to A.10.5.2.2.2 or, for the more complex approach (a random wave time domain random dynamic analysis), go to A.10.5.2.2.3.

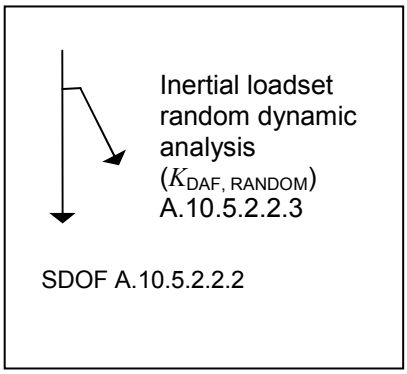

A.10.5.2.2.2 **The classical SDOF analogy**
(DAFs and inertial loadset)

DAFs:

This is an efficient first pass approach to evaluating the dynamic response.

Calculate the DAF ($K_{DAF,SDOF}$):

Ω = T_n/T,

where

T_n = 8,04 s (e.g. sand case non-linear period for 80 % rotational fixity)

T = $0{,}9T_{p(apparent)}$ = 14,94 s

Ω = 0,54, noted to be > 0.5 and therefore flagged as possibly unconservative

ζ = 0,07 from (A.10.4.3)

$$K_{DAF,SDOF} = \frac{1}{\sqrt{[(1-\Omega^2)^2 + (2\zeta\Omega)^2]}} \geq 1{,}20 \qquad \text{(A.10.5-1)}$$

= 1,40

Inertial loadset:

To obtain F_{in} it is necessary to inspect the hydrodynamic force data calculated using the in-house program Force-3.

Examples based on sand foundation condition assessment and hydrodynamic loads include the 1,15 environmental load factor.

60° heading:

$F_{BS,(QS)Max}$ = maximum hydrodynamic load
= 20 209 kN

$F_{BS,(QS)Min}$ = minimum hydrodynamic load
= –1 969 kN

so

$F_{BS,Amplitude}$ = 11 089 kN

and

F_{in} = (1,40 – 1,00) × 11 089
= 4 436 kN

90° heading:

$F_{BS,(QS)Max}$ = maximum hydrodynamic load
= 20 585 kN

$F_{BS,(QS)Min}$ = minimum hydrodynamic load
= –1 935 kN

so

$F_{BS,Amplitude}$ = 11 260 kN

and

F_{in} = (1,40 – 1) × 11 260
= 4 504 kN

120° heading:

$F_{BS,(QS)Max}$ = maximum hydrodynamic load
= 19 987 kN

$F_{BS,(QS)Min}$ = minimum hydrodynamic load
= –1 909 kN

so

$F_{BS,Amplitude}$ = 10 948 kN

and

F_{in} = (1,40 – 1) × 10 948
= 4 379 kN

These loads should now be applied through the hull centre of gravity along with the G, G_v and E_e loads from the previous calculations described above, under the flag where ISO 19905-1:2012, 8.8 is discussed, in a response calculation including second order sway effects, to generate the (G + G_v + E_e + D_e) P-Δ response.

The F_{in} loads are applied through the hull centre of gravity by means of a conveniently located hull centre of gravity node which is rigidly connected to the rest of the hull structure.

See ISO 19905-1:2012, 10.5.2 (discussed below) for the second stage of the two stage analysis.

A.10.5.2.2.3 Inertial loadset based on random dynamic analysis ($K_{DAF,RANDOM}$)

The dynamic response has been calculated following the guidance given in ISO 19905-1:2012, 10.4 with the masses presented in above under the flag where ISO 19905-1:2012, 8.7 is discussed.

The storm should be qualified against specified limits for assessment; see ISO 19905-1:2012, 10.5.3.

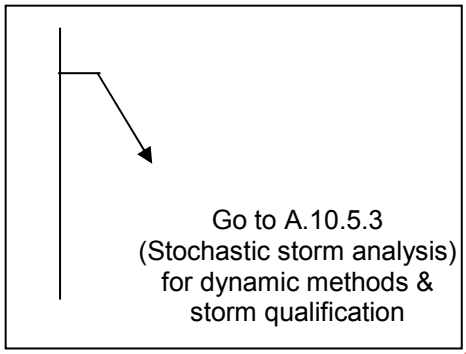

A.10.5.3 Stochastic storm analysis

Several detailed dynamic analysis methods are now considered. It is expected that in many analyses, this section can be called upon to produce responses of increasing levels of sophistication.

The storm generated for the sand case is considered in this section. The (different) storm generated for the clay case used exactly the same approach.

The following details apply to all methods.

— Although the underlying statistics are Gaussian, the non-linear forcing makes the excitation non-Gaussian, and this must be included.

— The spudcan-foundation interface should be modelled as a pin joint, except when fixity has been justified. Here fixity has been justified and is included.

— The relative velocity formulation has already been shown to apply in this case. From ISO 19905-1:2012, Table A.10.4-1, total global damping (% of critical) has already been determined as 4 % (structure + foundation) with an additional 3 % which is introduced by the hydrodynamics.

For stochastic analyses (for the sand case), the significant waveheight in ISO 19905-1:2012, A.6.4.2.6 is applied:

$$H_s = \left[1 + \left(\frac{10 H_{srp}}{T_p{}^2}\right) e^{\left(\frac{-d}{25}\right)}\right] H_{srp} \qquad \text{(A.6.4-9)}$$

$$H_s = 14{,}46$$

for: d = 121,9 m

H_{srp} = 14,4 m

ISO 19905-1 does not support frequency domain analyses so only the time domain is considered here. See ISO 19905-1:2012, A.7.3.3.3.2 for more information regarding the following section.

A random sea has been generated using 200 divisions of the spectrum with equal energy content (and finer divisions in the “tail”) and has been qualified at 3 h, 6 h and 9 h.

The airy wave height has been corrected for use in the stochastic storm (ISO 19905-1:2012, A.6.4.2.6), the calculation for which is shown below:

$$H_s = \left[1 + \left(10\frac{H_{srp}}{T_p{}^2}\right)e^{\left(\frac{-d}{25}\right)}\right]H_{srp}$$

This gives a corrected H_s = 14,47 m

The storm qualification criteria are calculated as follows:

Correct mean wave elevation

Standard deviation = $(H_s/4)$ ± 1 %

3,58	<	Standard deviation	<	3,65
–0,03	<	Skewness	<	0,03
2,90	<	Kurtosis	<	3,10

Maximum crest elevation = $\frac{H_s}{4}\sqrt{2\ln(N)}$ –5 % to +7,5 %

where: $N \approx \frac{Duration}{T_z}$

13,60	<	Maximum crest elevation (Duration = 9 h)	<	15,39

The storm qualification is shown below:

	Lower bound	Upper bound	Qualification duration		
			3 h	6 h	9 h
Standard deviation	3,582	3,655	3,608	3,592	3,594
Skewness	–0,030	0,030	–0,012	–0,02	–0,001
Kurtosis	2,90	3,10	3,076	3,091	3,04
Max. crest elev. 3 h	12,61	14,27	14,41[a]	-	-
Max. crest elev. 6 h	13,24	14,99	-	14,67	-
Max. crest elev. 9 h	13,60	15,39	-	-	14,86

[a] This maximum crest elevation is slightly too high but given the 3 h assessment is used for comparison purposes only it is considered acceptable. The final DAFs will be taken from the 9 h simulation.

The wave simulation therefore satisfies the checks.

Select the integration time step:

T_z / 20 = 0,65 s
T_n / 20 = 0,43 s (time step of 0,40 s selected)

Avoid transients by skipping 100 s of response simulation.

Select simulation length: This depends on the method selected and the quantities used. This is discussed further in ISO 19905-1:2012, C.5.3, where the length of the storm used for the analysis is justified.

A.10.3.2 Application of partial factors

The use of partial factors is only applicable to two stage deterministic analyses. For fully integrated stochastic analyses, the partial factors are set to unity, but the metocean inputs are scaled up to compensate. For more information regarding partial factors, see ISO 19905-1:2012, A.10.5.3.2.

Perform simulations as required in ISO 19905-1:2012, A.10.4.4.1.2.

Simulations were carried out using the in-house non-linear random dynamics software inclusive of P-Δ effects. Combined wave/current particle velocities were used in determining the hydrodynamic loading on the legs.

A.10.5.3.4 Methods for determining the MPME

Three approaches to detailed dynamic time domain analysis are recommended:

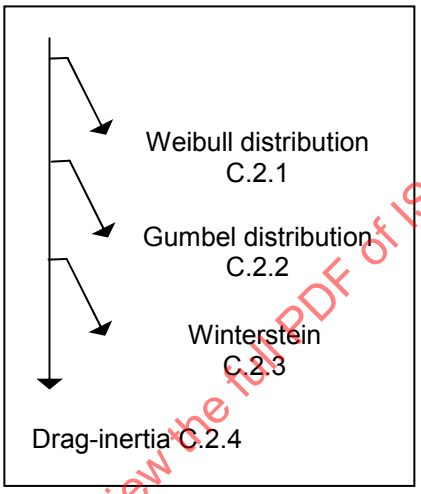

C.2.1 Weibull

Fit Weibull distribution to results of a number of time domain simulations to determine responses at required probability level and average the results.

i
C.2.1

C.2.2 Gumbel

Fit Gumbel distribution to histogram of peak responses from a number of time domain simulations to determine responses at required probability level.

i
C.2.2

C.2.3 Winterstein

Apply Winterstein's Hermite polynomial method to the results of time domain simulations.

This option has been chosen to calculate the DAFs for determination of the inertial loadset. The following analyses refer to the sand case only; a different storm was generated for the clay case following exactly the same procedure.

The input seastate has been checked for Gaussianity.

The method requires stable skewness, kurtosis and zero upcrossing rate in addition to the mean and standard deviations. The adequacy of the simulation length has been checked by qualifying the same storm at 3 h, 6 h and 9 h and calculating MPMEs and then DAFs at the 3 h probability level for each simulation length.

Storm heading 60˚		
Simulation duration	Overturning DAF	Base shear DAF
3 h	1,354	1,205
6 h	1,345	1,205
9 h	1,357	1,213
Storm heading 90˚		
Simulation duration	Overturning DAF	Base shear DAF
3 h	1,296	1,178
6 h	1,311	1,191
9 h	1,325	1,198
Storm heading 120˚		
Simulation duration	Overturning DAF	Base shear DAF
3 h	1,265	1,141
6 h	1,283	1,161
9 h	1,288	1,162

The DAF's for 15˚ and 45˚ have also been calculated as recommended in ISO 19905-1:2012, C.3 for comparison with the 60˚, 90˚ and 120˚ headings.

Storm heading 15˚		
Simulation duration	Overturning DAF	Base shear DAF
3 h	1,272	1,152
6 h	1,287	1,169
9 h	1,296	1,172
Storm heading 45˚		
Simulation duration	Overturning DAF	Base shear DAF
3 h	1,344	1,202
6 h	1,343	1,205
9 h	1,357	1,213

The results of these analyses show a slight upward trend over the increasing duration, which indicates that (at least) a 9 h storm is required to best assess the DAFs.

The moment responses for the 90° heading 9 h simulation and 3 h exposure are presented in more detail below:

Step	Quantity	Symbol	Full dynamic	Quasi-static
1	mean	μ	201 100 kNm	206 600 kNm
	std. dev.	σ	326 900 kNm	177 200 kNm
	skewness	α_3	0,1671	1,3500
	kurtosis	α_4	3,785	5,864
2	upcrossings	N	3 097	2 345
3	variables	h_3, h_4 & K	automatically calculated by software	
4		U_{mpm}	3,726	3,783
5		z_{MPM}	5,038	6,702
6		R_{MPMe}	1 848 000 kNm	1 395 000 kNm

With step 6 the required quantities are obtained and the DAF can be determined as:

$$DAF = \frac{R_{\text{MPM dyn}}}{R_{\text{MPM static}}} = \frac{1\,848\,000}{1\,395\,000} = 1{,}325$$

C.2.4 Drag-inertia method

Determine DAF for a two-stage deterministic storm analysis from the response of the jack-up for four conditions:

— full dynamic response;

— full static response;

— static response to inertia only wave loading (setting C_d = 0);

— static response to drag only wave loading (setting C_m = 0).

The DAF is then scaled based on ISO 19905-1:2012, Figure C.2.4-2 based on the ratio of T_n/T_p to ensure the DAF values are not underestimated for cases where T_n approaches T_p.

This approach is not considered further herein.

i
C.2.4 &
ISO/TR 19905-2

Detailed time-series methods

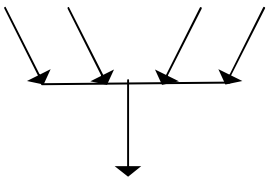

All detailed dynamic analysis methods have now been considered.

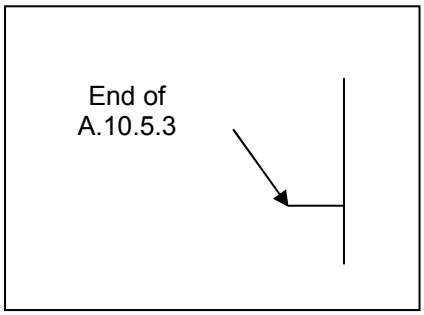

A.10.5.2.2.3 **Inertial loadset based on random dynamic analysis ($K_{DAF,RANDOM}$)**

The BS and OTM DAFs have been calculated as the ratios of the MPME of the dynamic response to the MPME of the static response in accordance with ISO 19905-1:2012, A.10.5.3 using Winterstein's Hermite polynomial method for the calculation of the MPME. The resulting DAFs are shown below:

Assessment case	Storm heading	Overturning DAF	Base shear DAF
Sand	015°	1,30	1,17
	045°	1,36	1,21
	060°	1,36	1,21
	090°	1,33	1,20
	120°	1,29	1,16
Clay	060°	1,48	1,32
	090°	1,43	1,29
	120°	1,36	1,24

The DAFs for 15° and 45° headings for the sand case have been calculated in accordance with the advice given in ISO 19905-1:2012, C.2, which recommends using the DAF calculated for one of these headings around the clock. GL Noble Denton's usual procedure for smoothing the DAFs involves calculating weighted average DAFs using 50 % of the DAF for that heading and then adding 25 % from each of the DAFs of the two adjacent headings (typically for 15° increments).

The flowing chart shows a comparison between using the weighted average of DAFs produced for 60°, 90° and 120° (sand case) and using the DAFs calculated for 15° and 45° around the clock as suggested in ISO 19905-1:2012, C.3.

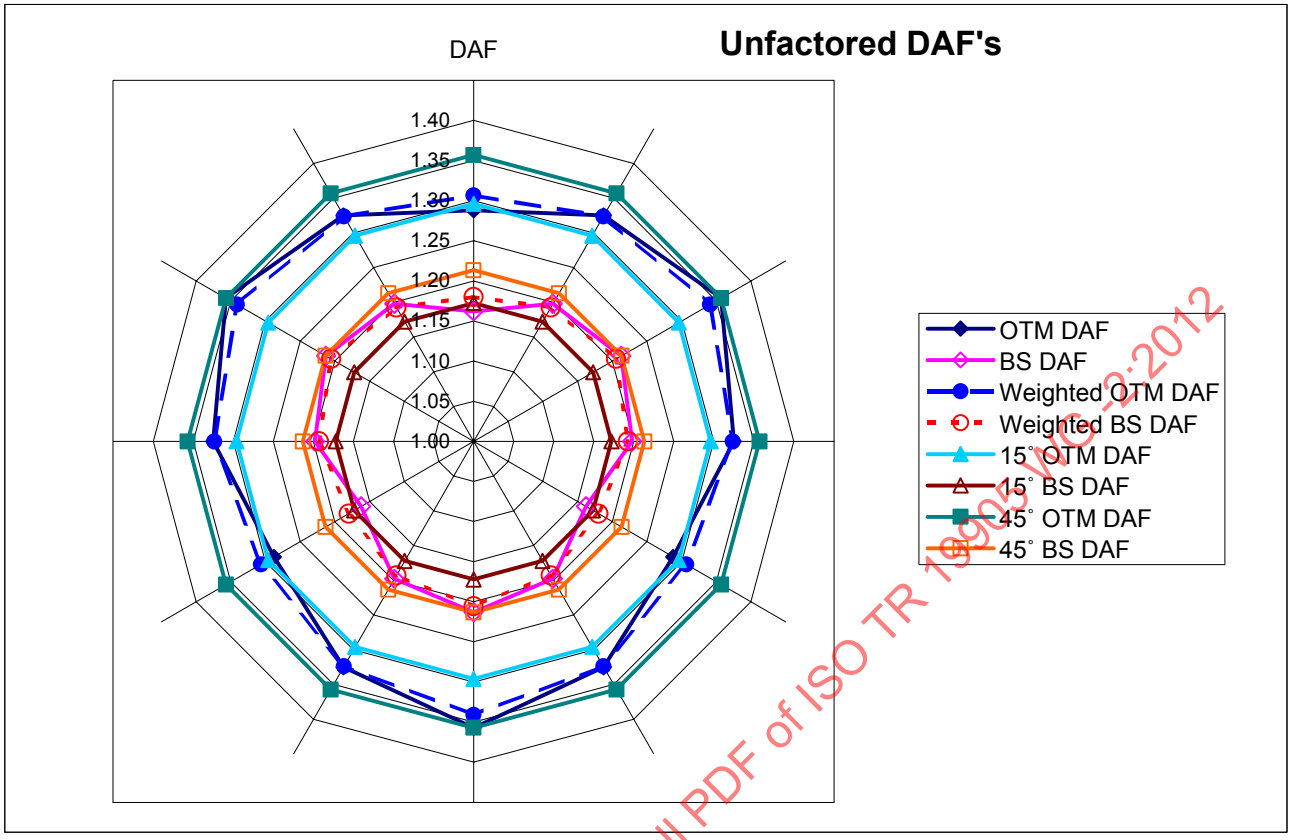

The chart shows a much better approximation is made by using weighted average DAFs than mid-point heading DAFs, where 45˚ would be conservative and 15˚ non-conservative even for the limited storm loading directions being considered.

Therefore, the weighted average DAF approach is adopted in this assessment, which results in the following DAFs.

Assessment case	Storm heading	Overturning DAF	Base shear DAF
Sand	060˚	1,34	1,20
	090˚	1,32	1,19
	120˚	1,30	1,18
Clay	060˚	1,48	1,32
	090˚	1,44	1,29
	120˚	1,38	1,25

Inertial loadset

The inertial loadset, F_{in}, normally should be such that it increases both the BS and the OTM from the deterministic quasi-static analysis by the same ratios as those determined between the random quasi-static (zero mass) analysis and the random dynamic analysis. In such cases, the structural model (used for dynamic analysis) may be simplified and it is not necessary that it contain all the structural details, but it should nevertheless be a multi degree-of-freedom model. See A.8.8.5 for guidance on applying an inertial loadset to the model that matches both dynamic BS and OTM.

Caution should be exercised when the wave period approaches resonance, and additional load cases should be considered when (T_n/T_p) is greater than 0,9. These extra load cases account for the changing phase between the forcing action and the inertial action as (T_n/T_p) approaches and exceeds 1,0 (see ISO 19905-1:2012, Figure A.10.5-3 and Note 1).

The basic load case is the inertial loadset applied in phase with, and to increase the response to, the metocean actions; see ISO 19905-1:2012, Equation (A.10.5-4). This load case is required for all ratios of (T_n/T_p). Three additional load cases, ISO 19905-1:2012, Equations (A.10.5-5) to (A.10.5-7), should be considered when (T_n/T_p) is greater than 0,9. Four sample load cases are shown diagrammatically in ISO 19905-1:2012, Figure A.10.5-3. In each case, the inertial loadset should be applied to the structure as described with A.8.8.5, using the same directional pair of $K_{DAF,RANDOM}$ values calculated for base shear and overturning moment.

Check:

T_n = 8,04 s (e.g. sand case non-linear period for 80 % rotational fixity)

T = $0{,}9T_{p(apparent)}$ = 14,94 s

T_n/T_p = 0,54

Therefore, the additional dynamic loadcases (ISO 19905-1:2012, Equations (A.10.5-5 to A.10.5-7)) do not need to be considered.

Example calculations following ISO 19905-1:2012, Equations (A.10.5-5) to (A.10.5-7) are provided in A.12, Appendix A.A.

i
A.12 Appendix A.A

The base shear inertial loadsets are calculated as given in ISO 19905-1:2012, Equation (A.10.5-3):

$$F_{in,PHASE}(a) = K_{DAF,RANDOM} F_{STATIC} - F_{STATIC,PHASE}(a) \quad \text{(A.10.5-3)}$$

To obtain F_{in} it is necessary to inspect the hydrodynamic force data calculated using the in-house program Force-3.

Note that the stochastic DAFs calculated refer to the increase in maximum BS and OTM as opposed to the increase in amplitude. As such, the maximum wave/current BS and OTM are used to calculate F_{in} as opposed to the amplitude.

Examples based on sand foundation condition assessment and hydrodynamic loads include the 1,15 environmental load factor.

60° heading:

$F_{BS,(QS)Max}$ = maximum hydrodynamic BS
= 20 209 kN

$F_{OTM,(QS)Max}$ = maximum hydrodynamic OTM
= $1{,}864 \times 10^6$ kN

Loadsets need to be applied to achieve the correct BS:

$F_{in\,(BS)}$ = $(1{,}203 - 1{,}00) \times 20\,209$
= 4 103 kN

And OTM:

$M_{in\,(OTM)}$ = $(1{,}34 - 1{,}00) \times 1{,}864 \times 10^6$
= $636{,}0 \times 10^3$ kNm

These loads are to be applied to the model in the same direction as the metocean conditions.

The inertial loads for the other headings have been calculated in a similar way. The resulting inertia loads are presented below.

Case/ Storm heading	Wave/Current		Required inertia force	Required inertia moment
	OTM (kNm)	BS (kN)	F_{in} (kN)	M_{in} (kNm)
Sand assessment				
60°	$1{,}86 \times 10^6$	$20{,}21 \times 10^3$	$4{,}10 \times 10^3$	$636{,}0 \times 10^3$
90°	$1{,}90 \times 10^6$	$20{,}58 \times 10^3$	$3{,}94 \times 10^3$	$610{,}9 \times 10^3$
120°	$1{,}84 \times 10^6$	$19{,}99 \times 10^3$	$3{,}61 \times 10^3$	$560{,}1 \times 10^3$
Clay assessment				
60°	$2{,}08 \times 10^6$	$20{,}12 \times 10^3$	$6{,}49 \times 10^3$	$1\,002{,}1 \times 10^3$
90°	$2{,}09 \times 10^6$	$20{,}31 \times 10^3$	$5{,}90 \times 10^3$	$911{,}7 \times 10^3$
120°	$2{,}02 \times 10^6$	$19{,}63 \times 10^3$	$4{,}94 \times 10^3$	$763{,}1 \times 10^3$

Given that there is only 5,2 m of leg above the upper guide for the sand case and 1,9 m for the clay case, no inertia forces have been applied to the legs above the upper guide.

ISO 19905-1:2012, A.8.8.5 offers guidance on applying an inertial loadset to the model that matches both dynamic BS and OTM.

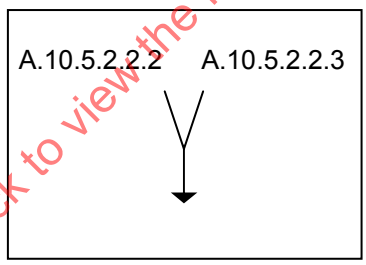

A.9.5 Determine quasi-static response

10.5.2 **Two stage deterministic (inertial loadset) approaches (Stage 2)**

The quasi-static response is calculated by applying the following actions to the unit:

G_F actions due to fixed load

G_v actions due to maximum or minimum variable load

E_e metocean action due to the extreme storm event

D_e actions representing dynamic extreme storm effects

The maximum quasi-static wave action is determined by stepping the maximum wave through the structure. The details of the wave are shown above, under the flag where ISO 19905-1:2012, 6.4 is discussed, but are reproduced here for continuity purposes.

H_{srp} = 14,4 m, and H_{max} = 26,8 m

NOTE Unlike some assessment methods which utilize a reduced deterministic wave weight, ISO 19905-1 uses the full maximum wave height and subsequently factors down the kinematics using a kinematics reduction factor (KRF) which is also used to account for the effects of wave spreading.

The hydrodynamic actions should be calculated using the Morison equation, utilizing the appropriate hydrodynamic model and wave theory as shown below.

(A.7.3.3.2) Check for applicability of Morison's equation

wavelength $\approx$ 427 m (from theory) for the extreme wave

tubular diameter = 0,71 m (maximum chord effective diameter)

Therefore the wavelength is greater than five times the reference diameter and so Morison's equation is applicable.

An appropriate wave theory is to be selected using ISO 19905-1:2012, A.7.3.3.3.1.

Refer to ISO 19905-1:2012, Figure A.7.3-5.

$$\left.\begin{array}{l} H_{\max} = 26{,}8 \text{ m} \\ T_{\text{ass}} = 16{,}6 \text{ s} \\ g = 9{,}81 \text{ m/s} \\ d = 123{,}1 \text{ m} \end{array}\right\} \quad \begin{array}{l} H / gT^2 = 0{,}009\,9 \\ d / gT^2 = 0{,}046 \end{array}$$

This indicates that Stokes fifth order wave theory can be used.

(A.7.3.3) Wave and current actions

The formulations given in ISO 19905-1:2012, A.7.3.3 for the drag and inertia forces are used in the in-house programs. The terms C_{D}, C_{M}, A and D are calculated elsewhere. The velocity terms v_{n} and u_{n} and $\dot{r}$ and acceleration terms $\dot{u}_{\text{n}}$ and $\ddot{r}_{\text{n}}$ are variables within the program.

Note that the relative fluid particle velocity is only included in stochastic analyses and not quasi-static analyses. See ISO 19905-1:2012, A.7.3.3.2.

Current velocities for this analysis have been defined at two points, the intermediate current values are linearly interpolated between these points by the software, allowing for current velocity reduction due to interference; see the discussion on A.7.3.3.4 above.

The wind actions are presented in A.7.3.4 in this document.

(9.3.1) The spudcan-foundation interface for use in the quasi-static model can be found in ISO 19905-1:2012, 9.3.1

(5.4.3) A range of heading should be considered to pick out the most onerous for each assessment case. The worst case loading directions for preload and foundation bearing capacity, leg and holding system strength and overturning capacity have been defined as 60°, 90° and 120° anticlockwise from the bow respectively for this assessment.

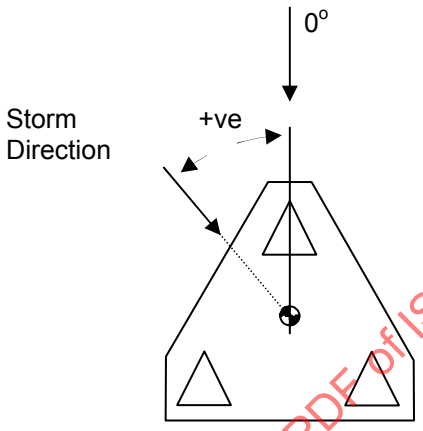

For each heading the wave is to be stepped through the modelled structure to find the worst wave phase. This can be done using the in-house program Force-3 which bolts on to the PAFEC FE package. The simulation is run for 100 s with a small, e.g. 0,5 s, time step to pick out the most severe instant. The program then allows the user to specify this instant in the final quasi-static analysis.

Two assessment loadcases F_{dmax} and F_{dmin} (for maximum and minimum variable load respectively) are required to satisfy the limit state checks listed in ISO 19905-1:2012, Table A.10.5-2. The actions to be applied to each of these loadcases are determined by the following generalized forms where partial factors are applied before undertaking the structural response analysis.

$$F_{dmax} = \gamma_{f,G}\, G_F + \gamma_{f,V}\, G_{Vmax} + \gamma_{f,E}\, [E_e + \gamma_{f,D}\, D_e]$$

$$F_{dmin} = \gamma_{f,G}\, G_F + \gamma_{f,V}\, G_{Vmin} + \gamma_{f,E}\, [E_e + \gamma_{f,D}\, D_e]$$

Where the actions are defined in ISO 19905-1:2012, 8.8.1, as discussed above, and duplicated here for completeness:

Fixed loads, G_F: Actions due to fixed load located at the appropriate position.

Variable loads, G_V: Actions due to max. or min. variable load positioned at the most onerous centre of gravity location applicable to the configurations under consideration.

Metocean loads, E_e: Actions due to metocean conditions during the extreme storm event (or zero for an earthquake assessment).

Inertia loads, D_e: Actions due to dynamic response (zero for stochastic storm assessment).

The two assessments (sand and clay foundations) were performed using GL Noble Denton's FORCE-3 bolt on to the PAFEC-FE package using the loadcases defined above. The following tables show the breakdown of the actions applied in each case and the response of the unit for each loadcase for both sand and clay cases.

Sand:

Storm direction	Wind	Wave/Current	Inertia		Total loading	
			Max.	Min.	Max.	Min.
60	9 204	20 209	4 103	4 535	33 515	33 948
	1 505 844	1 863 575	636 035	703 077	4 005 454	4 072 496
90	8 863	20 584	3941	4358	33 388	33 805
	1 448 481	1 898 349	610 929	675 513	3 957 758	4 022 342
120	7 728	19 987	3 613	4 072	31 328	31 787
	1 275 239	1 839 374	560 069	631 350	3 674 682	3 745 963

Clay:

Storm direction	Wind	Wave/Current	Inertia		Total loading	
			Max.	Min.	Max.	Min.
60	9 000	20 115	6 487	6 243	35 601	35 357
	1 467 572	2 076 011	1 002 060	964 376	4 545 643	4 507 959
90	8 657	20 312	5 902	5 511	34 871	34 480
	1 410 100	2 090 847	911 703	851 382	4 412 652	4 352 331
120	7 535	19 630	4 939	4 735	32 105	31 900
	1 239 536	2 019 945	736 081	731 493	4 022 561	3 990 974

Sand — Maximum hull weight:

Storm direction	Hull sway (m)	Leg	Moment (kNm)	Shear (kN)	Axial (kN)	Moment (kNm)	Shear (kN)	Axial (kN)
			In leg below lower guide			(At base of legs)		
60	3,46	1	1 517 607	4 719	25 231	73 271	12 213	42 046
		2	1 522 512	4 856	22 975	64 256	12 243	39 878
		3	1 711 845	3 590	148 798	0	9 064	165 053
90	3,42	1	1 523 493	3 787	65 668	131 748	11 713	82 482
		2	1 508 778	5 680	6 229	0	12 233	10 683
		3	1 673 586	3 188	137 556	0	9 437	153 821
120	3,13	1	1 439 127	2 806	101 789	117 916	10 144	118 603
		2	1 371 438	5 346	8 535	0	11 125	8 378
		3	1 444 032	3 041	103 751	113 600	10 055	120 006

Sand — Minimum hull weight:

Storm direction	Hull sway (m)	Leg	Moment (kNm)	Shear (kN)	Axial (kN)	Moment (kNm)	Shear (kN)	Axial (kN)
			In leg below lower guide			(At base of legs)		
60	3,51	1	1 554 885	4 885	17 364	29 764	12 380	34 178
		2	1 567 638	4 934	15 039	0	12 321	31 941
		3	1 727 541	3 777	143 962	0	9 251	160 217
90	3,42	1	1 518 588	3 914	58 791	126 745	11 841	75 606
		2	1 506 816	5 857	13 077	0	12 410	3 826
		3	1 662 795	3 306	130 640	0	9 555	146 895
120	3,11	1	1 414 602	2 982	94 559	138 419	10 320	111 373
		2	1 363 590	5 454	14 705	0	11 232	2 197
		3	1 420 488	3 227	96 511	135 084	10 232	112 766

Clay — Maximum hull weight:

Storm direction	Hull sway (m)	Leg	Moment (kNm)	Shear (kN)	Axial (kN)	Moment (kNm)	Shear (kN)	Axial (kN)
			In leg below lower guide			(At base of legs)		
60	3,33	1	1 482 291	5 513	25 741	391 027	13 420	82 532
		2	1 486 215	5 690	23 515	385 631	13 459	80 393
		3	1 798 173	4 179	146 718	1	8 731	202 930
90	3,17	1	1 447 956	3 826	65 325	374 055	12 233	122 115
		2	1 402 830	6 955	1 609	388 672	13 204	55 270
		3	1 649 061	3 669	132 258	114 090	9 427	188 470
120	2,83	1	1 326 312	2 570	97 296	312 056	10 310	154 086
		2	1 228 212	6 926	383	388 868	11 586	56 506
		3	1 333 179	2 874	99 052	304 502	10 202	155 273

Clay — Minimum hull weight:

Storm direction	Hull sway (m)	Leg	Moment (kNm)	Shear (kN)	Axial (kN)	Moment (kNm)	Shear (kN)	Axial (kN)
			In leg below lower guide			(At base of legs)		
60	3,23	1	1 436 184	5 366	20 052	387 593	13 273	76 842
		2	1 437 165	5 582	17 884	390 536	13 342	74 772
		3	1 740 294	4 189	137 379	5 332	8 741	193 600
90	3,05	1	1 367 514	3 581	58 448	377 195	11 988	115 238
		2	1 329 255	6 563	4 473	388 476	12 812	52 415
		3	1 529 379	3 914	121 340	206 402	9 682	177 561
120	2,73	1	1 260 585	2 570	89 026	336 777	10 320	145 816
		2	1 183 086	6 710	4 424	385 435	11 370	52 464
		3	1 269 414	2 884	90 713	328 145	10 212	146 934

From the analyses presented above and further detailed preliminary analyses, the most onerous cases for the different assessment parameters are:

60° maximum variable — For preload and foundation bearing capacity

90° maximum variable — For leg and holding system strength

120° minimum variable — For overturning and sliding

These will be considered in detail below.

Detailed leg model:

Given that the most onerous case for leg and holding system strength has been identified as 90° maximum variable, the loads associated with this case are applied to the detailed leg model to calculate the structural utilizations.

In this case further preliminary analyses identified that the most onerous loading was on the port and starboard legs and as such only these legs have been assessed.

Jackcase:

Although ISO 19905-1 recommends that the jackcase should be modelled with the detailed leg, in this case it has been deemed unnecessary given that the guide stiffnesses used in the analyses are arbitrary and that the subject jack-up has opposed chock and pinion pairs which are generally not significantly affected by the stiffness of the jackcase in the way that unopposed pinions are.

Fixation system:

For this specific jack-up unit the holding system is designed such that the pinions continue to hold the deadload ($G + G_v$) of the unit even while the chocks are installed. The chocks then hold all of the axial load in the chords over and above the deadload. There are several techniques for modelling this behaviour but in this case this the chocks were given negative gaps effectively preloading them in the opposite direction to the deadload. Once the deadload is applied the chocks become unloaded and any load over and above the deadload is held by the chocks.

Leg Position:

Three leg positions are to be considered: one with lower guide level with a horizontal brace (nod), one with lower guide level with a diagonal brace node (mid) and one with lower guide level with a chord mid-span (qrt). Note that in order to ensure the most accurate load distribution in the hull region, the loading of the leg changes slightly for each case due to the different length of leg below the lower guide.

Application of loads to the detailed leg model:

With the detailed model that has been set up earlier there are two primary methods of applying loads to achieve the correct loading in the correct parts of the leg.

Application of simple point loads

If the most onerous member utilizations are known to be at the position of the lower guide or spudcan connection, a simple approach can be taken to loading, where the user applies a limited number of point loads at a number of bays below the lower guide or above the spudcan to simulate the correct axial, shear and bending moment in the most onerous leg section which has been identified during preliminary detailed analyses.

Application of a complete loadset

If the most onerous member utilizations are at other positions in the leg then a compete loadset accounting for the hydrodynamic, wind, gravitational, buoyancy and P-Δ effects is required to simulate the correct axial, shear and moments in each part of the leg.

Preliminary analyses showed in this case that the worst chord utilizations were at the level of the lower guide and the worst brace utilizations at the leg section change at around 42 m above the spudcan tip. Given that the most onerous brace utilizations were neither at the spudcan connection or the lower guide, the application of a complete loadset was required and is described below.

The following diagram shows the loading configuration of the leg.

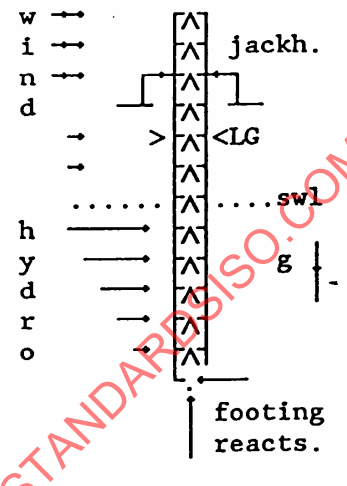

Weight and buoyancy loads:

Weight and buoyancy loads are represented in the model by nodal loads applied to each chord along the length of the leg. These loads simulate the correct distribution of weight and buoyancy and include the weight and buoyancy of the spudcan at the bottom of the leg

Footing loads:

As the model is not earthed at its footing, a set of loads is required to simulate the axial, shear and moment reactions. These reactions are taken from the quasi-static analyses performed earlier.

Hydrodynamic and wind loads:

Distributed hydrodynamic and wind loads are applied as nodal loads at the relevant elevations in the model to accurately simulate the environmental forces on the leg.

P-Δ loads:

P-Δ loads are applied to the leg as sets of vertical load couples applied at each bay below the lower guide in both horizontal orthogonal axes. The P-Δ loadset is derived from the assumed shape of the deflected leg accounting for the relative stiffness of the leg to hull connection and the spudcan foundation.

A.10.5.4 Leg inclination loads

In the absence of further information, the offset is 0,5 % of the length of leg below the lower guide.

Sand and clay

offset = 0,005 × 159,5* = 0,80 m (*approximate value)

additional moment = seabed reaction × 0,80 m

The resultant moment after all adjustments is applied by means of sets of vertical couples distributed along the length of the leg.

Lower guide loads:

The applied loads described above provide an accurate load distribution, noting that care must be taken to ensure that the correct overall reactions are achieved at the lower guide.

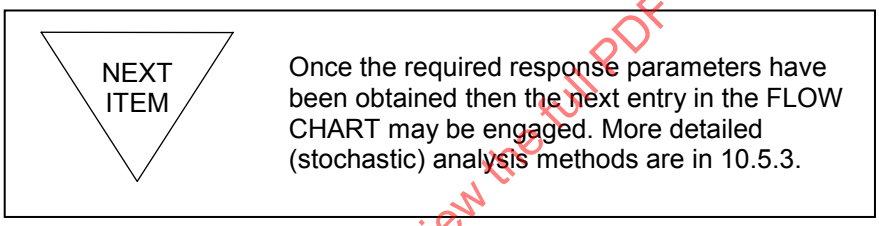

A.9.6 Effect of fixity on dynamic response

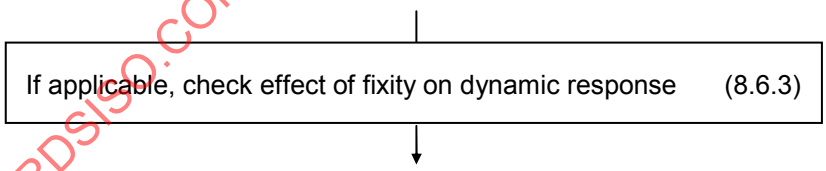

For the analysis of an independent leg jack-up unit in the elevated storm mode, the foundations may be assumed to behave as pinned supports, which are unable to sustain moment. This is a conservative approach for the bending moment in the leg in way of the leg-to-hull connection.

For the detailed example calculation, the inclusion of rotational foundation fixity is justified and the non-linear soil-structure interaction effects have been taken into account in the structural analysis. The model used includes the interaction of rotational, lateral and vertical soil forces as described in ISO 19905-1:2012, Clause 9 and A.9.

For the purpose of this assessment a single foundation fixity has been modelled, although it is noted that it may be required to consider the effects of upper or lower bound fixity values to address different areas of the structure under consideration.

When it is necessary to check the spudcans, the leg-to-can connection and the lower parts of the leg, appropriate calculations should be carried out to determine the upper bound spudcan moment considering soil-structure interaction; this has not been considered for the purpose of the detailed example calculations.

For earthquake screening analyses the simplest adequate spudcan-soil models should normally be used, incorporating the maximum interpreted small strain stiffnesses and capacities (clause 9) and not allowing for foundation degradation.

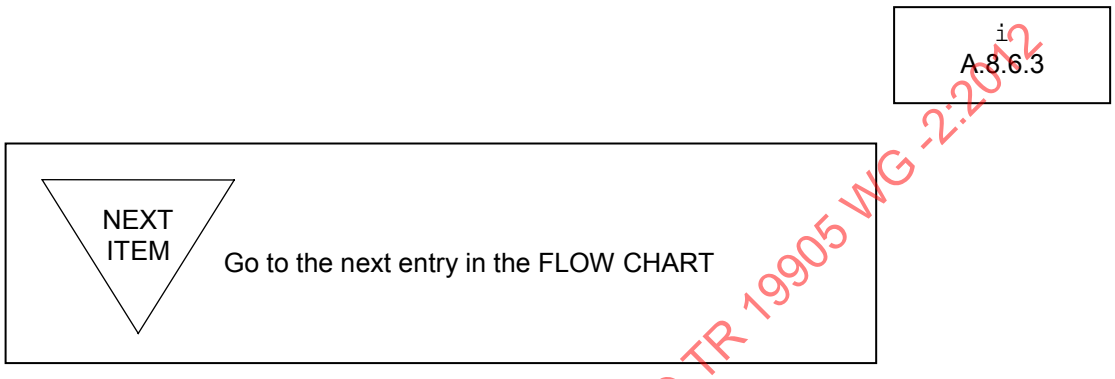

A.10 Structural and overturning assessment

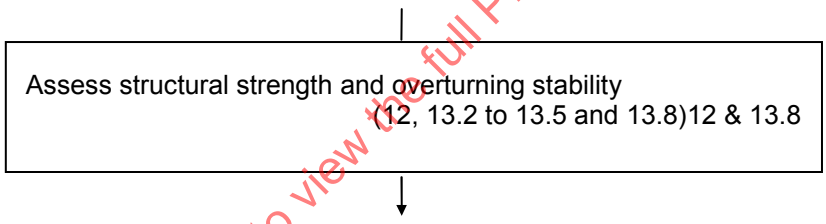

This is the first part of the load and resistance assessments. Additional penetration (if required), leg length and foundation checks are considered in the next two FLOW CHART items.

If the unit cannot satisfy the requirements of ISO 19905-1 at this stage, this may lead to either a more detailed response calculation (with or without foundation fixity), or to the unit being found unsuitable.

Structural strength — local route

General formulation	(13.2)
Leg members:	
Classification	(12.2 & A.12.2)
Section Properties	(12.3 & A.12.3)
Effects of axial force on bending moment (Moment Amplification)	(12.4 & A.12.4)
Leg strength - tubulars	(12.5 & A.12.5)
Leg strength - prismatic members	(12.6 & A.12.6)
Leg strength - joints	(12.7 & A.12.7)
Holding system	(12.1.4 & 13.5)
Spudcan strength	(12.1.5 & 13.4)

A.10.1 Acceptance criteria

13.2 **General formulation**

The intent of the structural checks is to satisfy the general utilization formula:

$$U \leq 1{,}0 \qquad (13.2\text{-}1)$$

where:

U is the utilization to one significant decimal place:

$$U = \frac{\text{action effect, } A_E \text{ , due to factored actions, } F_d}{\text{factored resistance, } R} \qquad (13.2\text{-}2)$$

For assessments where the relevant action effect consists of a combination of responses, the individual action effects and factored resistances combine into an interaction equation I. In these cases the utilization U is equal to the value of I.

For assessments where the resistance is given by the yield interaction surface (for foundations) or the plastic interaction surface (for strength of non-circular prismatic members) the utilization is of the following general form:

$$U = \frac{\text{length of the vector from a specified origin to the action effect, } A_E}{\text{length of the vector from the same origin to the factored interaction surface}} \qquad (13.2\text{-}3)$$

Factored actions are determined in accordance with the assessment load case F_d in ISO 19905-1:2012, 8.8.

NOTE Normally both partial action and partial resistance factors are greater than unity: actions are multiplied by partial action factors and resistances are divided by partial resistance factors.

Hull strength and jack house to deck connections are considered to be covered by classification unless special circumstances apply.

A.10.2 Structural strength assessment

12 **Structural strength**

In-line with ISO 19905-1, this detailed example calculation addresses strength checks for a truss-type leg per the “typical jack-up” being considered. It is noted that some of the checks included in ISO 19905-1:2012, Clause 12 are applicable to either tubular or box-type legs but this clause should be supplemented with other documents to address stiffened sections, e.g. ISO 19905-1:2012, References [12.1-1] to [12.1-4].

12.2 & A.12.2 **Member classification**

Leg brace members:

For circular tubulars the members are classified as Class 1 when:

$$D/t \leq 0{,}0517\ E / F_y \qquad (A.12.2\text{-}1)$$

where:

D = outside diameter

t = wall thickness

F_y = yield strength in stress units

E = elastic modulus

For all leg brace members:

E = 205 000 N/mm^2

F_y = 620,7 N/mm^2 (lower leg)
= 586,3 N/mm^2 (upper leg)

Leading to:

0,0517 E / F_y = 17,08 (lower leg)
= 18,08 (upper leg

Member	D (m)	t (m)	D/t	**Class 1**
Lower leg horizontal	0,406	0,032	12,69	Yes
Lower leg diagonal	0,406	0,032	12,69	Yes
Upper leg horizontal	0,356	0,025	14,02	Yes
Upper leg diagonal	0,356	0,025	14,02	Yes

Classification of tubular members to Class 1 is only relevant when undertaking earthquake, accidental or alternative strength analyses (see 10.7, 10.8 and 10.9). In all other cases the distinction between class 1 (plastic) and class 2 (compact) is irrelevant to the assessment but included herein for completeness.

A.12.2.3.2 **Non-circular prismatic member classification (Leg chord members)**

The “split-tubular” leg chord members are prismatic members that contain both curved and flat components, each of which is classified individually.

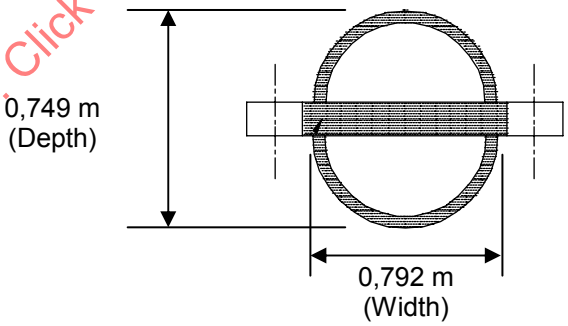

Simplified schematic of leg chord section — Constant cross-section

Curved components:

Prismatic members that contain curved or tubular components should have the curved components classified based on the values given in ISO 19905-1:2012, Table A.12.2-1

The curved components of the split-tubular chord taper in thickness toward the rack-plate; in-line with the recommendations in ISO 19905-1:2012, A.12.2.3.2 the average thickness over the width of the component has been adopted for classification:

D = outside diameter = 0,559 m

t = wall thickness
= 0,108 m (thickest section)
= 0,099 m (average thickness)

E = 205 000 N/mm^2

F_y = 690,0 N/mm^2

Therefore:

$(D/t)/(E/F_y)$ = 0,019

For the tubular component details presented and based on the classification guidance given in ISO 19905-1:2012, Table A.12.2-1, the tubular components are classified as Class 1 elements ($D/t \leq 0{,}052\ E/F_y$) regardless of whether the member is in bending or compression.

Table A.12.2-1 — Classification limits for non-circular prismatic members containing curved components

Class	D/t limits	
	Section in bending	Section in compression
1	$D/t \leq 0{,}052\ E/F_y$	$D/t \leq 0{,}052\ E/F_y$
2	$D/t \leq 0{,}103\ E/F_y$	$D/t \leq 0{,}077\ E/F_y$
3	$D/t \leq 0{,}220\ E/F_y$	$D/t \leq 0{,}102\ E/F_y$
4	$D/t > 0{,}220\ E/F_y$	$D/t > 0{,}102\ E/F_y$

Lateral torsional buckling

Non-circular prismatic members which do not satisfy the following simplified lateral torsional buckling criteria should be assessed further to determine a reduced member bending strength M_b using the guidance given in ISO 19905-1:2012, A.12.6.2.6.

Singly symmetric open sections, from F2-5 of AISC (see ISO 19905-1:2012, Reference [A.12.5-1]):

$$\frac{L_b}{r_{ltb}} \leq 1{,}76\sqrt{\frac{E}{F_{y,ltb}}} \qquad \text{(A.12.2-2)}$$

or for any closed section, derived from BS 5400-3 (see ISO 19905-1:2012, Reference [A.12.5-2]):

$$\frac{L_b}{r_{ltb}} \leq \frac{0{,}36 I_2 E}{Z_p F_{ymin}}\sqrt{\frac{AJ}{(I_1 - I_2)(I_1 - J/2{,}6)}} \qquad \text{(A.12.2-3)}$$

where the chord section in this case is a closed section and the following variables apply:

I_y = major axis second moment of area of the gross cross-section
= 0,009 7 m^4

I_z = minor axis second moment of area of the gross cross-section
= 0,006 7 m^4

L_b = effective length of beam-column between supports
= 5,105 m

A = gross cross-sectional area
= 0,247 m^2

J = torsion constant = 4 $A_o^2 / \Sigma(b/t)$

in which

A_o = the area enclosed by the median line of the perimeter material of the section
= 0,265 m^2

$\Sigma(b/t)$ = the sum of the width and thickness, respectively, of each component (wall of the section) forming the closed perimeter.

= 19,750 (assuming 0,108 m thickness around whole circumference)

r_z = radius of gyration about the minor axis as defined in ISO 19905-1:2012, Equation (A.12.3-7).
= 0,165 m

$F_{y,ltb}$ = yield strength, F_y, of the material that first yields when bending about the minor axis. Conservatively, F_y may be taken as the maximum yield strength of all the components in a non-circular prismatic cross-section

= 689,6 MPa

Z_p = fully plastic effective section modulus about the major axis determined from ISO 19905-1:2012, Equation (A.12.3-2)

= 0,040

F_{ymin} = minimum yield strength of the cross-section as defined in ISO 19905-1:2012, A.12.2.2
= 689,6 MPa

Therefore:

31,0 ≤ 425,3

Section passes the lateral torsional buckling criteria and therefore a reduced member bending strength need not be determined.

Flat plates

Non-circular prismatic members that contain flat components should have these components classified based on ISO 19905-1:2012, Tables A.12.2-2, A.12.3-3 and A.12.2-4.

When classifying non-circular prismatic components in accordance with ISO 19905-1:2012, Tables A.12.2-2, A.12.3-3 and A.12.2-4, a distinction is made between internal components and outstand components as follows:

— Internal components: components that are supported by other components along both longitudinal edges, i.e. the edges parallel to the direction of compression stress, and include:

  — *Flange internal components:* internal components parallel to the axis of bending

  — *Web internal components:* internal components perpendicular to the axis of bending

— Outstand components: components that are supported by other components along one longitudinal edge and at both ends of the member under consideration, with the other longitudinal edge free.

Classification of the flat plate leg chord members follow on the subsequent pages.

NOTE Classification detailed herein is based on the minimum cross-section (not included any rack tooth) — specifically relevant to classification of “outstand” components.

Flange internal components

b = width of base plate = 0,486 m

t_f = thickness = 0,191 m

E = 205 000 N/mm^2

F_y = 690,0 N/mm^2

Therefore:

$(b/t_f) / \sqrt{(E/F_y)} = 0,148$

For the flange internal component details presented and based on the classification guidance given in Table A.12.2-2, this component is classified as follows:

Section in bending:

$b/t_f \leq 1,03\sqrt{(E/F_y)}$

Therefore Class 1: Plastic

Section in compression:

$b/t_f \leq 1,03\sqrt{(E/F_y)}$

Therefore Class 1: Plastic

Table A.12.2-2 — Cross-section classification — Flange internal components

Limiting width-to-thickness ratios for compressed internal components			
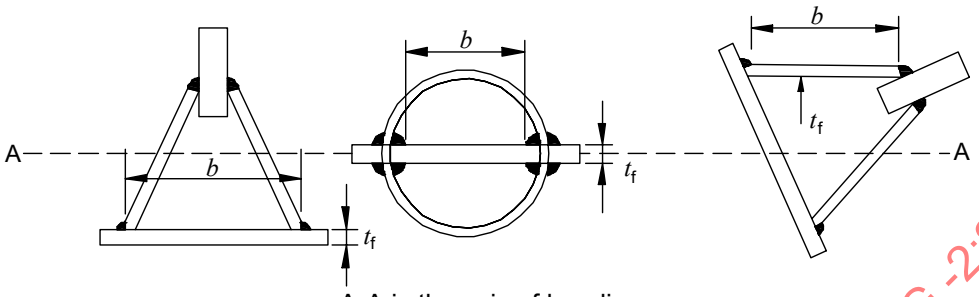 A-A is the axis of bending			
Class	**Type**	**Section in bending**	**Section in compression**
Plastic stress distribution in component and across section (compression positive)		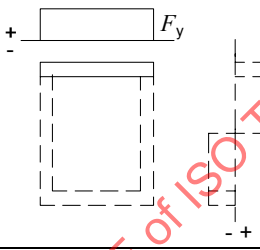	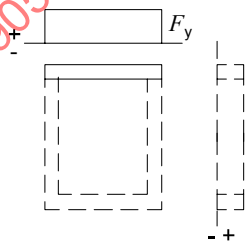
Plastic — Class 1	Rolled or welded	$b/t_f \leq 1{,}03\sqrt{(E/F_y)}$	$b/t_f \leq 1{,}03\sqrt{(E/F_y)}$
Compact — Class 2	Rolled or welded	$b/t_f \leq 1{,}17\sqrt{(E/F_y)}$	$b/t_f \leq 1{,}17\sqrt{(E/F_y)}$
Elastic stress distribution in component and across section (compression positive)		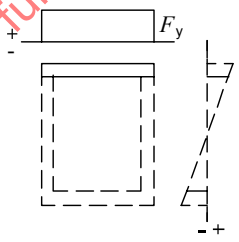	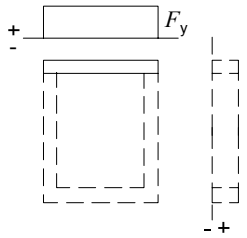
Semi-compact — Class 3	Rolled or welded	$b/t_f \leq 1{,}44\sqrt{(E/F_y)}$	$b/t_f \leq 1{,}44\sqrt{(E/F_y)}$
Slender — Class 4	Rolled or welded	$b/t_f > 1{,}44\sqrt{(E/F_y)}$	$b/t_f > 1{,}44\sqrt{(E/F_y)}$

Flange outstand components

Based on the cross-section classification for flange outstand components given in Table A.12.2-3:

b = width of outstand
= 0,014 m (at minimum cross-section)

t_f = thickness = 0,191 m

E = 205 000 N/mm^2

F_y = 690,0 N/mm^2

Therefore:

$(b/t_f) / \sqrt{(E/F_y)} = 0{,}004$

For the flange internal component details presented and based on the classification guidance given in Table A.12.2-3 for welded components, this component is classified as follows:

Flange subject to compression

$b/t_f \leq 0{,}30\sqrt{(E/F_y)}$ — therefore Class 1: Plastic

Flange subject to compression and bending (loading dependant):

Tip in compression:

$b/t_f \leq (0{,}30/\alpha)\sqrt{(E/F_y)}$ — therefore Class 1: Plastic

Tip in tension

$b/t_f \leq [0{,}30/(\alpha\sqrt{\alpha}]\sqrt{(E/F_y)}$ — therefore Class 1: Plastic

NOTE For the purposes of the classification example above, a conservative α value of 1,0 has been assumed. Member classification and subsequent strength checks should be based on the specific load distribution of individual load-case conditions.

Table A.12.2-3 — Cross-section classification — Outstand components

Limiting width-to-thickness ratios for outstand components				
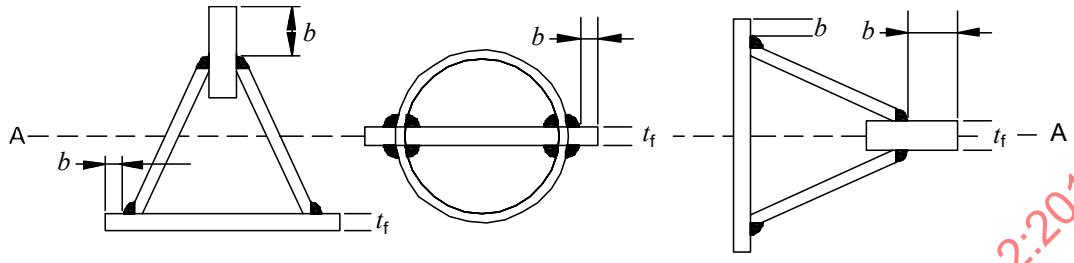 A-A is the axis of bending				
Class	**Type**	**Outstand subject to compression**	**Outstand subject to compression and bending**	
			Tip in compression	**Tip in tension**
Plastic stress distribution in component (compression positive)		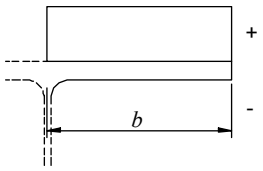	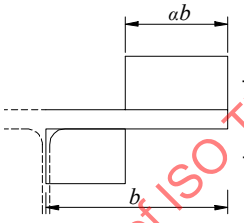	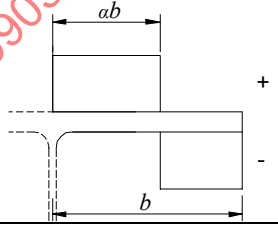
Plastic — Class 1	Rolled Welded	$b/t_f \le 0{,}33\sqrt{(E/F_y)}$ $b/t_f \le 0{,}30\sqrt{(E/F_y)}$	$b/t_f \le (0{,}33/\alpha)\sqrt{(E/F_y)}$ $b/t_f \le (0{,}30/\alpha)\sqrt{(E/F_y)}$	$b/t_f \le [0{,}33/(\alpha\sqrt{\alpha})]\sqrt{(E/F_y)}$ $b/t_f \le [0{,}30/(\alpha\sqrt{\alpha})]\sqrt{(E/F_y)}$
Compact — Class 2	Rolled Welded	$b/t_f \le 0{,}37\sqrt{(E/F_y)}$ $b/t_f \le 0{,}33\sqrt{(E/F_y)}$	$b/t_f \le (0{,}37/\alpha)\sqrt{(E/F_y)}$ $b/t_f \le (0{,}33/\alpha)\sqrt{(E/F_y)}$	$b/t_f \le [0{,}37/(\alpha\sqrt{\alpha})]\sqrt{(E/F_y)}$ $b/t_f \le [0{,}33/(\alpha\sqrt{\alpha})]\sqrt{(E/F_y)}$
Elastic stress distribution in component (compression positive)		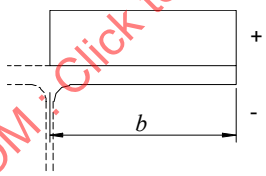	**Maximum compression at tip** 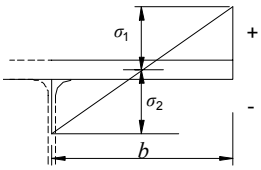	**Maximum compression at connected edge** 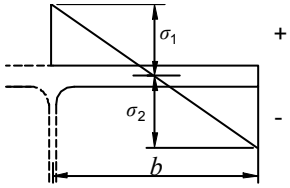
Semi-compact — Class 3	Rolled Welded	$b/t_f \le 0{,}55\sqrt{(E/F_y)}$ $b/t_f \le 0{,}50\sqrt{(E/F_y)}$	$b/t_f \le 0{,}84\sqrt{(k_\sigma E/F_y)}$ $b/t_f \le 0{,}76\sqrt{(k_\sigma E/F_y)}$ $\psi = \sigma_2/\sigma_1$ $k_\sigma = 0{,}57 - 0{,}21\psi + 0{,}07\psi^2$ for $1 \ge \psi \ge -1$	$b/t_f \le 0{,}84\sqrt{(k_\sigma E/F_y)}$ $b/t_f \le 0{,}76\sqrt{(k_\sigma E/F_y)}$ $\psi = \sigma_2/\sigma_1$ $k_\sigma = 0{,}578 / (\psi + 0{,}34)$ for $1 \ge \psi \ge 0$ $k_\sigma = 1{,}7 - 5\psi + 17{,}1\ \psi^2$ for $0 > \psi \ge -1$
Slender — Class 4	Rolled or Welded	$b/t_f >$ than for Class 3	$b/t_f >$ than for Class 3	$b/t_f >$ than for Class 3
In the figures relating to stress distributions, the dimension b is illustrated only in the case of rolled sections. For welded sections, b should be assigned as shown in the diagrams at the top of the table.				
When determining α for Class 1 and 2 members, the loads should be scaled to give a fully plastic stress distribution. For all classes it is conservative to use the relevant compression case.				

Web internal components

Based on the cross-section classification for web internal components given in Table A.12.2-4:

d = depth of web
= 0,486 m

t_w = thickness
= 0,191 m

E = 205 000 N/mm^2

Therefore:

$(d/t_w) / \sqrt{(E/F_y)} = 0,148$

For the web internal component details presented, and based on the classification guidance given in Table A.12.2-4 for welded component members, this component is classified as follows:

Web subject to bending:

$d/t_w \leq 2,56\sqrt{(E/F_y)}$ — therefore Class 1: Plastic

Web subject to compression:

$d/t_w \leq 1,03\sqrt{(E/F_y)}$ — therefore Class 1: Plastic

Web subject to bending and compression (example):

if $\alpha > 0,5$ $\quad d/t_w \leq [5,18\sqrt{(E/F_y)}] / (6,043\alpha - 1)$ — therefore Class 1: Plastic

or:

if $\alpha \leq 0,5$ $\quad d/t_w \leq 1,28\sqrt{(E/F_y)} / \alpha$ — therefore Class 1: Plastic

NOTE Member strength checks should be based on the α value specific to the load distribution of individual member and load-case conditions.

Table A.12.2-4 — Cross-section classification — Web internal components

Limiting width-to-thickness ratios for web internal components			
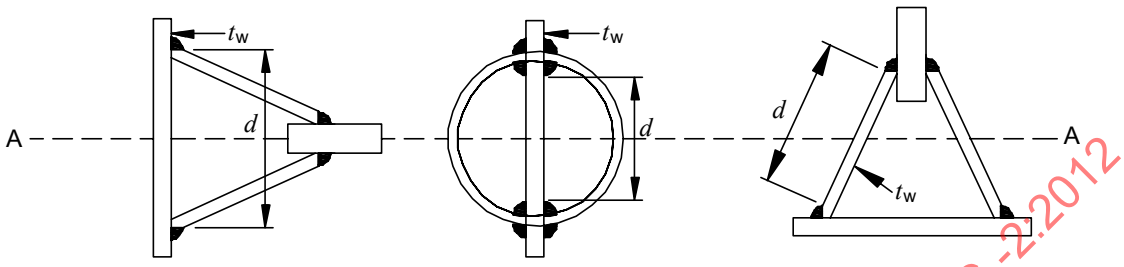 A-A is the axis of bending			
Class	**Web subject to bending**	**Web subject to compression**	**Web subject to bending and compression**
Plastic stress distribution in component (compression positive)	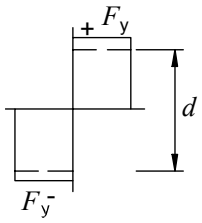	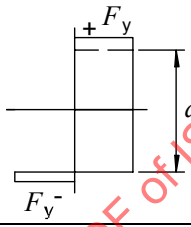	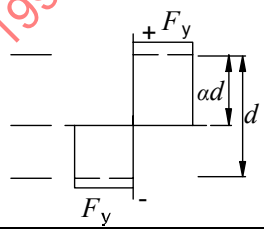
Plastic — Class 1	$\alpha = 0,5$ $d/t_w \le 2,56\sqrt{(E/F_y)}$	$\alpha = 1,0$ $d/t_w \le 1,03\sqrt{(E/F_y)}$	when $\alpha > 0,5$ $d/t_w \le \frac{5,18\sqrt{(E/F_y)}}{(6,043\alpha - 1)}$ when $\alpha \le 0,5$ $d/t_w \le 1,28\sqrt{(E/F_y)}/\alpha$
Compact — Class 2	$d/t_w \le 3,09\sqrt{(E/F_y)}$	$d/t_w \le 1,17\sqrt{(E/F_y)}$	when $\alpha > 0,5$ $d/t_w \le \frac{4,82\sqrt{(E/F_y)}}{(5,12\alpha - 1)}$ when $\alpha \le 0,5$ $d/t_w \le \frac{1,55\sqrt{(E/F_y)}}{\alpha}$
Elastic stress distribution in component (compression positive)	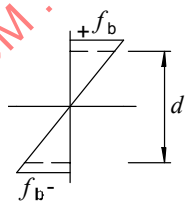	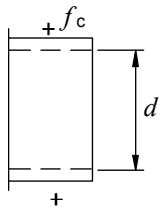	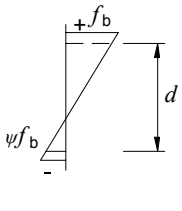
Semi-Compact — Class 3	$d/t_w \le 4,14\sqrt{(E/F_y)}$	$d/t_w \le 1,44\sqrt{(E/F_y)}$	when $\psi > -1,0$ $d/t_w \le \frac{1,44\sqrt{(E/F_y)}}{(0,674+0,327\psi)}$ when $\psi \le -1,0$ $d/t_w \le 2,07(1-\psi)\sqrt{(-\psi)}\sqrt{(E/F_y)}$
Slender —- Class 4	$d/t_w >$ than for Class 3	$d/t_w >$ than for Class 3	$d/t_w >$ than for Class 3
When determining α for Class 1 and 2 members, the loads should be scaled to give a fully plastic stress distribution. For all classes it is conservative to use the relevant compression case.			

NOTE The use of Tables A.12.2-3 and A.12.2-4 to classify cross-sections subject to axial compression and bending is complicated and requires knowledge of the cross-section stress distribution. It is always acceptable to conservatively base the cross-section classification on the relevant axial compressive case.

A.12.2.3.3 Reinforced components

No reinforced component members are present on the leg members of the “typical jack-up” being considered; reference should be made to ISO 19905-1:2012, A.12.2.3.3.

12.3 & A.12.3 Section properties

A.12.3.1 General

The cross-section properties used when assessing member strengths can differ from those used in the stiffness model (e.g. when determining structural deflections and natural periods). For example, leg chord properties for strength checks should be based on the minimum cross-sectional area (no rack tooth contribution) whereas stiffness areas may include approximately 10 % of the maximum rack tooth area. However, these increased cross-section properties may be used when determining the radii of gyration used in the determination of the column buckling strength (ISO 19905-1:2012, A.12.6.2.4) and moment amplification (ISO 19905-1:2012, A.12.4) only.

A.12.3.2.1 Axial properties — Class 1 and class 2 sections

For the “typical jack-up” being considered the leg horizontal and diagonal brace (tubular) members are single components with yield strengths:

F_y = 620,7 N/mm^2 (lower leg)
= 586,3 N/mm^2 (upper leg)

Likewise, the leg chord (non-circular prismatic) members are comprised of two half-rounds and a central rack-plate all with the same yield strength:

F_y = 690,0 N/mm^2

In this instance

F_{yeff} = F_y .

Axial strength is therefore calculated as $A_p . F_{yeff}$ for the following members:

Horizontal brace members:

lower leg: 0,037 × 620,7 = 23,17 MN

upper leg: 0,026 × 586,3 = 15,45 MN

Diagonal brace members:

lower leg: 0,037 × 620,7 = 23,17 MN

upper leg: 0,026 × 586,3 = 15,45 MN

Leg chord strength: constant:

0,246 × 690,0 = 169,74 MN

(no rack tooth)

Guidance is given in ISO 19905-1:2012, A.12.3.2.1 for members comprising components of different yield strength.

i
A.12.3.2.1

A.12.3.2.2 Flexural properties — Class 1 and class 2 sections

The second moment of area I_t is determined for the leg members as follows:

Horizontal brace members:

lower leg: $I_t = 6{,}60 \times 10^{-4}$ m^4

upper leg: $I_t = 3{,}61 \times 10^{-4}$ m^4

Diagonal brace members:

lower leg: $I_t = 6{,}60 \times 10^{-4}$ m^4

upper leg: $I_t = 3{,}61 \times 10^{-4}$ m^4

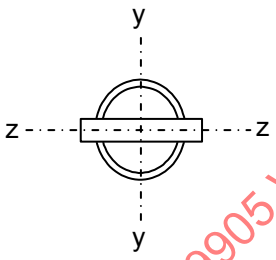

Leg chord members:

$I_{tyy} = 6{,}70 \times 10^{-3}$ m^4

$I_{tzz} = 9{,}68 \times 10^{-3}$ m^4

A.12.3.3 Semi-compact sections

The leg chord and brace members do not have any components classified as “class 3 — semi-compact members” for the “typical jack-up” being considered. No further guidance on semi-compact sections is included in this detailed example calculation.

A.12.3.4 Slender sections

The leg chord and brace members do not have any components classified as “class 4 — slender members” for the “typical jack-up” being considered. No further guidance on slender sections is included in this detailed example calculation.

12.4 & A.12.4 Moment amplification

For the “typical jack-up” being considered the elastic centroid is the same as the plastic centroid for all sections; therefore no moment resulting from the eccentricity between the elastic and plastic centroids of class 1 members exists in the case being considered.

For the case being reported here, the Euler moment amplification, p-δ, effects are included in the strength checks [“B” factor per ISO 19905-1:2012, Equation (A.12.4-2)] in lieu of being specifically accounted for in the structural response analysis.

The global large displacement effects (P-Δ) are included in the structural response analysis (per Clause 8).

The effective length factors and moment reduction factors (C_m) used in the strength checks are based on the values presented in ISO 19905-1:2012, Table A.12.4-1:

Effective length factors (K):

Chords with or without lateral loading $K = 1{,}0$

Tubular braces $K = 0{,}8$ (for split-X brace members)

Moment reduction factors (C_m):

Moment reduction factors, C_m, are member and load dependant, calculated for each member and loadcase as follows:

Chords with transverse loading:

$$C_m = 1,0 - 0,2\, P_u / P_E$$

where

P_u = member axial force inclusive of global P-Δ effects

P_E = $(\pi^2 A_c E) / (K L/r)^2$ (calculated for the plane of bending)

P_{Ey} = 734,3 MN

P_{Ez} = 510,0 MN

A_c = A_p for class 1 components (per ISO 19905-1:2012, A.12.3.5.2)
= 0,247 m^2

K = 1,0 (per above)

L = unbraced length of member for plane of flexural buckling taken as braced point to braced point for chords

= 5,105 m

r = radius of gyration for the plane of flexural buckling

r_y = 0,198 m

r_z = 0,165 m

Tubular braces (with transverse loading):

C_m = $1,0 - 0,2\, P_u / P_E$

Calculated per above but with:

L = unbraced length of member for plane of flexural buckling taken as face to face for braces.

12.5 & A.12.5 Leg strength — Tubulars

A.12.5.1 Applicability

The D/t ratio for tubular members must be less than 120 [ISO 19905-1:2012, Equation (A.12.5-1)] and of yield strength no more than 700 N/mm^2 for the strength check approach detailed in ISO 19905-1 to apply:

Member		D (m)	t (m)	D/t	F_y (N/mm^2)
Horizontal:	Lower leg	0,406	0,032	12,80	620,7
	Upper leg	0,356	0,025	16,00	586,3
Diagonal:	Lower leg	0,406	0,032	12,80	620,7
	Upper leg	0,356	0,025	16,00	586,3

All tubulars therefore satisfy these requirements.

Likewise, the D/t ratio (for member, m, at depth d), for which the effects of hydrostatic pressure can be ignored, is given by Equation (A.12.5-2):

$$(D/t)_m \leq 211 / d^{0,335} \quad \text{(A.12.5-2)}$$

where:

d = effective head of water applicable to the tubular in question;
= depth below the water surface (including penetration into the seabed where applicable) + $p\ \gamma'/(\rho_w)$;

p = depth below the sea floor in metres (zero if above sea floor);

γ' = submerged unit weight of the soil
= 11,0 kN/m^3 for sand case being considered (see 6.5)
= 5,0 kN/m^3 (average) for clay case being considered

ρ_w = mass density of water (1,025 for seawater);

$(D/t)_m$ = maximum D/t ratio possible given d

Case	Leg section	Waterdepth[a]	Penetration[a]	d	$211/d^{0,335}$
Sand	Lower	116,5	N/A	116,5	42,9
	Upper	80,8	N/A	80,8	48,5
Clay	Lower	85,0	35,8	294,5	31,4
	Upper	85,0	N/A	85,0	47,6

[a] Penetration and water depths reflect the position of the deepest tubular brace member, and not spudcan tip (leg brace members start at 6,4 m above spudcan tip).

The maximum D/t ratio of 16,0 is below the limiting value $(D/t)_m$ for all tubulars; therefore the effects of hydrostatic pressure can be ignored.

A.12.5.2 Tension, compression and bending strength of tubular members

A.12.5.2.1 Axial tensile strength check

Tubular members subjected to axial tensile forces, P_{ut}, should satisfy:

$$P_{ut} \leq A\ F_y / \gamma_{R,Tt} \quad \text{(A.12.5-3)}$$

where:

F_y = yield stress as defined in ISO 19905-1:2012, A.12.2.2

A = total cross-sectional area

$\gamma_{R,Tt}$ = partial resistance factor for axial tension, 1,05

The limiting axial force for tubular members in tension is tabulated below:

Member		A (m^2)	F_y (N/mm^2)	Limiting P_{ut} (MN)
Horizontal:	Lower leg	0,037	620,7	21,87
	Upper leg	0,026	586,3	14,52
Diagonal:	Lower leg	0,037	620,7	21,87
	Upper leg	0,026	586,3	14,52

All tubular members in tension have loads lower than the limiting values above with a maximum lower leg utilization of 0,23 and a maximum upper leg utilization of 0,33 therefore satisfying the requirements of ISO 19905-1.

A.12.5.2.2 Axial compressive strength check

Tubular members subjected to axial compressive forces, P_{uc}, should satisfy:

$$P_{uc} \leq P_a / \gamma_{R,Tc} \qquad (12.5\text{-}4)$$

where

P_a = representative compressive strength as determined in A.12.5.2.4

$\gamma_{R,Tc}$ = partial resistance factor for axial compressive strength, 1,15

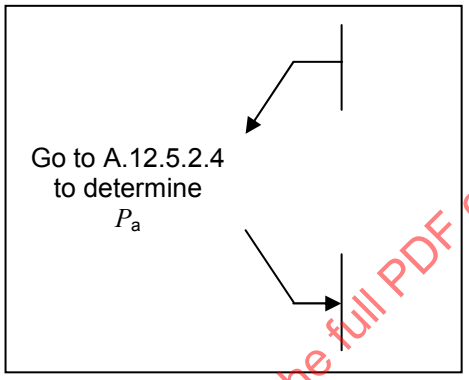

The limiting axial force for tubular members in compression is tabulated below:

Member		A (m^2)	F_y (N/mm^2)	P_a (MN) (from A.12.5.2.4)	Limiting P_{uc} (MN)
Horizontal:	Lower leg	0,037	620,7	18,73	16,29
	Upper leg	0,030	586,3	11,79	10,26
Diagonal:	Lower leg	0,037	620,7	18,73	15,62
	Upper leg	0,030	586,3	11,79	9,71

All tubular members in compression have loads lower than the limiting values above with a maximum lower leg utilization of 0,36 and a maximum upper leg utilization of 0,47 therefore satisfying the requirements of ISO 19905-1.

A.12.5.2.3 Local buckling strength

The representative local buckling strength, P_{yc}, should be determined from:

$$P_{yc} = A F_y \quad \text{for } A F_y / P_{xe} \leq 0{,}170 \qquad (A.12.5\text{-}5)$$
$$P_{yc} = [1{,}047 - 0{,}274\, A F_y / P_{xe}]\, A F_y \quad \text{for } 0{,}170 < A F_y / P_{xe} \leq 200\, F_y / E$$

where

F_y = yield stress as defined in ISO 19905-1:2012, A.12.2.2

A = total cross-sectional area

P_{xe} = representative elastic local buckling strength
P_{xe} = 2 C_x E A (t / D) (A.12.5-6)

C_x = critical elastic buckling coefficient
= 0,3 (recommended value for determining P_{xe})

Member		A (m^2)	F_y (N/mm^2)	P_{xe} (MN)	$A F_y / P_{xe}$	Limiting P_{yc} (MN)
Horizontal:	Lower leg	0,037	620,7	358,7	0,064	22,97
	Upper leg	0,026	586,3	224,6	0,068	15,24
Diagonal:	Lower leg	0,037	620,7	358,7	0,064	22,97
	Upper leg	0,026	586,3	224,6	0,068	15,24

The calculation of AF_y / P_{xe} indicates that the first Equation (A.12.5-5) should be used throughout.

A.12.5.2.4 Column buckling strength

The representative axial compressive strength of tubular members, P_a, should be determined from:

P_a = [1,0 – 0,278λ^2] P_{yc} for $\lambda \leq 1{,}34$ (A.12.5-7)
P_a = 0,9 P_{yc} /λ^2 for $\lambda > 1{,}34$

λ = [P_{yc}/P_E]^{0,5} (A.12.5-8)

where:

P_{yc} = representative local buckling strength (see A.12.5.2.3)

λ = column slenderness parameter

P_E = smaller of the Euler buckling strengths about the y or z direction
= π^2 E I / $(KL)^2$

E = Young's modulus as defined in ISO 19905-1:2012, A.12.1.1
= 205 000 N/mm^2

K = effective length factor in y or z direction, see ISO 19905-1:2012, A.12.4.3
= 0,8 for diagonals and horizontals (split-X brace design)

L = unbraced length in y or z direction measured between centre-lines
= 7,775 m for horizontals
= 8,446 m for diagonals

= second moment of area of the tubular.

Member		I (m^4)	P_E (MN)	λ	Limiting P_a (MN)
Horizontal:	Lower leg	$6{,}62 \times 10^{-4}$	34,62	0,81	18,73
	Upper leg	$3{,}58 \times 10^{-4}$	18,72	0,90	11,79
Diagonal:	Lower leg	$6{,}62 \times 10^{-4}$	29,34	0,88	17,97
	Upper leg	$3{,}58 \times 10^{-4}$	15,87	0,98	11,17

A.12.5.2.5 Bending strength check

Tubular members subjected to bending moments, M_u, should satisfy:

$M_u \leq M_b/\gamma_{R,Tb}$ (A.12.5-9)

where

M_u = M_{uy} or M_{uz} is the bending moment due to factored actions about member y- and z-axes, respectively, determined in an analysis that includes global P-Δ effects;

M_b is the representative bending moment strength, determined from:

$$\left.\begin{array}{lll} M_b = M_p & \text{for} & (F_y\, D)/(E\, t) \le 0{,}051\ 7 \\ M_b = [1{,}13 - 2{,}58\ (F_y\, D)/(E\, t)]\ M_p & \text{for } 0{,}051\ 7 < & (F_y\, D)/(E\, t) \le 0{,}103\ 4 \\ M_b = [0{,}94 - 0{,}76\ (F_y\, D)/(E\, t)]\ M_p & \text{for } 0{,}103\ 4 < & (F_y\, D)/(E\, t) \le 120\ (F_y / E) \end{array}\right\} \quad \text{(A.12.5-10)}$$

M_p is the plastic moment strength

$$M_p = F_y\ [D^3 - (D - 2t)^3] / 6 \quad \text{(A.12.5-11)}$$

$\gamma_{R,Tb}$ is the partial resistance factor for bending strength, $\gamma_{R,Tb}$ = 1,05.

Member		M_p	$(F_y\, D)/(E\, t)$	M_b	Limiting M_u (MNm)
Horizontal:	Lower leg	2,79	0,038	2,79	2,66
	Upper leg	1,61	0,041	1,61	1,53
Diagonal:	Lower leg	2,79	0,038	2,79	2,65
	Upper leg	1,61	0,041	1,61	1,53

All tubular members subject to bending have loads lower than the limiting values above with a maximum lower leg bending-only utilization of 0,07 and a maximum upper leg bending-only utilization of 0,06 therefore satisfying the requirements of ISO 19905-1.

A.12.5.3 Tubular member combined strength checks

ISO 19905-1 requires that tubular members be checked for combined axial forces and bending and for beam shear and torsional shear. Although all members have been checked in the analysis, only example calculations are presented here with a full table of maximum member utilizations presented at the end of this section.

A.12.5.3.1 Axial tension and bending strength check

Tubular members subjected to combined axial tension and bending forces should satisfy the following condition along their length:

$$\gamma_{R,Tt}\ P_{ut} / (A\ F_y) + \gamma_{R,Tb}\ (M_{uy}^{\ 2} + M_{uz}^{\ 2})^{0,5} / M_b \le 1{,}0 \quad \text{(A.12.5-12)}$$

where:

P_{ut} = axial tensile force due to factored actions

A = total cross-sectional area

F_y = yield stress as defined in ISO 19905-1:2012, A.12.2.2

M_{uy}, M_{uz} = bending moments about member y- and z-axes respectively due to factored actions determined in an analysis which includes global P-Δ effects

M_b = representative moment strength, as defined in Equation (A.12.5-9)

$\gamma_{R,Tt}$ = partial resistance factor for axial tension, 1,05

$\gamma_{R,Tb}$ = partial resistance factor for bending, 1,05

Example:

The following example is based on a diagonal brace in tension in the upper leg section in the area of highest brace utilizations (note all of the highest utilizations occur for braces in compression; see A.12.5.3.2 below). The following forces and moments are calculated in the brace:

Axial force = 4,57 MN (tension)

Bending moment Y = 0,08 MNm

Bending moment Z = 0,01 MNm

From the data derived in A.12.5.2:

Limiting P_{ut} = 14,52 MN (from A.12.5.2.1)

M_b = 1,61 MNm (from A.12.5.2.5)

Therefore:

Tension and bending strength check:

$$\left(\frac{4,57}{14,52}\right)+1,05\left(\frac{\sqrt{0,08^2+0,01^2}}{1,61}\right)=0,37$$

Member UC = 0,37

A.12.5.3.2 Axial compression and bending strength check

Tubular members subjected to combined axial compression and bending forces should satisfy the following conditions at all cross-sections along their length:

Beam-column check:

$$(\gamma_{R,Tc}\,P_{uc}/P_a) + (\gamma_{R,Tb}/M_b)\,(M_{uay}^{\ 2} + M_{uaz}^{\ 2})^{0,5} \le 1,0 \qquad \text{(A.12.5-13)}$$

Local strength check:

$$(\gamma_{R,Tc}\,P_{uc}/P_{yc}) + (\gamma_{R,Tb}/M_b)\,(M_{uy}^{\ 2} + M_{uz}^{\ 2})^{0,5} \le 1,0 \qquad \text{(A.12.5-14)}$$

where

P_{uc} = axial compressive force due to factored actions

P_{yc} = representative local buckling strength in A.12.5.2.3

P_a = as defined in A.12.5.2.4

M_{uy} = corrected effective bending moment about member y-axis due to factored actions determined in an analysis which includes global P-Δ effects

M_{uz} = corrected effective bending moment about member z-axis due to factored actions determined in an analysis which includes global P-Δ effects

M_{uay} = amplified bending moment about member y-axis due to factored actions from A.12.4.3

M_{uaz} = amplified bending moment about member z-axis due to factored actions from A.12.4.3

M_b = representative bending strength, as defined in Equation (A.12.5-9)

$\gamma_{R,Tb}$ = partial resistance factor for bending, 1,05

$\gamma_{R,Tc}$ = partial resistance factor for axial compressive strength, 1,15

Example:

The highest brace utilization for the sand case occurs is a diagonal brace in the upper leg section just above the section change. The following forces and moments are calculated in the brace:

Axial force = 4,83 MN (compression)

Bending moment Y = 0,09 MNm

Bending moment Z = 0,01 MNm

From the data derived in A.12.5.2

P_{yc} = 15,24 MN (from above under the flag where ISO 19905-1:2012, A.12.2.5.3 is discussed)

P_a = 11,17 MN (from above under the flag where ISO 19905-1:2012, A.12.2.5.4 is discussed)

M_b = 1,61 MNm (from above under the flag where ISO 19905-1:2012, A.12.5.2.5 is discussed)

Therefore:

Beam-column strength check:

$$1{,}15\left(\frac{4{,}83}{15{,}24}\right)+1{,}05\left(\frac{\sqrt{0{,}09^2+0{,}01^2}}{1{,}61}\right)=0{,}42$$

Local strength check:

$$1{,}15\left(\frac{4{,}83}{11{,}17}\right)+1{,}05\left(\frac{\sqrt{0{,}09^2+0{,}01^2}}{1{,}61}\right)=0{,}56$$

Member UC = 0,56

A.12.5.3.3 Beam shear strength check

Tubular members subjected to beam shear forces should satisfy:

$$V \leq P_v/\gamma_{R,Tv} \qquad \text{(A.12.5-15)}$$

where:

V = beam shear due to factored actions

P_v = representative shear strength
= $A\,F_y/(2\sqrt{3})$ (A.12.5-16)

A = total cross-sectional area

$\gamma_{R,Tv}$ = partial resistance factor for beam shear strength, 1,05

Following from the example given above:

Shear force = 0,012 MN

$P_v = A\,F_y/(2\sqrt{3})$ = 4,40 MN

Therefore:

$$\text{Shear strength UC} = 1{,}05\left(\frac{0{,}01}{4{,}40}\right) = 0{,}00$$

A.12.5.3.4 Torsional shear strength check

Tubular members subjected to torsional shear forces should satisfy:

$$T_u \leq T_v / \gamma_{R,Tv} \qquad \text{(A.12.5-17)}$$

where:

T_u = torsional moment due to factored actions

T_v = representative torsional strength
= $2\,I_p\,F_y/(D\sqrt{3})$

I_p = polar moment of inertia
= $(\pi/32)\,[D^4 - (D - 2t)^4]$

Following from the example given above:

Torsional moment = 0,002 MN

I_p = 7,16E-04 m^4

T_v = 1,36 MN

Therefore:

$$\text{Torsional strength unity check (UC)} = 1{,}05\left(\frac{0{,}002}{1{,}36}\right) = 0{,}00$$

The highest brace utilizations for the 90° heading (identified as the worst heading for structural UCs) are presented below with the UC shown in **bold** used in the example calculations above. (Although not apparent when reported to two decimal places, small differences exist between the brace strength checks for mid-bay, node and quartering cases.)

Case	Leg 2 mid	Leg 2 nod	Leg 2 qrt	Leg 3 mid	Leg 3 nod	Leg 3 qrt
Sand	0,56	0,56	**0,56**	0,47	0,47	0,47
Clay	0,60	0,60	**0,60**	0,46	0,46	0,46

NOTE Although ISO 19905-1 only requires utilizations to be reported to one decimal place, for the purpose of transparency, utilizations are reported in these detailed example calculations to two decimal places.

The maximum structural utilizations for the braces are all below 1,0 with the maximum UC of 0,60 reported for the clay case. Therefore, the unit brace strength checks are passed for both sand and clay conditions.

12.6 & A.12.6 Leg strength — Strength of non-circular prismatic members

ISO 19905-1 requires that non-circular prismatic members be checked for combined axial forces and bending and for shear and torsional shear. Although all members have been checked in the analysis, only example calculations are presented here with a full table of maximum member utilizations presented at the end of this section.

It should be noted that member utilizations from the analysis have been calculated using software which calculates the plastic interaction curves for the specific chord section in question, and as such although the analysis methodology follows the interaction surface approach, the equations for M'_{px} and M'_{py} given in ISO 19905-1:2012, Annex F have not been used.

A.12.6.2 Non-circular prismatic members subjected to tension, compression, bending or shear

A.12.6.2.2 Axial tensile strength check

Non-circular prismatic members subjected to axial tensile forces, P_{ut}, should satisfy:

$$P_{ut} \leq P_t / \gamma_{R,Pt} \quad \text{(A.12.6-1)}$$

where

P_t = axial tensile strength of non-circular prismatic members
= $\Sigma(F_{yi}A_i)$ (A.12.6-2)
= 170,46 MN

F_{yi} = yield strength of the i^{th} component comprising the structural member (as defined in ISO 19905-1:2012, A.12.2.2)
= 689,6 MN/m^2 (constant across cross-section)

A_i = cross-sectional area of the i^{th} component comprising the structural member
= 0,247 m^2
(yield stress constant across the section)

$\gamma_{R,Pt}$ = partial resistance factor for axial tension, 1,05

therefore:

limiting P_{ut} = 162,3 MN

A.12.6.2.3 Axial compressive local strength check

Non-circular prismatic members subjected to axial compressive forces, P_{uc}, should satisfy:

$$P_{uc} \leq P_{pl} / \gamma_{R,Pcl} \quad \text{(A.12.6-3)}$$

where

P_{pl} = the local compressive axial strength of non-circular prismatic members
= $\Sigma F_{yi}A_i$ for class 1 and 2 members (A.12.6-4)
= 170,5 MN

F_{yi} = yield strength of the i^{th} component comprising the structural member (as defined in ISO 19905-1:2012, A.12.2.2)
= 689,6 MN/m^2 (constant across cross-section)

A_i = cross-sectional area of the i^{th} component comprising the structural member
= 0,247 m^2 (yield stress constant across the section)

$\gamma_{R,Pcl}$ = partial resistance factor for local axial compressive strength, 1,1

therefore:

limiting P_{uc} = 155,0 MN

A.12.6.2.4 Axial compressive column buckling strength

The representative compression strength of all member classifications subject to flexural buckling should be determined from the following equations for **high strength steels**:

$$P_n = (0{,}762\ 5^{\lambda_c^{3,22}})\ P_{pl} \text{ for } \lambda_c \leq 1{,}2 \quad \text{(A.12.6-18)}$$

$$= (0{,}860\ 8/\lambda_c^{1{,}854})\ P_{pl} \text{ for } \lambda_c > 1{,}2 \quad \text{(A.12.6-19)}$$

where

$$\lambda_c = \left\{\frac{P_{pl}}{P_E}\right\}^{0,5} \quad \text{(A.12.6-20)}$$

P_{pl} = compressive axial strength as defined in A.12.6.2.3
= 170,46 MN

P_E is the minimum Euler buckling load for plane of bending
[defined in ISO 19905-1:2012, A.12.4.3 (including rack teeth of chords; see A.12.3.1)]

P_{Ey} = 734,3 MN

P_{Ez} = 510,0 MN

therefore:

λ_c = 0,578

P_n = 162,7 MN

A.12.6.2.5 Bending strength

The classification of member cross-sections in ISO 19905-1:2012, A.12.2 is used to identify the potential for local buckling.

Lateral torsional buckling checks have been performed according to ISO 19905-1:2012, A.12.2.3.2. The chord passed these checks and therefore the bending strength need not be reduced due to this effect.

A.12.6.2.5.2 Class 1 plastic and class 2 compact section bending strength

The representative bending strength, M_b, is given by the plastic bending moment of the entire section:

$$M_b = Z_p F_{ymin} \quad \text{(A.12.6-21)}$$

where

M_b = representative bending moment strength

M_{by} = 27,43 MNm

M_{bz} = 24,53 MNm

Z_p = fully plastic section modulus determined from ISO 19905-1:2012, Equation (A.12.3-2) (see section above addressing ISO 19905-1:2012, A.12.6.2.5.2)

Z_{py} = 0,040 m^3

Z_{pz} = 0,036 m^3

F_{ymin} = minimum yield strength of the cross-section as defined in ISO 19905-1:2012, A.12.2.2 (see section above addressing ISO 19905-1:2012, A.12.2.2)
= 689,6 MN/m^2

A.12.6.2.6 Bending moment strength affected by lateral torsional buckling

The chord passes the lateral torsional buckling criteria specified in ISO 19905-:2012, A.12.2.3.2 and hence no further assessment of lateral torsional buckling has been made.

A.12.6.2.7 Bending strength check

Non-circular prismatic members subjected to bending moments, M_u, should satisfy:

$$M_u \leq M_b / \gamma_{R,Pb} \quad \text{(A.12.6-37)}$$

where

M_u = M_{uy} or M_{uz} the bending moment about member y- and z-axes respectively due to factored actions

M_b = representative bending moment strength, determined from A.12.6.2.5 and A.12.6.2.6

M_{by} = 27,43 MNm

M_{bz} = 24,53 MNm

$\gamma_{R,Pb}$ = partial resistance factor for bending, 1,1

therefore:

limiting M_{uy} = 24,94 MNm

limiting M_{uz} = 22,30 MNm

A.12.6.3 Non-circular prismatic member combined strength checks

Non-circular prismatic member analysis can utilize one of two methods:

a) the interaction equation approach (see ISO 19905-1:2012, A.12.6.3.2), applicable to all member classifications;

b) the plastic-interaction surface approach (see ISO 19905-1:2012, A.12.6.3.3), applicable to class 1 and 2 members.

The following sections demonstrate both methods although the structural utilizations for the unit in consideration have been calculated using the interaction surface approach.

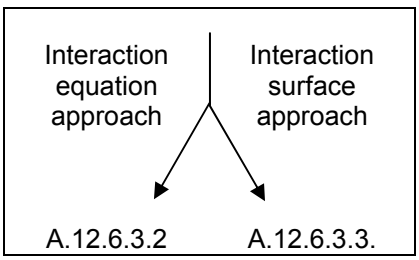

A.12.6.3.2 Interaction equation approach

The following example demonstrates the interaction equation approach for a specific chord member in compression:

Case	Sand
Storm heading	90°
Leg	Port leg
Position of lower guide	Quarter bay
Chord	Port (with respect to global axes system)

Loads in the chord section at level of lower guide:

Axial load	–93,7 MN
Bending Y_1	–0,39 MNm
Bending Y_2	–4,70 MNm
Bending Z_1	0,00 MNm
Bending Z_2	0,00 MNm
Shear Y	0,00 MN
Shear Z	–1,69 MN
Torsion	0,00 MNm

Bending 1 and 2 about each axis refer to the moments at each end of the chord section considered. This calculation assesses the section at node 2 but the moments at node 1 are required for calculation of the C_m terms.

Each non-circular prismatic structural member should satisfy the following conditions.

Note that when the shear due to factored actions is greater than 60 % of the shear strength, the bending moment strength should be reduced parabolically to zero when the shear equals the shear strength (P_v in A.12.6.3.4):

Local strength check (for all members):

$$\frac{\gamma_{R,Pa} P_u}{P_{pls}} + \left[\left\{ \frac{\gamma_{R,Pb} M_{uey}}{M_{by}} \right\}^{\eta} + \left\{ \frac{\gamma_{R,Pb} M_{uez}}{M_{bz}} \right\}^{\eta} \right]^{\frac{1}{\eta}} \leq 1,0 \qquad \text{(A.12.6-38)}$$

Beam-column check (for members subject to axial compression):

If $\gamma_{R,Pa} P_u / P_p > 0,2$

$$\frac{\gamma_{R,Pa} P_u}{P_p} + \frac{8}{9} \left[\left\{ \frac{\gamma_{R,Pb} M_{uay}}{M_{by}} \right\}^{\eta} + \left\{ \frac{\gamma_{R,Pb} M_{uaz}}{M_{bz}} \right\}^{\eta} \right]^{\frac{1}{\eta}} \leq 1,0 \qquad \text{(A.12.6-39)}$$

where

P_u = applied axial force
= 93,7 MN

P_{pls} = representative axial strength of a non-circular prismatic member
= 170,5 MN

P_p = representative axial strength of non-circular prismatic member
= 162,7 MN

M_{uey} = corrected bending moment (for local strength checks) about member y-axis due to factored actions from ISO 19905-1:2012, A.12.4

= –4,70 MNm (in this example e = 0 so $M_{uy} = M_{uey}$)

M_{uez} = corrected bending moment about member z-axis due to factored actions from A.12.4
= 0,00 MNm (in this example e = 0 so $M_{uz} = M_{uez}$)

M_{ua} = amplified bending moment (for beam column component checks) about member y-axis due to factored actions from ISO 19905-1:2012, A.12.4

= $M_{ue}\,B$

M_{uay} = –3,38 MNm

M_{uaz} = 0,00 mNm

where

B = Member moment amplification factor for the axis under consideration
$C_m/(1{,}0 - P_u/P_E)$

B_y = 0,72

B_z = 0,30

C_m = $0{,}6 - 0{,}4M_1/M_2$

(where M_1/M_2 is the ratio of the smaller to the larger non-amplified end moments of the member in the plane of bending under consideration; M_1/M_2 is positive for the segment subject to reverse curvature and negative when subject to single curvature)

C_{my} = 0,63

C_{mz} = 0,30

M_{1y} = 0,39 MNm

M_{2y} = 4,70 MNm

M_{1z} = 0,00 MNm

M_{2z} = 0,00 MNm

M_b = representative moment strength, as defined in A.12.6.2.5 or A.12.6.2.6; in this example the shear is less than 60 % of the shear strength so the full moment strength can be used

M_{by} = 27,43 MNm

M_{bz} = 24,53 MNm

$\gamma_{R,Pb}$ = partial resistance factor for bending = 1,1

$\gamma_{R,Pa}$ = partial resistance factor $\gamma_{R,Pc}$ for axial compressive strength = 1,1

η = exponent for biaxial bending

= 2,0

Therefore:

Local strength check:

$$\frac{1,1\times 93,7}{170,5}+\left[\left\{\frac{1,1\times 4,70}{27,43}\right\}^2+\left\{\frac{1,1\times 0,00}{24,53}\right\}^2\right]^{\frac{1}{2}}=0,79\le 1,0$$

Beam-column check (for members subject to axial compression) with $\gamma_{R,Pa} P_u / P_p$ > 0,2:

$$\frac{1,1\times 93,7}{162,7}+\frac{8}{9}\left[\left\{\frac{1,1\times 3,38}{27,43}\right\}^2+\left\{\frac{1,1\times 0,00}{24,53}\right\}^2\right]^{\frac{1}{2}}=0,75\le 1,0$$

A.12.6.3.3 Interaction surface approach

The following example demonstrates the interaction surface approach for a specific chord member; see ISO 19905-1:2012, A.12.6.3.2, as discussed above, for the specific chord details and applied loads.

The interaction surface approach requires the assessor to develop a plastic strength interaction surface in terms of the axial strength and biaxial moment strengths. In this case the surface has been generated using the GL Noble Denton software PLASTIC written by Dyer (see ISO 19905-1:2012, Reference [A.12.6-2]) for the assessment of plastic chord sections. The signs of the applied moments are considered very carefully as advised by ISO 19905-1, although this is less important for the symmetric section considered than for non-symmetric sections.

A measure of the interaction ratio can, then, be obtained as the ratio between the vector lengths from the functional origin to the member forces and the vector length from the functional origin to the nearest point on the surface. The generic equation describing the interaction surface for a family of split tubular chords is shown below:

i
Annex F.31 & F.3.3

$$\frac{P}{P_y}+\left(1-\frac{P}{P_y}\right)\left\{\left(\frac{M_z}{M'_{pz}}\right)^2+\left(\frac{M_y}{M'_{py}}\right)^2\right\}^{1/2}\le 1,00$$

(For both local strength check where $P_y = P_{Pl}$ and for the beam-column check where $P_y = P_n / \gamma_{R,Pa}$)

where

M'_p = adjusted local y and z axis bending strengths used in simplified interaction equations

M'_{py} = $M_{py}\left(1-\left(\frac{P}{P_y}\right)^{1,85}\right)$ for (P/P_y) <1,0

= 15,11 MNm for local strength check

= 14,22 MN for beam column check

M'_{pz} = $M_{pz}\left(1-\left(\frac{P}{P_y}\right)^{2,25}\right)$ for (P/P_y) <1,0
= 15,11 MNm
= 14,32 MN for beam column check

where

P = chord member axial force
= 93,7 MN

P_y = chord member axial strength (P_{pl} / $\gamma_{R,Pa}$) for local strength check
= 155,0 MN

P_{pl} = axial compressive local strength
= 170,5 MN

P_y = chord member axial strength (P_n / $\gamma_{R,Pa}$) for beam-column check
= 147,9 MN

P_n = representative compressive column buckling strength
= 162,7 MN

M_y, M_z = y and z axis bending moments for local strength checks, M_{uey} and M_{uez} (see A.12.6.3.2)

M_{uey} = –4,70 MNm

M_{uez} = 0,00 MNm

M_y, M_z = y and z axis bending moments for beam column checks, M_{uay} and M_{uaz} (see A.12.6.3.2)

M_{uay} = –3,38 MNm

M_{uaz} = 0,00 MNm

M_{py}, M_{pz} = local y and z axis plastic bending strengths (M_b / $\gamma_{R,Pb}$)

M_{py} = 24,94 MNm

M_{pz} = 22,30 MNm

M_b = representative moment strength, as defined in A.12.6.2.5 or A.12.6.2.6; in this example the shear is less than 60 % of the shear strength so the full moment strength can be used

M_{by} = 27,43 MNm

M_{bz} = 24,53 MNm

$\gamma_{R,Pa}$ = partial resistance factor $\gamma_{R,Pc}$ for axial compressive strength = 1,1

$\gamma_{R,Pb}$ = partial resistance factor for bending = 1,1

Therefore:

Local strength check:

$$\left(\frac{93,7}{155,0}\right)+\left(1-\frac{93,7}{155,0}\right)\left\{\left(\frac{0,00}{15,11}\right)^2+\left(\frac{4,70}{15,11}\right)^2\right\}^{1/2}=0,73\le 1,00$$

Beam-column check (for members subject to axial compression):

$$\left(\frac{93,7}{147,9}\right)+\left(1-\frac{93,7}{147,9}\right)\left\{\left(\frac{0,00}{14.32}\right)^2+\left(\frac{3,38}{14,22}\right)^2\right\}^{1/2} = 0,73 \le 1,00$$

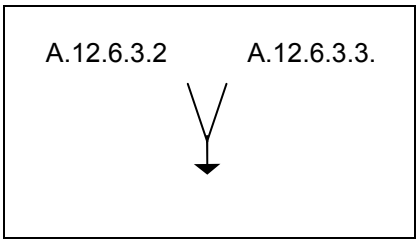

A.12.6.3.4 Beam shear

Non-circular prismatic members subjected to beam shear forces due to factored actions should satisfy the following:

$$V_y \le P_{vy} / \gamma_{R,Pv} \quad \text{(A.12.6-44)}$$

$$V_z \le P_{vz} / \gamma_{R,Pv} \quad \text{(A.12.6-45)}$$

where

V_y, V_z = beam shear due to factored actions in the local y and z directions

V_y = –0,00 MN

V_z = –1,69 MN

P_{vy}, P_{vz} = representative shear strength in the local y and z directions

= $(A_v F_{ymin} / \sqrt{3})$ (A.12.6-46)

P_{vy} = 74,96 MN

P_{vz} = 74,96 MN

A_v = effective shear area in the direction being considered (for split tubular chords this is taken as the area of the rack plus half the area of the split tube)

A_{vy} = 0,188 m^2

A_{vz} = 0,188 m^2

$\gamma_{R,Pv}$ = partial resistance factor for beam shear strength = 1,1

therefore:

$$\text{shear UC in } y = \frac{0,00}{74,96} 1,10 = 0,00$$

$$\text{shear UC in } z = \frac{1,69}{74,96} 1,10 = 0,02$$

The shear forces in both y and z are both significantly below 60 % of the shear strength, therefore allowing the use of the full bending strength M_b in the combined strength checks.

A.12.6.3.5 Torsional shear

Closed-section non-circular prismatic members subjected to torsional shear moments should satisfy the following:

$$T \leq T_v / \gamma_{R,Pv} \qquad \text{(A.12.6-47)}$$

where

T = torsional moment due to factored actions
= 0,00 MNm

T_v = representative torsional strength
= $I_p F_{ymin} / (r \sqrt{3})$
= 20,77 MNm

I_p = polar moment of inertia
= 0,020 m^4

r = maximum distance from centroid to an extreme fibre
= 0,374 m

Torsional unity check (UC) = $\frac{0,00}{20,77} 1,10 = 0,00$

The section passes the torsional shear check with a UC of 0,00.

Chord structural utilizations

The highest chord utilizations for the 90° heading (identified as the worst heading for structural UCs) are presented below for information with the UCs shown in **bold** used in the example calculations above.

Case	Leg 2 mid	Leg 2 nod	Leg 2 qrt	Leg 3 mid	Leg 3 nod	Leg 3 qrt
Sand	0,69	0,72	0,73	1,02	1,04	1,07
Clay	0,64	0,66	0,70	0,99	1,02	1,03

The maximum structural utilizations for the chords are above 1,0 for both the sand and clay assessment cases. The unit therefore fails the chord strength check for both the sand and clay example calculations detailed herein.

12.7 & A.12.7 Leg strength — Joints

ISO 19905-1 states that joint strength should be assessed when the site conditions (metocean combinations, eccentric spudcan loading, etc.) fall outside the limits that are normally assessed by the RCS.

Joint strength details may be made available by the designer; assessment of joint strength is considered outside the scope of this annex.

The leg strength checks have been completed.

i
ISO 19902 and ISO 19901-3

12.1.4 & 13.5 **Holding system strength**

Strength of the elevating and fixation system would typically be provided by the manufacturer. Values for the "typical jack-up" being considered herein are:

ultimate holding capacity of the pinions = 28,5 MN / pinion pair

ultimate holding capacity of rack chocks = 105,5 MN / chord (pair of chocks)

The capacities above represent the unfactored ultimate strength of the system, to which the holding system resistance factor, $\gamma_{R,H}$, of 1,15 should be applied:

factored allowable holding capacity of the pinions = 24,8 MN / pinion pair

factored allowable holding capacity of rack chocks = 91,8 MN / chord

This unit retains 100 % of the "functional weight" on the pinions when the rack-chock holding system is installed; see the data sheet in A.12, Appendix A.B. This system is modelled accurately in the fully detailed leg models.

Both the pinion and rack chock holding system strength utilization calculations are based on the maximum loads in the most heavily loaded leg chord at the level of the holding system determined from the final quasi-static assessments of the maximum hull weight case.

Pinion strength utilization calculation (both assessment cases)

Sand assessment:

Load in leg chord = 146,8 MN

Load taken by rack chocks = 87,2 MN

Load taken by 1st pinion pair = 16,2 MN

Load taken by 2nd pinion pair = 15,1 MN

Load taken by 3rd pinion pair = 14,3 MN

Load taken by 4th pinion pair = 14,0 MN

Factored allowable pinion capacity (per pair) = 24,8 MN

Therefore:

Pinion strength utilization = 0,65 < 1,0

Clay assessment:

Load in leg chord = 144,7 MN

Load taken by rack chocks = 75,0 MN

Load taken by 1st pinion pair = 15,6 MN

Load taken by 2nd pinion pair = 14,5 MN

Load taken by 3rd pinion pair = 13,8 MN

Load taken by 4th pinion pair = 13,5 MN

Factored allowable pinion capacity (per pair) = 24,8 MN

Therefore:

Pinion strength utilization = 0,63 < 1,0

The pinion holding system strength check therefore satisfies the requirements of ISO 19905-1.

Rack chock holding system strength utilization calculation

Sand assessment:

Load in leg chord = 146,8 MN

Load taken by pinions = 59,6 MN

Load taken by rack chocks (per pair) = 87,2 MN

Factored allowable rack chock capacity (per pair) = 91,8 MN

Therefore:

Rack chock strength utilization = 0,95 < 1,0

Clay assessment:

Load in leg chord = 144,7 MN

Load taken by pinions = 57,4 MN

Load taken by rack chock (per chock pair) = 87,3 MN

Factored allowable rack chock capacity (per pair) = 91,8 MN

Therefore:

Rack chock strength utilization = 0,95 < 1,0

The rack chock holding system strength checks therefore satisfy the requirements of ISO 19905-1.

Hull strength

Hull strength and jackhouse to deck connections are considered to be covered by classification unless special circumstances apply.

A detailed hull model including plate elements would be amenable to a detailed strength analysis. Extreme loads could be determined from a simpler structural model, and applied via portions of leg model, in reverse of the application of loads to a detailed leg model.

A.10.3 Spudcan strength assessment

12.1.5 & 13.4 **Spudcan strength**

The strength of the spudcan is normally supplied by the manufacturer. The manufacturer's data are expected to represent the unfactored ultimate strength of the spudcan and spudcan to leg connection.

ISO 19905-1:2012 specifies that the effects of the forces on the top and bottom of the spudcan due to factored actions for any of the applicable assessment situations shall be checked against the factored ultimate strength derived from the manufacturer's specification using $\gamma_{R,S}$ = 1,15.

If the spudcan vertical and rotational reactions are within the limits set by the manufacturer, it is not normally necessary to check the strength of the leg to spudcan connection.

No spudcan limits are known for the "typical jack-up" being considered and therefore it is not possible to check the spudcan strength implicitly. Instead, given that the preload capacity check is less than 1,0, it would be a fair assumption that the spudcan loading is within limits.

A detailed spudcan model including plate elements would be amenable to a detailed strength analysis. Extreme loads could be determined from a simpler structural model, and applied via portions of leg model, in reverse of the application of loads to a detailed leg model.

A.10.4 Overturning stability assessment

13.8 **Overturning stability**

It is noted that the overturning check serves only the purpose of a traditional benchmark; the assessment is governed by the foundation checks — this has been included for completeness.

The critical heading for overturning was determined to be 120° for both the "sand" and "clay" assessment cases. For this there are two leeward legs.

The margin of safety against overturning of the jack-up is assessed based on the general formula for assessment checks given in Equation (13.2-2):

$$\alpha_i = \left(\frac{\text{action effect } (A_E) \text{ due to factored action } (F_d)}{\text{factored resistance } (R)} \right)_i \qquad (13.2\text{-}2)$$

based on:

M_{OTM} = overturning moment due to factored actions F_d

$R_{d\,OTM}$ = the factored stabilizing moment based on the representative stabilizing moment $R_{r,OTM}$ [See ISO 19905-1:2012, Equation (13.8-1).]

with:

$\gamma_{R,OTM}$ = the resistance factor on representative stabilizing moment
= 1,05

The overturning moment is calculated from factored actions about the overturning axis:

Sand assessment

Moment loads in MN:

Wind overturning moment $\times \gamma_{f,E}$	(1 109 × 1,15)
Wave & current overturning moment $\times \gamma_{f,E}$	(1 599 × 1,15)
Inertial overturning moment $\times \gamma_{f,E}$	(549 × 1,15)
P-Δ overturning contribution $\times \gamma_{f,G}$	(612 × 1,00)

Therefore:

Total: 4 357 MNm

The stabilizing moment $R_{r,OTM}$ calculated about the same axis for the same assessment situation accounting for:

Self weight righting moment / $\gamma_{R,OTM}$

= (minimum total weight × lever arm[1]) / 1,05

= (228,8 x 19,2) / 1,05

= 4 184 MNm

[1] Hull sway can be accounted for in the overturning check by incorporating P-Δ load in the overturning moment or by using a righting moment "lever-arm" reduced by the hull sway. In this case the first approach has been used.

Stabilizing moments due to seabed foundation fixity / $\gamma_{R,OTM}$

= (274 / 1,05)

= 260 MNm

Therefore:

- Total: 4 444 MNm

Overturning utilization = 0,98 < 1,0 for the "sand" assessment case

Therefore, the unit satisfies the overturning stability assessment for the "sand" assessment case.

Clay assessment

Moment loads in MN:

Wind overturning moment $\times \gamma_{f,E}$	(1 078 × 1,15)
Wave & current overturning moment $\times \gamma_{f,E}$	(1 756 × 1,15)
Inertial overturning moment $\times \gamma_{f,E}$	(636 × 1,15)
P-Δ overturning contribution $\times \gamma_{f,G}$	(552 × 1,00)

Therefore:

Total: 4 542 MNm

The stabilizing moment $R_{r,OTM}$ calculated about the same axis for the same assessment situation accounting for:

Self weight righting moment / $\gamma_{R,OTM}$

= (minimum total weight × lever arm[1]) / 1,05

= (228,4 × 19,2) / 1,05

= 4 176 MNm

[1] Hull sway can be accounted for in the overturning check by incorporating P-Δ load in the overturning moment or by using a righting moment "lever-arm" reduced by the hull sway. In this case the first approach has been used.

Stabilizing moments due to seabed foundation fixity / $\gamma_{R,OTM}$

= (1 050 / 1,05)

= 1 000 MNm

Therefore:

Total: 5 176 MNm

Overturning utilization = 0,88 < 1,0 for the "clay" assessment case

Therefore, the unit satisfies the overturning stability assessment for the "clay" assessment case.

ISO 19905-1 notes: "The overturning check serves only the purpose of a traditional benchmark; the assessment is governed by the foundation checks."

NEXT ITEM

The structure has now been assessed and overturning stability considered.

Foundations are now assessed.

A.11 Assessment of foundation

Assess foundation, Sections A.9.3.3 & A.9.3.6/Figure A.9.3-17

Rather than produce a local route sign, the flow chart in Figure A.9.3-17 is referenced.

A.9.3.6 Acceptance checks

ISO 19905-1:2012, A.9.3.3 is referenced for this section. The flow chart in Figure A.9.3-17 may be followed at this stage and is reproduced below for easy reference.

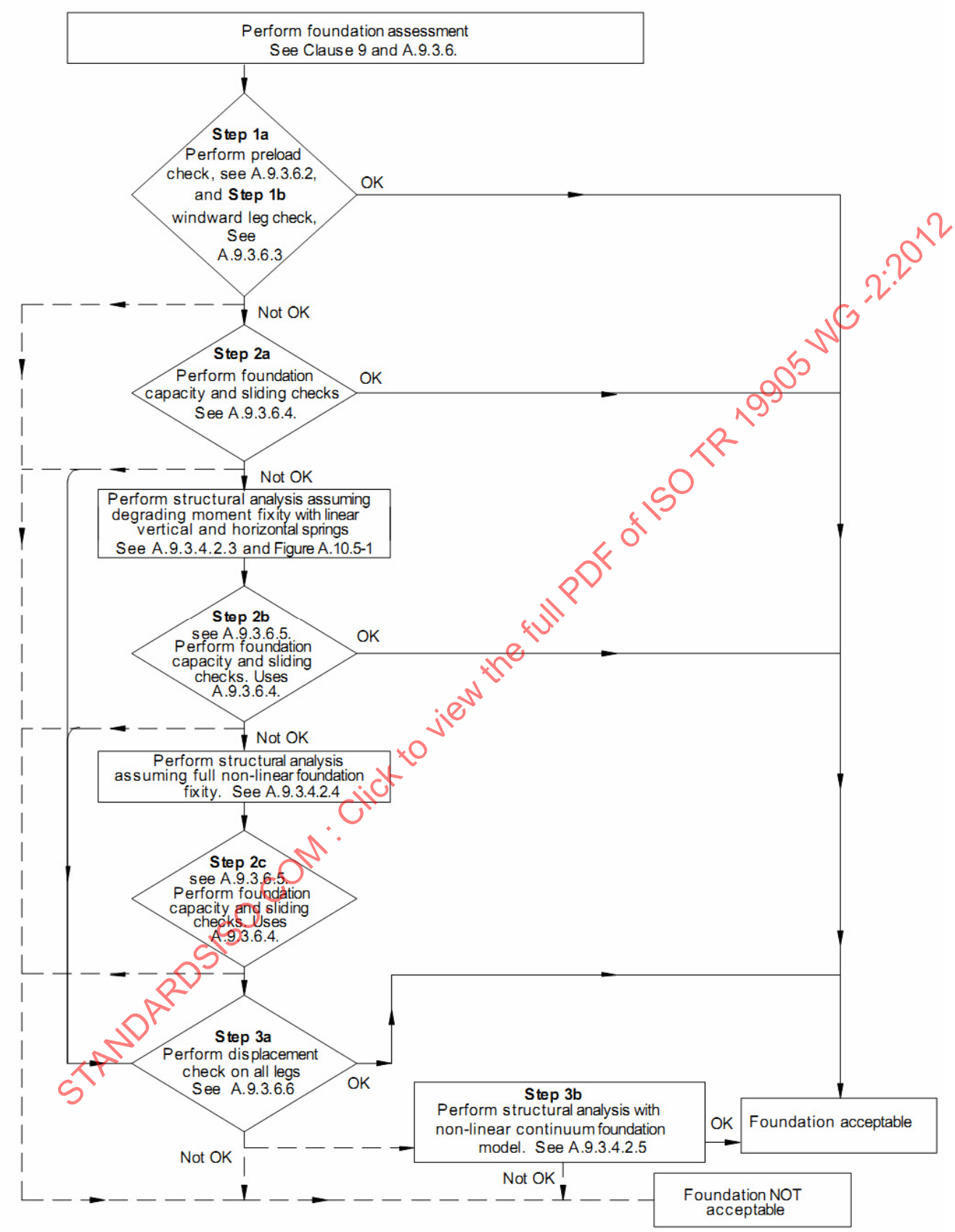

Figure A.9.3-17 — Approach to foundation acceptance checks

A.9.3.6.2 Level 1, Step 1a — Ultimate bearing capacity for vertical loading — Preload check

The simple preload check should be applied only when the horizontal force on the leeward leg spudcan, F_H, is no greater than F_{H1} (see ISO 19905-1:2012, Table A.9.3-7) and when the forces are determined from an analysis model with pinned condition for all spudcans (see ISO 19905-1:2012, Table A.9.3-1).

Although the assessment detailed herein has allowed for inclusion of foundation fixity the process is detailed below for completeness.

The following check is based on the starboard leg (leeward leg) for the 60° storm direction for both the sand and clay conditions.

From the quasi-static analysis, leeward leg vertical loads are as follows.

Location 1 (sand):

According to ISO 19905-1:2102, Table A.9.3-7, the limiting horizontal capacity, F_{H1}, for a Step 1a bearing capacity check to apply for a partially penetrated spudcan in sand is given by:

$$F_{H1} = [0,1 - 0,07\ (B/B_{max})^2]Q_{Vnet}$$

For this example calculation, $F_{H1} = 0,055Q_{Vnet}$ = 8,6 MN.

However, the horizontal component of the storm footing reaction being examined, F_H = 9,1 MN.

Given $F_H > F_{H1}$ the unit can not be checked using the Level 1, Step 1a assessment.

Location 2 (clay):

According to ISO 19905-1:2012, Table A.9.3-7, the limiting horizontal capacity, F_{H1}, for a Step 1a bearing capacity check to apply for a spudcan in clay is given by:

$$F_{H1} = 0,03\ Q_{Vnet}$$

For this example calculation, F_{H1} = 4,4 MN

However, the horizontal component of the storm footing reaction being examined, F_H = 8,7 MN

Given $F_H > F_{H1}$ the unit can not be checked using the Level 1, Step 1a assessment.

The calculated storm footing reactions for the unit for either soil profile do not comply with the conditions for a Level 1, Step 1a check. The foundation will therefore be assessed according to Level 2a.

Had the unit passed this Step 1a check then the analysis would proceed to the windward leg sliding check described in ISO 19905-1:2012, A.9.3.6.3.

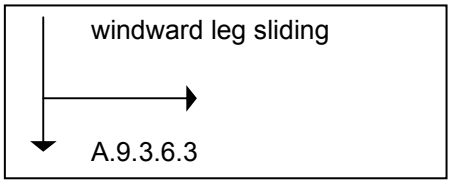

[not applicable here]

A.9.3.6.4 Level 2, Step 2a — Foundation capacity and sliding check

The foundation capacity check depends on the footing model. If a pinned footing has been used then ISO 19905-1:2012, A.9.3.6.4 is applicable. If a degree of footing fixity has been used then ISO 19905-1:2012, A.9.3.6.5 is applicable.

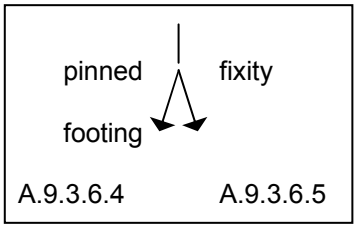

A.9.3.6.4 Level 2, Step 2a — Foundation capacity and sliding check — Pinned spudcan

Both the “sand” and “clay” assessment cases presented in these detailed example calculations incorporate foundation fixity at the spudcan restraint level. No assessment of the foundation bearing capacity check for a “pinned” foundation restraint condition has been made. However, ISO 19905-1:2012, Equation (A.9.3-56), describing the foundation bearing capacity envelope, applies to the foundation bearing capacity check for both the “pinned” assessment approach (Step 2a check per ISO 19905-1:2012, A.9.3.6.4) and assessment inclusive of spudcan fixity (Step 2b check per ISO 19905-1:2012, A.9.3.6.5).

A.9.3.6.5 Level 2, Step 2b — Foundation capacity and sliding check — Spudcan with moment fixity and vertical and horizontal stiffness

Factored loads for the case of a footing with moment fixity are treated in much the same way as for the pinned footing, except that the vector formed of the vertical, horizontal and moment loads has already been modified such that it either lies within the yield envelope or lies on the vertical-horizontal plane with the moment degraded to zero.

The foundation interaction envelope, as defined in ISO 19905-1:2012, A.9.3.6.4 (Figure A.9.3-18), is applicable to both “pinned” and “foundation fixity” assessment approaches.

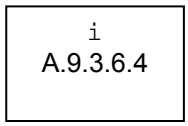

The partial resistance factor is applied to the Q_{VH} yield surface prior to the assessment of the load vectors.

The foundation capacity to withstand vertical, horizontal and moment loadings F_V, F_H and F_M is defined by the yield surface function encountered in the fixity calculations. To apply the resistance factors to this surface, the points on the yield surface must be written as vectors from the point of zero net reaction, i.e. (F_H = 0, $F_V = W_{BF,o} - B_S$), and then reduced in magnitude accordingly.

The resistance term is the foundation capacity to withstand the combined vertical and horizontal storm foundation loads (F_H, F_V), which is obtained according to ISO 19905-1:2012, A.9.3.3.2, as shown below.